Synthesis of bisquinolines, naphthyridines and pyronaridine to elucidate the mechanism of antimalarial drug action

Said Alizadeh-Shekalgourabi

A thesis submitted in partial fulfilment of
The requirement of the University of Hertfordshire
For the degree of Doctor of Philosophy

The programme of research was completed in the Pharmacy Department at University of Hertfordshire.

June 2024

Seek the cure, the science with encompassing parallel challenges, leave no stone unturned, look for the key to this enigma, wonder the world in search of knowledge, read all published and ask all questions to wipe away this unforgiving disease.

Do not weaken in pursuit, not to fall sleep, not to fall behind, not to get tired, not to slow down, not to allow any doubt in, not to fear any upheaval, and believe one can achieve one's goal, keep away from liars and the ones who are not in the know, do one's outmost to wage war on this parasite, and promise to light the way like a burning star and blaze numerous trails for others to follow….

Said Alizadeh-Shekalgourabi **September 1991**

Honour and Glory demands Blood and Sweat. You only fail if you quit…

Ahmad Alizadeh-Shekalgourabi **(1930-2002)**

"When you have eliminated the impossible, whatever remains, however improbable, must be the truth."

Arthur Conan Doyle, Sr. **(Scottish writer 1859-1930)**

Declaration.

No part of this thesis may be reproduced without the express permissions of the author and my Supervisors Dr F.M.D. Ismail and Dr D.G. Griffiths. I declare that the contents of this thesis are novel and it is to remain confidential until it is published in peer reviewed journals and/or conferences.

Said Alizadeh-Shekalgourabi

Dr. Fyaz M. D. Ismail

Dr. David G. Griffiths

Acknowledgements.

I would like to thank my supervisors Dr. Fyaz M. D. Ismail and Dr. David G. Griffiths for their expert guidance, patience, helpful discussions as well as provision of laboratory facilities and continued access to members of the Medicinal Chemistry Research Group. Also, I would like to thank Dr. Paul Bassin, Professor Anwar Baydoun and Professor Satyajit Sarker (LJMU) for believing in and supporting medicinal chemistry group.

The former staff of the Chemistry Department who, despite the closure of the Department, continued to assist me in realizing my goal of completing my doctoral dissertation. I thank Professor M. G. B. Drew of Reading University for providing single crystal X-ray diffraction facilities and also performing numerous Density Functional Theory calculations which have greatly aided the understanding of antimalarial haem drug receptor interactions detailed herein.

I also wish to thank one of my former supervisors, Dr. Pamela Carr assisted with the initial molecular modelling experiments (Macromodel and APEX) which were then supplanted with more sophisticated molecular mechanics studies (Cerius2) and DFT experiments in collaboration with Professor Michael G. B. Drew (University of Reading) and Dr. Sam P. de Visser (Manchester University). My deepest gratitude to Dr Martin J. Frearson (University of Hertfordshire) for valuable discussions involving electron ionisation mass spectrometry.

Dr. Mark Scott (UH) and Mr. Roy Bird who valiantly maintained the EI-mass spectrometer until it was finally scrapped. Consequently, Dr. Martin J. Frearson deserves special thanks for providing an alternative service by acquiring numerous ion trap GC-MS mass spectra for our research group and his expert guidance and fruitful discussions on deciphering fragmentation patterns contained in both EI-and CI- mass spectra.
Mr. David Clarke, latterly, Wendy Poursaeedi-Brownhill performed NMR experiments. In addition, thanks are due to Mr. Andrew J. Blackaby for providing multidimensional NMR experiments (500 MHz) and LC-MS experiments at Glaxo-Wellcome when, for whatever reason, such facilities became unavailable within the Chemistry Department.

Dr. Nicola J. Dempster of the School of Pharmacy (LJMU) provided DSC and Electrospray measurements on the drug receptor complexes for which I am most grateful. Dr. Giles Edwards of Waters PLC, latterly Nizwa University, assisted with the MS-MS fragmentation experiments involving various antimalarials, especially pyronaridine. Dr. Harry Morris (LJMU) assisted with the mathematical and statistical analysis of the drug binding (UV studies) involving all the antimalarials detailed in this study and wrote the

Fortran programs to unravel the nature and type of drug binding between haem and various putative drugs. Dr. Philip Evans (currently at PeakDale) is due special mention for assisting in repeating several key experiments involving the Jacob-Goulds reaction and Hoffman rearrangements.

Mr. Brian Robinson of Northwick Park Institute was most kind in providing a small but vital sample of authentic pyronaridine (**15**). A more generous quantity (2g) was available both from the stalwarts of malaria research, Professors Wallace Peters and David Warhurst. Ms Victoria Deering (Cancer research) who kindly and meticulously went through chemical reactions and provided much needed technical support. Dr. Michael J. Dascombe (University of Manchester) kindly provided antimalarial pharmacology *in-vivo* (*Plasmodium berghei*) over two decades to our research group whereas Prof. Prapon Wilairat tested various analogues against wild type K1 multi-drug resistant *Plasmodium falciparum* strain of parasite at Mahidol University, Thailand.

Special thanks to Mr. Ricardo Adamcik for his advice and technical expertise in keeping my computers in working order, formatting my thesis so many times and being supportive throughout my studies. Also, many thanks to Elizabeth. G. Stone and daughters Jane and Anne for believing in me whilst morally supporting and encouraging me to march this endeavour to fruition.

Finally, thanks are due to Lisa, Sami, Sara, David, Jasper, my parents and the rest of my family and friends for being the wind beneath my wings, as well as their immeasurable support, belief and encouragement throughout my studies.

Abbreviations.

AAQM	Alkyl amino quinolinyl methanol
ADMET	Absorption, distribution, metabolism, elimination and toxicology
ADF	Accurate & efficient DFT programme
AIDS	Acquired immune deficiency syndrome
AMU	Atomic mass unit
APT	Attached proton test
ATR	Attenuated total reflectance
Aq	Amodiaquine
CF3	Trifluoromethyl group
COSY	Correlation spectroscopy
CQ	Chloroquine
CTZ	Clotrimazole
Da	Dalton (unit of atomic mass)
DDT	Dichlorodiphenyltrichloroethane (dicophane)
DEPTQ	Distortionless Enhancement by Polarization Transfer. This experiment allows to determine multiplicity of carbon atom substitution with hydrogens
DFT	Density functional theory
DMF	N-N-dimethylformamide
DMSO	Dimethyl sulfoxide
DNA	Deoxyribonucleic Acid
Dowtherm	A heat transfer fluid of biphenyl ($C_{12}H_{10}$) and diphenyl oxide ($C_{12}H_{10}O$)
DSIR	Department of Scientific and Industrial Research
ED50	Dose producing an effect 50% of maximum
ED90	Dose producing an effect 90% of maximum
ESI	Electrospray mass spectrometry
FDA	Food and drug administration
Fe(III)PPIX	Ferriprotoporphyrin IX
FTIR	Fourier transform Infra-red
GSH	Glutathione
Hm	Haem
HETCOR	Heteronuclear correlation (HETCOR) spectroscopy
HIV	Human immunodeficiency virus
HMBC	Heteronuclear multiple bond correlation, experiment gives correlations between carbons and protons that are separated by two, three, and, sometimes in conjugated systems, four bonds.
HMPA	Hexamethyl phosphoramide
HMQC	Heteronuclear multiple quantum coherence, a ^{13}C spectrum is displayed on one axis and a ^{1}H spectrum is displayed on the other axis. Cross-peaks show which proton is attached to which carbon. COSY spectra show 3-bond coupling (from H-C-C-H)
^{1}HNMR	Proton nuclear magnetic resonance is the application of nuclear magnetic resonance in NMR spectroscopy with respect to hydrogen-1 nuclei within the molecules of a substance, in order to determine the structure of its molecules.
HPLCMS	High performance liquid chromatography spectroscopy mass spectrometry
HRESMS	High resolution electro spray mass spectrometry
HTS	High throughput screen
IC_{50}	Concentration inhibiting response by 50%
IQ	Isoquine
IG	Interessen Gemeinschaft

INS	International numbering system for food additives
Kd	Dissociation constant
LDH	Lactate dehydrogenase
MEP	Molecular electrostatic potential
MJF	Dr Martin J Frearson
MMV	Medicines for malaria venture
MRC	Medical research council
MS	Microwave synthesis
m.p.	Melting point
NADH	Nicotinamide adenine dinucleotide (H for hydrogen)
NCE	Novel chemical entity
NIMR	National institute for medical research
NMR	Nuclear magnetic resonance
P.	*Plasmodium*
PIHRESMS	Positive ion high resolution electrospray mass spectrometry
Pyr	Pyronaridine
Scd	Single crystal X-ray diffraction
SN	Survey number
Qn	Quinine
Qd	Quinidine
QSAR	Quantitative structure-activity relationships
RR	Resonance Raman
s.e.m	Standard error of the mean vs. standard deviation
S_NAr	Nucleophilic aromatic substitution
TB	Tuberculosis
TLC	Thin layer chromatography
UK	United Kingdom
USA	United states of America
WRAIR	Walter reed army institute of research
WHO	World health organisation

Abstract.

In recent years *Plasmodium falciparum* has become resistant to many clinically used antimalarial agents. This reinforces the need to develop Novel antimalarial drugs.

This study details the synthesis of improved antimalarials based on *bis*quinolines. The synthesised molecules were studied for their potential activity, both *in silico* and *in-vitro* and in an attempt to understand the structural determinants of their antimalarial activity. Further *in-vivo* studies were performed on a variety of quinoline based compounds to determine their possible mode/s of action, possibly associated with their interaction with haem and haem derived complexes.

The synthesis of various *bis*quinolines, and consequently, the development of an extra thermodynamic pharmacophore model that has allowed identification of a potent, soluble, orally bioavailable antimalarial *bis*quinoline, *meta*-quine (*N*,*N*-*bis*(7-chloroquinolin-4-yl)benzene-1,3-diamine) (dihydrochloride), which is active against *Plasmodium berghei in-vivo* (oral ID_{50} 25 μmol/kg) and multidrug-resistant *Plasmodium falciparum* K1 *in-vitro* (0.17 μM). *Meta*-quine shows strong affinity for the putative antimalarial receptor, haem at pH7.4 in aqueous DMSO.

In an effort to find compounds superior to *meta*-quine, the *de*-halogeno-amination/S_NAr Displacement reaction in *N*-methylpyrollidinone was used to construct both a fluorinated analogue of RO 47-7737, and an inactive 4-aminoquinoline/ mefloquine hybrid, and observed lack of antimalarial activity of this compound against *Plasmodium berghei* infection in mice. The latter Structure determined by X-ray crystallography, revealed hydrogen bonding to solvent (methanol).

The site and order of protonation of these quinolines was investigated using quantum mechanics calculations (Courtesy of Prof Drew, Reading University).

Results suggested that protonation was impeded at the endocyclic nitrogen in mefloquine due to electronic rather than steric factors and the molecule was protonated preferentially at the piperidine side chain in Mefloquine. In contrast, both *mono*- and *bis*-4-aminoquinolines were protonated at the endocyclic quinoline nitrogen. This suggested that trifluoromethyl groups buttressing the endocyclic quinolinyl nitrogen was detrimental to 4-aminoquinoline receptor binding, but not quinoline methanols; suggesting that these two classes of molecules act by different mechanisms/binding modes within the acidic vacuole of Plasmodia.

4-Hydroxy-1,5-naphthyridine (SN 13,639), a key intermediate in the production of certain azasubstituted antimalarials, is normally synthesised by a multistep route comprising cyclization, de-esterification and decarboxylation. An unexpected and direct formation of 4-hydroxy-1,5-naphthyridine by Gould-Jacob cyclization in refluxing diphenyl ether was found.

This occurred under microwave conditions, to produce ethyl 4-hydroxy-1,5-naphthyridine-3-carboxylate, which spontaneously underwent a rare retro-fries rearrangement to form 4-hydroxy-1,5-naphthyridine, which also identified the transition state involved. The product was unambiguously characterised by X-ray crystallography and 2D-NMR experiments. Various adducts and solvated forms were examined by DFT experiments.

An examination of the large downfield shifts observed for the molecule in TFA-*d* were rationalised by proposing protonation at N-5 accompanied by the formation of a novel hydrogen bonded complex with the solvent. Similar interactions may occur between naphthyridines and the acidic side chain of the haem receptor. Although antimalarial activity of 4-hydroxy-1,5-naphthyridine is weak against multi-drug resistant strains of *Plasmodia*, the compound allows rapid access to various known antimalarial naphthyridines and could act as fluorescent probe of drug action.

Pyronaridine (4-[(7-chloro-2-methoxybenzo[b][1,5]naphthyridin-10-yl)amino]-2,6-*bis*[(pyrrolidin-1-yl)methyl]phenol). The first European synthesis of pyronaridine 4-(7-Chloro-2-methoxy-benzo[b][1,5]naphthyridin-10-ylamino)-2,6-*bis*-pyrrolidin-1-ylmethyl-phenol (**15**), a potent antimalarial, from commercially available starting materials, namely 2,4-dichlorobenzoic acid and 2-methoxy-5- aminopyridine. The copper mediated Ullmann synthesis of 4-chloro-2-(methoxy-3-pyridylamino) benzoic acid in *n*-pentanol was accompanied by the formation of its pentyl ester complicating isolation and purification.

An alternative Ullmann-Goldberg procedure was developed using DMF, both successfully replaced the *n*-pentanol and also produced the pyridylamino-benzoic acid under anhydrous, oxygen free, conditions, in which cyclodehydration was followed by dehydrochlorination using anhydrous $POCl_3$, the desired product 7,10-dichloro-2-methoxy-benzo [b][1,5] naphthyridine was accompanied by an unexpected (and undesired) trichlorinated product in which the methoxy group had been displaced to form 2,7,10-trichloro-benzo [b][1,5] naphthyridine.

The trichlorinated molecule was the dominant product (>50%) if the reaction was continued beyond four hours as confirmed by GC-MS spectrometry. Subsequent S_NAr reaction whereby the halogen situated at the 10 position in 7,10-dichloro-2-methoxy-benzo [b][1,5] naphthyridine was displaced by *p*-aminophenol produced 4-(7-chloro-2-methoxy-benzo[b][1,5]naphthyridin-10-yl(amino)-phenol as a bright yellow solid, as opposed to a brown solid as reported by Zheng *et al.* (**1982**). The presence of oxygen during the reflux period proved detrimental and rapidly oxidized the material to various compounds including a red-brown product identified as the corresponding quinone-imine. The target substance was produced by refluxing the air sensitive 4-(2,7-dichloro-benzo [b][1,5] naphthyridin-10-ylamino)-phenol with excess pyrrolidine and aqueous formaldehyde (Mannich Reaction) under argon.

Pyronaridine was isolated as a moderately air sensitive free base using flash column chromatography on silica developed with methanol: ammonia (9:1, v/v under argon), and proved identical to an authentic sample when examined by a variety of analytical techniques (NMR, HRMS, HPLC-MS and TLC). The solid was, however, stable as the known yellow tetraphosphate salt. Hence, a superior, enhanced reliable synthetic procedure, but lower in overall yield (9-19%), when compared to the original method (33%) published in the Chinese language (Zheng *et al.* **1982**) has been developed. Our spectroscopic (NMR and accurate MS) confirms that the published structure coincides with the data presented herein. The biological activity of pyronaridine, pyracrine and the aromatic head group was determined *in-vivo*.

The side chain/head group was completely inactive at the doses tested whereas both pyracrine and pyronaridine were highly active against the *Plasmodium berghei* drug sensitive strain N/13/1A/4/20 and are suitable for further development.

Index of contents chapters.

Chapter 1

Haemoglobin and drug interaction.

Index of contents chapter 1.

Figure of contents chapter 1.

Table of contents chapter 1.

Aim.

Familiarise the reader with antimalarial drugs and antimalarial drug receptor complex for 4-aminoquinolines and related compound.

1. Introduction: clinical aspects of malaria.

Half of the world's population involving roughly 3.3 billion people, are at risk of contracting malaria. According to the latest estimates (**2020**), there were approximately 241 million cases of Malaria infection and an incredible 627,000 deaths in 2020 (World Health Organisation, **2022**). *Plasmodium falciparum* is the most prevalent malaria parasite in the WHO African Region, accounting for 96% of estimated malaria cases in 2020, as well as in the WHO South-East Asia Region (50%), the WHO Eastern Mediterranean Region (71%) and the WHO Western Pacific Region (65%). Children aged under 5 years are the most vulnerable group affected by malaria. In 2020, they accounted for 80% (500,000) of all malaria deaths worldwide (World Health Organisation, **2022**).

Consequently, it is estimated that a person dies every 50 seconds (World Health Organisation, **2022**). The prevalence of this disease is increasing globally with over 40-45% of the world's population estimated to be currently at risk (Ziegler *et al*., **2001**) and it is more than likely that climate change and Covid-19 will lead to an increase in infections.

Table 1-1. Specific risk groups amongst the population worldwide (WHO, 2022).

Young children	Children living in stable transmission areas that have not yet developed protective immunity against the most severe forms of the disease. Young children constitute the bulk of malaria deaths worldwide.
Non-immune pregnant women	Non-immune pregnant women are at risk since malaria causes high rates of miscarriage (up to 60% in *P. falciparum* infection) and maternal death rates of 10–50%.
Semi-immune pregnant women	Affects pregnant women predominantly living in areas of high disease transmission. Malaria can result in miscarriage and low birth weight, especially during the first and second pregnancies. An estimated 200,000 infants die annually as a result of malaria infection during pregnancy.
Semi-immune HIV-infected pregnant women	Women in stable transmission areas are at increased risk of malaria during all pregnancies. Also, women with the malaria infection of the placenta have a higher risk of passing HIV infection onto to their new-born offspring.
People with HIV/AIDS/TB	Dramatic increase in the risk of malaria disease when infected by either HIV or TB or both
International travellers from non-endemic areas	These groups are at high risk of malaria and its consequences because they lack immunity.
Immigrants from endemic areas and their children	Such transient populations living in non-endemic areas and returning to their home countries to visit friends and relatives are similarly at risk because of waning or absent immunity.

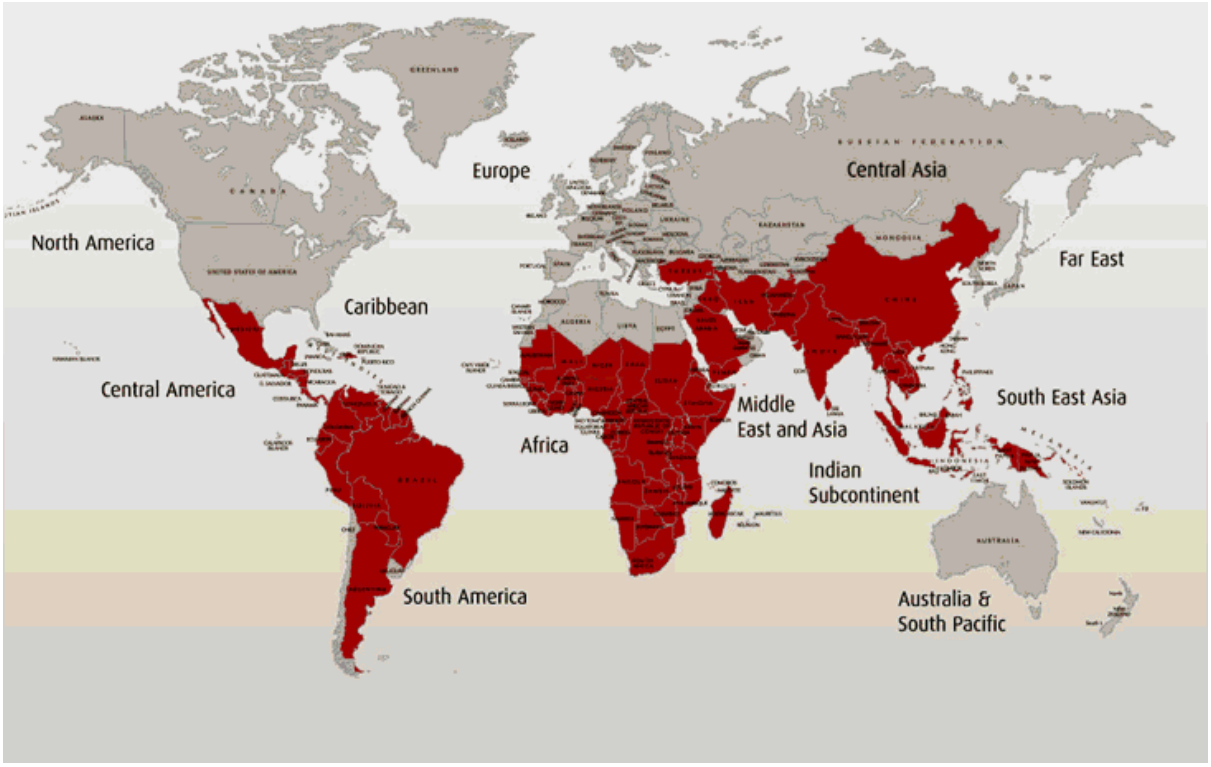

Figure 1.1. A depiction of high-risk malaria hotspots worldwide.

The efficacy of clinically used anti-malarial drugs available is limited, due to problems of toxicity, resistance and cost. The emergence of persistent parasite resistance since the 1960s, especially in *P. falciparum* strains, one of four (perhaps five) species infecting man, has been a major contributor to the global resurgence of malaria in the last three decades (Marsh, **1998**).

Emergence of drug resistant strains as well as increased reporting and diagnosis has resulted in a doubling of malaria-attributable child mortality in Eastern and Southern Africa (Korenromp *et al*., **2003**). Elucidation of the *P. falciparum* genome sequence (Gardner *et al*., **2002**), affords opportunities for understanding *Plasmodium* biochemistry, interaction with the human host thereby assisting drug and possibly, vaccine development (Figure 1.1). There is a pressing need to synthesize novel antimalarials, due to limitations on supplies of naturally occurring antimalarials, coupled with the increased resistance to antimalarials in common use (Ismail *et al*., **1996**). Consequently, the design and synthesis of novel, safe and affordable therapies to treat the disease are needed.

1.1. What is malaria?

Malaria is a complex mosquito-borne infectious disease caused by a diverse group of eukaryotic microorganisms of the genus of Apicomplexan parasites. Four species of the *Plasmodium* parasite can infect humans directly, these being (*P*. for *Plasmodium*) *P. vivax, P. ovale* and *P. malariae*, with *P. falciparum* being the most serious form of the disease.

The fifth species, known as *Plasmodium knowlesi*, is a zoonosis that causes malaria in macaques, a type of monkey, and which can also infect humans (Singh *et al*, **2004**). Malaria is generally confined to tropical and subtropical areas (Martin *et al*., **2007**). However, due to climate change, malaria may become endemic both to mainland Europe as well as the United Kingdom (Jane *et al*., **2008**).

1.1.1. The malaria life cycle.

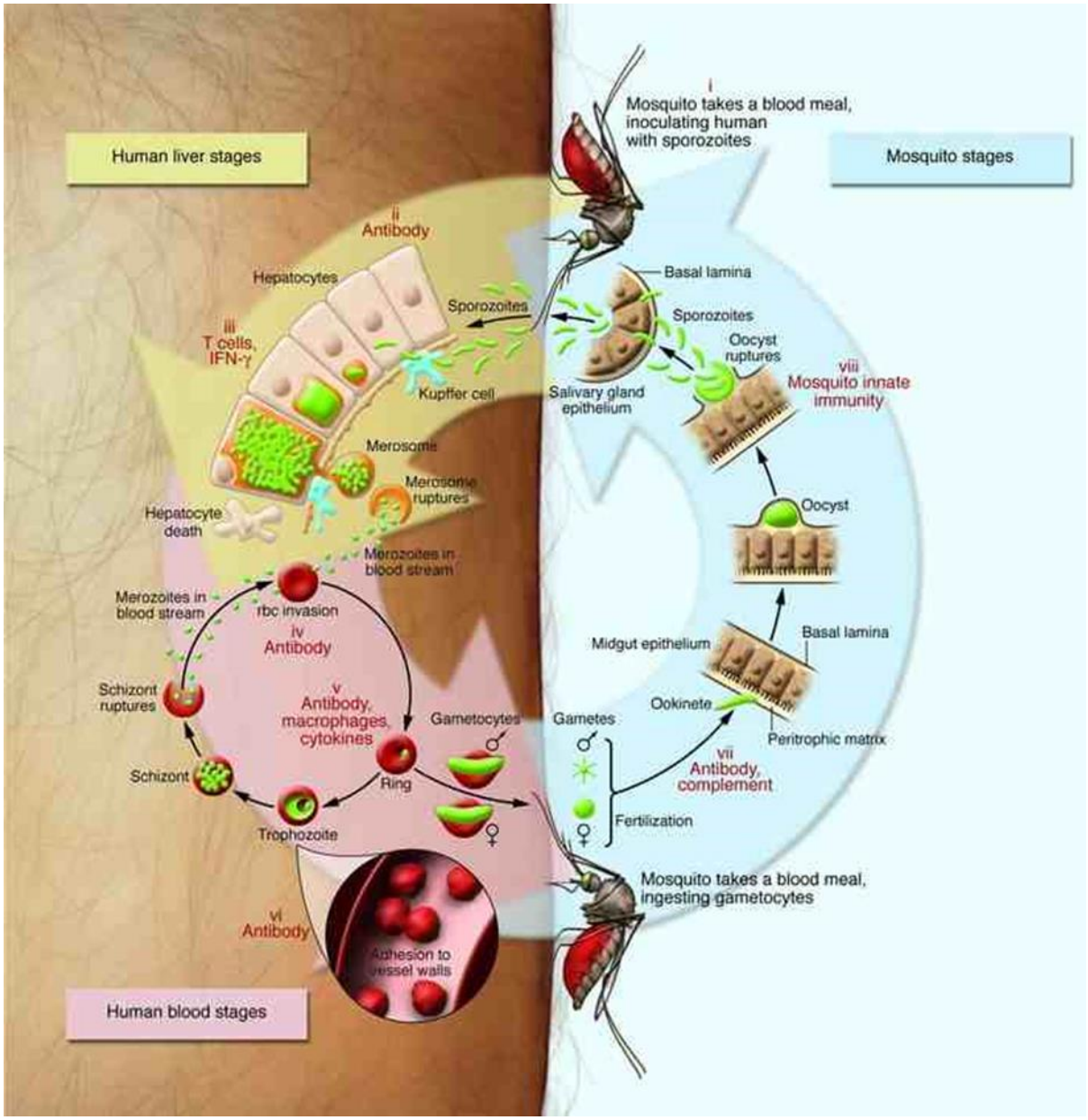

Figure 1.2. The life cycle of the malaria parasite (Greenwood *et al*., 2008).

The parasite develops within the female mosquito, and eventually mix with the mosquito's saliva (i.e. sporozoites), and are injected into the host once bitten, after which they migrate to the host liver. This hepatic system infection is known as the exoerythrocytic phase. After a period lasting between two weeks to several months, and occasionally years of

occupying the human hosts liver cells (hepatocytes), develop into merozoites (Figure 1.2). The liver cells rupture, with the merozoites wrapping themselves around hepatocytes, the cell membrane of the infected host liver cell (Stern *et al*., **2008**). This allows merozoites to escape, undetected by the host, into the bloodstream entering the so called erythrocytic phase, they asexually develop into merozoites (Bledsoe, **2005**).

Then their host, the liver cells, ruptures, whilst wrapping itself in the cell membrane of the infected host liver cell (Stern *et al*., **2008**). This allows merozoites to escape undetected by the host into the bloodstream entering the so called erythrocytic phase (Bledsoe, **2005**).

Once freed of a cellular environment, merozoites rapidly swim as flagellates to red blood cells, invading, and then multiplying asexually into ring forms, trophozoites and schizonts. The mechanics of parasitic invasion are still poorly understood (Koch & Baum, **2016**). The parasite, resides in this haemoglobin rich environment.

Within the blood trophozoites produce replicates to form new merozoites, causing anaemia. The resulting light-headedness, shortness of breath and tachycardia is accompanied by fever, chills, nausea and a flu-like illness caused by cytokine release (Holding, **2001**).

Waves of fever (paroxysms) have been known in both ancient Greek and Hindu civilizations, which coincide with the simultaneous escape of merozoites from hepatic cells which infect new red blood cells. The periodicity between attacks of fever can be used to diagnose which *Plasmodial* strain is present and, consequently, which therapy to administer. Sexual forms, called gametocytes, are also produced which can infect a mosquito after piercing the skin of an infect human host, thus continuing the life cycle of the malaria parasite (Figure 1.3).

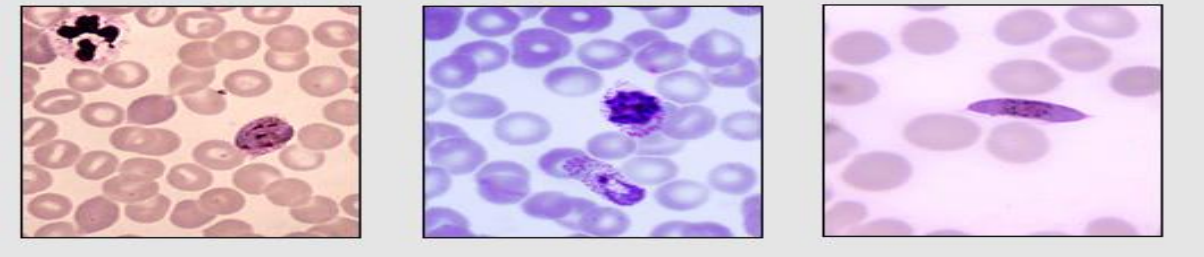

Figure 1.3. Left to right: infected host hepatocytes, are released from ruptured schizont, and consequently lead to further infection of nearby red blood cells. It is this release of merozoites into the bloodstream which causes the trademark malaria disease. (Garcia, 2010).

1.1.2. Novel drug targets.

The search for novel drug targets within *Plasmodia* may be achieved through functional proteomics and genomics allowing rational, structure based, drug design of NCEs (novel chemical entities) (Cowman *et al*., **2012**; Dascombe *et al*., **2005**). An additional tool, combinatorial chemistry in its myriad forms, allows construction of large libraries of compounds suitable for high throughput screening (HTS). Acceleration of the antimalarial

drug discovery process is currently limited, in part, by the expense of maintaining cultured parasites, the reliable availability of fresh disease free, human blood, and the lack of cheap automated equipment. In contrast, although animal models are considered expensive, they remain the only effective tool for monitoring efficacy *in-vivo*, whilst simultaneously monitoring toxicity at an early stage of the drug discovery process. This approach allows for the early rejection of toxic prototypes, thus decreasing the chances of developing inappropriate NCEs.

Potential drug targets within *Plasmodia* can be sorted into four categories targeting:

1) processes occurring within the digestive vacuole (Warhurst, **2001**),
2) enzymes involved in metabolite and macromolecular synthesis (Coombs *et al*., **2001**),
3) membrane processes (Calas, **2000**),
4) cell signalling (Harmse, **2001**).

1.2. A brief historical review of clinically useful antimalarials.

1.2.1. Quinoline.

Quinoline has been used for the production of a precursor in the synthesis of various antimalarials including the 8-aminoquinolines (such as primaquine (**6**) and pamaquine (**7**)) and 4-aminoquinolines (like such as chloroquine (**1**) (Figure 1.4) and or amodiaquine (**9**)) (Dascombe *et al*., **2007**). It has been suggested that compounds with a bulky *bisquinoline* structure may be less efficiently removed by chloroquine-resistant *Plasmodia*, therefore enabling them to maintain anti-malarial activity (O'Neil *et al*., **1998**).

Pamaquine (**7**), commonly used in conjunction with quinine (**2**) (Figure 1.4)helps to prevent relapses by effecting malarial hypnozoites. This combination has also shown its efficacy towards the erythrocytic stages of all four human malarias. Pamaquine (**7**) when used as a prophylactic agent against malarial parasites lacked effectiveness.

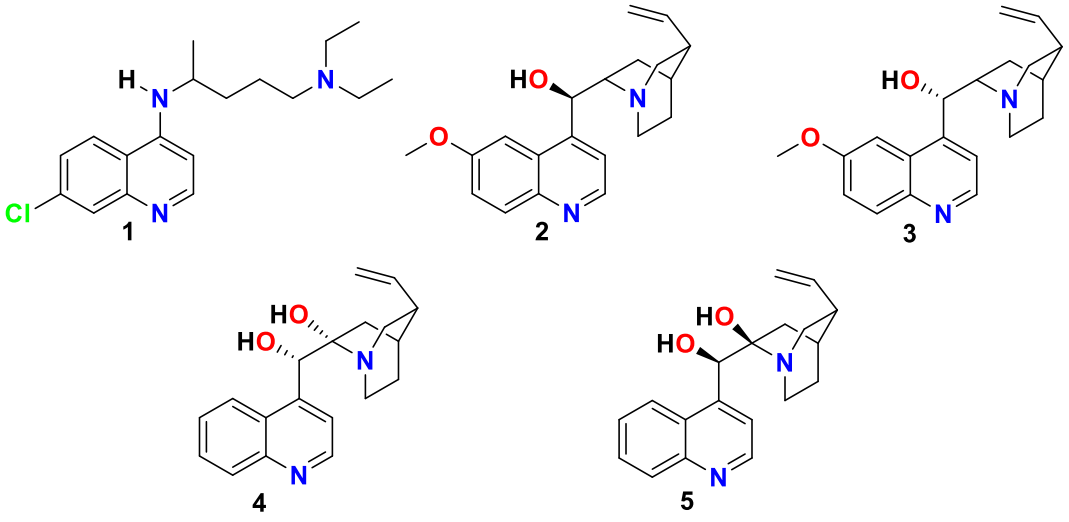

Figure 1.4. chloroquine (**1**), quinine (**2**), quinidine (**3**), cinchonine (**4**), cinchonidine (**5**).

Its high toxicity in humans subsequently led to the development of the successful casual prophylactic, primaquine (**6**).

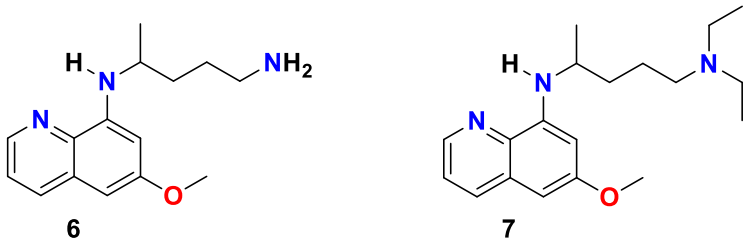

6 **7**

Figure 1.5. Primaquine (**6**), pamaquine (**7**).

Primaquine (**6**) (Figure 1.5) became the drug of choice for anti-relapse therapy especially against *P. vivax* and *P.ovale* where it acts on the hypnozoite stage (Wolfe. **1997**). Primaquine (**6**) also acts as a gametocytocidal agent (Chavalitshewinkoon-Petmitr *et al*., **2000**).

1.2.2. Quinine.

Quinine (**2**) is an extensively used alkaloid by many inhabitants of Peru before it was brought to Europe in 1600, and eventually isolated from the bark of the native cinchona tree by Joseph-Bienaime Caventou and Pierre-Joseph Pelletier in 1820 (Gringauz, **1997**). Quinine (**2**) acts by interfering with the exoerythrocytic stage of the parasite's life cycle, as a blood schizonticidal and gametocide against *Plasmodium vivax* and *Plasmodium malariae*.

Its effects are mediated towards the inhibition of haemozoin crystallisation within the food vacuoles. The drug was further developed during World War II, although due to its complicated structure, it proved very expensive to synthesise. Quinine (**2**) has been rendered largely obsolete by the introduction of improved antimalarials i.e. chloroquine (**1**), which display greater efficacy. Its mechanism of action is believed to be inhibition of haem detoxification by forming a covalent adduct (De Villiers *et al*., **2008**). The secondary alcohol coordinates centrally to the iron atom allowing the endocyclic nitrogen to interact with the carboxylic acid of the haem.

Before the development of malarial resistance, chloroquine (**1**) was the most widely used anti-malarial in the world. Chloroquine (**1**) was first synthesised in Germany in 1934 during the antimalarial drug discovery effort following World War I by Hans Andersag at Bayer I.G. Farbenindustrie. Testing at Bayer mistakenly showed that chloroquine (**1**) toxicity made it unsuitable as a chemotherapeutic drug. Subsequent work on the compound by the British and the United States Armies during World War II showed that the initial toxicity testing was incorrect and chloroquine (**1**) was, in fact, a very promising antimalarial (Slater *et al*., **2009**).

However, the drug was not produced on a commercial scale until after WWII when chloroquine (**1**) replaced quinine (**2**) as the first line of treatment for malaria due to its low cost, straightforward synthesis and low toxicity (Slater *et al*., **1993**). The antimalarial mode of action is commonly known to occur within food vacuoles of the parasite, most probably

against haem, the action towards inhibiting the biosynthesis of *Plasmodium* nucleic acids by the formation of complexes with haem or DNA is now considered incorrect.

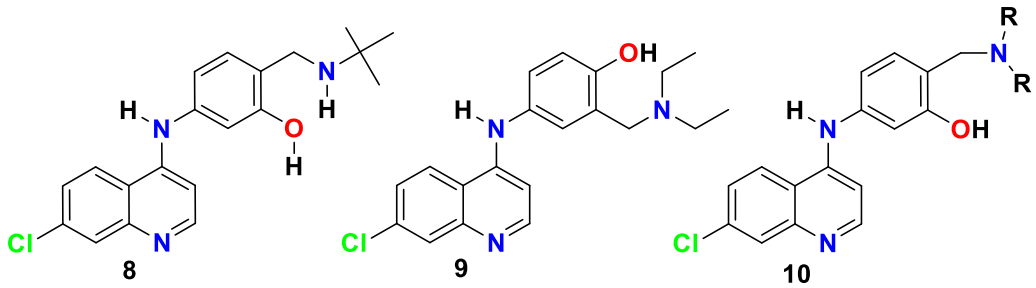

Figure 1.6. *N*-tert-butyl isoquine (GSK369796) (**8**) amodiaquine (SN10751) (**9**) SN-13,730 (**10**) (Bhattacharya *et al*., 2009).

The drug has activity against both gametocytes and schizonts (not resistant strains) of *P. vivax, P. malariae, P. ovale* as well as the immature gametocytes of *P. falciparum*, an assumption contradicted by Wolff *et al*. Amodiaquine (**9**) (Figure 1.6) was first synthesised in 1948 (Wislogle Burckhalter *et al*., **1948**) and improved by an alternative route in 1950 (Burckhalter *et al*., **1950**). The drug is a fast-acting blood schizonticide (Wolff *et al*., **1997**). In 1980s, it was demonstrated that amodiaquine (**9**) was effective against both chloroquine-resistant and chloroquine-sensitive strains of *P. falciparum* (Watkins *et al*., **1984**). It is also cheap to synthesise, making the drug commercially viable. Its use was hindered by unforeseen side effects i.e. hepatic toxicity and agranulocytosis, caused by the oxidation of the amine head group subsequently producing toxic semi quinone-imine free radicals or a quinone-imine. Production of such intermediates allows irreversible binding to proteins, especially in the liver (Jewell *et a1*., **1995**) and may induce immunotoxicity.

Heterocycles with aliphatic side chains were first developed by researchers at IG Farben due to the presence of this privileged ring system within the prototypical antimalarial investigations using quinine (**2**) (Figure 1.4). They focused on aryl bridged quinolines of the amodiaquine (**9**) class originally developed by Burckhalter at Parke Davis (Burckhalter *et al*., **1950**). This class of drug is most widely used for the treatment of erythrocytic *Plasmodial* infections (Bray *et al*., **1996**). Interestingly, the original report that disclosed amodiaquine (then called camoquine) also tabulated the synthesis of the reversed isomer now dubbed isoquine (**10**) (Figure 1.6).

The compendium by Wiselogle detailed all of the antimalarial data from the American war effort on discovering clinically useful battlefield antimalarials (Wiselogle, **1946**; Burckhalter *et al*., **1948**). Subsequently, Barlin *et al* (Barlin & Yan, **1989**; Barlin *et al*., **1992**). Eventually O'Neil *et al* worked on these *meta*–amino phenol antimalarials (O'Neil *et al*., **2008**).

1.2.3. Quinacrine.

Quinacrine (**11**) (Figure 1.7), an acridine (**12**) (Figure 1.7) synthesised in 1931 at Bayer,

Germany, was one of the first synthetic substitutes for quinine (Figure 1.4), which due to

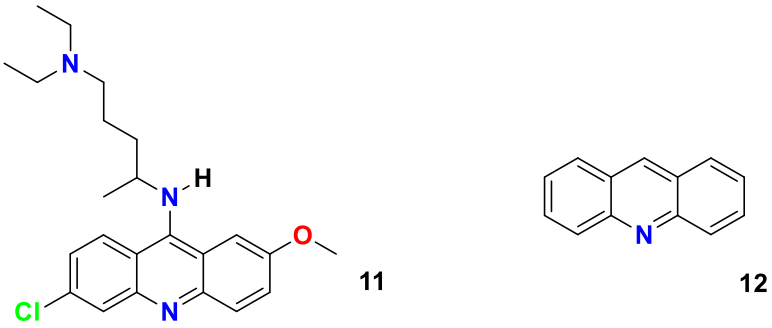

Figure 1.7. Quinacrine (**11**) acridine ring (**12**).

the outbreak of the World War II was in short supply. The drug is an exoerythrocytic schizonticide, similar to quinine, with the ability to control symptoms of *P. vivax*. For a limited number of susceptible individuals, this antiprotozoal has side effects including jaundice and toxic psychosis, possibly causing permanent damage (Gringauz *et al*., **1997**) thus limiting its use. The main problem associated with its use was noncompliance due to it staining the skin yellow. These reasons prompted its substitution for the improved chloroquine, which were used by allied forces during the later stages of World War II.

1.2.4. Mefloquine.

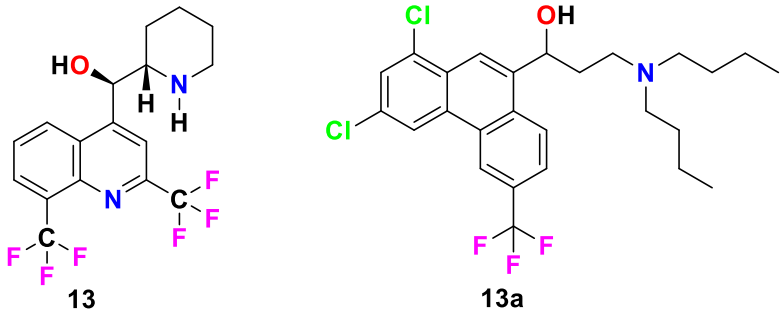

Figure 1.8. Mefloquine (**13**) halofantrine (**13a**)

Mefloquine (**13**) (Figure 1.8) was developed in the 1970s during the Vietnam conflict at the Walter Reed Army Institute of Research (WRAIR), as a synthetic analogue of quinine (**2**) (Figure 1.4). The drug was developed in order to protect American troops abroad in tropical high-risk malaria areas, to help protect against multi-drug resistant strains of *P. falciparum*. The mode of action is focused towards the food vacuole, and acts by interfering with the intraerythrocytic stages of the parasite's life cycle, but has no effect on mature gametocytes (Wolfe *et al*., **1997**).

Mefloquine (**13**) (Figure 1.8) probably has the same mechanism of action as disclosed for halofantrine (**13a**) (De Villiers *et al*., **2008**), and targets haem by axial coordination. It is used for prophylaxis during acute therapy, is effective against all malaria strains capable of infecting humans, and is renowned for its long half-life.

Due to presence of trifluoromethyl (CF_3) group at position 2, which prevents oxidative metabolism causing the drug to have half-life of 15 days (Gringauz *et al*., **1997**). This promotes the opportunity for clearing drug sensitive strains but also encourages resistant strains to develop (Wolfe *et al*., **1997**). The American society of tropical medicine and hygiene reported on 44 U.S. Marines who contracted *P. falciparum* whilst dosed on prescribed mefloquine (**13**) when deployed in Liberia in 2003 (Whitman *et al*., **2010**).

1.2.5. Methylene blue.

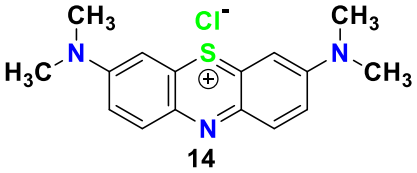

14

Figure 1.9. Methylene blue (**14**)

Methylene blue (**14**) (Figure 1.9) was discovered in 1891 by Paul Ehrlich as a successful treatment for malaria. Experiments have shown it (and some of its analogues) to be highly effective antimalarial against certain strains of *Plasmodia*. All compounds tested suppressed the growth of *P. Vinckei Petteri in-vivo* with IC_{50} in the 1.2-5.2 mg/kg range, and Methylene blue (**14**) and azure Blue (a synthetic structural analogue of methylene blue) suppressed *P. yoelii* nigeriensis in the 9-11 mg/kg range (Atamna *et al*., **1996**). The drug was used throughout the pacific war during World War II, although lost popularity amongst the troops and faded out due to its disliked side effects i.e. green urine and the ability to turn the sclera (whites of the eyes) blue. However, because it is cheap, its use as an antimalarial has been revived (Schirmer *et al*., **2011**). Methylene blue (**14**) (Figure 1.9) has been trialled in combination with chloroquine (**1**), results have proved promising (Meissner *et al*., **2019**), as well as antiviral activity against covid-19 (Buckwald *et al*., **2021**).

Haynes *et al*., (**2011**) have suggested a unified redox theory of antimalarial drug action which may explain in part how these phenazines kill parasites.

1.2.6. Pyronaridine.

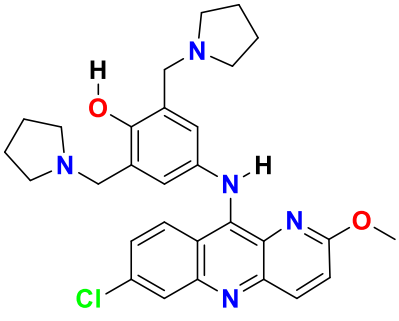

15

Figure 1.10. Pyronaridine (**15**).

Pyronaridine (**15**) (Figure 1.10) was first synthesised in 1970s at the Institute of Parasitic

diseases in Shanghai, China (Chen & Zheng., **1992**) and has been in clinical use in China since the 1980's (Chang *et al*., **1992**). Pyronaridine targets the erythrocytic stage, and the ability of Pyronaridine (**15**) to hold both schizontocidal and gametocytocidal actions is a very useful and attractive capability, whilst at the time, primaquine (**6**) was the only known gametocytocidal on the market (Chavalitshewinkoon-Petmitr *et al*., **2000**).

Also, studies prove that pyronaridine (Figure 1.10) acts effectively against chloroquine-resistant and sensitive strains of *P. falciparum*, displaying less toxicity than chloroquine (**1**) (Chen & Zheng., **1992**; Croft *et al*., **2012**). Its discovery and development have been extensively reviewed by Dascombe *et al*., **2007**.

1.2.7. Importance of hydrogen bonding in drug interaction at receptor sites.

Pharmacodynamics is study of the biochemical and physiological effects of drugs (especially pharmaceutical drugs). The effects can include those manifested within animals (including humans), microorganisms, or combinations of organisms (for example, infection). The effect of the organism on the drug (or xenobiotic) is collectively referred to as pharmacokinetics (ADME; absorption, distribution metabolism and elimination).

Pharmacodynamics and pharmacokinetics are the main branches of pharmacology, being itself, a topic of biology interested in the study of the interactions between both endogenous and exogenous chemical substances with living organisms. Pharmacodynamics is the study of how a drug affects an organism, whereas pharmacokinetics is the study of how the organism affects the drug. Pharmacodynamics relates to the study of the action of drugs upon an organism (usually at a receptor). Drug action at receptors includes enzymes, ion channels, transporter proteins, RNA, DNA, RNAase and membranes (for anaesthetic action) and usually involve two types of drugs which are either agonists or antagonist. Agonists stimulate and often activate the receptor. Antagonists compete with agonists and prevent them from activating the receptors. Ion channels act on enzymes or transporter proteins. Stimulation of receptors more often than not leads to an amplification of response, inducing an alteration of cellular and physiological processes, a release of hormones, etc.

Drugs interact at receptors by bonding at specific binding sites. Since most receptors are composed of proteins, the drug's interaction with specific amino acids causes conformational changes within the proteins. The strongest interactions are those involving ionic bonds, which vary with the reciprocal of the distance squared between interacting sites (Foreman *et al*., **2010**). When a dissociative event occurs upon binding (e.g. between a basic drug and a carboxyl group on an amino acid side chain), Cation π-interactions can fall within this category, for instance when a cation, e.g. acetylcholine, interacts with the negative π bonding cloud upon an aromatic group buried within its receptor (Zhong *et al*., **1998**). Ion-dipole and dipole-dipole bonds have similar interactions, but are more complex in nature and are weaker than ionic bonds. Receptors can also act by binding to drugs via hydrogen bonding, which

will be discussed in detail.

1.2.8. Hydrogen bonding in receptors.

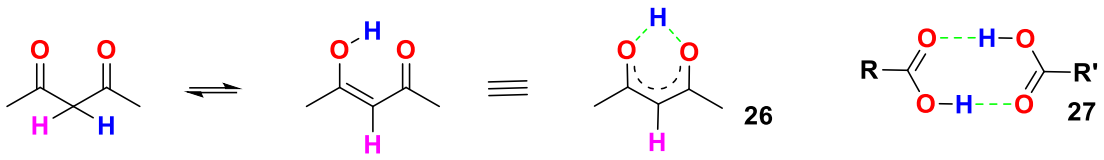

Figure 1.11. Pentane-2,4-dione tautomerises to 4-hydroxypent-3-en-2-one Carboxylic acids often form dimers in the gas phase and in solution (depending on the concentrations) and in the solid state as found in x-ray crystallography databases (green lines) (Vishweshwar *et al*., 2002; Mirzaei *et al*., 2020).

A hydrogen bond is an electromagnetic attractive interaction between polar molecules where a hydrogen atom is bonded with a select range of electronegative atoms which include nitrogen, oxygen and halogens (especially fluorine).

The hydrogen must be covalently bonded to another electronegative atom to create a hydrogen bond (Figure 1.11). The Nature of the Chemical Bond, Linus Pauling (first published **1939**) credits Moore and Winmill with the first printed description of the hydrogen bond concept (Moore *et al*., **1912**; Weinhold & Kein, **2014**). These bonds can arise intermolecularly between sets of molecules or intramolecularly i.e. within different parts of a single molecule, for instance, pentane-2,4-dione (acetylacetone), in which hydrogen bonding assists stabilisation of the enolic tautomer.

The 3-D shape of a drug modulates its effects upon a receptor and each potential conformer can interact to varying extents and this modulates the potency of each drug.

1.2.9. Potency.

Potency is a measure of how much of a drug is required in order to produce a desired effect. Consequently, only a small dosage of a high potency drug is required to induce a large response in an organism. ‘Intrinsic activity’ is defined as full for agonists possessing intrinsic activity = 1 whereas antagonists possess an intrinsic activity = 0, therefore, a partial agonist lies between these two values. Notably, intrinsic efficacy also quantifies the various activated state(s) of receptors as well as the ability of a drug to induce maximum response without occupying and or binding to all of the receptors.

1.3. Drug specificity.

In order to afford specific, desired interactions and minimise interactions at other unwanted sites, a knowledge of the binding arrangement between the drug and its receptor is essential. For instance, the endogenous drug acetylcholine (ACh) within the parasympathetic nervous system activates muscarinic receptors but in the neuromuscular system it activates nicotinic receptors. Since the compounds muscarine and nicotine can each preferentially interact at one of two receptor types, this allows them to preferentially activate only one of the two systems, whereas ACh itself can activate both.

The affinity of a drug quantifies how "tightly" a drug binds to the receptor. Weak binding results in a limited duration of action (measured numerically by a dissociation constant K_D). The magnitude of K_D equates to the concentration of drug at 50% receptor occupancy. Specifically: K_D = [Drug][Receptor]/[Complex]

This value is modulated by conformational effects, type of bonding involved between drug and receptor, as well as the shape and volume of the drug. In general, the higher the values of KD, the lower the affinity of the drug to that specific receptor.

1.3.1. Food vacuole redox metabolism.

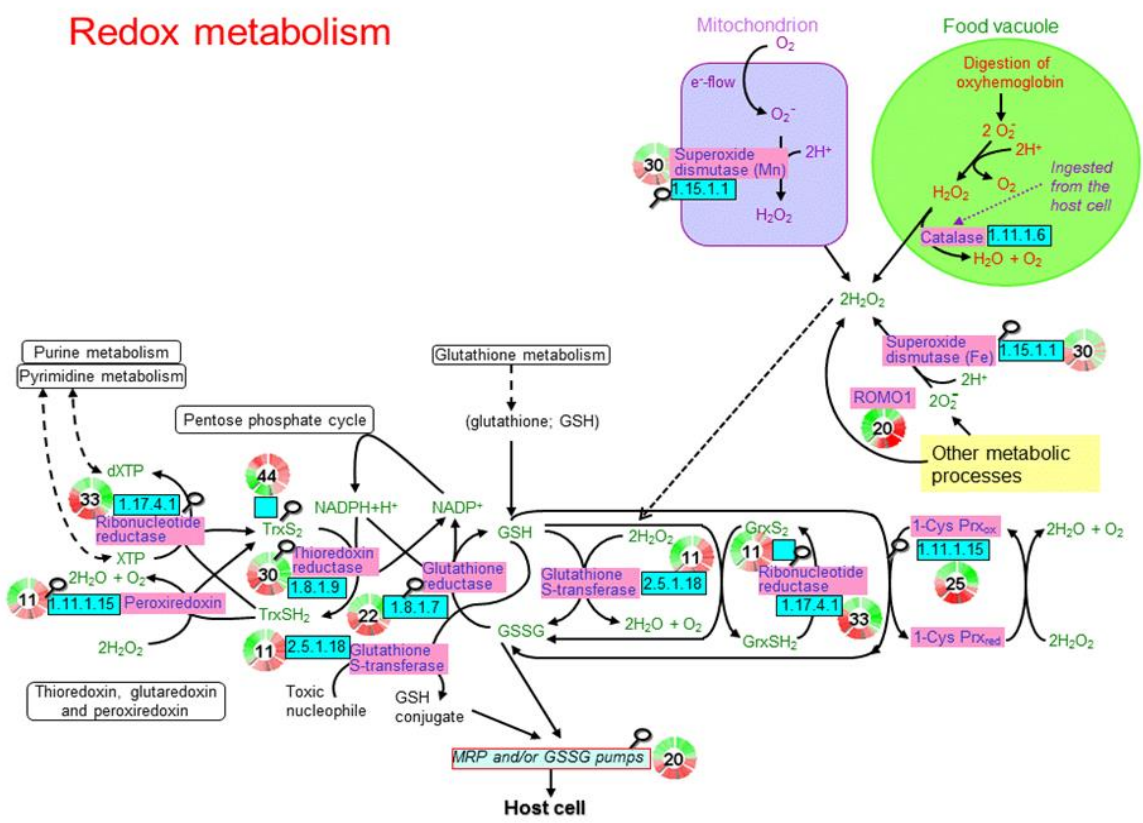

Figure 1.12. Redox within the parasite food vacuole(http://mpmp.huji.ac.il/maps/redoxmetpath.html).

The amino acids produced from the degraded globin are used as building blocks for the parasite's own metabolism (Choi *et al*., **1999**). Conversely, four molecules of non-protein bound 'free Haem' (ferrous-protoporphyrin IX, Fe(II)PP(IX)) are concurrently released from each molecule of haemoglobin, each of which is highly redox active and therefore cytotoxic by generating Reactive oxygen species (ROS•) which disrupt cell membranes.

Free haem is toxic to the parasite and the unavailability of haem parasite oxygenase suggests that haem cannot undergo detoxification through catabolism. Accumulation of free haem (up to 400μm) is lethal to the parasite, causing disruption to metabolic functions by generating free radicals, peroxidation of membranes, inhibition of enzymes and disruption of DNA synthesis and associated processes (Ziegler *et al*., **2001**).

However, this is not an infinite chain but consists of ferric iron of one haem coordinated to the propionate carboxylate group of an adjacent haem (Choi *et al*., **1999**). The model suggested by Fitch and Kanjananggulpan (**1987**), has been supplanted by a new model by pagola (Pagola *et al*., **2000**).

Solution of a high resolution powder X-ray diffraction pattern (Figure 1.13) using synchrotron radiation reveals a hydrogen bonded network of haem dimers linked by reciprocating propionate carboxylate side chains co-ordinating to the Fe(III) from the propionate side chains of each porphyrin, and to the iron(III) co-ordination centre of the next porphyrin. The model has been further refined by Klonis (Klonis *et al*., **2010**) (Figure 1.13).

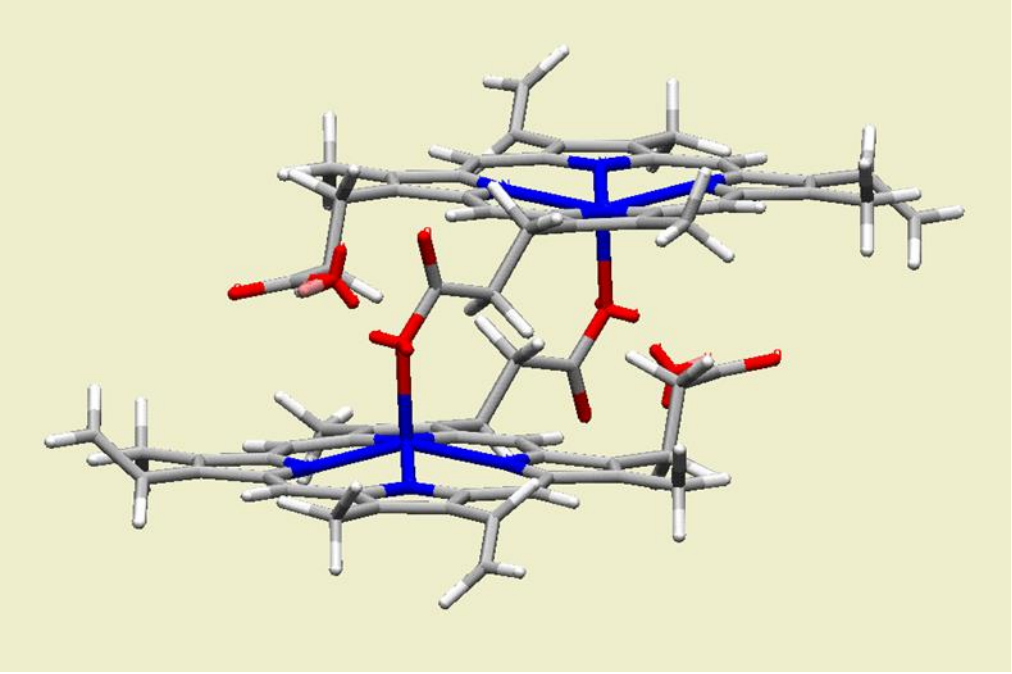

Figure 1.13. X-ray model reciprocally bonded (*in Silico*) depicts the reciprocal coordination bonds between the central iron (Fe) atom of one unit of haem with the propionate oxygen side chains of another unit of haem, resulting in biomineralisation. The dimers are consequently hydrogen bonded at right angles to the mean porphyrin plane (Klonis *et al*., 2010).

Classic antimalarials such as chloroquine (**1**) are currently believed to target processes

occurring within the parasite digestive vacuole including *haemoglobin* catabolism (Egan and Marques, **1999**). During this trophozoite stage, host *haemoglobin* is catabolised to amino acids for the *de novo* parasite protein synthesis. Recently, lipid nanospheres have been suggested to aid this process and certain amino acids may also be required to aid the biomineralisation (Egan *et al*., **2008**; Coronado *et al*., **2014**).

The currently accepted mechanism of action of quinoline antimalarials is through inhibition of haemozoin formation (Egan and Marques, **1999**). The quinoline ring of these antimalarials is an essential feature of many existing drugs. Essential elements of a quinoline pharmacophore have been proposed by Ismail *et al* (**1996**, **1998**) and by Egan *et al* (**2000**). Ridley & Hudson (**1998**) suggested that this pharmacophore was consistent with haem. Subsequently, Dascombe *et al* (**2005**) showed that *bis*quinoline compounds such as *meta*-quine did indeed interact with haem (See chapter 3).

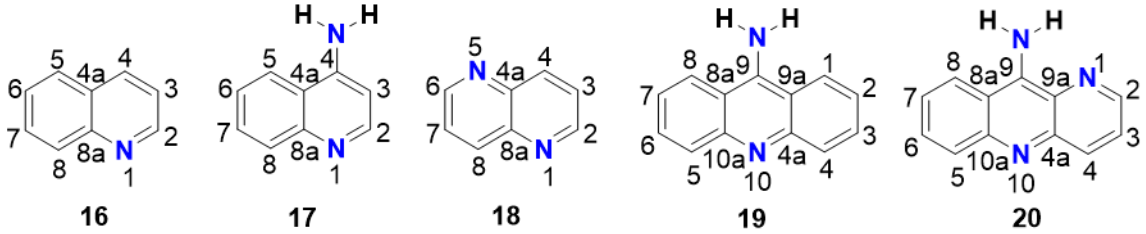

Figure 1.14. Numbering system adopted in this study for various heterocycles.

Both 4-aminoquinolines and 9-aminoacridines can target haem biomineralisation, and is essential for parasite survival, unique to the parasite, these compounds will remain important as chemotherapeutic agents for the foreseeable future (Ziegler *et al*., **2001**), The various numbering systems adopted in this study are demonstrated above (Figure 1.14).

A variety of different assays are available to investigate the inhibition of haemozoin formation, differing primarily in reaction conditions; the spectroscopic methodologies; and the aggregation templates used, include:

a) parasitic extracts;
b) parasite-derived or synthetic haemozoin;
c) histidine rich proteins, and/or;
d) various lipids.

X-ray diffraction techniques by (Bohle *et al*., **1996**; Bohle & dodd. **2014**) demonstrated that haemozoin was identical to β-haematin, and was not the result of extraction or purification artefact.

Consequently, haem aggregation activity of antimalarials *in-vitro*, by methodologies for the preparation of synthetic β-haematin is considered reasonable. However, the use of conventional spectroscopic methods for such studies are ineffective under the acidic conditions required for the reaction, since the starting material and product are insoluble at the concentrations used (Egan *et al*., **1997**). This process was followed at vacuolar pH using

positive-ion electrospray mass spectrometry (Ismail *et al*., **2009**).

The *in-vitro* chemical synthesised *β*–haematin (Egan *et al*., **1994**), enabled the effects of antimalarials on *β*-haematin formation to be assessed by Fourier transform infrared spectroscopy (FTIR)(Egan *et al*., **1994**), thereby demonstrating a direct relationship between intra-erythrocytic antimalarial activity and inhibition of spontaneous *β*-haematin formation, suggesting that the binding of drug to haem at low pH was the underlying mechanism of drug action. However, this was challenged by Pandya (Pandya *et al*., **2001**), who suggested that the product previously accepted to be *β*-haematin was instead a haem-acetate complex, and expressed concerns about extrapolating biologically relevant results from experiments with such high, non-physiological, concentrations of acetate. In response, (Egan and Marques, **1999**) admirably validated their assay system demonstrating both through FTIR spectroscopy and X-ray powder diffraction that the assay products were identical to those produced by other synthetic methods. Also, there was no evidence of a haem-acetate complex, even in 11.4 M acetate solution. Although the acetate in this system catalyses the formation of synthetic *β*-haematin, it does so by acting as a phase transfer catalyst, increasing the solubility of haematin, which is the rate limiting factor. Novel substances structurally distinct from existing drugs have been identified that target haem catabolism by using an HTS screen based on haem biomineralisation (Sandlin *et al*., **2014**), suggesting that drugs unrelated and therefore not cross resistant with chloroquine (**1)** could be developed provided they show corresponding efficacy against parasites *in-vitro* and *in-vivo.*

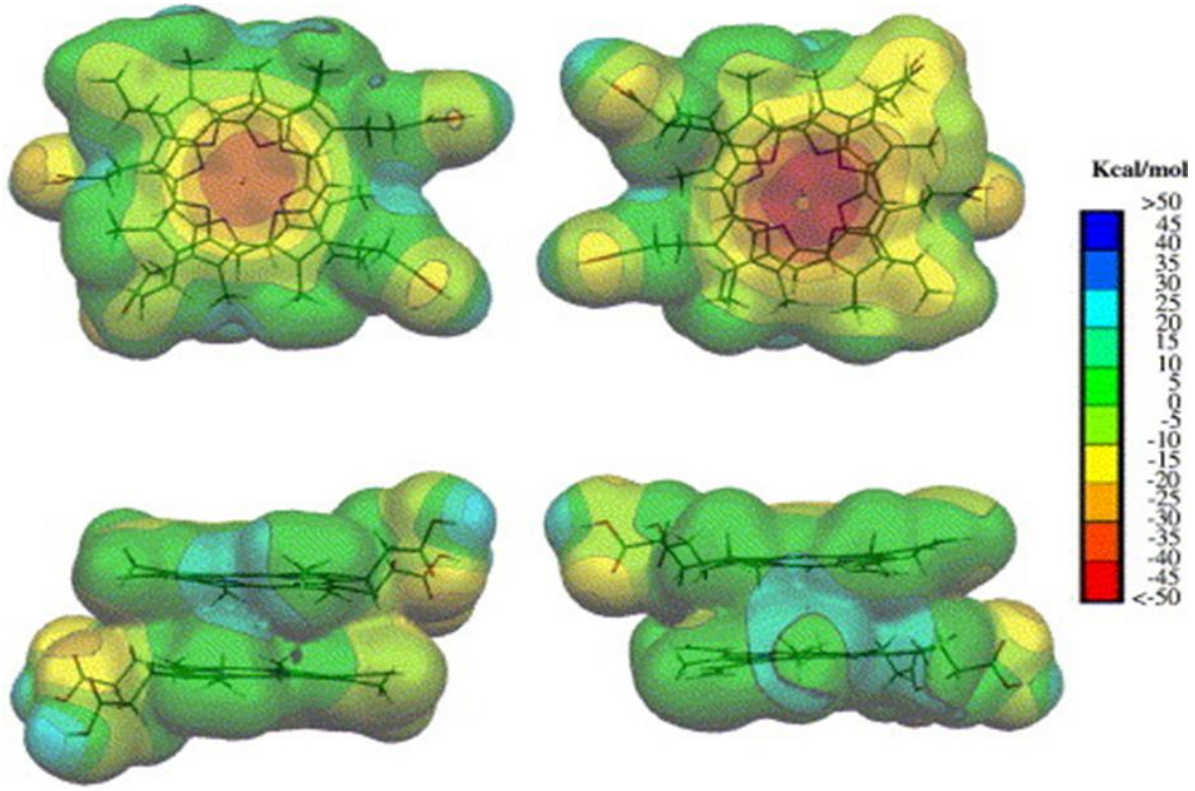

Figure 1.15. MEPs (molecular electrostatic potential) superimposed onto total electron density for the hematin l-oxo-dimer (Portela *et al*., 2004).

Molecular electrostatic potential (MEP) surfaces generated using the CUBEGEN. These MEP iso-energy contours were generated in the range of -50 to 50 kcal/mol, superimposed onto a surface of constant electron density (0.0002 e/au^3), to provide a measure of the electrostatic potential at roughly the van der Waals surface of the molecule. Notably, this colour-coded surface provides a measure of the overall size of the molecule, as well as the location of negative or positive electrostatic potentials. The regions of positive electrostatic potential indicate excess positive charge, leading to repulsion of the positively charged test probe, while regions of negative potential indicate areas of excess negative charge, leading to attraction of the positively charged test probe (Figure 1.15).

Three-dimensional surfaces of molecular electrostatic potential at the constant values of −5 and −10 kcal/mol were generated to determine the profile of the electrostatic potential of a molecule when approaching the receptor (Portela *et al*., **2004**)

1.3.2. Drug receptor targets: Haem binding.

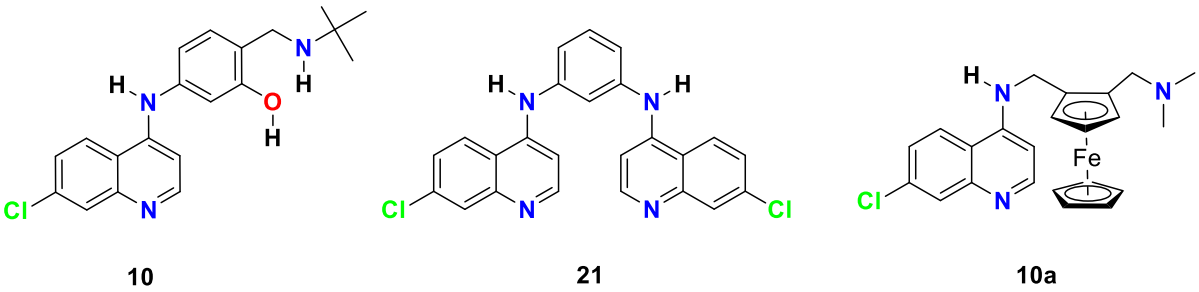

Figure 1-16. N-*tert*-butyl isoquine (GSK369796) (**10**) *meta*-quine (**21**) ferroquine (**10a**).

Antimalarial drugs mediate their effects by disrupting processes or metabolic pathways in different subcellular organelles. There are two phases in which the *Plasmodium* parasite infects its host, exoerythrocytic and erythrocytic. Most relevant to the current study, the quinoline class of compounds, have been the subject of intensive and ongoing study. In drug:haem binding, 4-aminoquinolines target processes within the erythrocytic stages of the parasite development, where the parasite invades red blood cells and digests haem. The 4-aminoquinolines, which include chloroquine (**1**) (Figure 1.4), amodiaquine (**9**) (Figure 1.6), *meta*-quine (**21**) (Figure 1.16) and more recently studied experimental candidate: *N*-tert-butyl isoquine (GSK369796)(**8**) (O'Neil *et al*., **2008**), concentrate inside the acidic digestive vacuole, where they are believed to bind *β*-haematin and interfere with haem detoxification (Fidock *et al*., **2004**).

The quinoline drug molecule binds to the haem molecule, preventing further biomineralisation. Views as to the stoichiometry and geometry of the drug-receptor complex differ between investigators and sometimes rely on fitting spectroscopic data to pre-existing models of drug receptor geometry.

Briefly, by binding to monomeric, dimeric, and oligomeric or biomineralised haem, chloroquine is commonly assumed to interact with the porphyrin ring of the haematin by a π–π stacking interaction of the quinoline ring. Subsequent accumulation of the haem-drug complex within the erythrocyte ultimately poisons the parasite (Hawley *et al*., **1998**; O'Neil *et al*., **1998**). This structure is referred to as a drug-haematin complex. This has a toxic and lethal effect on the parasite through the generation of free radicals near sensitive structures such as membrane lipids or proteins. Haemozoin formation is thought to be inhibited by quinoline antimalarials (O'Neill *et al*., **1998**). *In-vitro* experiments have shown slow spontaneous, pH driven, biomineralisation of haematin to *β*-haematin in cell-free systems, which is inhibited by antimalarials such as chloroquine (**1**) (Figure 1.4) and quinine (**2**) (Egan *et al*., **1994**).

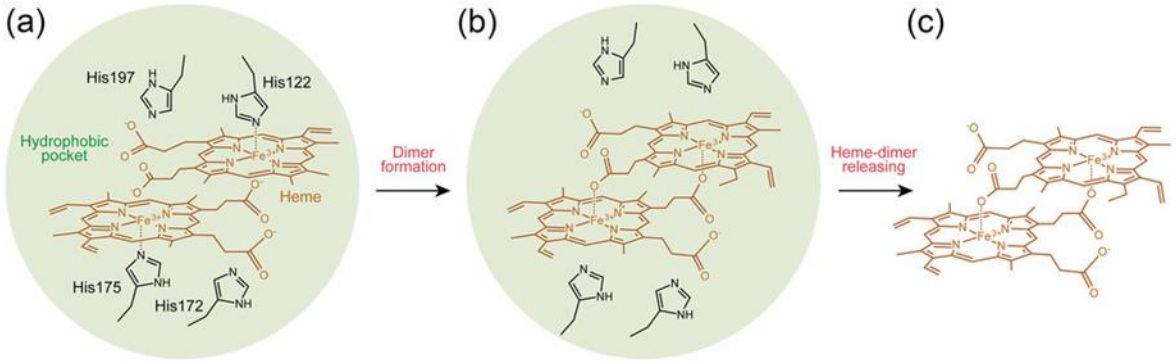

Figure 1.17. Proposed mechanism for the haem detoxification protein process (Nakatani *et al*., 2014).

Chloroquine (**1**) (Figure 1.4), for example, exploits haemoglobin degradation pathways in *P. falciparum*. As the parasite catabolises human haemoglobin, the haematin by-product is detoxified by crystallization to haemozoin.

An identified haem detoxification protein in *P. falciparum* has been shown to be one of the most potent of the haemozoin-producing enzymes. The reaction mechanisms have recently been clarified by Nakatani (Nakatani *et al*., **2014**) (Figure 1.17).

As the production and accumulation of inert *β*-haematin is interrupted within the food vacuole, this toxic substance can generate free radicals (especially if reduced outside the vacuole) and kill the parasite (Hrycyna *et al.*, **2013**).

Here, the drug forms complexes, probably in a 1:2 stoichiometry with respect to 4-aminoquinoline and acridines with haematin probably, which then escapes the vacuole and contributes to cell lysis by oxidising and disrupting cell membranes (Croft *et al*., **2012**). Therefore, targeting the inhibition of haem biocrystallisation is a specific mode of action for combating malarial parasites and is an attractive drug target and this is further discussed below. In terms of monomeric haem, (Dascombe *et al.*, **2005**) have suggested that the inter-actions can be below the axially ligated iron substituent in haematin (below-face) on the same

side or at the periphery involving hydrogen bonds (Ismail *et al.*, **2010**).

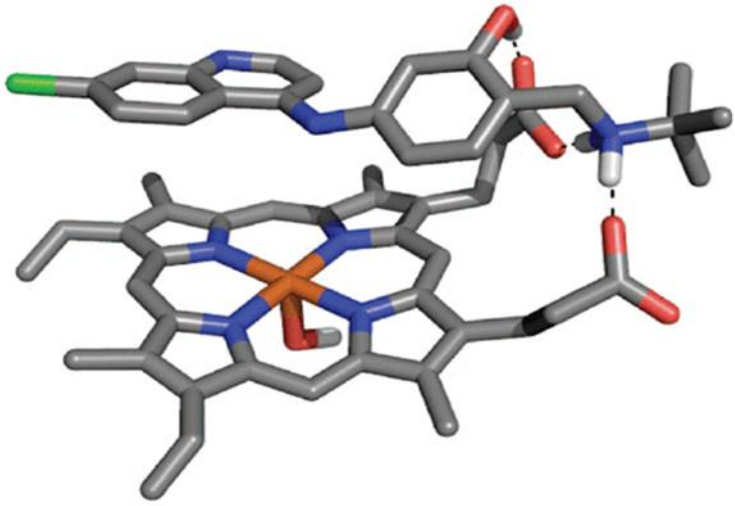

Figure 1.18. Molecular mechanics binding between porphyrin and *N*-tert-butyl isoquine (O'Neill *et al*., 2009).

Other investigators invoke π–π interactions as being responsible for drug action. The haem μ-oxo-dimer being the target has been downgraded by some but Roepe and Egan suggest it can still form under certain conditions, for instance high ionic strength (Dascombe *et al.*, **2005**). Ismail *et al* have shown that this μ-oxo dimer is undetectable in normal positive-ion electrospray mass spectrometry. A previous sandwich complex of haem-μ-oxo- dimer, drug- haem-μoxo dimer (Figure 1.22) was not detected using electrospray mass spectrometry studies. It has been shown conclusively that the drug-haematin complex could be accompanied by below-face, above-face and edge-on motifs (Dascombe *et al*., **2005**, **2007**), of which the last is most energetically stable since it involves hydrogen bonding (Figure 1.18).

The use of docking algorithms employing a MM2 field has been used to show how *meta*-quine binds by top-face interaction to haem (Figure 1.18) (i.e. the same face as the axial substituent). It depicts the chemical structure of the haematin molecule (Haematin is a brown to black iron-containing oxygen-transport metalloprotein in the red blood cells of all vertebrates), a pigment formed by decomposition of haemoglobin. For instance, with the antimalarial cryptolepine, Ismail et al have shown this to be the most likely mode of drug binding (Ismail *et al*., **2010**) which is consistent with the mode of action of chloroquine (**1**), showing 1:1 stoichiometry with the receptor involved with haem binding (Dascombe *et al*., **2005**).

Binding to haemozoin has also been investigated for ferroquine (**10a**) (Dubar *et al*., **2011**). The inhibition of nucleation and/or growth of haemozoin crystals as induced by ferroquine (**10a**) may be explained by the stereoselective binding of FQ to the principal faces.

In their study, the conformational energy of FQ was then minimized with the COMPASS force field. Ferroquine (**10a**) can possibly interact with the {0,0,1} and {1,0,0} faces of haemozoin, blocking crystal growth. With respect to the structure-activity relationship, the

antimalarial activity on 15 different *P. falciparum* strains showed that the activity of FQ did not correlate with CQ, confirming lack of cross resistance (Dubar *et al*., **2011**).

It is possible to form hydrogen bonds between a diprotonated FQ molecule and charged CO_2 groups of haemozoin (Dubar *et al*., **2011**).

It is unclear how adsorption onto an inert pigment will cause oxidative stress unless it also inhibits crystal growth of haemozoin. However, in resistant *Plasmodial* strains, there is decreased drug accumulation within the food vacuole and so the parasite is more likely to survive and cause further damage and infection to the host. Chloroquine (**1**) is associated with weak base properties, properties believed to be responsible for chloroquine accumulation in parasites *in-vivo* (Ginsburg *et al*., **1990**; Geary *et al*., **1990**).

1.3.3. DFT and molecular mechanics interactions.

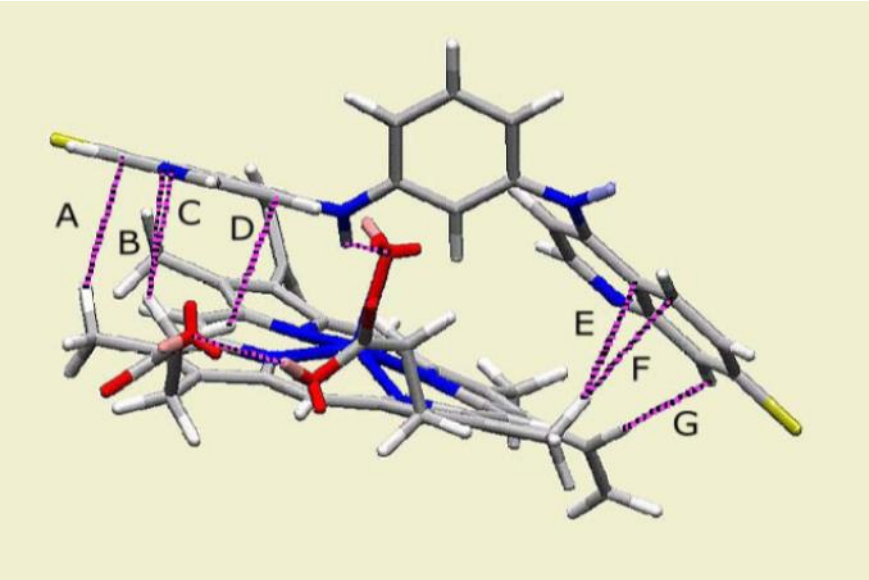

Figure 1.19. A molecular mechanics interaction face binding model of the most favourable porphyrin: *N*-tert-butyl isoquine (**8**) complex (carbon, grey: hydrogen, white: oxygen, red: nitrogen, blue: chlorine, green: iron, orange). Hydrogen bonds are indicated with black and pink dashed lines. Lowest energy Conformer of 1:1 haematin: *meta*-quine (**21**) top-face binding complex illustrating close contacts (A-G) between haematin and *meta*-quine (Dascombe *et al.,* 2005)

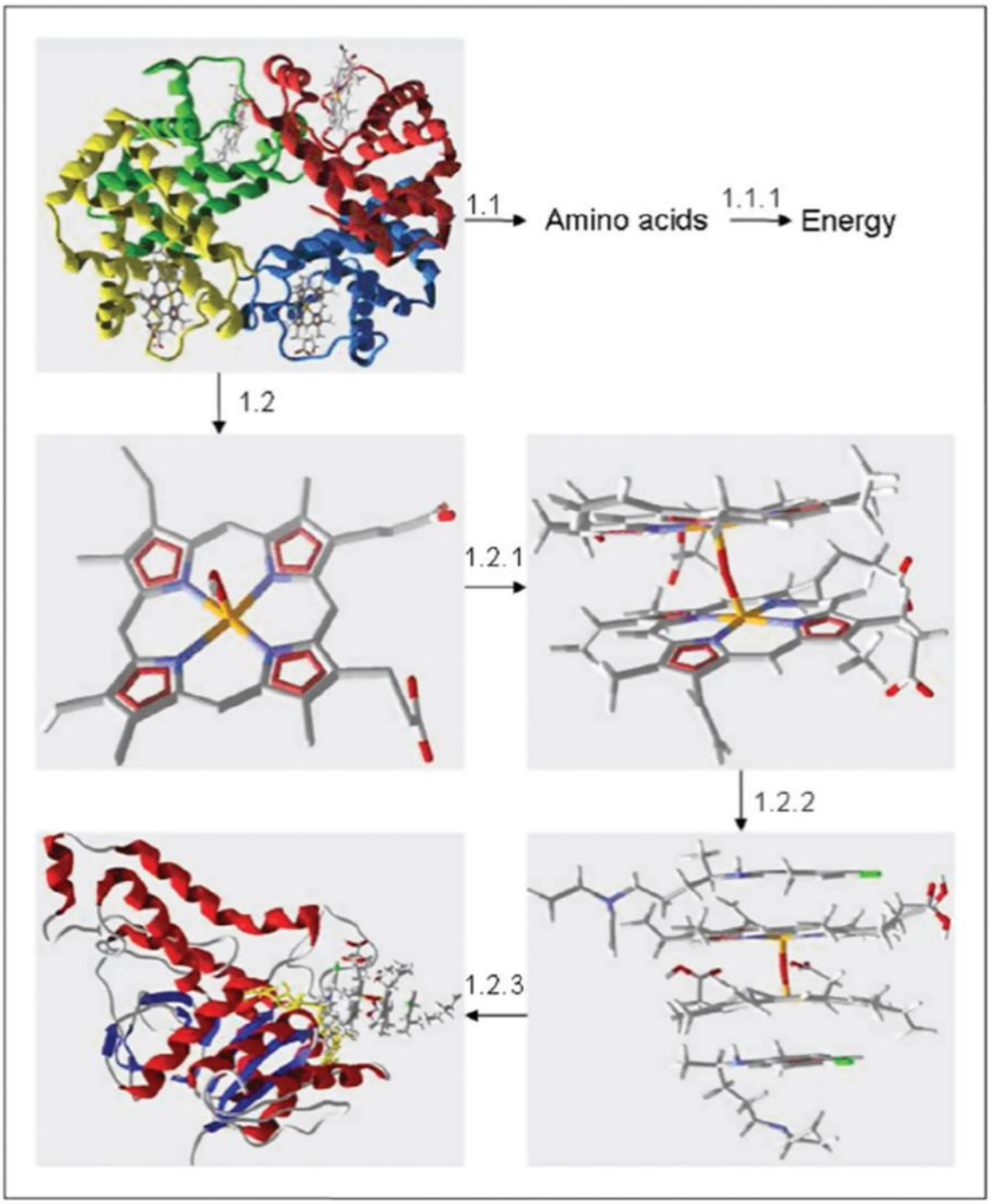

Figure 1.20. Haemoglobin breaks down to route 1.1, amino acids and route 1.2, to haematin, route 1.2.1 assumed μ-oxo dimer formation and 1.2.2, Wireframe Model of a 1:2 chloroquine-haematin π–π sandwich-type complex. Postulated food vacuole dynamics. (Cortopassi *et al*., 2011).

The docking energies of NADH and some quinoline derivatives were calculated (in the free forms and in complex with dimeric haematin) in the active site of the *Plasmodium falciparum* LDH (*Pf* LDH) (Figure 1.20). The results showed better docking score values to the complexes when compared to the free compounds, highlighting them as more efficient inhibitors of *Pf* LDH. Furthermore, the performed Molecular dynamics (MD) simulation studies on the best docking conformation of the chloroquine-μ-oxo dimer complex with *Pf* LDH, and suggested the results *in silico* corroborate experimental data, indicating a possible action route for the quinoline derivatives in the inhibition of *Pf* LDH (Cortopassi *et al.*, **2011**)

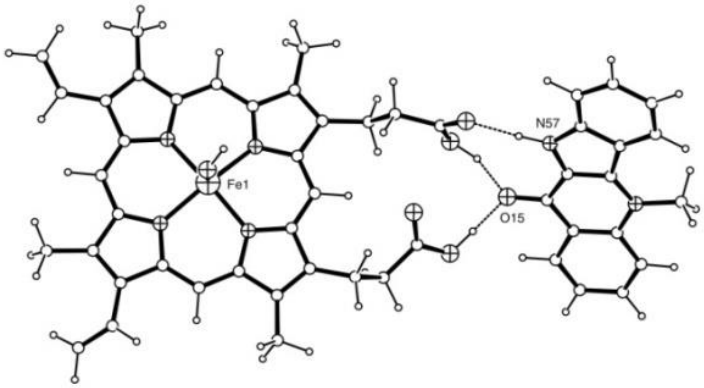

Figure 1.21. An optimised DFT generated structure of haematin-hydroxycryptolepine complex (keto tautomer) in edge binding mode. Hydrogen bonds shown as dotted lines are 1.761, 1.570, 1.570 Å reading from top to bottom. High resolution positive-ion electrospray mass spectrometry (HRPIESMS), e.g. pH 14, $C_{50}H_{44}FeN_6O_5^+$; predicted: 864.2717 (courtesy of Prof Drew)

1.3.4. Haem binding and fragmentation.

Compare this (Figure 1.21) to chloroquine geometry depicted in the top RHS corner showing chloroquine and haematin (Figure 1.22). All studies conducted using Macromodel™ (Ismail and Carr; unpublished work, Modelled in **1994**). Magnolia panel below (Figure 1.22) demonstrates haem-drug binding of various monomer and dimer formations between haematin and *meta*-quine, revealing close contacts as shown (Dascombe *et al*., **2005**). These potential interactions suggest opportunities for drug design. For example, bio-isosteric substitution of the C-5 methine by nitrogen (position F) makes symmetrical metazaquines (e.g. N^1,N^3-*bis*(7-chloro-1,5-naphthyridin-4-yl)benzene-1,3-diamine).

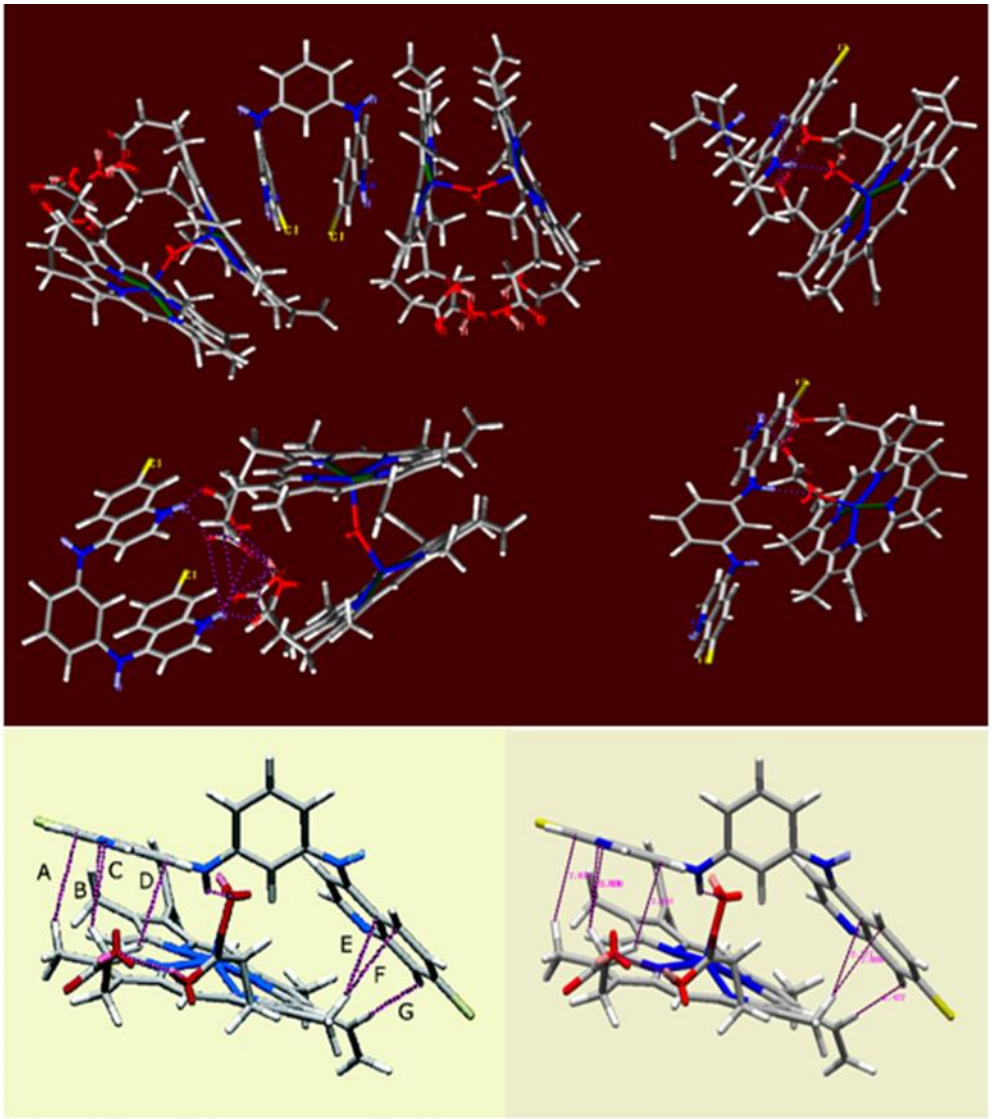

Figure 1.22. Top brown panel: From top LHS; proceeding anticlockwise: *meta*-quine sandwiched between haematin μ-oxo dimer and interactions; hydrogen bonded to the four propionic acid moieties and positioned above-face upon the upper, axially coordinated. Lower energy form of *meta*-quine bound to receptor by enhanced hydrogen-bonding (dotted lines).

In contrast, Dascombe *et al* (**2005**) have reported no binding to μ-oxo dimeric species (in mass spectrometry) when samples are mechanically ground with various drugs or exposed to the haem in solution at various pH (Dascombe *et al*., **2005**). Instead, they have reported binding to both free haem and the reciprocal dimeric subunit of haemozoin. Initially, following literature precedent, various π–π models were generated. The speciation of ferriprotoporphyrin IX (Fe(III)PPIX) in aqueous and mixed aqueous-organic solvents has been investigated by UV-Vis, proton NMR, magnetic, and diffusion measurements.

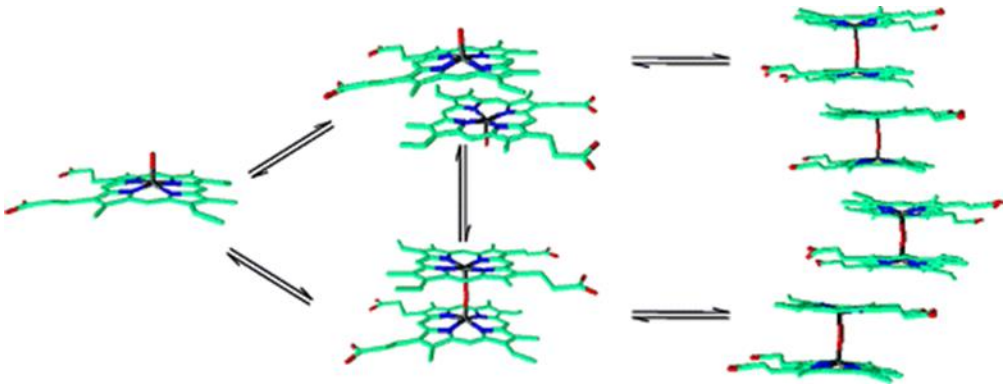

Figure 1.23. The speciation of ferriprotoporphyrin IX (Fe(III)PPIX)(De Villiers *et al.*, 2009).

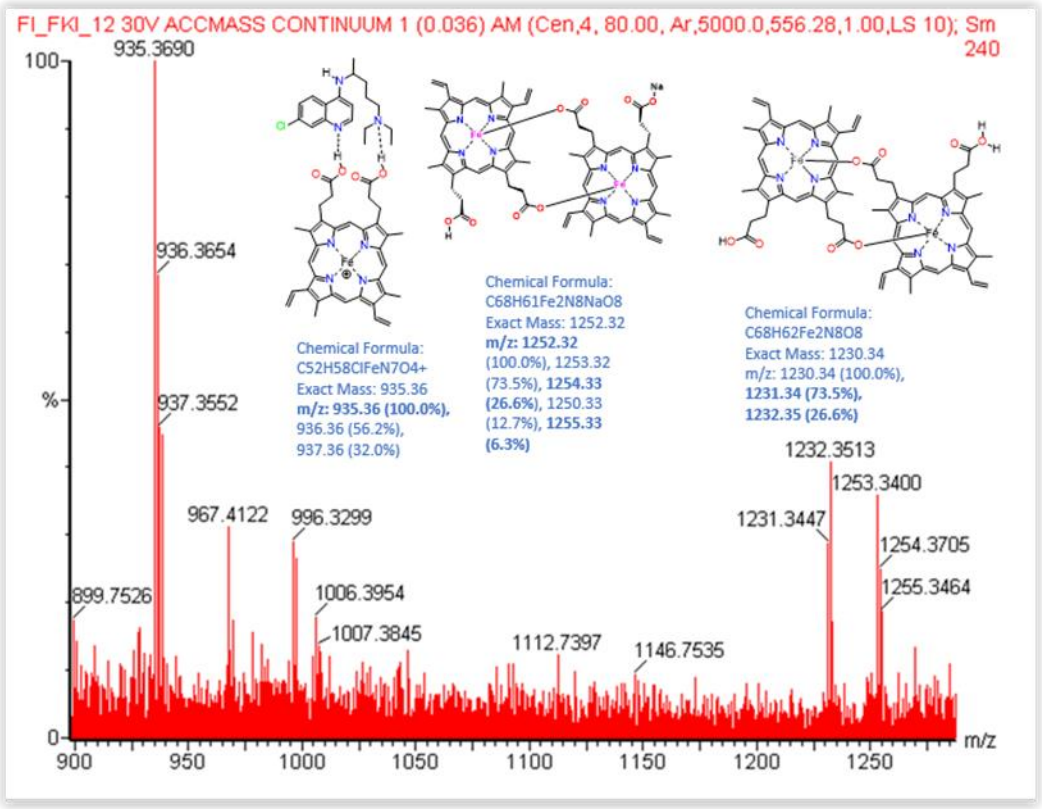

Figure 1.24. Fragmentation of CQ: haem complex.

1.3.5. Manich reaction.

The mannich reaction (Mannich & Krosche, 1912), so named after Carl Ulrich Franz Mannich is an important carbon-carbon-bonding reaction that is utilized in the synthesis of alkaloid natural products, and is a versatile building block within a range of biosynthetic pathways. This chemistry exploited the known nucleophilic addition reaction between a primary or secondary amine with a non-enolizable carbonyl group (i.e. formaldehyde, followed by dehydration to form Schiff base) (Figure 5.41. Scheme 52).

The Schiff base intermediate reacts with an acidic proton (in this case from the corresponding cyclohexa-2, 4-dienone) subsequently forming the substituted *β*-amino carbonyl compound, also known as the Mannich base (aminomethylation) (Tramontini & Angiolini, **1994**).

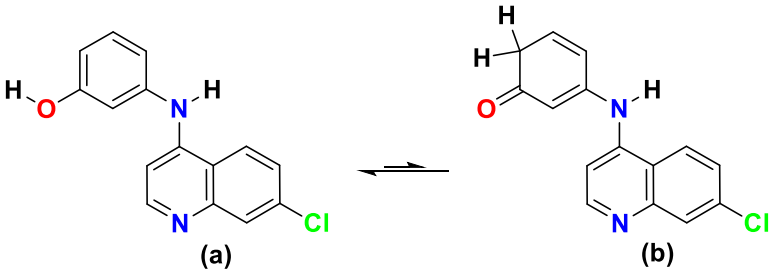

Figure 1.25. Enol form a) 3-(7-chloroquinolin-4-ylamino) phenol; b) Keto form: 3-(7-chloroquinolin-4-ylamino) cyclohexa-2,4-dienone.

This three-component condensation reaction allows the construction of a common heterocyclic scaffold appended to a wide range of compounds with differing side chains. Consequently, a range of compounds can be constructed, from which we can select candidate antimalarials possessing the best pharmacological and pharmaceutical properties (e.g. water solubility, salt formation ability, etc). The Mannich reaction initially forms an iminium ion from formaldehyde and amine. The enolizable carbonyl group can then tautomerize to the enol form due to the acidic reaction conditions, after which it can attack the iminium ion at the electrophilic carbon atom. This involves the movement of a proton and a shifting of bonding electrons (Figure 1.25).

1.3.6. Mechanism of the mannich reaction.

The C-H activated component is usually an aliphatic or aromatic aldehyde or ketone, carboxylic acid derivatives, *β*-dicarbonyl compounds, nitroalkanes, electron rich aromatic compounds, such as phenols (activated at their *ortho* position) and terminal alkynes. To obtain high concentrations of iminium ion, protic solvents such as ethanol, methanol, acetic acid or water are used as a reaction medium, ensuring maximum rate aminoalkylation. Aromatic amines have a low reaction profile, therefore primary and secondary aliphatic

amines are favoured. Over-alkylation forms tertiary amines, and use of primary amines can be an issue, overcome by using secondary amines. Unsymmetrical ketones give rise to regio-isomeric Mannich bases, unlike the more substituted α-positioned derivatives. The Mannich base can react further in three ways in comparison to the route described above. If it is a primary or secondary amine it may further condense with one or two additional molecules of aldehyde and an active compound, for example If the active hydrogen compound has two or three active hydrogens, the Mannich base may condense with one or two additional molecules of aldehyde and ammonia or amine (Figure 1.26).

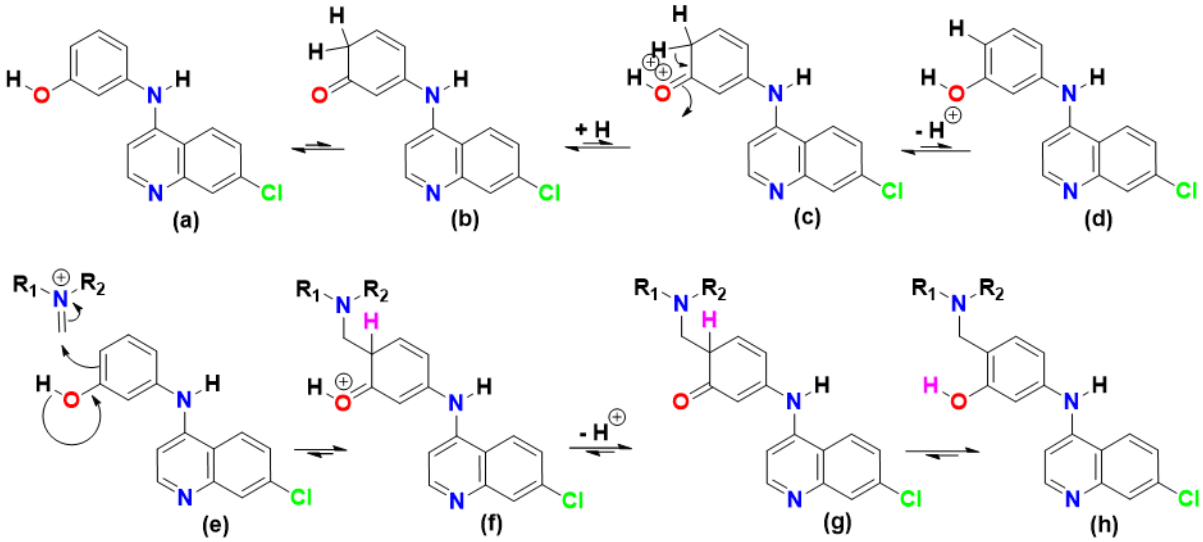

Figure 1.26. Mechanism of the mannich reaction.

1.4. References.

Atamna, H., Krugliak, M., Shalmiev, G., Deharo, E., Pescarmona, G., Ginsburg, H. 1996. Mode of antimalarial effect of methylene blue and some of its analogues on *Plasmodium falciparum* in culture and their inhibition of *P. vinckei petteri* and *P. yoelii nigeriensis in-vivo*. *Biochem Pharmacol*. 51, 693-700.

Bhattacharya, S., Saha, C. N., Chetia, D. 2009. Synthesis and Evaluation of Some New *Isoquine* Analogues for Antimalarial Activity. *E-Journal of Chemistry*. 6, S381-S389.

Barlin, G. B., Jiravinyu, C., Butcher, G. A., Kotecka, B., Rieckmann, K. 1992. The *in vitro* and *in-vivo* antimalarial activity of some Mannich bases derived from 4-(7'-trifluoromethyl-1',5'-naphthyridin-4'-ylamino)phenol, 2-(7'-trifluoromethyl-quinolin-4'-ylamino)phenol, and 4'-chloro-5-(7"-trifluoromethylquinolin-4"-ylamino)biphenyl -2-ols. *Ann Trop Med Parasitol*. 86, 323-331.

Barlin, G. B., Yan, J. 1989. Potential Antimalarials. VIII. Mono- and Di-mannich Bases of 2-(7'-Trifluoro-methylquinolin-4'-ylamino)phenol Via 2-Nitrophenols. *Australian Journal of Chemistry*. 42, 2191.

Bledsoe, G. H. 2005. Malaria primer for clinicians in the United States. *South Med J*. 98, 1197-1204.

Bohle, D. S., Dinnebier, R. E., Madsen, S. K., Stephens, P. W. 1996. Characterization of the products of the haem detoxification pathway in malarial late trophozoites by X-ray diffraction. *Molecular Pharmacology*. 50, 1559-1566.

Bohle, D. S., Dodd, E, L. 2014. Orienting the heterocyclic periphery: a structural model for chloroquine's antimalarial activity. *Chem. Commun*. 50, 13765.

Bray, P. G., Hawley, S. R., Mungthin, M., Ward, S. A. 1996. Physiological properties correlated with drug resistance and the reversal of drug resistance in *Plasmodium falciparum*. *J Biol Chem*. 272, 713-716.

Burckhalter, J. H. 1950. The Mannich reaction with *o*-Phenylphenol. *J. Am. Chem. Soc*. 72, 5309-5310.

Burckhalter, J. H., Tendick 1948. Aminoalkylphenols as antimalarials (heterocyclicamino)-alpha-amino-o-cresols; the synthesis of camoquin. *J Am Chem Soc*. 70, 1363-1373.

Calas, M., Ancelin, M. L., Cordina, G., Portefaix, P., Piquet, G., Vidal-sailhan, V., Vial, H. 2000. Antimalarial activity of compounds interfering with *Plasmodium falciparum* phospholipid metabolism: comparison between mono- and *bis*quaternary ammonium salts. *J Med Chem*. 43, 505-516.

Camacho, J. E., Batista, F. M. 2008. Effectiveness of official development aid and new principles and tools for health development aid. 2008 *Sespas Report*. Gac Sanit, 22 Suppl 1, 237-243.

Chang, C., Lin-hua, T., Jantanavivat, C. 1992. Studies on a new antimalarial compound: pyronaridine. *Trans R Soc Trop Med Hyg*. 86, 7-10.

Chang, C., Zheng, X. 1992. Development of the New Antimalarial Drug Pyronaridine. *Biomedical and Environmental Sciences*. 5, 149-160.

Chavalitshewinkoon-petmitr, P., Pongvilairat, G., Auparakkitanon, S., Wilairat, P. 2000. Gametocytocidal activity of *pyronaridine* and DNA topoisomerase II inhibitors against multidrug-resistant *Plasmodium falciparum in vitro*. *Parasitol Int*. 48, 275-280.

Choi, C. Y., Cerda, J. F., Chu, H. A., Babcock, G. T., Marletta, M. A. 1999. Spectroscopic characterization of the haem-binding sites in *Plasmodium falciparum* histidine-rich protein 2. *Biochemistry*. 38, 16916-24.

Coombs, G. H., Goldberg, D. E., Klemba, M., Berry, C., Kay, J., Mottram, J. C. 2001. Aspartic proteases of *Plasmodium falciparum* and other parasitic protozoa as drug targets. *Trends Parasitol*. 17, 532-537.

Coronado, L. M., Nadovich, C. T., Spadafora, C. 2014. Malarial Hemozoin: From target to tool, *Biochim Biophys Acta*, 1840, 6, 2032–2041.

Cortopassi, W.A., Oliveira, A. A., guimaraes, A. P., Renno, M. N., Krettli, A. U., Franca, T. C. 2011. Docking Studies on the Binding of Quinoline Derivatives and Hematin to *Plasmodium Falciparum* Lactate Dehydrogenase, *Journal of Biomolecular Structure and Dynamics*. 29:1, 207-218, DOI: 10.1080/07391102.2011.10507383.

Cowman, A. F., Berry, D. Baum, J. 2012. The cellular and molecular basis for malaria parasite invasion of the human red blood cell. *J Cell Biol*. 198, 961-971.

Croft, S. L., Duprac, S., Arbe-barnes, S. J., Craft, J. C., Shin, C., Fleckenstein, L., borghini-fuhrer, I., Rim, H. 2012. Review of *pyronaridine* anti-malarial properties and product characteristics. *Malarial Journal*. 11, 270-298.

Dascombe, M., Drew, M., Evans, P. Ismail, F. 2007. Rational Design Strategies for the Development of Synthetic Quinoline and Acridine Based Antimalarials. *Frontiers in Drug Design & Discovery*. 3, 559-609.

Dascombe, M. J., Drew, M. G., Morris, H., Wilairat, P., Auparakkitanon, S., Moule, W. A., Alizadeh-shekalgourabi, S., Evans, P. G., Lloyd, M., Dyas, A. M., Carr, P. Ismail, F. M. 2005. Mapping antimalarial pharmacophores as a useful tool for the rapid discovery of drugs effective *in-vivo*: design, construction, characterization, and pharmacology of *meta*-quine. *J Med Chem*. 48, 5423-5436.

De villiers, K. A., Marques, H. M. Egan, T. J. 2008. The crystal structure of *halofantrine*-ferriprotoporphyrin IX and the mechanism of action of arylmethanol antimalarials. *J Inorg Biochem*, 102, 1660-1667.

De villiers, K. A., Asher, C., Egan, T. J. 2009. Speciation of ferriprotoporphyrin IX in aqueous and mixed aqueous solution is controlled by solvent identity, pH, and salt. *J Inorg Chem*. 48(16), 7994–8003.

Drew, M. G. 2014. Emiretus. University of reading. *Private Communications*.

Dubar, F., Egan, T. J., Pradines, B., Kuter, D., Ncokazi, K. K., Forge, D., Paul, J. F., PIerrot, C., Kalamou, H., Khalife, J., Buisine, E., Rogier, C., Vezin, H., Forfar, I., Slomianny,

C., Trivelli, X., Kapishnikov, S., Leiserowitz, L., Dive, D., Biot, C. 2011. The antimalarial ferroquine: role of the metal and intramolecular hydrogen bond in activity and resistance. *ACS Chemical Biology.* Mar;6(3):275-287. DOI: 10.1021/cb100322v.

Egan, T., Marques, H. 1999. The role of haem in the activity of chloroquine and related antimalarial drugs. *Coordination Chemistry Reviews*. 493-517.

Egan, T. J. 2008. Haemozoin formation. *Mol Biochem Parasitol*. 157, 127-136.

Egan, T. J., Hunter, R., Kaschula, C. H., Marques, H. M., Misplon, A. Walden, J. 2000. Structure-function relationships in aminoquinolines: effect of amino and chloro groups on quinoline-haematin complex formation, inhibition of *beta*-haematin formation, and antiplasmodial activity. *J Med Chem*. 43, 283-291.

Egan, T. J., Mavuso, W. W., Ross, D. C., Marqués, H. M. 1997. Thermodynamic factors controlling the interaction of quinoline antimalarial drugs with ferriprotoporphyrin IX. *J Inorg Biochem*. 68, 137-145.

Egan, T. J., Ross, D. C., Adams, P. A. 1994. Quinoline anti-malarial drugs inhibit spontaneous formation of *beta*-haematin (malaria pigment). *FEBS Lett*. 352, 54-57.

Fidock, D., Rosenthal, P., Croft, S., Brun, R., Nwaka, S. 2004. Antimalarial drug discovery: efficacy models for compound screening. *Nat Rev Drug Discov*. 3, 509–520. https://doi.org/10.1038/nrd1416.

Fitch, C. D., Kanjananggulpan, P. 1987. The state of ferriprotoporphyrin IX in malaria pigment. *J Biol Chem*. 262, 15552-15555.

Foreman, J. C., Johnson, T., Gibb, A. J. 2010. Textbook of Receptor Pharmacology, (3rd Ed), *CRC Press*.

Garcia, L. S. 2010. Malaria. *Clinics in Laboratory Medicine.* 30, 93-129.

Gardner M. J., Hall, N., Fung, E., White, O., Berriman, M., Hyman, R. W., Carlton, J. M., Pain, A., Nelson K,E., Bowman, S., Paulsen, I,T., James, K., Eisen, J,A., Rutherford, K., Salzberg, S. L., Craig, A., Kyes, S., Chan, M. S., Nene, V., Shallom, S. J., Suh, B., Peterson, J., Angiuoli, S., Pertea, M., Allen, J., Selengut, J., Haft, D., Mather, M. W., Vaidya, A. B., Martin, D. M., Fairlamb, A. H., Fraunholz, M. J., Roos, D. S., Ralph, S. A., McFadden, G. I., Cummings, L. M., Subramanian, G. M., Mungall, C., Venter, J. C., Carucci, D. J., Hoffman, S. L., Newbold, C., Davis, R. W., Fraser, C. M., Barrell, B. 2002. Genome sequence of the human malaria parasite *Plasmodium falciparum*. *Nature*. 419(6906):498-511. doi: 10.1038/*nature*01097.

Geary, T. G., Divo, A. D., Jensen, J. B., Zangwill, M. and Ginsburg, H. 1990. Kinetic modelling of the response of *Plasmodium falciparum* to chloroquine and its experimental testing *in vitro*. Implications for mechanism of action of and resistance to the drug. *Biochem Pharmacol*. 40, 685-691.

Ginsburg, H., Stein, W. D. 1991. Kinetic modelling of chloroquine uptake by malaria-infected erythrocytes. Assessment of the factors that may determine drug resistance. *Biochem Pharmacol*. 41, 1463-1470.

Greenwood, B. M., Fidock, D. A., Kyle, D. E., Kappe, S. H., Alonso, P. L., Collins, F. H., Duffy, P. E. 2008 Malaria: progress, perils, and prospects for eradication. *J Clin Invest*. 118, 4, 1266–1276.

Gringuaz, A. 1997. Introduction to medicinal chemistry : how drugs act and why, New York, *Wiley-VCH*.

Harmse, L., Van Zyl, R., Gray, N., Schultz, P., Leclers, S., Meijer, L., Doerig, C., Havlik, I. 2001. Structure-activity relationships and inhibitory effects of various purine derivatives on the *in vitro* growth of *Plasmodium falciparum*. *Biochem Pharmacol*. 62, 341-348.

Hawley, S. R., Bray, P. G., Mungthin, M., Atkinson, J. D., O'neill, P. M., Ward, S. A. 1998. Relationship between antimalarial drug activity, accumulation, and inhibition of heme polymerization in *Plasmodium falciparum in vitro*. *Antimicrob Agents Chemother*. 42, 682-686.

Haynes, R. K., Chen, K. W., Li, K. Y., Tang, M. M., Wong, H. N., Chen, M. J., Guo, Z, F., Guo, Z, H., Coghi, P., Monti, D. 2011. A partial convergence in action of methylene blue and artemisinins: antagonism with chloroquine, a reversal with verapamil, and an insight into the antimalarial activity of chloroquine. *ChemMedChem*. 6, 9, 1603-1615.

Holding, P. A., Snow, R. W. 2001. Impact of *Plasmodium falciparum* malaria on performance and learning: review of the evidence. *Am J Trop Med Hyg*. 64, 68-75.

Hrycyna, C. A., Summers, R. L., Lehane, A. M., Pires, M. M., Namanja, H., Bohn, K., Kuriakose, J., Ferdig, M., Henrich, P. P., Fidock, D. A., Kirk, K., Chmielewski, J., Martin, R. E. 2014. *Quinine* dimers are potent inhibitors of the *Plasmodium falciparum* chloroquine resistance transporter and are active against quinoline-resistant *P. falciparum*. *ACS Chem Biol*. 9, 722-730.

Ismail, F. M., Dascombe, M. J., Carr, P., Merette, S. A., Rouault, P. 1998. Novel aryl-*bis*quinolines with antimalarial activity *in-vivo*. *J Pharm Pharmacol*. 50, 483-492.

Ismail, F. M., Dascombe, M. J., Carr, P., North, S. E. 1996. An exploration of the structure-activity relation-ships of 4-aminoquinolines: novel antimalarials with activity *in-vivo*. *J Pharm Pharmacol*. 48, 841-850.

Ismail, F. M., Levitsky, D. O., Dembitsky, V. M. 2009. Aziridine alkaloids as potential therapeutic agents. *Eur J Med Chem*. 44, 3373-3387.

Ismail, F. M., Dempster, N. M., Ford, J. L. 2009b. Rapid and efficient isolation of *cryptolepine* from *Cryptolepis sanguinolenta* using focused microwave extraction methods: a haem-binding antimalarial, *J. Pharm. Pharmacol*. 61 Meeting Abstract.

Ismail, F. M., Dempster, N. M., Edwards, G., Morris, H., Saleem, I., Alrawahi, A., Azam, M., Dascombe, M. J., Smith, M., Parker, A. W., Clark, I. P., Alizadeh-shekalgourabi, S., Drew, M. G. 2010. Invited Lecture: Quantification of Haem: Antimalarial Drug Receptor Geometry by Crystallography, DFT, *Spectroscopic and Spectrometric Methods in-vitro and in silico*. 31st BMSS 3-Day Meeting Mass Spectrometry for a Changing

World Sunday to Wednesday: 5–8th September, Cardiff City Hall.

Jewell, H., Maggs, J. L., Harrison, A. C., O'neil, P. M., Ruscoe, J. E., Park, B. K. 1995. Role of Hepatic Metabolism in the Bioactivation and Detoxification of *Amodiaquine*. *Xenobiotica*. 25, 199-217.

Klonis, N., Dilanian, R., Hanssen, E., Darmanin, C., Streltsov, V., Deed, S., Quiney, H., Tilley, L. 2010. Haematin-haematin self-association states involved in the formation and reactivity of the malaria parasite pigment, hemozoin. *Biochemistry,* 49, 6804-6811.

Koch, M., Baum, J. 2016. The mechanics of malaria parasite invasion of the human erythrocyte - towards a reassessment of the host cell contribution. *Cell Microbiol*. Mar 18(3):319-29. doi: 10.1111/*cmi*.12557.

Korenromp, E. L., Williams, B. G., Gouws, E., Dye, C., Snow, R. W. 2003. Measurement of trends in childhood malaria mortality in Africa: An assessment of progress toward targets based on verbal autopsy. *Lancet Infect Dis.* 3, 349-358.

Mannich, C., Krosche, W. 1912. Ueber ein Kondensationsprodukt aus Formaldehyd, Ammoniak und Antipyrin. *Archiv der Pharmazie.* 250, 647–667.

Marsh, K. 1998. Malaria disaster in Africa. *Lancet*. 352, 924.

Martin, R. E., Kirk, K. 2007. Transport of the essential nutrient isoleucine in human erythrocytes infected with the malaria parasite *Plasmodium falciparum*. *Blood*. 109, 2217-2224.

Meissner, P., Mendes J, M., Ouermi, L., Compaore, G., Coulibaly, B., Nebie, E., Krisam, J., Klose, C., Kieser, M., Jahn, A., Lu, G., D'alessandrol, U., Sie, A., Mockenhaupt, F. P., Muller, O. 2019. Safety and efficacy of artesunate-amodiaquine combined with either methylene blue or primaquine in children with *falciparum* malaria in Burkina Faso: A randomized controlled trial. *PloS one*. 14(10), e0222993.

Mirzaei, M., Sadeghi, F., Molconov, K., Zareba, J, K., Gomila, R, M., Frontera, A. Recurrent Supramolecular Motifs in a Series of Acid−Base Adducts Based on Pyridine-2,5-Dicarboxylic Acid N-Oxide and Organic Bases: Inter- and Intramolecular Hydrogen Bonding. 2020. *Cryst. Growth Des*. 2020, 20, 1738−1751.

Moore, T., Winmill, T. 1912. The state of amines in aqueous solution. *Journal of the Chemical Society, Transactions*. 101, 1635-1676.

Nakatani, K., Ishikawa, H., Aono, S. Mizutani, Y. 2014. Identification of essential histidine residues involved in haem binding and Hemozoin formation in haem detoxification protein from *Plasmodium falciparum*. *Sci Rep*. 4, 6137.

O'neill, P. M., Bray, P. G., Hawley, S. R., Ward, S. A. Park, B. K. 1998. 4-Aminoquinolines: past, present, and future, a chemical perspective. *Pharmacol Ther*. 77, 29-58.

O'neill, P. M., Shone, A. E., Stanford, D., nixon, G., Asadollahy, E., Park, B. K., Maggs, J. L., Roberts, P., Stocks, P. A., Biagini, G., Bray, P. G., Davies, J., Berry, N., Hall, C., Rimmer, K., Winstanley, P. A., HIndley, S., Bambal, R. B., Davis, C. B., Bates, M.,

Gresham, S. L., Brigandi, R. A., Gomez-de-las-heras, F. M., Gargallo, D. V., Parapini, S., Vivas, L., Lander, H., Taramelli, D., Ward, S. A. 2009. Synthesis, antimalarial activity, and preclinical pharmacology of a novel series of 4'-fluoro and 4'-chloro analogues of amodiaquine. Identification of a suitable "back-up" compound for N-tert-butyl isoquine. *J Med Chem*. 52, 1828-1844.

Pagola, S., Stephens, P. W., Bohle, D. S., Kosar, A. D. Madsen, S. K. 2000. The structure of malaria pigment beta-haematin. *Nature*. 404, 307-310.

Pandya, T., Pandey, S. K., Tiwari, M., Chaturved, S. C. Saxena, A. K. 2001. 3-D QSAR studies of triazolinone based balanced AT1/AT2 receptor antagonists. *Bioorg Med Chem*. 9, 291-300.

Ploscariu, N. 2014. Nanomechanical properties of single protein molecules and peptides.

Portela, C., Afonso, C. M., Pinto, M. M. Ramos, M. J. 2004. Definition of an electronic profile of compounds with inhibitory activity against haematin aggregation in malaria parasite. *Bioorg Med Chem*. 12, 3313-3321.

Ridley, R. G., Hudson, A. T. 1998. Chemotherapy of malaria. *Curr Opin Infect Dis*. 11, 121-136.

Sandlin, R. D., Fong, K. Y., Wicht, K. J., Carrell, H. M., Egan, T. J., Wright, D. W. 2014. Identification of *β*-haematin inhibitors in a high-throughput screening effort reveals scaffolds with *in vitro* antimalarial activity. *Int. J. Parasitol. Drugs Drug Resist*. *4*, 316-325

Schirmer, H., Meuller, T., Johann, L., Jannack, B., Breuckner, G., Lanfranchi, D, A., Bauer, H., Sanchez, S., Yardley, V., Deregnaucourt, C., Schrevel, J., Lanzer, M., anzer, R., Davioud-charvet, M. 2011, Glutathione Reductase-Catalyzed Cascade of Redox Reactions To Bioactivate Potent Antimalarial 1,4-Naphthoquinones; A New Strategy to Combat Malarial Parasites. *Journal of the American chemical society*. 133, 30, 11557–11571.

Siddiqui, G., Giannangel, C., De Paoli, A., Schuh, A.K., Heimsch, K. C., Anderson, D., Brown, T.G., Macraild, C.A., Wu, J., Wang, X., Dong, Y., Vennestrom, J.L., Becker, K., Creek. D.J. 2022. *ACS Infectious Diseases.* 8 (1), 210-226. DOI: 10.1021/acsinfecdis.1c00550

Singh, B., Kim Sung, L., Matusop, A., Radhakrishan, A., Shamsul, S. S., Cox-singh, J., Thomas, A., Conway, D. J. 2004. A large focus of naturally acquired *Plasmodium knowlesi* infections in human beings. *Lancet* (London, England). 363(9414), 1017–1024. https://doi.org/10.1016/S0140-6736(04)15836-4

Slater, A. F. 1993. Chloroquine: mechanism of drug action and resistance in *Plasmodium falciparum*. *Pharmacol Ther*. 57, 203-235.

Slater, L. B. 2009. War and Disease: Biomedical Research on Malaria in the Twentieth Century. *Rutgers University Press*. Piscataway, NJ, USA, 272.

Stern, L., Slobedman, B. 2008. The Economics of Climate Cha Human Cytomegalovirus Latent Infection of Myeloid Cells Directs Monocyte Migration by Up-Regulating Monocyte Chemotactic Protein-1. *J Immunol.* 2008; 180:6577-6585.

Smith, M. B., March, J. 2001. March's advanced organic chemistry reactions, mechanisms, and structure sixth edition. *wiley-interscience a john wiley & sons, inc*.

Tramontini, M. R., Angiolini, L. 1994. Mannich Bases-Chemistry and Uses (*New Directions in Organic & Biological Chemistry*). *Science*. 1-304.

Vippagunta, S. R., Dorn, A., Matile, H., Bhattacharjee, A. K., Karle, J. M., Ellis, W. Y., Ridley, R. G., Vennerstrom, J. L. 1999. Structural specificity of chloroquine-haematin binding related to inhibition of haematin polymerization and parasite growth. *J Med Chem*. 42, 4630-4639.

Vishweshwar, P., Nangia, A., Lynch, V, M. 2002. Recurrence of Carboxylic Acid−Pyridine Supramolecular Synthon in the Crystal Structures of Some Pyrazinecarboxylic Acids. *J. Org. Chem*. 67, 556-565.

Warhurst, D. C. 2001. A molecular marker for chloroquine-resistant *falciparum* malaria. *The New England journal of medicine*. 344, 4, 299-302.

Watkins, W. M., Sixsmith, D. G., Spencer, H. C., Boriga, D. A., Kariuki, D. M., Kipingor, T., Koech, D. K. 1984. Effectiveness of amodiaquine as treatment for chloroquine-resistant *Plasmodium falciparum* infections in Kenya. *Lancet*. 1, 357-359.

Weinhold, F., Klein, R. A., 2014. What is a hydrogen bond? Resonance covalency in the supramolecular domain. *Chem. Educ. Res. Pract.* 2014, 15, 276-285. DOI: 10.1039/C4RP00030G.

Wiselogle, F. Y., National Research Council (U.S.) 1946. A survey of antimalarial drugs, *1941-1945,* Ann Arbor, Mich. *Edwards.*

Whitman, T. J., Coyne, P, E., Magill, A. J., Blazes, D. L., Green, M. D., Milhous, W. K., Burgess, T. H., Freilich, D., Tasker, S. A., Azar, R. G., Endy, T. P., Clagett, C. D., Deye, G. A., Shanks, D., Martin, G, Y. 2010. An Outbreak of *Plasmodium falciparum* Malaria in U.S. Marines Deployed to Liberia. *Am J Trop Med Hyg*. 83(2), 258–265.

Wolfe, H, L. 1997. *Plasmodium* ovale in Zambia, Malariologist, *Ministry of Health*. Box 205, Lusaka, Zambia.

WHO. *World Health Organisation*. 2022.

Zhong, W., Gallivan, J. P., Zhang, Y., Li, L., Lester, H. A., Dougherty, D. A. 1998. From ab initio quantum mechanics to molecular neurobiology: A cation–π binding site in the nicotinic receptor. *Proc. Natl. Acad. Sci.* USA 95, 21, 12088–12093.

Ziegler, J., Linck, R., Wright, D. W. 2001. Haem Aggregation inhibitors: antimalarial drugs targeting an essential biomineralization process. *Curr Med Chem*. 8, 171-189.

Chapter 2

An exploration of the structure-activity relationship of mono- and *bis*-4-aminoquinolines bridged by aliphatic and aromatic rings: various antimalarials with superior *in-vivo* activity.

Index of contents chapter 2.

Figure of contents chapter 2.

Table of contents chapter 2.

AIM.

Synthesise compounds to deduce Geometry of the antimalarial drug receptor complex for 4-aminoquinolines and related compounds.

2.1. *Bis*quinolines.

A new series of *mono*- and *bis*quinolines, including a proven group of novel antimalarial drugs active *in-vivo*, were synthesised. Three different approaches were used to synthesise the molecules namely:

a) S_NAr reactions in phenol (a high boiling protic solvent).
b) *N*-methyl pyrrolidin-2-one (NMP, a non-nucleophilic high boiling, aprotic solvent).
c) Methanol (a mildly-nucleophilic low boiling, protic solvent).

Phenol (a nucleophilic and participating solvent) provided compounds in variable yield but high purity, whereas NMP provides compounds in high yield but lower purity compared to phenol. The high-temperature (180-250°C) synthesis of 4-aminoquinolines, including *bis*quinolines, by nucleophilic displacement was both fast and efficient in both of these solvents. Unlike NMP, methanol, failed to promote reactions with aliphatic side chains under conventional reflux at atmospheric pressure.

Three types of side chains were investigated:

a) Side chains possessing one amine bound to an aryl or alky substituent.
b) An aliphatic diamine which was linear or cyclic.
c) Aryl-diamines.

It was discovered in the current study that the previously described, efficient three-day synthesis of *meta*-quine (in refluxing methanol at ambient pressure) could be accelerated to two minutes using commercial sealed vessels by conducting reactions in superheated methanol at 180°C (focused microwave irradiation). Using aromatic phenylene diamines, the crystal structures of aromatic bridged compounds, *ortho*-, *meta*- and *para*-quine were then obtained after screening numerous reaction conditions that promoted crystal growth. Each had only four rotatable torsional angles around the bonds.

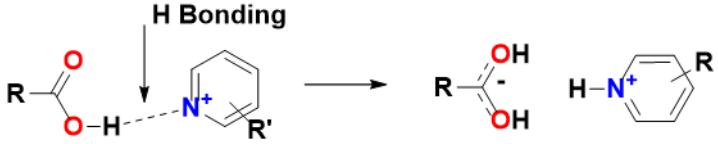

Figure 2.1. Example of salt formation.

Examination of solvent interactions of alcohols and carboxylic acids with the *quinoline* rings using both NMR (Ismail & Alizadeh., unpublished study) and crystallography (Ramon *et al*. **2014**), allowed hydrogen bonding patterns to be deduced, setting the scene for understanding how such compounds interact with proton donors (including haem) (Figure 2.5, Figure 2.6).

Surprisingly, examination of NMR chemical shifts of the proton at the 5th position (the proton on position 5 in quinoline molecule appears to be deshielded), suggest that that it is as

deshielded (or more de-shielded) as that bound at the 2nd position. Accordingly, *aza* substitution of this site may allow retention of antimalarial activity whilst changing its effect during xenobiotic drug metabolism reactions. This substitution typically reduced the lipophilicity of compounds when compared to the parent compounds.

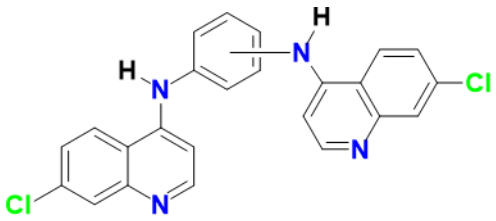

Figure 2.2. Aromatic bridged compounds, *ortho*-, *meta*- and *para*-quine.

2.1.1. Quinoline.

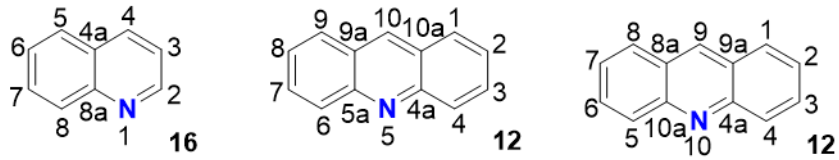

Figure 2.3. A quinoline (**16**) and an acridine (**12**).

Quinoline, (C_9H_7N 1-*aza*- naphthalene) (Figure 2.3), was first extracted from coal tar in 1834 by Friedlieb Ferdinand Runge (Anft, **1955**).

Notably, Ludwig Knorr had already synthesised this liquid as early as **1883** but this is consistent with Runge's endeavours who was noted for independently discovering many substances including quinine and caffeine. In its unsubstituted form, quinoline is rare and occurs naturally only in the phasmid (*Oreophoetes peruana*), a stick insect (Eisner *et al*., **1997**). Consequently, coal tar remains the most economic and viable source of commercial quinoline. This heterocycle can be used as a high boiling solvent (108-110°C/11mm Hg) especially for performing decarboxylation reactions (Patel *et al*., **2014**). In its substituted form, it is a useful building block to access more complex molecules, including natural products and pharmaceuticals (Patel *et al*., **2014**).

This study was principally concerned with the chemical 4,7-dichloroquinoline (Figure 2.4) (Price and Roberts, **1946**) and the compounds discussed were analogues/derivatives of the quinoline ring system, of which a limited number of compounds contain the acridine ring system (**23a**) (Figure 2.4).

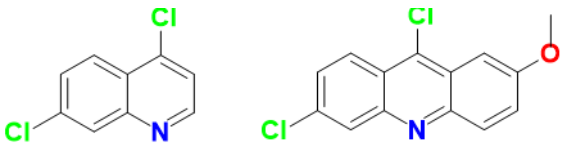

23 **23a**

Figure 2.4. Dichloroquinoline (**23**) and 6,9-dichloro-2-methoxyacridine (**23a**).

The first approach to facilitating the discovery of superior antimalarials to those currently in clinical use required examination of molecular features associated with antimalarial activity collated from the literature, especially those involving quantitative structure-activity relationships *in-vivo*. Consequently, correlation of published data relating to the *in-vivo* antimalarial activity of numerous chloroquine (**1**) and acridine analogues with the three-dimensional orientation of functional groups decorating these compounds allowed formulation of certain empirical rules and using appropriate methods, the pharmacophore (Dascombe, **2005**). These rules have previously proved useful in predicting which compounds should be synthesised and some of these can be screened both *in-vitro* and *in-vivo* to assess their usefulness as potential drug development candidates.

In the literature, not all of the compounds have been tested under identical conditions nor against the same parasite (or even species) or host making it important to re-test new and known compounds using a standardised antimalarial test system. Ideally, the Peters 4-day antimalarial test *in-vivo* is used (Peters, **1975**; Nogueira & Rosario, **2010**), with the data subsequently analysed using QSAR (Dearden *et al*., **2009**). However, this is time consuming and expensive and is only carried out using compounds possessing useful antimalarial activity against clones of human malarias cultured *in-vitro*.

Secondly, inexpensive antimalarial drugs are required due to the evolution of drug resistance within parasites exposed to drugs in current use in the developing world. The relatively high cost of existing antimalarial drugs makes them unaffordable to patients in affected areas especially in regions of sub-Saharan Africa, the far east and selected regions of South America.

2.1.2. The role of the bridging unit.

The apparent lack of cross-resistance between clinically useful antimalarial compounds that contain an aryl side chain i.e. amodiaquine (**9**) as well as those that contain an alkyl side chain e.g. chloroquine (**1**), makes amodiaquine (**9**) a potential treatment for malarial infections (Muller *et al*., **1996**; Olliaro *et al*., **1996**) but is marred with concerns about toxicity, generating semi quinone-imine.

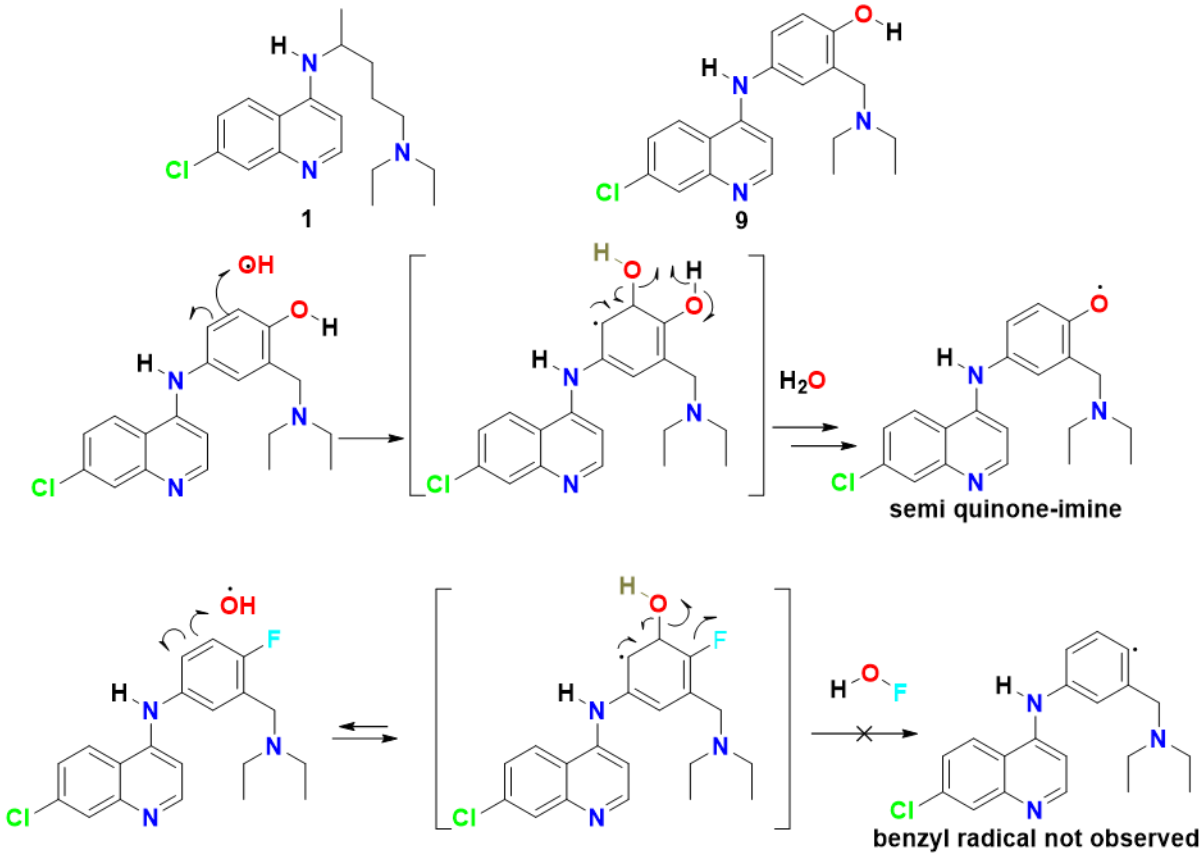

Figure 2.5. Reaction of amodiaquine (**9**) with a hydroxyl radical (Bisby, 1990).

For instance, prophylactic administration of amodiaquine (**9**) can induce severe adverse effects including agranulocytosis and hepatitis in sensitive individuals (Neftel *et al.*, **1986**; Cook, **1995**). Such adverse effects are associated with oxidation of the phenolic group, generating a free radical of amodiaquine (**9**) (Figure 2.5).

Irreversible binding of such intermediates to proteins, especially in liver microsomes prepared from human livers might explain the observed toxicity (Maggs *et al.*, **1988**; Bisby, **1990**; Harrison *et al.*, **1992**). Consequently, the oxidisable OH group has been bioisosterically replaced with a relatively inert fluorine atom or the amino methyl side chain transposed to a position that cannot form quinine imines. In the latter approach, even the supposedly superior compound **9** (SN-10,751) (Chapter **1**, page 20), first synthesised by Burckhalter *et al* (**1949**), subsequently named isoquine by investigators at University of Liverpool (O'Neill *et al.*, **2003**), has apparently been withdrawn from further development.

One reason for its poor toxicological profile may be a consequence of its potential to form

quinone-methides (Figure 2.6), which can also react with cysteine or glutathione, as well as thiols within protein side chains (Ismail & Alizadeh., unpublished study). Consequently, the apparent benefits of so called isoquine (**9**a) are outweighed by their poor toxicity profile.

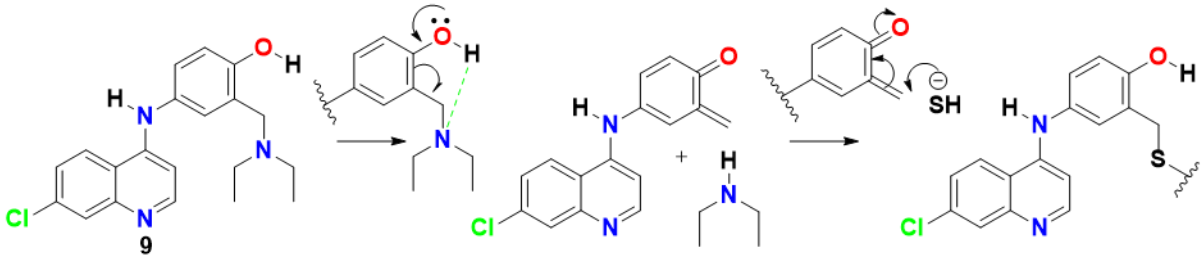

Figure 2.6. Mechanism illustrating potential toxication of isoquine(**9**a), forming toxic (**9**b) by interacting with cellular thiols such as glutathione or cysteine (RSH)(Ruscoe *et al*., 1995)

Any carbon atom bonded to the fluorine (Figure 2.5) is relatively electron poor since electron density coalesces around the fluorine, imparting ionic character to the bond.

O'Neill *et al* have studied the same compound suggesting it will have a better toxicological profile than amodiaquine (O'Neill *et al.,* **2009**). The mechanism above shows that the formation of HOF will be thermodynamically unfavourable (Figure 2.6). Two alternative strategies have been reported:

a) The replacement of the hydroxyl group by a bioisosteric hydrogen, and.
b) Reduction of the ring to a cycloalkyl compound (and concurrent replacement of the amino methylene side chain of amodiaquine (**9**)).

However, this side chain is considered vital for antimalarial activity (Werbel *et al.,* **1986**; Ruscoe *et al.,* **1995**).

In this investigation, amino methylene side chain has been replaced by a second proton acceptor, an additional 7-chloro-4-aminoquinoline ring which introduces an element of symmetry. In the second modification, the OH group on the aryl bridge is absent, consequently eliminating the possibility of inducing immediate quinone-imine toxicity *in-vitro* and *in-vivo*.

The rationale for synthesising aromatic bridge compounds is not only to avoid metabolism mediated formation of quinine imines but also:

a) To introduce a symmetry into *cyclo*-alkyl-bridged compounds generating *bis*quinolines (in which the 4-amino group corresponding to the amino methylene group (Ismail *et al.,* **1996**) is replaced by an aryl or heterocyclic amine, which may also be effective in antimalarial drug-receptor interactions (Ismail *et al.,* **1998**).
b) To produce achiral compounds, making both synthesis and purification easier.
c) To identify affordable compounds.

The two-step synthetic route detailed in this study is an affordable, one-pot synthesis since it utilises the 4,7-dichloroquinoline used in the manufacture of both amodiaquine (**9**) and chloroquine (**1**). *Bis*quinolines investigated: *ortho, meta, para*-quine (Figure 2.7).

The bridging unit should be chosen so that it minimises potential mutagenicity and

carcinogenicity of any molecules incorporating the precursor amine (Doubleday *et al*., **2006**).

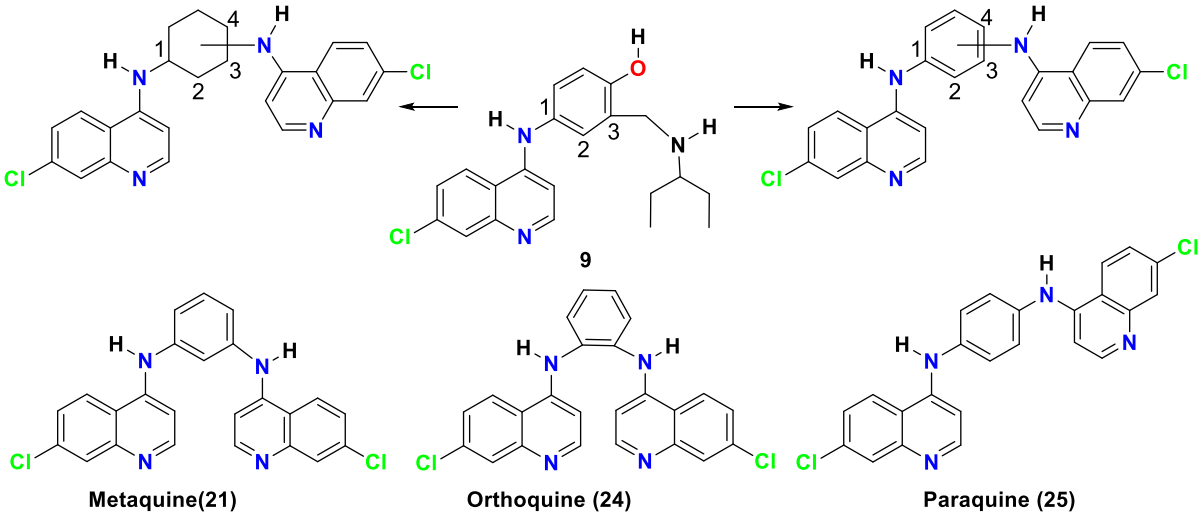

Figure 2.7. Diagram of *bis*quinolines: *ortho*, *meta*, *para-quine*.

Cycloalkyl bridged compounds with potential antimalarial activity have been constructed *in silico*. These explore some of the previously mentioned design criteria, especially *bis*quinolines similar to (±)- N^1,N^2-*bis*(7- chloroquinolin-4-yl)cyclohexane-l,2-diamine, *ortho*-quine (24) (Figure 2.7) (Vennerstrom *et al*., **1992**). Notably, both (±)-*trans*- and *cis*-N^1,N^2-*bis*(7-chloro-quinolin-4-y1)cyclohexane-1,2-diamine are active against *Plasmodium berghei* in mice (Ismail *et al*., **1996**; Ridley *et al*., **1997**) but their mechanism of antimalarial action requires further refinement.

The question to be considered whether haem is a possible target for these compounds and if so, can these compounds be rationally designed to be superior in antimalarial activity to molecules in current clinical use? It maybe that the optimal compounds have already been identified.

By changing the hybridisation in the bridging unit, from (sp^3 to sp^2) in the cycloalkyl bridging unit to produce an aromatic ring, a planar non chiral molecule was designed. After testing its antimalarial activity *in-vivo*, a potent prototype, i.e. *N^1,N^2-bis(7-chloro-quinolin-4-y1)phenylene- 1,2-diamine* (*ortho*-quine) (**24**) (Figure 2.7) was produced. Hence other isomers were also examined since they should have the same lipophilicity but the averaged distances between the nitrogen atoms in the molecules have different distances. Originally this compound was considered useful as a potential amodiaquine substitute (Ismail *et al.*, **1996**; Dascombe *et al.*, **2005**).

The aryl-bridged *bis*quinolines have been reported and tested for antimalarial activity *in-vivo* against *Plasmodium berghei*, however, their mechanism of action was unknown at the time. The aryl-bridged *bis*quinolines were re-synthesised in the current study, using methods with improved yield and reduced reaction time to those reported by Ismail *et al* (**1998**).

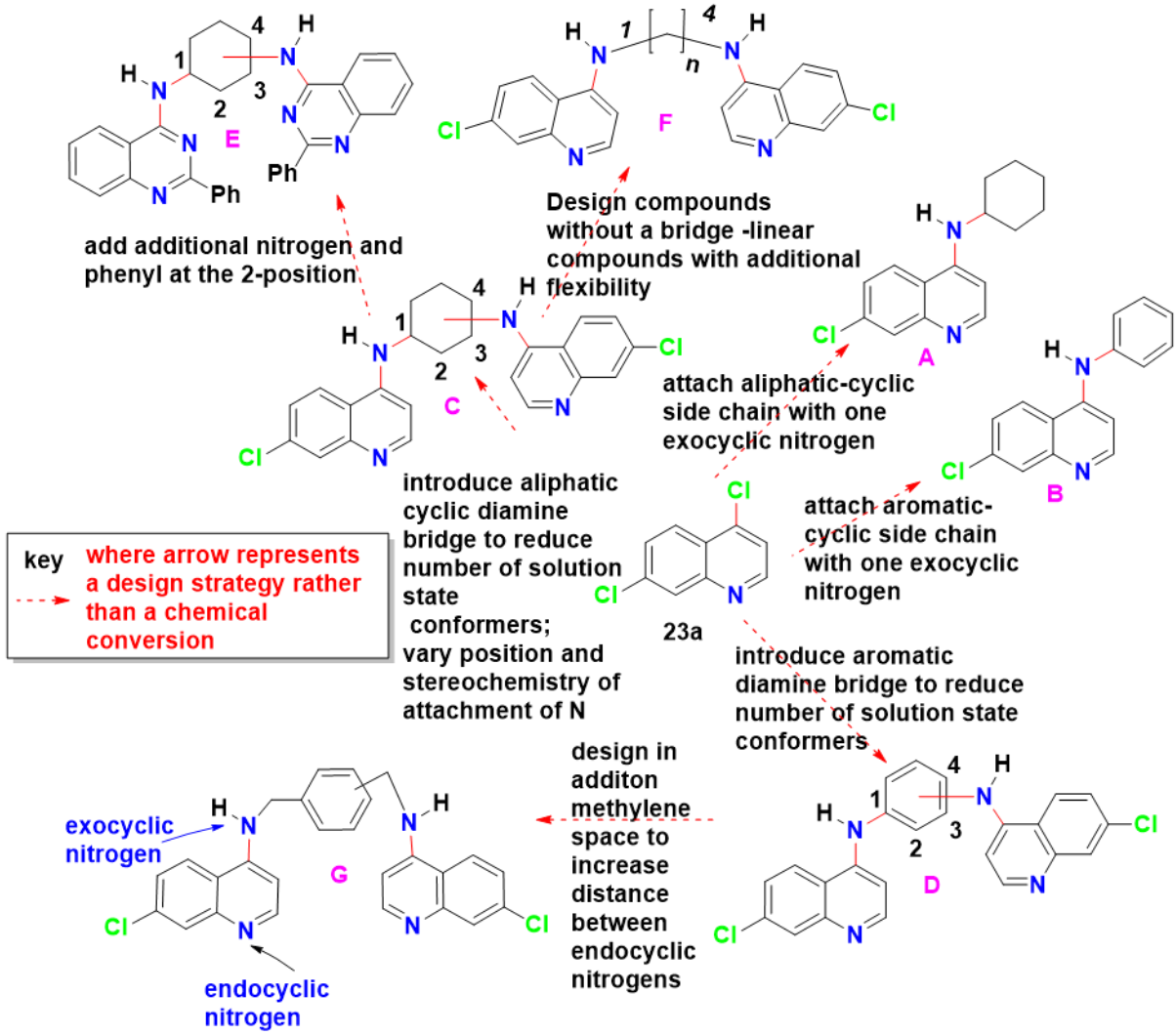

Figure 2.8. Diagram of various rotational bonds in aryl and cyclo-alkyl bridge compounds.

The cyclohexane bridging unit in (±)-*trans*- and *cis*-N^1,N^2-*bis*(7-chloroquinolin-4-yl)cyclohexane-1,2-diamine (**26**) allows these molecules to populate a restricted number of solution-state conformers (Figure 2.9) compared to chloroquine (**1**), which has a flexible side chain.

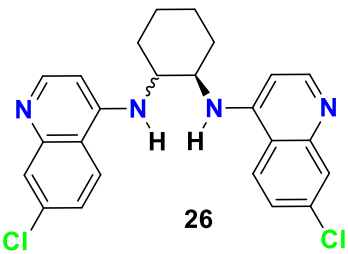

Figure 2.9. (±)-*trans* and *cis*-N^1,N^2-*bis*(7-chloroquinolin-4-yl)cyclohexane-1,2-diamine (**26**).

2.2. Synthesis.

An initial goal was to synthesise *bis*quinolines of type C-D (Fig 2.8). The use of a cyclic alkane diamine as the bridging unit restricted the number of state conformers of the *bis*quinolines (Basco *et al*., **1994**).

Therefore, in this study, a range of *bis*quinolines bearing a cyclohexyl, a piperidyl or a piperazine moiety were synthesised using 4,7-dichloroquinoline and the appropriate diamine.

The second series of compounds D were analogues in which a phenylene diamine ring was used, to further reduce a number of conformers since the molecules contained only four rotatable bonds. Both were compared to lipophilic monomeric counterparts. In addition, rigid molecules are known to have a markedly different log P profile than the corresponding flexible compounds.

Biological activity for such molecules seemed very promising as N^1,N^2- *bis*(7-chloroquinolin-4-yl)-phenylene-1,2-diamine and N^1,N^3- *bis*(7-chloroquinolin-4-yl) – phenylene-1,3-diamine were found to be active against *P. berghei in-vivo*.(ID_{50} = 30 mg /kg and ID_{50} = 1.2 mg /kg) (Ismail *et al.*, **1998**). In this model of malaria, chloroquine (**1**) was active *in-vivo* at ID_{50} = 4.3 mg /kg. Additionally, Elslager demonstrated that certain 2,4-disubstituted quinazolines proved to have some good antimalarial activity (Elslager *et al*., **1981**).

Though the *bis*quinolines do not possess any substituent on the 2-position, the insertion of a nitrogen on the 3-position of the quinoline ring could give additional information as to the kind of interaction involved at the 3-position of the quinazoline ring, if active or not. Thus, alkyl and aryl *bis*quinazolines (C and D respectively) were synthesised and their activity compared with those of corresponding *bis*quinolines.

2.2.1. Other solvents used in S_NAr reactions.

Useful replacements include methanol for aromatic di-amines, and *N*-methyl-2-pyrrolidone for aliphatic di-amines, but ethoxyethanol proved unsuitable (Vennerstrom *et al.*, **1992**).

2.2.2. Acid scavengers.

Nucleophilic substitution between 4,7-dichloroquinolines has also been conducted in the presence of a suitable acid scavenger which may be inorganic e.g. Na_2CO_3 (Singh *et al*., **1971**) or organic (e.g. triethylamine) (Vennerstrom *et al.*, **1992**). Triethylamine as hydrogen chloride scavenger has been used to construct both alkyl and aryl-bridged quinolines.

2.2.3. Electronic effects in the displacement of the chlorine at the 4-position using phenol.

The nature of the substituents on the quinoline ring and their position affect nucleophilic substitution. Early investigators divided the effects into the two regions of the quinoline ring (Baciocchi *et al*., **1958**). The first effect involves substituents on the carbocyclic ring, the second on the pyridine ring.

2.2.4. Effects of the substituents located on the carbocyclic ring.

Reactivity of a chlorine atom on the 4-position of the quinoline ring can be affected by remote substituents located on the 5-, 6-, 7- and 8-positions (Figure 1.14). Most investigations, however, have involved the 6- and 7- and 8- positions in the case of 4-chloroquinoline, since a substituent at the 5^{th} position causes steric hinderance to incoming nucleophile (Lutz *et al*., **1971**).

Two bulky substituents occupying the 4^{th} and 5^{th} positions exert an unfavourable *peri* interaction upon one another. For instance, (Baciocchi *et al*., **1958**) examined the reaction of 4-chloroquinolines (substituted at positions 5-,6-,7- or 8-) with various nucleophiles, especially the methoxide anion.

Their results indicate methoxy-dechlorination varied according to the nature of the substituent in the 6-position, the rate being accelerated with an electron-withdrawing group (-M effect), such as a nitro group and was depressed with an electron-donating group (+M effect), such as dimethyl amino group. Electron-donating (+M) groups in the 6-position exhibited a stronger deactivating conjugative effect on the 4-chloro than the same group at the 7-position, the situation being reversed by an electron-withdrawing group at the 6-position.

The presence of nitro groups at the 5- and 8-positions (Illuminati *et al*., **1964**) revealed that the 5-nitro group depressed the reaction rate in comparison to the 7-nitro group under comparable reaction conditions. One explanation is the unfavourable steric hindrance between the nitro group and the chlorine at the 4-position of the quinoline ring.

This effect has led to reaction failures if the group becomes excessively large, such as the trifluoromethyl group (Lutz *et al*., **1971**). The activating effect of the substituents decreases in the order: 6-NO_2 > 7-NO_2 > 7-Cl > 7-Br > 6-Cl > 6-H > 7-MeO (Illuminati *et al*., **1964**).

However, Surrey *et al* (**1946**) have shown that it is possible to react compounds containing a moderately bulky substituent such as chlorine on the 5^{th} position to form the corresponding benz-Dichloro-4-aminoquinoline derivatives in good yield (85-98%). (Surrey *et al*., **1946**).

Consequently, all of these substituents have been incorporated into 4-aminoquinolines

that have been used to explore antimalarial activity both *in-vitro* and *in-vivo*. In all cases, the best antimalarial activity *in-vivo* activity was shown by halogens occupying the 7th position, especially chlorine (Werbel & Thompson, **1972**; Vippagunta *et al*., **1999**).

2.2.5. Effects of substituents located on the pyridine ring.

As with the substituents in the carbocyclic ring, electron-withdrawing (-I) groups such as trifluoromethyl enhanced the S_NAr reaction rate, if present at the 2-position of the quinoline ring. Illuminati *et al* found that activation followed the following order: 2-*aza* > 2-CF_3 > 2-H > 2-Ph > 2-Me_2N (Illuminati *et al*., **1964**; Sample & Senge, **2021**). Alkoxy groups were strongly deactivating substituents, especially if located on the 2nd position (Belli *et al*., **1963**). One explanation may be mesomeric interactions present in the starting material (2-alkoxy-4-chloroquinoline) which cause a decrease in the electron-accepting ability of the quinoline (Figure 2.10).

2.2.6. Solvent effects in the displacement of the chlorine at the 4-position using Phenol.

Phenol as solvent/reagent was introduced by the investigators (Magidson & Grigorowski, **1933**). In a subsequent paper, they showed that 9-chloroacridines also react with phenol to form the 9-phenoxyacridines, which can be displaced by nucleophilic amines to form the 9-amino derivative such as mepacrine (Magidson & Grigorowski, **1936**; Staderini *et al*., **2013**).

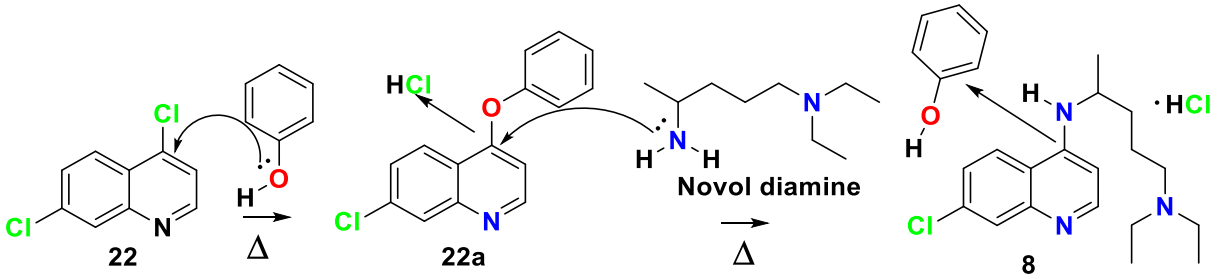

Figure 2.10. Nucleophilic substitution of an amine and a 4-chloroquinoline, with phenol as solvent.

Phenol acts as a nucleophile and solvent (Figure 2.10), serving a dual function (Surrey & Cutler, **1951**). In the mid 1940's, its use was extended to 4-aminoquinolines, especially with an alkyl side chain (Surrey & Cutler, **1951**). For instance, it was shown that 4,7-dichloroquinoline, dissolved in hot phenol in the presence of N^1-N^1-diethyl-1,4-pentanediamine (made by Winthrop Chemical Company and called Novol diamine) reacted via an intermediate which was identified as 7-chloro-4-phenoxyquinoline (**22a**) to give chloroquine (**1**) (Surrey & Cutler, **1951**, Cheruku *et al*., **2003**).

Racemic (±) chloroquine (**1**) is also prepared by condensation of N^1,N^1-diethyl-1,4-pentanediamine with 4,7-dichloroquinoline in anhydrous phenol (Surrey & Cutler, **1951**)

rather than the original IG Farben preparation of Resochin with high boiling mineral oil (Andersag, **1939**). The effect of the solvent on the reaction between 4-chloroquinoline and aliphatic amines was investigated by Surrey & Cutler (Surrey & Cutler, **1951**) whereby phenol improved the yield by 50%.

Physical organic studies involving piperidino dechlorination of 4-chloroquinoline and the influence of solvent on reaction rates have been reported (Chapman & Russel-Hill, **1956**; Baciocchi *et al*., **1958**).

These classical syntheses of 4-substituted quinoline antimalarial heterocycles involve thermal condensations between 4-haloquinolines and a suitable amine or, less frequently, a 4-aminoquinoline with an alkyl or aryl halide at around 180°C.

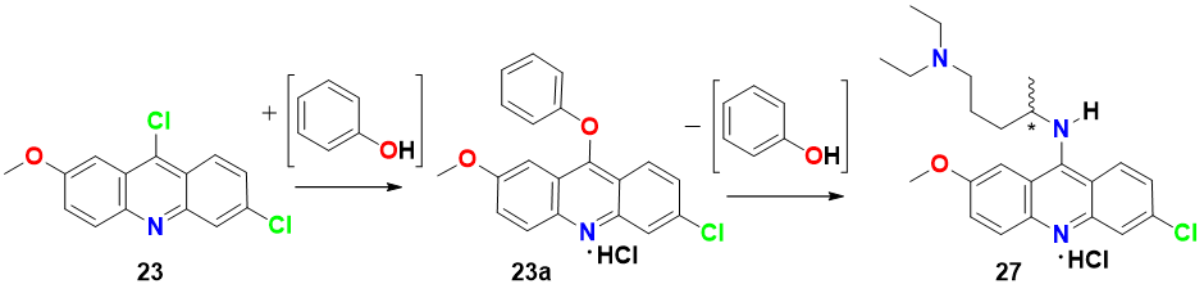

Figure 2.11. 9-chloroacridines also react with phenol to form the 9-phenoxyacridines, which can be displaced by nucleophilic amines to form the 9-amino derivative such as mepacrine (**27**) (Magidson *et al*., 1936).

Subsequently, phenol was adopted in the synthesis of 4-aminoquinolines (Surrey & Cutler **1951**; Staderini *et al*., **2013**). Some *bis*quinaldines were synthesised using phenol as solvent (Schock, **1957**) (Figure 2.11). Refluxing diamines with the appropriate halo-quinaldine (150-160°C for 4 to 5 hrs) provided the desired *bis*quinolines between 29 and 90% yield (Schock, **1957**). The *bis*quinolines obtained were variously substituted on the 6-position with amino, dimethylamino, methoxy, chlorine or nitro groups. Sinha and colleagues also used anhydrous phenol to prepare *bis*quinaldines (Sinha *et al*., **1977**), where a 4-chloro-7-nitroquinaldine (4-chloro-2-methyl-quinoline) was reacted with various diamines to produce various *bis*quinolines in good to excellent yields (52-99%, 130-135°C, 18 hrs). The reaction proceeded well especially with various alkyl or alkylamino groups. However, the use of phenol is currently unpopular due to its corrosive properties, high expense and environmental concerns.

In the above reactions, phenol (pKa = 10.0) serves simultaneously as solvent and proton donor. At room temperature, the phenol molecule has weak tendencies to lose the H^+ ion from the hydroxyl group, resulting in the highly water-soluble phenolate anion C_6H_5O-, (phenoxide anion) (March, **1985**). Compared to aliphatic alcohols, phenol is more acidic by a factor of 10^6. One explanation for the increased acidity is resonance stabilization of the phenoxide anion by the aromatic ring. Alternatively, it may be rationalised as an orbital overlap between the oxygen's lone pairs and the aromatic system. The dominant effect could

be inductive; the comparatively more powerful inductive withdrawal of electron density that is provided by the sp^2 system (compared to a sp^3 system) increases oxyanion stabilization.

When haloquinolines and halo acridines accept protons on to the endocyclic nitrogen, the carbon bearing the chlorine atom is the target for nucleophilic substitution (Smalley, **1977**).

After this study was complete, microwave accelerations were reported for the synthesis of various acridines (Staderini *et al*., **2013**) Since focused microwave irradiation of equimolecular mixtures of 9-chloroacridines, 4-chloroquinolines and 4-chloroquinazolines with amines in the presence of 2 equivalents of phenol allowed efficient synthesis of aminated heterocycles it is consistent with the results reported here that at least one molecule is required to displace the halogen and the other acts as solvent. Haloquinolines have been extensively reviewed in 1977 by Smalley.

2.2.7. Nucleophilic displacement of the chlorine atom from 4-chloroquinolines.

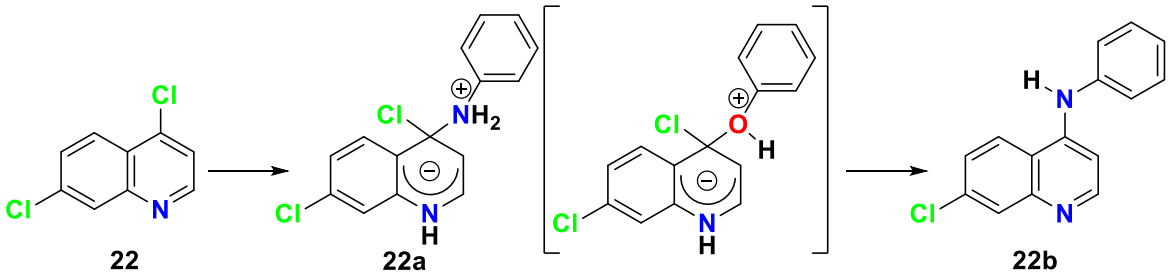

Figure 2.12. Substitution nucleophilic displacement of chlorine atom with a phenyl amine.

The endocyclic nitrogen heteroatom within halo-quinolines predisposes halogens at the 2- and 4- position towards nucleophilic substitution (Figure 2.12). One classical interpretation invokes intermediate anions that are stabilized by resonance effects. Expulsion of the halogen can occur by several routes. Six nucleophilic mechanisms are known namely S_NAr (addition elimination mechanism), the aromatic S_N1 mechanism, the benzyne mechanism, the free radical $S_{RN}1$ mechanism, ANRORC mechanism and Vicarious nucleophilic substitution.

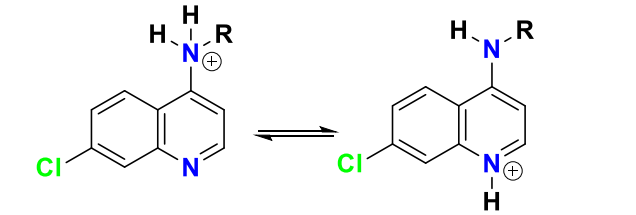

Figure 2.13. Classification of protonation sites.

Currently evidence favours, a nucleophilic aromatic substitution (S_NAr) mechanism (Bunnett *et al*., **1951**, **1970**) whereby the nucleophile displaces a good leaving group, which in this case is a halide anion (Figure 2.13).

Such a mechanism involves a bimolecular process whereby the transition state bears both

the incoming and the leaving groups, the so-called Jackson-Meisenheimer Complexes (Terrier, **1984**) (Figure 2.14). Benzyne type routes would lead to scrambling of the incoming amine to both termini of the quinolinyl-aryne (Figure 2.14).

In the case of 4,7-dichloroquinoline, to our knowledge, evidence for this later mechanism's involvement has never been encountered, the attack at the 4-position has been confirmed using crystallographic studies as well as MS investigations.

It is important not to reflux haloquinolines in pure amines (in the absence of solvent), since this led to highly exothermic reaction, including HCl liberated from the substitution reaction, entering a catalytic phase which is occasionally explosive (Figure 2.16).

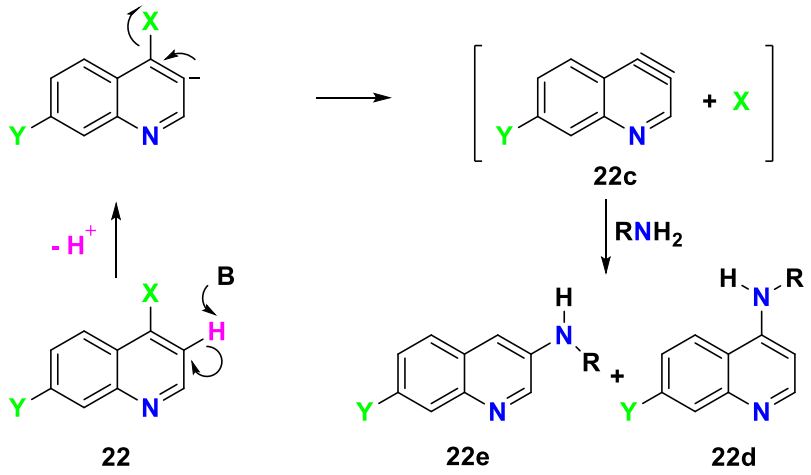

Figure 2.14. Benzyne type routes (Terrier, 1984)

The resultant reaction rate increases, promotes halogen lability of the 2nd and 4th positions, by protonation of the endocyclic ring nitrogen (NMR and DFT experimental evidence; Ismail &Drew unpublished) (Figure 2.15).

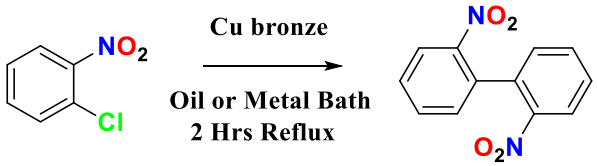

Figure 2.15. Example of the formation of a biaryl using Ullmann conditions.

A violent exothermic reaction, resulting in damage to CEM microwaves was one of those unfortunate events.

Figure 2.16. Example of haloquinolines exothermic reaction.

2.3. Results and discussion.

A number of solvents including high boiling mineral oil (B.P > 200^{o}C), Hexamethylphosphoramide (HMPA), sulfolane, NMP, diphenyl-ether, biphenyl, DMSO, water, methanol, ethanol, propanol and phenol were screened. Some of these solvents were found not suitable in synthesis of *mono* and *bis*quinolines: biphenyl and diphenyl-ether persisted in the products and their use was abandoned. Similarly, sulfolane, DMSO and hexamethyl phosphoramide (HMPA) proved too difficult to remove from the *bis*quinolines and often caused the products to decompose. The white mineral oil, INS No: 905e, and the boiling point of the mineral oil (INS), while above 200, varied from batch to batch, were also rejected. HMPA was considered especially noteworthy since it selectively solvates cations, and accelerates some difficult S_NAr reactions. Although, HMPA is considered only mildly toxic, its propensity to cause nasal cancers in rats led it to be abandoned. Of all the above solvents, only three proved sufficiently safe, versatile and easy to remove from the desired target compounds, namely, NMP, phenol and methanol.

2.3.1. Use of phenol as a solvent: advantages and disadvantages.

Solvent has effects in the displacement of the chlorine at the 4-position. Studies on the piperidino dechlorination of 4-chloroquinoline and the influence of solvent on reaction rates have been reported (Baciocchi *et al*., **1958**; Chapman & Russel-Hill, **1956**). The effect of altering the solvent on the reaction between 4-chloroquinoline and aliphatic amines were investigated (Surrey & Cutler, **1951**). Using phenol as a solvent improved the yield by 50%. It was shown that 4,7-dichloroquinoline dissolved in hot phenol in the presence of N^1-N^1-diethyl-1,4-pentanediamine reacted *via* an intermediate as 7-chloro-4-phenoxyquinoline (Surrey & Cutler, **1951**) to give chloroquine (**1**). Phenol acted in these cases as both reactant and solvent, in agreement with data for *mono*quinolines synthesised by Motiwala in 2007, using a domestic microwave oven (Motiwala *et al*., **2007**).

Consequently, when haloquinoline and halo acridines accept protons on to the endocyclic nitrogen, it activates the carbon bearing the chlorine atom towards nucleophilic substitution.

Phenol as solvent/reagent was introduced (Magidson and Grigorowski *et al*., **1933**), and in a subsequent paper these investigators showed that 9-chloroacridines also react with phenol to form the 9-phenoxyacridines, which can be displaced by nucleophilic amines to form the 9-amino derivative (Magidson & Grigorowski, **1936**). Subsequently, phenol was adopted in the synthesis of 4-aminoquinolines (Surrey & Cutler, **1951**).

Practical replacements for phenol have been sought due to its corrosive nature which, include methanol for aromatic di-amines and the polar aprotic solvent *N*-methyl-2-pyrrolidone for aliphatic di-amines.

Nucleophilic substitution between 4,7-dichloroquinoline and an amine have also been

conducted in the presence of a suitable acid scavenger which may be inorganic Sodium carbonate or organic (e.g. triethylamine) (Singh *et al*., **1971**;Vennerstrom *et al*., **1992**; Ismail *et al*., **1996**). Triethylamine as hydrogen chloride scavenger has been used to construct both alkyl and aryl bridge Quinolines. (Ismail *et al*., **1998**).

Though cycloalkyl bridged compounds such as (±)-N^1,N^2-*bis*(7-chloroquinolin-4-yl)cyclohexane-1,2-diamine were successfully synthesised in this study using phenol, the yields were poor (2-25%)(Fig 2-18).

The required *bis*quinolines were prepared in adequate yield (84%) using *N*-methyl-2-pyrrolidone, as a suitable solvent (Cain *et al*., **1978**).

Displacement of chlorine from 4,7-dichloroquinoline, which is a solvent-dependent process, should be promoted with protic solvents like ethanol compared with aprotic ones such as toluene. Ethanol, methanol and DMSO (Muller &, Siegfried, **1972**) were used as solvents in this study, they did not promote the formation of *ortho*-quine at reflux (Ismail *et al.*, **1998**) but were readily formed when microwave irradiation was employed. (this study).

The reaction time of 1-3 days for the synthesis of *bis*quinolines (Ismail *et al.*, **1998**) limited both the number of compounds and the cost effectiveness of the study. The suitability of diphenyl ether, a high boiling solvent for accelerating the formation of *ortho*-quine was, therefore, studied (Fig 2-18). However, prolonged heating under reflux in diphenyl ether, encouraged the formation of novel compounds containing three molecules of quinoline to one of the diamines and fast atom bombardment mass spectrometry (FAB MS) was used (Compounds **24a**, **26e**). They are completely insoluble in most deuterated solvents at room temperature. Some Mass spectral data indicated a possible trimer (not shown).

2.4. Synthesis of *bis*quinolines via Ullmann reaction, biaryl compounds.

The Ullmann reaction is routinely employed for the synthesis of biaryl compounds when aryl halides react with copper or other metals such as nickel, silver, palladium and platinum (Hassan *et al.*, **2002**). The postulated reaction mechanism invokes aryl radical formation which reacts with Cu^+ to form aryl-copper (I) complexes. The latter then couples with the precursor aryl halide to form a symmetrical biaryl compound. For instance, 2,2′-dinitrobiphenyl is synthesised from *o*-chloronitrobenzene in the presence of excess of activated copper (2.5 equivalents) to give yield 54%.

Although aryl iodides are used most often, chloride and bromides also undergo the reaction. The ease of formation follows normal bond strength mediated lability i.e. I>Br>Cl. For example, the molecule represented by CH_3X has a bond dissociation energy (BDE) of 57.6, 72.1, 83.7 kcal/mol representing carbon–X bonds to iodine, bromine and chlorine, respectively (Blanksby and Ellison, **2003**). Alternatively, by employing two different aryl halides, two symmetrical and one unsymmetrical compound is produced (Figure 2.17)

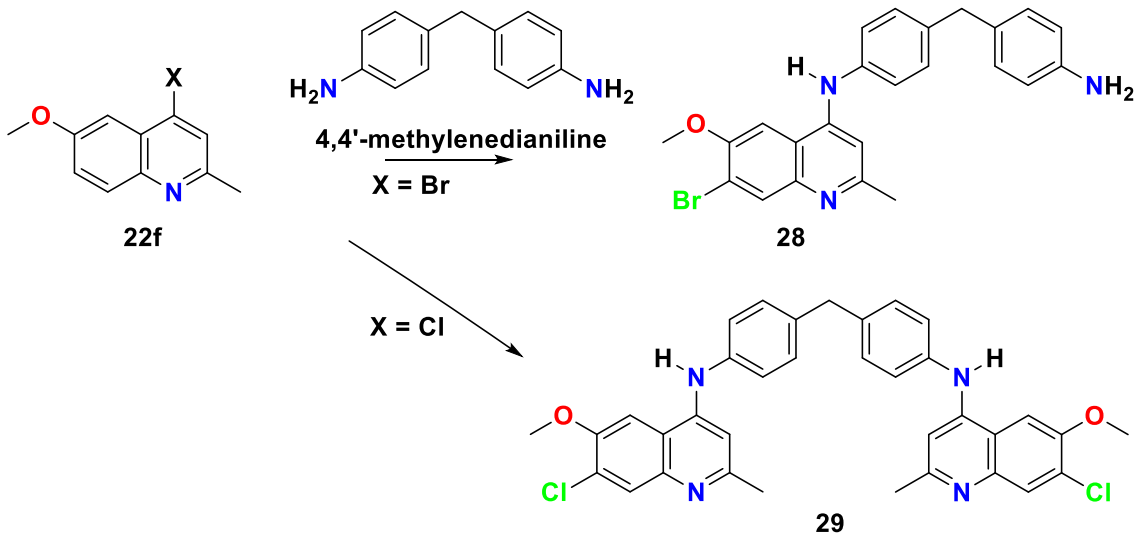

Figure 2.17. Synthesis of either *mono*quinolines vs. *bis*quinolines depending on nature of leaving group under copper catalysis.

However, depending on the reactivity of the halides and using steric hindrance on the aryl rings, one product is exclusively formed. For instance, the reaction between picryl chloride and iodobenzene gives solely 2,4,6-trinitrobiphenyl (March, **1985**).

As expected, the yields of Ullmann coupling reactions are highly influenced by the position and the nature of substituents on the aryl rings (Figure 2.17).

The reaction has been employed in 4-substituted quinolines. For instance, using Ullmann conditions (Slater *et al*., **1930**) when an excess of 4,4'-methylenedianiline was heated in the melt phase with 4-chloro-6-methoxy-2-quinoline, the *bis*quinoline *N,N'-(methylenebis(4,1-phenylene)bis(6-methoxy-2-methylquinolin-4-amine)* was exclusively produced (Figure 2.18).

Interestingly, the intermediate monomer was obtained when 4-bromo-6-methoxy-2-methylquinoline was used since it was more reactive than the 4-chlorocompound which required more forcing conditions leading to *bis*quinolines (Slater, **1931**).

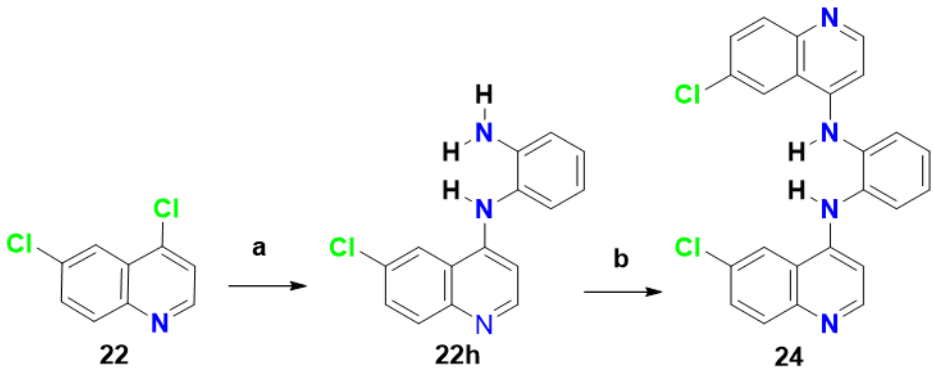

Figure 2.18. Vennerstrom *et al*., 1992 at Roche, who reported and produced certain *bis*quinolines.

The *bis*quinoline was produced during a study involving 2,3-benz-γ-carbolines

(Kermack and Storey, **1950**). Despite Kermack's WWII involvement in finding novel antimalarials, such compounds were not tested until 1998 (Ismail *et al.,* **1998**). Our group's renewed interest in aryl bridged quinolines began in early 1990's and the first preparation of *ortho*-, *meta*- and *para*-quine by looking at the work done by Vennerstrom (Vennerstrom *et al*., **1992**) (Figure 2.18a) who reported a variety of alkyl bridged *bis*quinolines one of which was further examined at Roche, produced a number of alkyl and aryl bridged *bis*quinolines (Hofheinz *et al*., **1998**).

A number of 4-amino substituted 2,8-*bis*(trifluoromethyl)quinoline derivatives were synthesised by Mital *et al* to evaluate activity against *Mycobacterium tuberculosis* (M.tb strain H37Rv) *in-vitro*. Most of the compounds demonstrated notable antimycobacterial activity and are comparable to first line antituberculosis drugs currently in use. However, they did not evaluate these compounds against *Plasmodia* (Mital, **2006**).

In the search for potential new anticancer drugs, Hu *et al* reported an efficient synthesis of *bis*-tetrahydroaminoacridine (*bis*-tacrine) and its congeners involving *bis*-amination of 9-chlorotetrahydro-acridine (Hu, **2001**, Zhu *et al*., **2002**). Subsequently, compounds that bind to DNA have also been investigated (Sebestik *et al.,* **2006**).

Newer trifluoromethyl containing *bis*quinolines have been described. (Kgokong *et al*., **2008**). A series of *N*,*N*-*bis*(trifluoromethylquinolin-4-yl)- and *N*,*N*-*bis*(2,8-*bis*(trifluoro-methyl)quinolin-4-yl) diamino alkane and piperazine derivatives were synthesised by reaction of both 4-chloro group on the 2-trifluoromethyl- and 2,8-*bis*(trifluoromethyl)-quinoline by diaminoalkane or piperazine groups (Kgokong *et al*., **2008**). Results of *in-vitro* antimalarial activity and evaluations of these compounds against the chloroquine (**1**)-sensitive (D10) and chloroquine (**1**) resistant (*K1*) strains of *Plasmodium falciparum* suggested that compounds with trifluoromethyl groups in both the 2nd and 8th positions, coupled with diaminoalkyl bridging chains of 2 to 6 carbon atoms exhibit a slightly higher activity than compound with only a trifluoromethyl group at position 2 (Kgokong *et al*., **2008**).

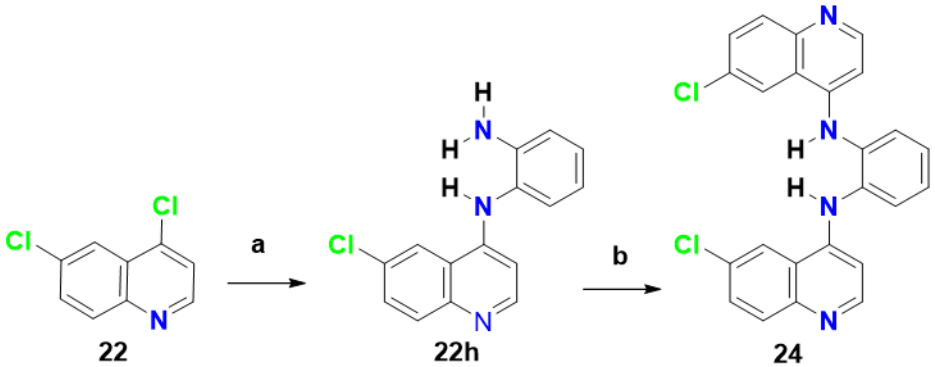

Figure 2.18a. General *bis*quinolines synthesis. (Vennerstrom *et al*., 1992)

2.4.1. Base scavengers.

Triethylamine was chosen as a convenient volatile and available HCl scavenger.

Although Singh *et al* have utilised both Na_2CO_3 and K_2CO_3, they proved ineffective at high temperatures as also found by Vennerstrom *et al* (**1992**). Notably, triethylamine was also miscible with NMP. Other tertiary amines, such as *N*-methylpiperidine could also be used, but offered no significant advantage over triethylamine in these studies. Furthermore, NMP's low volatility was a distinct disadvantage during work-up and purification (Figure 2.19).

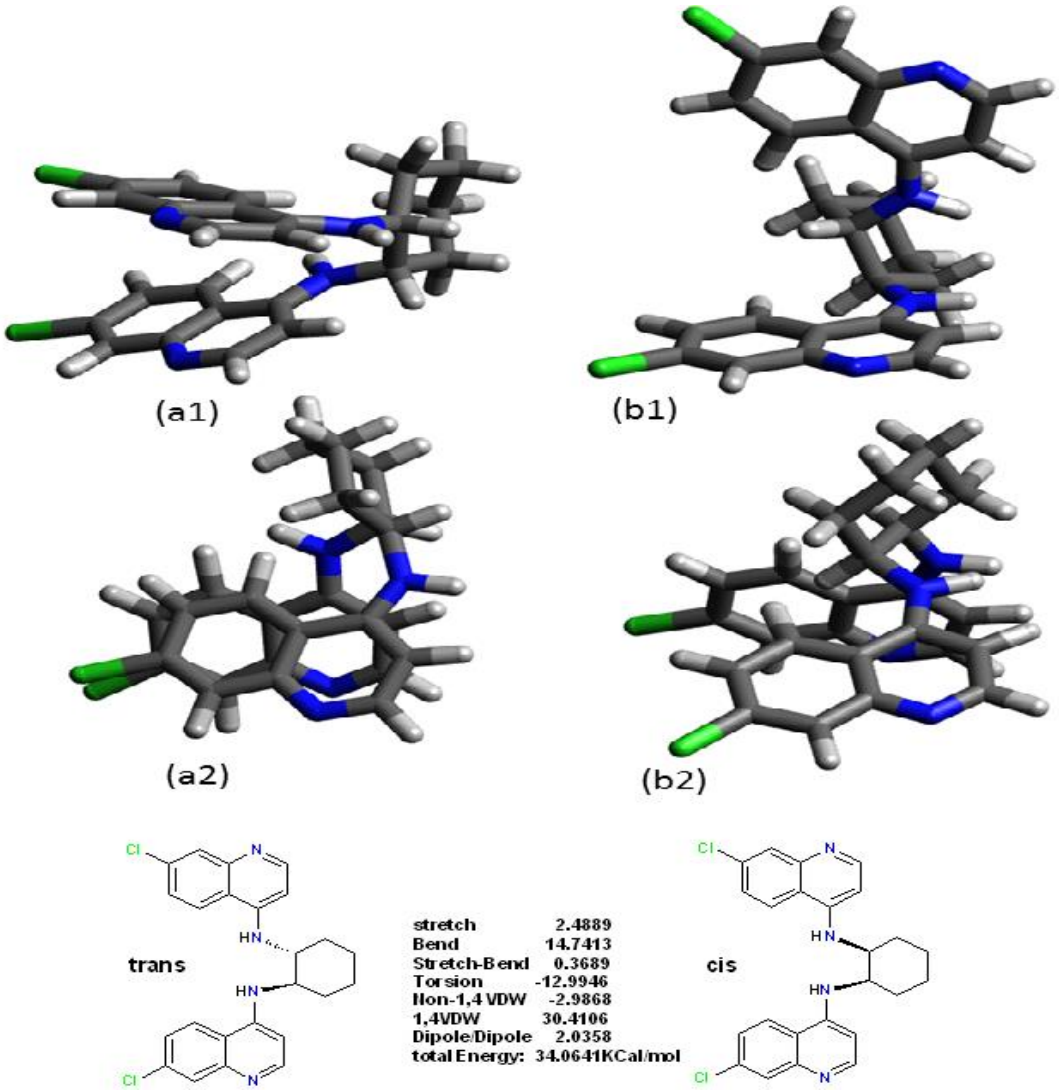

Figure 2.19. Structural formulae of compound: a) *trans*-(±)-N^1,N^2-*bis*(7-chloroquinolin-4-yl)cyclohexane-1,2-diamine and b) the *cis*-isomer.

2.4.2. Optimum temperature range.

A useful temperature range for bimolecular nucleophilic displacement of 4-haloquinolines in solution lies between 180-210°C, with 180°C being preferred since the aryl formation occur at lower temperatures, aliphatic compounds require higher temperatures. Reaction temperatures greater than 250°C always led to the formation of both, the desired compounds and high molecular weight products. *Mono*- or *bis*-4-aminoquinolines were not

formed when 4,7-dichloroquinoline was heated with aliphatic substances such as (±)-*trans*-1,2-diaminocyclohexane at temperatures below 170°C, the lowest temperature at which a thermally assisted nucleophilic displacement will take place, in acceptable yield.

2.4.3. Synthesis of aromatic *bis*quinolines.

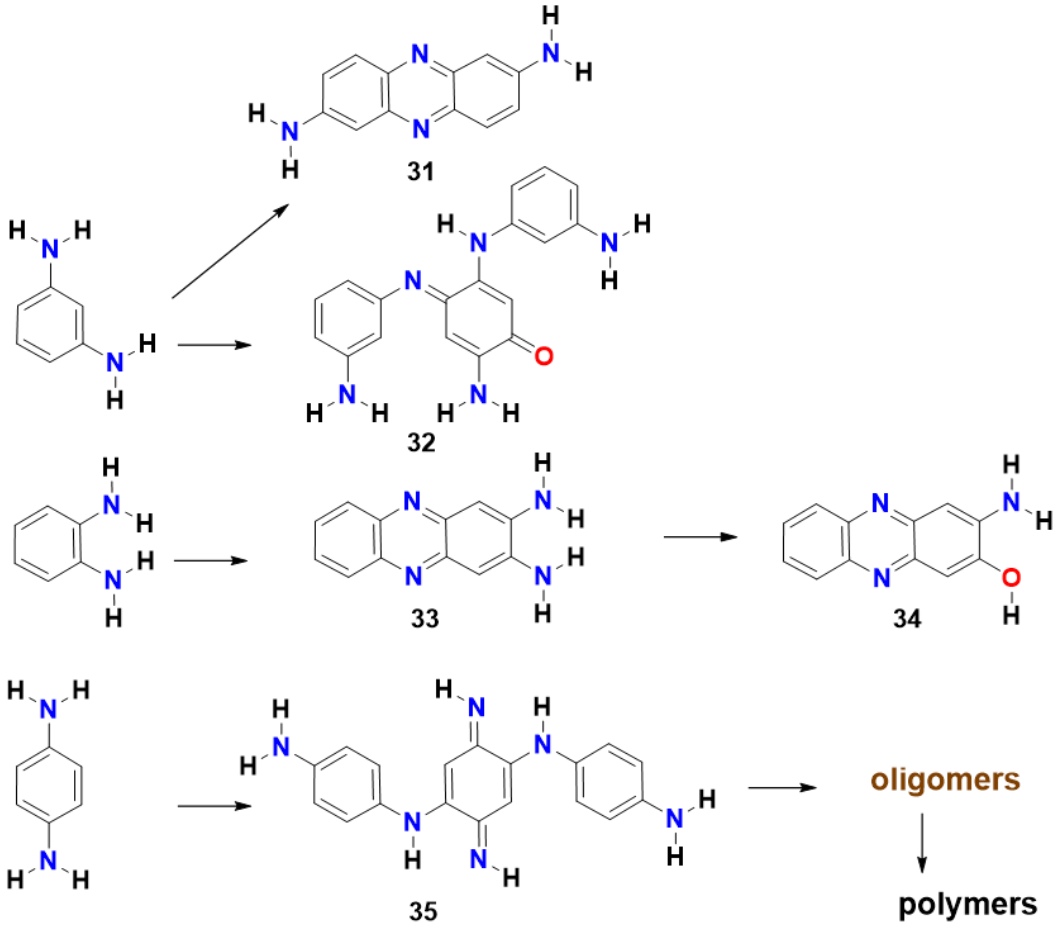

Figure 2.20. Putative Side products formed from oxidation of phenylenediamines including phenazines. (molecular ions consistent with Ms data)

Aryl bridged *mono*- and *bis*quinolines were synthesised using a published method (Barlin & Jiravinyu, **1991**) that uses HCl-MeOH (pH 4.7) as the solvent.

CH_3OH:water:hydrochloric acid (3:1: trace, pH 4.7) proved convenient for synthesising of aryl-bridged *bis*quinolines but failed for alky bridged diamines (Figure 2.19). Reaction side-products, in addition to the corresponding monomers, were complex oxidation products of the phenylenediamines (i.e. *ortho*, *meta* and *para*-quine) (Figure 2.20). In the presence of oxygen, products can be rather complex as shown above. Many of these compounds were highly coloured and can also be mutagenic.

For instance, Kami *et al*. have found that in the presence of ozone, the synthesis of one of the mutagens can be optimised (Kami *et al*., **2000**). In contrast, *m*-phenylene diamine can also form a 2,7-diaminophenazine (Watanabe *et al*., **1989**).

Exclusion of oxygen reduced the yields of these high molecular weight side products, (Barlin & Jiravinyu, **1991**) which were readily separated from the target compounds by

washing with excess acetone and if required re-crystallization of compounds such as *meta*-quine from pyridine and activated charcoal.

Accurate determination of the melting point transition of *bis*quinolines by visual observation proved impossible as these compounds either charred or decomposed into dark material. Investigation of *ortho*-quine by differential scanning calorimetry (DSC) indicated the onset of the phase transition to charring at 299°C for crude material and 316°C for acetone triturated material. Using methanol or ethanol rather than NMP may be considered a relatively eco-friendly process.

2.4.4. TLC/Flash chromatography.

Most compounds streaked on TLC plates since the log P values were high (log P estimated > 6.25). The most useful TLC system on silica gel found was *n*-butanol/water/Acetic acid (50/1.5/ 1.5, v/v/v).

2.4.5. Reaction mechanisms in aromatic bridged compounds.

The reaction mechanism involved in the formation of compounds *ortho*-quine, *meta*-quine and *para*-quine involves two sequential S_NAr substitutions (Bunnett & Zahler, **1951**). In aqueous acidic methanol (to increase acidity and allow solvent addition to the reaction, (Forrest *et al*., **1984**)) the reaction of 4,7-dichloroquinoline with 1,2-phenylenediamine initially produces the monomer (Compound 24a) as the major component and small quantities (10-15%) of the *bis*quinolines. In solution, solvation or steric hindrance (or both) of the monomer hinders the approach of the second 4,7-dichloroquinoline molecule, thereby reducing the probability of *bis*quinoline formation. The unreacted primary amino group of the monomer decreases in nucleophilicity (compared with *o*-phenylenediamine), because it is protonated under these conditions and is also attached to the aryl quinoline ring, consequently the amino group is electronically deactivated towards substitution reactions. As the temperature of the mixture increases, solvents are driven off producing a semi-solid mass which evolved a noxious gas, possibly HCl gas. These conditions favour the formation of aryl-bridged *bis*quinoline isolated as hydrochloride salts. The approach of the second quinoline during the formation of *bis*quinolines, *meta*-quine and *para*-quine is probably more favourable because of reduced steric hindrance. The increase in yield might be attributable to the phenomenon of acidity jump, i.e. when a strong acid is introduced into a weakly acidic solvent the overall Hammett acidity parameter (H_o) increases, partly because of the reaction generating HCl. The intention was to synthesise the HCl salt and recrystallize this for X-ray crystallographic analysis. The reaction was designed to employ the combination of a weak base and a strong acid to promote an acidity jump (Olah *et al.*, **2009**).

Overall, all our S_NAr reactions are standard acid-base reactions, since the hydrogen

chloride evolved is absorbed by the *bis*quinoline base to form a salt. The rate limitation appears to be related to inefficiency in stirring the entire solution during microwave heating (Scheme 1-27).

2.4.6. Mass spectrometry and NMR studies.

Mass spectrometry of compounds *ortho*-, *meta*- and *para*-quine proved useful in confirming the absence or presence of intermediates i.e. monomers, or side products such as 4-methoxy-7-chloro-quinoline and interestingly, coloured high oxidation products.

Using positive-ion electrospray mass spectrometry, clear evidence for the suggested molecular formulae (strong M-H^+ ions) was obtained for all compounds, even when they were insoluble for NMR studies. Solubility in common deuterated NMR solvents (CD_3OD, (CD_3SOCD_3)DMSO-*d_6*, and $CDCl_3$) was higher for *ortho*-quine and *para*-quine than for *meta*-quine.

Though the solubilities of *ortho*-quine and *meta*-quine were higher in trifluoroacetic acid (TFA-*d*) than in DMSO-*d_6*, the smaller (*meta*) coupling constant information was lost because of signal broadening. The problem was overcome by refluxing the compounds in ammonia and generating the free bases, usually under a blanket of inert atmosphere such as argon. Consequently, NMR spectra were readily obtained for all compounds except for *para*-quine. The poor solubility, even in TFA-*d*, probably arises due to π–π stacking of the compound by adoption of a planar conformer in the crystal state or through a hydrogen-bonded complex. Despite doubling of the number of scans to 96, the ^1H spectra remained broad. Addition of D_2O to the solution reduced the solubility of *para*-quine, and the smaller coupling constants within the quinoline ring were calculated by extending the number of scans to 1000. Compounds precipitated from TFA within 48 hrs, which complicated the automated acquisition of 2-D NMR data. Spectra of *para*-quine was obtained in hot DMSO-*d_6* in one experiment (360K, 64 scans), and the solubility of *para*-quine was insufficient to enable acquisition of 2D HETCOR or COSY information even at high temperatures (100°C). Towards the end of the study, samples were run as free bases in heated DMSO-*d_6* provided liquid nitrogen levels for the NMR magnet were carefully monitored.

It was noted that the introduction of a nitrogen substituent at the 5^{th} position would cause reduction of a *peri* interaction or perhaps "through bond interaction, causing H5 to be as deshielded as a proton found attached to the C3 position" (Osborne *et al*., **1993**). In 2,4-dihalogenoquinolines note that H5 was located downfield of H8 in contradiction to the earlier work by Beak *et al* (**1970**).

From the predicted ^1H –NMR data, it appears that the substituent at C4 has a pronounced effect on the predicted chemical shift position at H5 and is a through bond effect (rather than through space *peri* effect) since the *N*-dimethyl analogues do not affect predicted shift positions at H4.

2.4.7. Putative oxidation of isomeric *bis*quinolines.

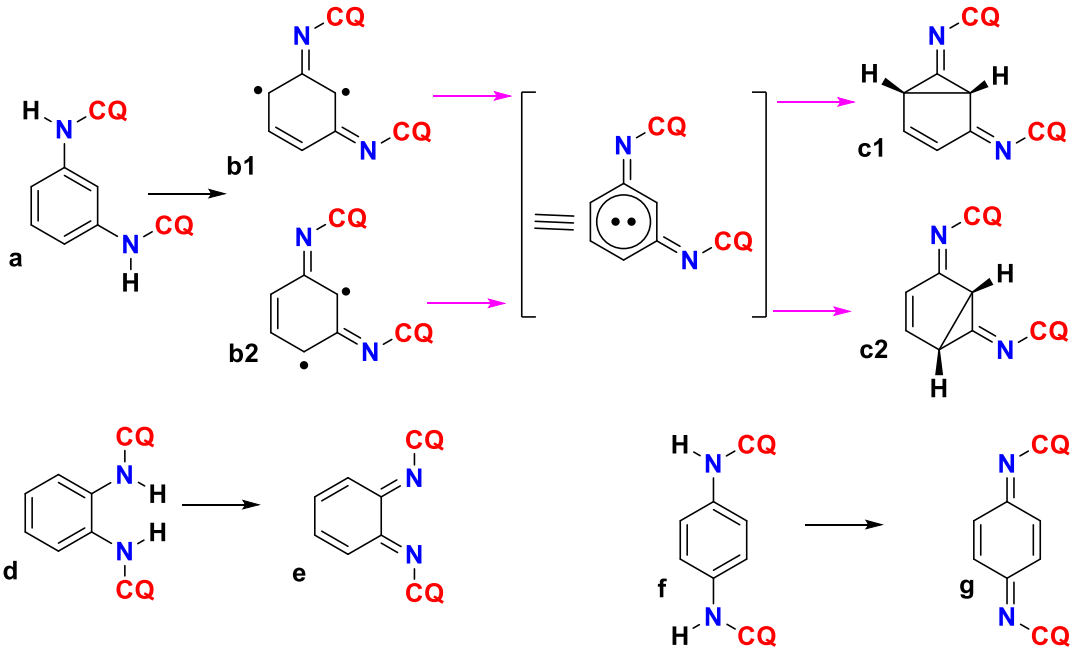

Figure 2.21. a) *meta*-quine, d) *ortho*-quine, f) *para*-quine and their computationally accepted isomeric (imine form) *bis*quinolines. (CQ stands for 4-7dichloroquine)

Putative oxidation of isomeric *bis*quinolines. (a): *meta*-phenylenediamine (b1 & b2): putative biradical intermediates; (c1) and (c2): (1S,2Z,5S,6Z)-N^2,N^6-*bis*(7-chloroquinolin-4-yl)bicyclo[3.1.0]hex-3-ene-2,6-diimine; (d): *ortho*-phenylenediamine; (e): *(1E,2E)*-N^1,N^2-*bis*(7-chloroquinolin-4-yl)cyclohexa-3,5-diene-1,2-diimine; (f): *para*- phenylenediamine; (g): *(1Z,4Z)*-N^1,N^4-*bis*(7-chloroquinolin-4-yl)cyclohexa-2,5-diene-1,4-diimine; selected *E/Z* isomers of quinone-imines shown. This strategy was found to be efficient, cost effective and fast. This suggested to us the most adventitious *aza*- substitution would be at C5 which may explain why compounds such as 1,5-napthyrdines show marked antimalarial activity both *in-vitro* and *in-vivo.* (Figure 2.21) (Barlin *et al.*, **1985**; McCaustland & Chen, **1970**).

Preliminary MM2 calculations (Using MM2 programme) confirm that the relative energies of the *ortho*, *para* and *meta* oxidation i.e. products (e,c1/c2 and g) have relative energies of e (0 kcal/mol), g (5.2167 kcal/mol) and c1/c2 (88.4049 kcal/mol) confirming that the *meta*- substituted phenylene bridged compound is the most stable to oxidative conditions. Notably, simpler analogues of chloroquinoline substituted (*1S,5S*)-bicyclo[3.1.0]hex-3-ene-2,6-diimine derivatives have been studied by The Houk group (Doubleday *et al.*, **2006**) (Figure 2.22).

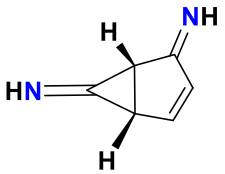

Figure 2.22. (1S,5S)-bicyclo[3.1.0]hex-3-ene-2,6-diimine

2.5. Materials and methods.

2.5.1. General.

Glassware was cleaned with detergent, then by repeated rinsing with ordinary, and distilled water. All Pyrex glassware was cleaned further by baking at its annealing temperature, eliminating adsorbed organic residues. All reactions were treated as both moisture and air-sensitive and the procedures outlined by Shriver & Drezdzon (**1986**) were used throughout. All materials used were of the highest purity available (Aldrich, Lancaster Synthesis). Substances were modified before use, using suitable procedures (Perrin & Armarego (**1988**) or the original literature as appropriate, except chloroquine (**1**) phosphate (Sigma Chemical Co.) which was used as received.

Reactions were treated as light- and air-sensitive and special synthetic procedures detailed were used throughout; reactions were performed using vacuum-line techniques under dry argon or nitrogen.

N-methyl-2-pyrrolidone was dried with barium oxide by addition and removal by distillation of one third its volume of anhydrous benzene, using a Dean-Stark trap. The residue was then distilled and the fraction boiling between 204 and 206°C was collected (anhydrous *N*-methyl-2-pyrrolidone, b.p. 81-82°C, 10 mmHg). Triethylamine was purified according to the procedure described by Perrin & Armarego (**1988**) under inert conditions. Moisture was rigorously excluded from the work up.

N-methyl-2-pyrrolidone, triethylamine, 4,7-dichloroquinoline, 1,2-phenylenediamine, 1,3-phenylenediamine and 1,4-phenylenediamine were purified before use (Perrin & Armarego, **1988**). All solvents were re-distilled under argon before use. Methanol was purified carefully by distillation from magnesium because reagent-grade methanol can contain measurable quantities of lead salts.

2.5.2. Analysis of compounds.

All substances were further purified by flash column chromatography before biological testing; separation was performed under pressurized argon (5 psi) on silica gel (Merck 60, 230- 400 mesh) or alumina (Laporte Industries UGl, 100 mesh).

Vacuum dry-column chromatography was performed in polythene tubing either on deactivated silica gel (grade 3) or basic alumina. Thin-layer chromatography (TLC) was performed on pre-coated silica gel 60 plates in tanks saturated with the vapour of the indicated solvent.

Substances were observed at 254 nm under UV light and detected for functional group tests, by spraying with a 5% solution of phosphomolybdic acid in ethanol, 5% sulphuric acid,

5% aqueous potassium permanganate, iodine vapour or by charring with a hot air gun, as appropriate. Most 4-aminoquinoline compounds are sensitive to the phosphomolybdic acid spray and develop intensely coloured blue spots.

Spectral and HPLC analysis were conducted using the facilities of the Chemistry Department, University of Hertfordshire. NMR was performed with a Bruker 250 MHz FT Aspect 2000, and Varian VXR400 (Liverpool University of John Moore); tetramethylsilane (TMS) was used as internal standard (chemical shifts in δ (ppm) and coupling constants in Hz) and unless otherwise specified the solvent used were $CDCl_3$ or dimethylsulphoxide-d_6. Substances such as the *bis*-(acridinyl-4-yl)ethane-1,2-diamines were sparingly soluble even in CD_3SOCD_3. In such cases the ^{I3}C NMR spectra were poorly resolved. IR spectra were acquired with a Mattson Galaxy series FTIR 5000; 1% compound KBr mixture was compressed into discs under vacuum.

Oils were dissolved in $CHCl_3$ and evaporated as a thin film on KBr discs. Mass spectrometry was performed with a VG 7070H with VG 2050 data system and heated probe. Spectra were recorded with an electron beam energy of 70eV and a trap current of 200PA. The ion source temperature was 200-240°C and the probe was operated at ambient temperature. Reversed-phase HPLC was performed with a Perkin Elmer series 10 chromatograph (C-18 column). The mobile phase (isocratic) was CH_3CN-THF-H_20, 55: 40: 5 (v/v/v). UV spectrometry was performed with a Philips PU8720 UV/VIS scanning spectrophotometer. A Gallenkamp capillary melting point apparatus was used to measure the melting points (m.p.) of each compound. The m.p. of compounds which sublimed were investigated in sealed tubes. Reported m.p. are uncorrected, however, verification was sought by differential scanning calorimetry (PerkinElmer DSC4).

2.5.3. Synthetic methods.

Reactions between 4-haloquinolines and amines were conducted in various solvents; acidified aqueous methanol (apparent pH 3.5) proved the cheapest and most convenient. The starting mixture was refluxed for 24-48 hrs under argon. The yields have not been optimised (Ismail *et al*., **1996**; Vennerstrom *et al*., **1992**). Crude reaction mixtures were quenched by allowing the hot reaction mixture to cool, washing with distilled water and then acetone, and vacuum filtration. If product did not precipitate out after work up, it was often triturated with dry acetone and suction-filtered. Compounds were oven-dried and then desiccated over KOH under dry argon and protected from light until analysis. Reaction mixtures were processed by using one of the following procedures:

2.5.3.1. Process I

The reaction mixture was left to cool in a Dewar flask. Mixture was filtered, producing

colourless crystals (triethylamine hydrochloride) which were then washed with anhydrous *N*-methyl-2-pyrrolidone (NMP). The filtrate was then concentrated under reduced pressure, poured on to ice, filtered and centrifuged. Unreacted starting materials were removed by extraction with boiling ethyl acetate (or acetone) and distilled water (10:90 ml).

2.5.3.2. Process II

The crude reaction mixture was mixed with ice and triturated with ethyl acetate. The precipitate was filtered and washed with distilled water (1 L). The solid was then slowly dissolved in 2M acetic acid, whilst cooling (liquid nitrogen) and the resulting solution was filtered. And extracted with ethyl acetate. The aqueous solution was cooled and made alkaline (pH 12) with 2M aqueous ammonia. purification was repeated to eliminate impurities. Dilute solutions of acetic acid and ammonia were used and ice was added during the purification process, as 4-aminoquinolines may decompose into 4-hydroxyquinolines. Quinolines containing trifluoro-methyl groups on the 2^{nd} and 8^{th} positions were more likely to decompose, as were all compounds with a *cis*-diaminocycloalkyl bridging unit.

2.5.3.3. Process III

The reaction mixture was triturated with acetone using a mortar and pestle. The resulting suspension was filtered and the solid was then slowly dissolved in 2M acetic acid, with cooling (liquid nitrogen), filtered and extracted with ethyl acetate. The aqueous solution was cooled and made alkaline (pH 12) with 2M aqueous ammonia. The procedure was repeated until the melting point of the compound was constant. Compounds were dried under vacuum.

2.5.4. Synthesis of *bis*quinolines.

Previously reported syntheses of 4-aminoquinoline antimalarial heterocycles use phenol (Surrey & Cutler, **1951**) to improve thermal condensations between 4-halo-quinolines and a suitable amine (Ismail *et al.,* **1996**; Tyman *et al.,* **1989**; Vennerstrom *et al.,* **1992**). Our attempts to synthesise *ortho*-quine using phenol as a solvent failed, they were difficult to clean up and characterise (0-20% yield).

The desired *bis*quinolines were synthesised in good yields (Monomers: Compound 36 at 85%, 38 at 82%, *bis*quinolines: Compound 26 at 78% and 84%), by heating the appropriate phenylenediamine under reflux with 4,7-dichloroquinoline in acidified aqueous methanol (pH 4.7 with 2M HCl). 1,3- and 1,4-phenylenediamines reacted with 4,7-dichloroquinoline (compounds **21a**, **24a**, **25a**) at lower temperatures than the bimolecular nucleophilic

displacement of 4-haloquinolines with alkylamines (120-210°C) (Ismail *et al*., **1996**). To synthesize the *ortho* compound an oil bath heated to 180°C was used. Compounds *ortho*-quine, *meta*-quine and *para*-quine were solid dihydrochlorides which decomposed without melting. NMR spectra of *meta*-quine were acquired in $(CD_3)_2SO$, those of *ortho*-quine and *para*-quine in CF_3CO_2D.

2.5.4.1 Ullmann coupling method in the presence of copper.

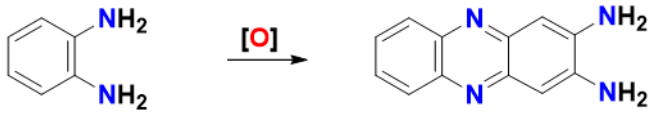

33

Figure 2.23. Oxidation to N^1,N^2-*bis*(6-chloroquinolin-4-yl)benzene-1,2-diamine.

Using microwaves, *ortho*-phenylenediamine was irradiated at 100W (10 minutes, 180°C) and left to stand for 2 days. After microwaving, a multi-layered sandwich of coloured products formed, including an orange, a blue and a brown solid. Some unreacted starter 4,7-dichloroquinoline sublimed to the top of each tube. Methanol (5.2 ml) was subsequently added, the suspension vortexed for 10 minutes or until all material had dissolved. The solution was then further re-irradiated at 100W power for 30 minutes attaining a temperature of 180°C.

A black liquid formed, when diluted with either water or acetone, it turned a yellow colour, which was then filtered to remove copper salts. After refluxing, charcoal was added (1%). The purple liquid which formed, was *ortho*-phenylenediamine being oxidised to the known phenazine-2,3-diamine (Iseminger *et al.*, **1997**) (Figure 2.23). To avoid oxidisation, solutions were filtered and solids washed with methanol immediately after irradiation. Oxidation of phenylenediamines can produce immunotoxins known as Bandrowski bases. This is well known for *p*-phenylene-diamine, other aromatic amines can behave in a similar fashion (Farrell *et al*., **2009**).

2.6. General synthetic procedures.

*Bis*quinolines can be constructed using focused microwave reactions, and for aryl bridged quinolines, acidified methanol proved suitable whereas alky bridged quinoline could be constructed in *N*-methyl pyrrolidine. NMR-structure activity relationships identified suitable positions for bioisosteric substitution (the 5th position) and a number of such compounds are described in Chapter 4.

2.6.1. Synthesis (monomers).

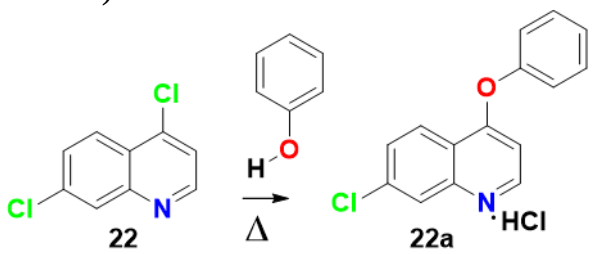

Figure 2.24. S_NAr displacement reaction, with phenol.

All compounds were prepared by a modification of Vennerstrom (Vennerstrom *et al.*, **1992**) (The chemicals synthesised are given Scheme numbers in this study. A total of 57 schemes in the whole thesis. This chapter contains 39 schemes. Schemes 40 to 42 are in chapter **3**, schemes 43-47 in chapter **4** and Schemes 48 to 57 in chapter **5**). The condensation reactions between the 4-Chloroquinolines and amines were conducted in various anhydrous solvents, especially *N*-methyl-2-pyrrolidone. Although heating the mixture of starting materials under reflux for 1-3 days under argon ensured high conversion to the required products, quoted yields have not been optimized (Quoted yields were around 78% and 84% as mentioned above). Crude reaction mixtures were processed using one of the following procedures. Infrared peaks were assigned using an online database: http://www.science-and-fun.de/tools/ (Socrates, **2004**).

1. (±)-N^1(7-chloroquinolin-4-yl)cyclohexylamine. compound **36**.

4,7-Dichloroquinoline (1.98 g, 0.01 mol), the cyclohexylamine (0.99 g, 0.01 mol) and triethylamine (1.012 g, 0.01 mol) were heated under reflux in *N*-methyl-2-pyrrolidone (25 ml) for 3 days to give a black oil that was worked up using process I. The yield from a single synthesis of **36** was 1.64 g, yield %85, (m.p. 82°C). FTIR (cm^{-1}): 3372(O-H bridge), 1617 (aryl conjugated, C=C) (Figure 2.25).

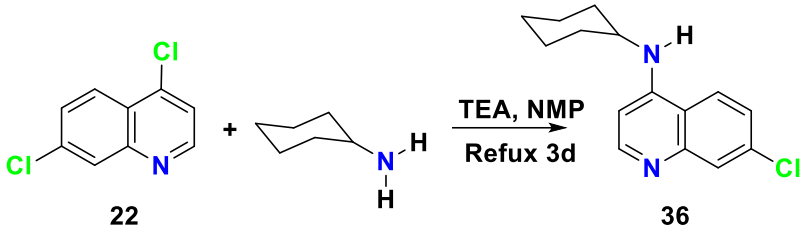

Figure 2.25. Scheme 1, S_NAr displacement, cyclohexylamine, NMP, reflux.

Molecular Formula = $C_{15}H_{17}ClN_2$. ^1H NMR (DMSO- d_6) δ (ppm) : 1.05-1.30 (4H, m), 1.58-2.0 (6H, m), 3.75-3.95 (1H, m), 6.91 (1H, d, $J_{2,3}$= 5.7 Hz), 7.50 (1H, dd, $J_{5,6}$=7.1 Hz, $J_{6,8}$=2.1 Hz), 7.88 (1H, s), 8.32 (1H, d, $J_{5,6}$= 8.9 Hz), 8.35 (1H, d, $J_{2,3}$= 5.7 Hz). ^{13}C NMR (DMSO- d_6) δ (ppm): 55.7, 30.59, 24.0, 25.0, 24.0, 30.59, 151.78 (C2, CH), 100.12 (C3, CH), 149.7 (C4, quaternary), 118.5 (C4a, quaternary)123.8 (C5, CH), 119.4 (C6, CH), 128.0 (C7, quaternary), 126.5 (C8, CH), 149.7 (C8a, quaternary). MS m/z: 260,262.

2. N^1(7-chloroquinolin-4-yl)-adamantyl-1-amine. compound **37**.

4,7-Dichloroquinoline (1.98 g, 0.01 mol), the 1-adamantanamine (1.51 g, 0.01 mol) and triethylamine (1.012 g, 0.01 mol) were heated under reflux in *N*-methyl-2-pyrrolidone (25 ml) for 3 days to give a black oil that was worked up by repeating process I three times. The yield from a single synthesis of **37** was 2.60g, 85% (m.p. 331-333°C by DSC) (Figure 2.26).

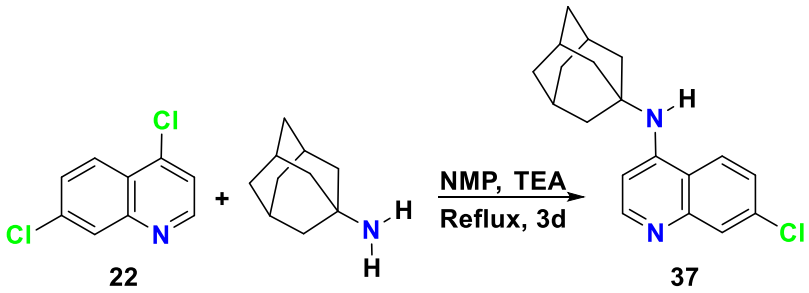

Figure 2.26. Scheme 2, S_NAr displacement, 1-adamantanamine, NMP, reflux.

Molecular Formula = $C_{19}H_{21}ClN_2$. ^1H NMR (DMSO-d_6) δ (ppm) 1.5-2.2 (15H', m), 6.74 (1H, d, $J_{2,3}$ = 5.7 Hz), 7.31 (1H, d, $J_{5,6}$ = 8.9 Hz, $J_{6.8}$ =2.1 Hz), 7.68 (1H, s), 8.18 (1H, d, $J_{5,6}$ = 8.9 Hz), 8.33 (1H, d, $J_{2,3}$=5.7 Hz). ^{13}C NMR (DMSO- d_6) δ (ppm): 53.7, 41.2, 29.7, 36.5, 29.7, 36.5, 29.7, 41.2, 41.2, 36.5, 151.7 (C2, CH), 100.2 (C3, CH), 154.5 (C4, quaternary), 118.5 (C4a, quaternary), 124.9 (C5, CH), 121.8 (C6, CH), 133.9 (C7, quaternary), 129.7 (C8, CH), 149.3 (C8a, quaternary). MS m/z: 312/314, 178/180.

3. N^1-(7-chloroquinolin-4-yl)-adamantyl-2-amine. compound **38**.

4,7-Dichloroquinoline (1.98 g, 0.01 mol), the 2-adamantanamine hydrochloride (1.87 g,

0.01 mol) and triethylamine (2.02 g, 0.02 mol) were heated under reflux in *N*-methyl-2-pyrrolidone (25 ml) for 3 days to give a black oil that was worked up by repeating Process I, two times. The yield from a single synthesis of **38** was 2.56g, 82% (m.p. 257-260°C by DSC). This compound decomposed in bright light over a period of one year (Figure 2.27).

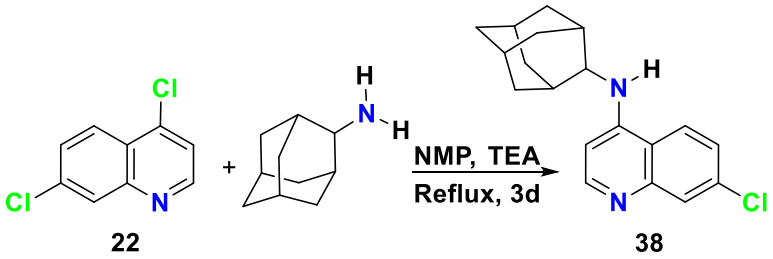

Figure 2.27. Scheme 3, S_NAr displacement, 2-adamantanamine, NMP, reflux.

Molecular Formula = $C_{19}H_{21}ClN_2$. ^1H NMR (DMSO-d_6) δ (ppm): 1.7-2.9 (15H', m), 6.74 (1H, d, $J_{2.3}$ = 5.7 Hz), 7.31 (1H, dd, $J_{5.6}$ = 8.9 Hz, $J_{6,8}$ = 2.1 HZ), 7.68 (1H, d, $J_{6,8}$ = 2.1 Hz), 8.23 (1H, d, $J_{5,6}$ = 8.9 Hz), 8.36 (1H, d, $J_{2,3}$ = 5.7 Hz). ^{13}C NMR (DMSO- d_6) δ (ppm): 62.8, 41.3, 30.2, 35.7, 36.6, 35.7, 30.2, 41.3, 30.2, 30.2, 152.5 (C2, CH), 100.2 (C3, CH), 154.5 (C4, quaternary), 118.5 (C4a, quaternary), 124.8 (C5, CH), 122.6 (C6, CH), 133.9 (C7, quaternary), 129.3 (C8, CH), 149.7 (C8a, quaternary). MS m/z: 312/314, 178/180.

4. N^1-(7-chloroquinolin-4-yl)-2,4-dichlorophenyl-1-amine. compound **39**.

4,7-Dichloroquinoline (1.97 g, 0.01 mol), the 2,4-dichloroaniline (1.62 g, 0.01 mol) and triethylamine (1.01 g, 0.01 mol) were heated under reflux in *N*-methyl-2-pyrrolidone (25 ml) for 3 days to give a black-green oil that was worked up by repeating process I three times.

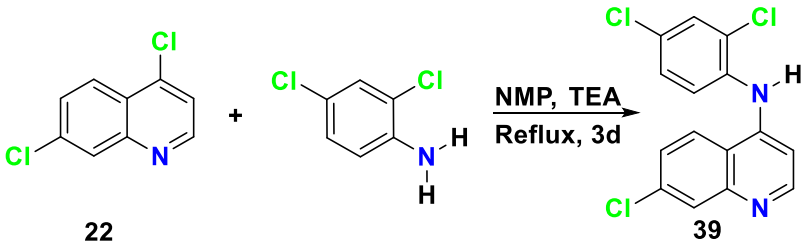

Figure 2.28. Scheme 4, S_NAr displacement, 2,4-dichloroaniline, NMP, reflux.

The yield from a single synthesis was 2.62g; 81% (greenish solid, m.p. 258°C by DSC); FTIR (cm^{-1}), 798 (C = C stretch). (C-H aromatic stretch), 1611 (N-bend, secondary amine), 1477 cm (C-H bend, CH_2). 1238, 1212 (C-N stretch, aromatic C-N bond), 652 (C-Cl stretch).

Molecular Formula = $C_{15}H_9Cl_3N_2$. ^1H NMR (DMSO-d_6) δ (ppm): 6.39 (1H, d, $J_{2,3}$=5.7 Hz), 7.39-7.67 (2H, H5', H6'), 7.86 (1H, dd, $J_{5,6}$= 7.1 Hz), 7.95 (1H, H3', m), 8.27 (1H, d, $J_{6,8}$=2.1 Hz), 8.59 (1H, d, $J_{2,3}$ = 5.7 Hz), 9.00 (1H, d, $J_{5,6}$ = 7.1 Hz). ^{I3}C NMR (DMSO-d_6)

δ (ppm): 134.4 (C1', quaternary), 126.6 (C2' , quaternary), 131.2(C3',CH), 125.7(C4', quaternary), 127.7(C5',CH), 119.1 (C6',CH), 155.1 (C2, CH), 100.91 (C3, CH), 154.3 (C4,quaternary), 119.7 (C4a, quaternary), 126.2 (C5, CH); 129.7 (C6, CH), 135.9 (C7, quaternary), 129.4(C8,CH), 154.6 (C8a,quaternary). MS m/z: 288,290,322/324/326 with a base ion m/z = 288.

5. (1S,2S)-N^1,N^2-*bis*(6-chloro-2-methoxyacridin-9-yl)cyclohexane-1,2-diamine. compound **40**.

6,9-Dichloro-2-methoxyacridine (5.56 g, 0.02 mol), (±)-1,2-diaminocyclohexane (1.14 g, 0.01 mol) and triethylamine (1.01 g, 0.01 mol) were heated under reflux in *N*-methyl-2-pyrrolidone (25 ml) for 12 h. The reaction mixture was allowed to cool to room temperature, triethylamine (1.01 g, 0.01 mol) was added again. This mixture was refluxed for 48 hrs, cooled to room temperature and worked up using process I and then Process II to give a yellow solid in 5.07g, 85% yield.

This yellow compound charred above 350°C (onset of charring: 268°C determined by DSC and because of its poor solubility precipitated before NMR spectra could be satisfactorily acquired. Molecular Formula = $C_{34}H_{30}Cl_2N_4O_2$. This experiment was repeated and it had a slightly different results. The expected molecular ion was seen at m/z = 596, 598 together with the base ion at m/z 259 (Figure 2.29).

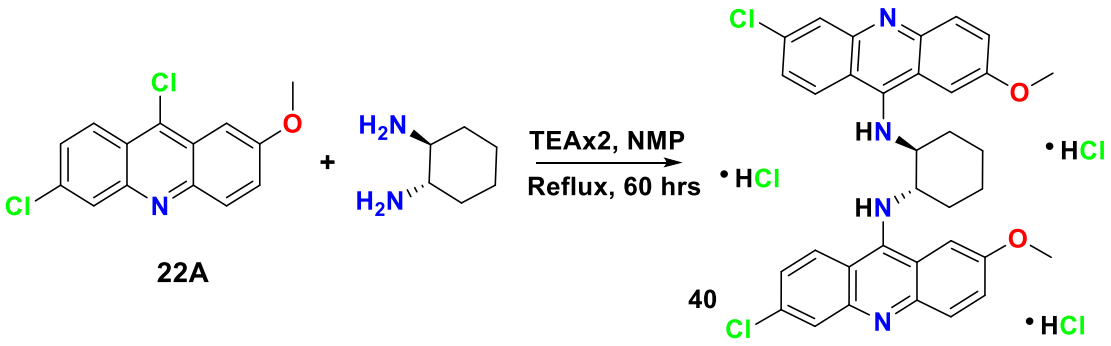

Figure 2.29. Scheme 5, S_NAr displacement, (±)-1,2-diaminocyclohexane, NMP, reflux.

2.6.2. Synthesis of aliphatic bridged *bis*quinolines (phenol method).

A mixture of 4,7-dichloroquinoline (19.8 g; 0.1mole) and 1,6-hexamethylenediamine (6.07g, 0.052 moles) were suspended in anhydrous phenol (47.05g; 0.05 moles) and were refluxed for 2 hrs using an air condenser. The resulting mixture was cooled then was cautiously poured into an excess of sodium hydroxide solution (10% in water; 100 ml). The resultant product was filtered (glass fibre filter paper) and then washed with copious quantities of water to remove excess alkali. Subsequently, it was triturated with 300 ml of anhydrous methanol; 50 g of crude base was obtained. These results were compared with the

NMP solvent method detailed blow.

6. (±)-*trans*-N^1,N^2-*bis*(7-chloroquinolin-4-yl)cyclohexane-l,2- diamine, compound **26**.

4,7-Dichloroquinoline (3.96 g, 0.02 mol), the *trans*-1,2-diaminocyclohexane (1.14 g, 0.01 mol) and triethylamine (2.02 g, 0.02 mol) were heated under reflux in *N*-methyl-2-pyrrolidone (25 ml) for 3 days to give a dark brown liquid that was worked up using process II (Figure 2.30). Yields from two separate syntheses of compound **26** were 3.41, 78% and 3.67, 84%. The cream-coloured powder obtained after purification was recrystallized from aqueous ethanol to give greenish crystals (m.p. 331.4°C, lit: Vennerstrom *et al* (**1992**)). m.p. 330-333°C, by DSC. FTIR (cm^{-1}): 3446 (N-H stretch, quinoline), 3442, 3257 (N-H stretch, secondary amine), 3233 (secondary amine), 2930 (C-H aromatic stretch), 1571 (N-H bend, secondary amine), 1416 (C=C stretch), 1083 (C-Cl aromatic stretch), 859 (C-H bend), 767, 643 (C-Cl stretch) 3096, 2938, 2766, 1631, 1584, 1550.

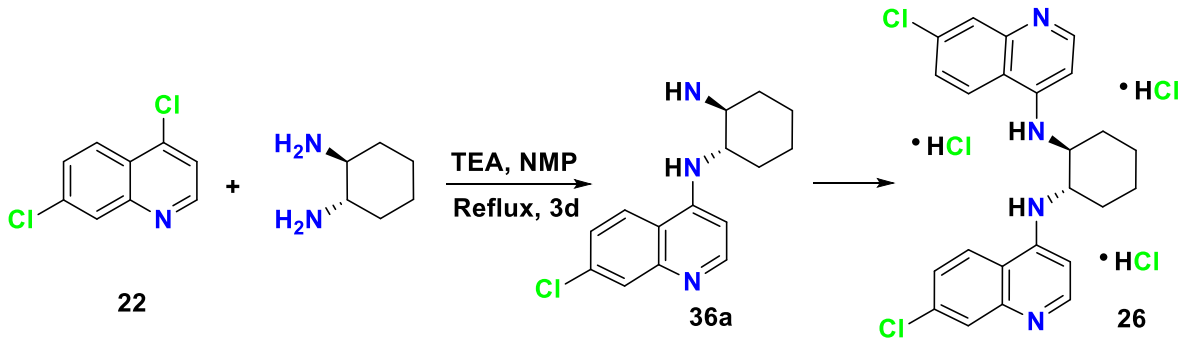

Figure 2.30. Scheme 6, S_NAr displacement, *trans*-1,2-diaminocyclohexane, NMP, reflux.

Molecular Formula = $C_{24}H_{22}Cl_2N_4$. ^{1}H NMR (DMSO-d_6) δ (ppm): 1.34-1.69 (4H', m), 1.7-1.91 (4H', m), 2.0-2.2 (2H', m) 3.75-3.95 (2H, m), 6.74 (2H, d, $J_{2,3}$=5.7 Hz), 7.31 (2H, dd, $J_{5,6}$ = 8.9 Hz, $J_{6,8}$ = 2.1 Hz), 7.58-7.68 (2H, d, $J_{6,8}$ = 2.1 Hz), 8.22-8.35 (2H, d, $J_{2,3}$ = 5.7 Hz) (the intensities are 1:3:3:1, ABX pattern, type 1 according to the classification used by Haigh *et al* (**1965**). The absolute positions of the quinoline ring protons are concentration dependent and, therefore, differ from those reported by Vennerstrom *et al* (**1992**). The mass spectrum indicates presence of both compound **26** and **36a**, (with a relative molecular mass (RMM) of 440 and 275 atomic mass units. Upon purification only the *bis*quinoline was detected. The purified compound shows molecular ions 436 and 438 and a base ion at 205. MS m/z: 437.13 confirming $C_{24}H_{22}Cl_2N_4$. Attempts to synthesize the *mono*quinoline **36a**, shown in (Figure 2.30) resulted solely in the formation of **26**, which was confirmed both by NMR and TLC analysis. Attempted purification of this *mono*quinoline by dissolution in 2M acetic acid and subsequent reprecipitation with 2M ammonia, caused it to decompose to 4-hydroxy-7-chloroquinoline. Similarly, the 1R,2R-(-)-, 1S,2S-(+)- compounds had identical spectra to that of **26** whereas the *cis* isomer differed significantly by the appearance of three broad

singlets between 1 and 3 (ppm):6.74 (2H, d, J2,3 = 5.7 Hz), 6.88-7.03 (2H, 16 Hz, NH).

7. *Cis*-N^1,N^2-*bis*(7-chloroquinolin-4-yl)clohexane-1,2-diamine, compound **26b**

4,7-Dichloroquinoline (3.96 g, 0.02 mol), the *cis*-1,2-diaminocyclohexane (1.14 g, 0.01 mol) and triethylamine (2.02 g, 0.02 mol) were heated under reflux in *N*-methyl-2-pyrrolidone (25 ml) for 3 days to give a dark brown oily liquid that was worked up using process I. The yield from synthesis of **26b** was 55% (Figure 2.31). Purification of **26b** was by trituration with analytical grade acetone and recovery of the insoluble product by filtration (process III) (The reaction mixture was triturated with acetone using a mortar and pestle. The suspension was filtered and the solid was then slowly dissolved in 2M acetic acid, with cooling (liquid nitrogen), filtered and extracted with ethyl acetate. The aqueous solution was cooled and made alkaline (pH 12) with 2M aqueous ammonia. The procedure was repeated until the melting point of the compound was constant. Purified compounds were dried under vacuum. The presence of steric hindrance (Figure 2.31), arising from unfavourable interactions between the two quinoline rings, may contribute to the instability of this compound (m.p. 290°C). FTIR (cm^{-1}): 3446 (N-H stretch, quinoline).

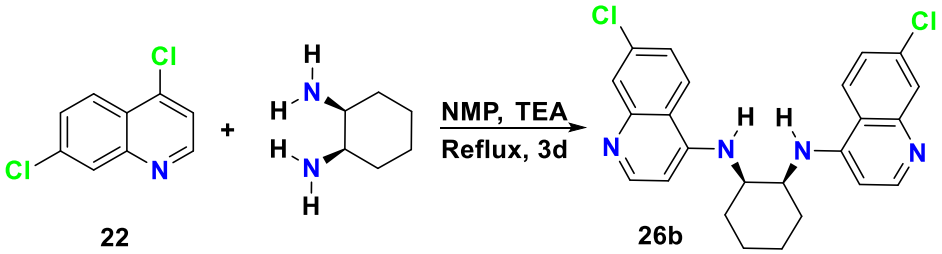

Figure 2.31. Scheme 7, S_NAr displacement, *cis*-1,2-diaminocyclohexane, NMP, reflux.

Molecular Formula = $C_{24}H_{22}Cl_2N_4$. 400 MHz ^1H NMR (DMSO-d_6) δ (ppm): 1.56 (2H, m, H3'ax), 1.79 (2H, m, H3'eq), 1.89 (2H, m, H2'ax), 2.52 (2H, m, H2'eq), 2.49-2.57 (2H, m, H1'ax), 7.00 (2H, d, 6.6 Hz, H3), 7.67 (2H, d, J = 9.2 Hz, H6), 8.06 (2H, s, H8), 8.55 (2H, d, J = 6.6 Hz, H2), 9.21 (2H, d, J = 9.2 Hz, H5). The cycloalkyl peaks were broadened owing to slow ring inversion resulting in loss of fine couplings ($2'_{H-H}$ < 3Hz).

^{13}C NMR (DMSO-d_6) δ (ppm): 21.8 (C3', CH_2), 26.5 (C2', CH_2), 51.9 (C1', CH), 144.6 (C2, CH), 99.3 (C3, CH), 153.7 (C4, quaternary), 116.12 (C4a, quaternary), 125.9 (C5, CH), 120.4 (C6, CH), 126.7 (C7, quaternary), 137.0 (C8, CH), 147.6 (C8a, quaternary). Accurate MS m/z: 437.13 confirming $C_{24}H_{22}N_4Cl_2$.

8. 1R,2R-(-)-N^1,N^2-*bis*(7-chloroquinolin-4-yl)cyclohexane-1,2- diamine, &1S,2S-(+)-N^1,N^2-*bis*(7-chloroquinolin-4- yl)cyclohexane-I,2-diamine, compound **26c**.

4,7-Dichloroquinoline (**22**) (3.99 g, 0.02 mol), the 1R,2R-(-)-1,2-diaminocyclohexane (1.14 g, 0.01 mol) and triethylamine (2.02 g, 0.02 mol) were heated under reflux in *N*-methyl-2-pyrrolidone (25 ml) for 3 days to give a dark brown oily liquid that was worked up using process III (The crude reaction mixture was triturated with analytical grade acetone using a mortar and pestle. The suspension was filtered and the solid was then slowly dissolved in 2M acetic acid, with cooling (liquid nitrogen), filtered and extracted with ethyl acetate. The aqueous solution was cooled and made alkaline (pH 12) with 2M aqueous ammonia. The procedure was repeated until the melting point of the compound was constant. Purified compounds were dried under vacuum before chromatography and biological testing) (Figure 2.32). The yield from synthesis of **26c** was 3.37g, 77%. The cream-coloured powder obtained after purification was recrystallized from aqueous ethanol to give crystals (m.p. 224-228°C by DSC).

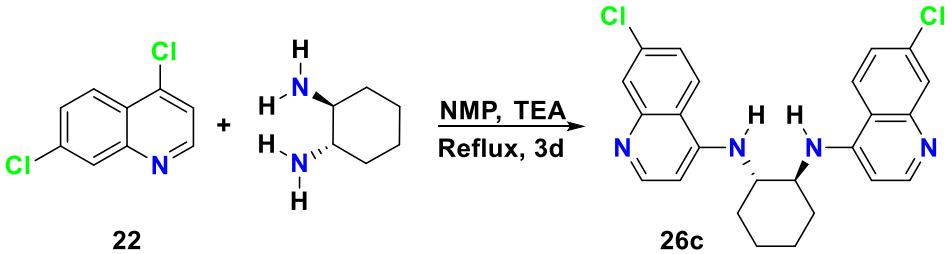

Figure 2.32. Scheme 8, S_NAr displacement, 1R,2R-(-)-1,2-diaminocyclohexane, NMP, reflux.

Molecular Formula = $C_{24}H_{22}Cl_2N_4$ 250 MHz ^{1}H NMR (DMSO-d_6) δ (ppm): 1.19-1.28 (2H, m, H3'ax), 1.44-1.48 (2H, m, H3'eq), 1.81-1.83 (2H, m, H2'ax), 2.06 (2H, broad s, H2' eq), 2.52-2.62 (2H, m, Hl' ax), 6.80 (2H, d, $J_{2,3}$ = 5.7 Hz), 7.32 (2H, dd, $J_{5,6}$ = 8.9 Hz), 7.67 (2H, d, $J_{6,8}$ = 2.1 Hz), 8.14 (2H, d, $J_{5,6}$ = 8.9 Hz), 8.28 (2H, d, $J_{2,3}$ = 5.7 Hz).

^{13}C NMR: (DMSO-d_6) δ (ppm): 24.6 (C3', CH_2), 31.5 (C2', CH_2), 55.6 (Cl', CH), 153.7 (C2, CH), 99.0 (C3, CH), 154.2 (C4, quaternary), 124.1 (C5, CH), 127.0 (C6, CH), 149.9 (C7, quaternary), 133.2 (C8, CH), 123.5 (C9, quaternary), 154.2 (C10, quaternary). Accurate MS m/z: 437.13 confirming $C_{24}H_{22}N_4Cl_2$.

1S,2S-(+)-N^1,N^2-*bis*(7-chloroquinolin-4-yl)cyclohexane-I,2-diamine, was made in similar conditions using 1S,2S-(+)-1,2-diaminocyclohexane giving %55 yield (m.p. 291°C).

9. 1S,2S-(-)-N^1, N^2-*bis*(7-chloroquinolin-4-yl) cyclohexane-1,2-diamine. compound **26d**.

Compound **26d** was prepared in a similar fashion as 1S,2S-(+)-1,2-diaminocyclohexane (55% yield); it had similar spectra as **26c** when run under the same concentration and conditions and the m.p. of the compound was 290-293°C by DSC (Figure 2.33).

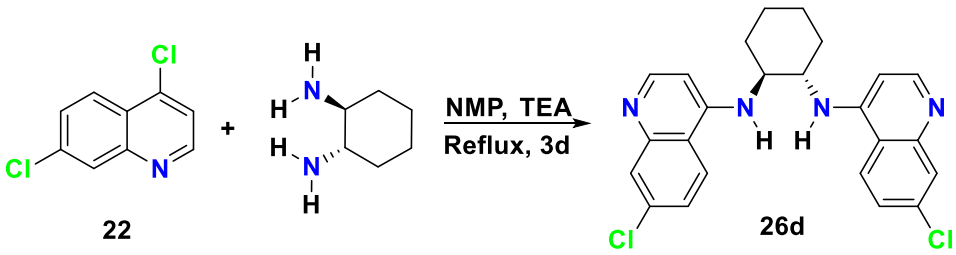

Figure 2.33. Scheme 9, S_NAr displacement, 1S,2S-(+)-1,2-diaminocyclohexane, NMP, reflux.

10. (±)-*trans*- N^1, N^2-*bis*(7-(trifluoromethyl)-quinolin-4-yl)cyclohexane-1,2-diamine, compound **26e**.

4-Chloro-7-(trifluoromethyl)quinoline (4.63 g, 0.02 mol), the (±)-1,2-diaminocyclohexane (1.14 g, 0.01 mol) and triethylamine (2.02 g, 0.02 mol) were heated under reflux in *N*-methyl-2-pyrrolidone (25 ml) for 3 days to give a dark brown viscous liquid that was worked up using process I to give a white powder 4.43 g, 88% (m.p. 333-336°C by DSC). FTIR (cm^{-1}): 1092 (C-F stretch), 798 (C=C stretch) (Figure 2.34).

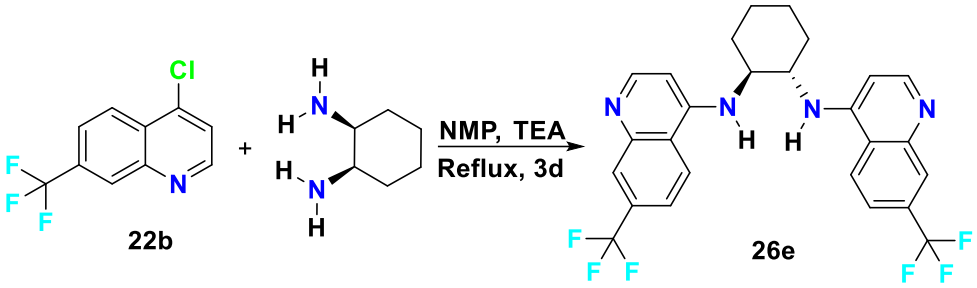

Figure 2.34. Scheme 10, S_NAr displacement, (±)-1,2-diaminocyclohexane, NMP, reflux.

Molecular Formula = $C_{26}H_{22}F_6N_4$. ^{1}H NMR (DMSO-d_6) δ (ppm): 1.34-1.69 (4H', m), 1.7-1.91 (4H', m), 2.0-2.2 (2H', m), 3.75-3.95 (2H, m,), 6.91 (2H, d, $J_{2,3}$ = 5.7 Hz), 7.50 (2H, dd, $J_{5,6}$ = 7.1 Hz), 7.88 (2H, d, $J_{6,8}$=2.l Hz), 8.32 (2H, d, $J_{5,6}$ = 8.9 Hz), 8.35 (2H, d, $J_{2.3}$ = 5.7 Hz).

^{I3}C NMR DMSO-d_6 δ (ppm): 55.77 (Cl', CH), 30.59 (C2', CH_2), 24.0 (C3', CH_2), 151.78 (C2, CH), 100.12 (C3, CH), 149.70 (C4 quaternary), 122.5 (C7", quaternary, CF3), 123.8 (C5, CH), 117.0 (C6, CH), 128.0 (C7, quaternary), 126.5 (C8, CH), 147.5 (C9, quaternary), 118.5 (C10, quaternary). MS m/z: 504 (l00%), 484 (M-HF), FAB (M + H) 505.

11. (±) *trans*-N^1,N^2-*bis*(2,8-*bis*(trifluoromethyl)quinolin-4-yl)cyclohexane-1,2-diamine, compound **26f**.

4-Chloro-2,8-*bis*(trifluoromethyl)quinoline (0.69 g, 0.002 mol), the (±)-1,2-diaminocyclo- hexane (0.11 g, 0.001 mol) and triethylamine (0.20 g, 0.02 mol) were heated

under reflux in *N*-methyl-2-pyrrolidone (5 ml) for 3 days to give a dark brown viscous liquid that was worked up using process I which produced a brown compound. Suspension and vortexing in chloroform/ conc. NH_3 (15 ml/15 ml, V/V) for one hour, filtering at the pump and washing with chloroform (5 x 25 ml) at the pump produced a tan solid 0.32 g (50%) (Figure 2.35).

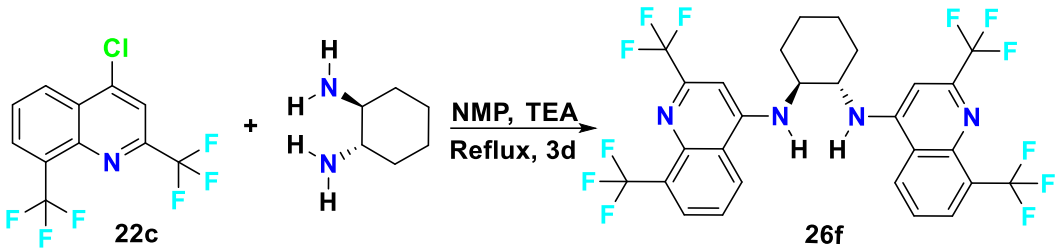

Figure 2.35. Scheme 11, S_NAr displacement, (±)-1,2-diaminocyclohexane, NMP, reflux.

Molecular Formula = $C_{28}H_{20}F_{12}N_4$. Free base: ^{1}H NMR: δH (DMSO-d_6) 1.49-1.51 (4H', m, ^3J H_{ax}-H_{ax} = 9.48 Hz), 1.77-1.89 (4H', m), 2.06 (2H', d, ^3J H_{ax}-H_{ax} = 12.64 Hz), 4.00 (2H, m), 7.16 (2H, s, H3), 7.89 (2H, d, H5, $^3J_{H\text{-}H}$ = 7.20 Hz), 8.27 (2H, d, $3J_{H\text{-}H}$ = 8.49 Hz). Methanol peak at 3.33 ppm.

^{13}C NMR: APT (75.5 MHz): δC (DMSO-d_6) 24.6 (C3', CH_2), 31.2 (C2', CH_2), 56.8 (C1', CH), 145.3 (C2, quaternary, distorted), 95.1 (C3, CH), 114.6 (C2", quartet, $^2J_{C\text{-}F}$ = 33 Hz), 152.0 (C4, quaternary), 123.7 (C5, CH), 128.5 (C6, CH), 125.8 (C7, CH), 129.2 (C8", quartet, $^2J_{C\text{-}F}$ = 29 Hz), 143.5 (C8, quaternary,), 147.3 (C9, quaternary), 126.3 (C10, quaternary).

The dihydrochloride was a grey solid: (decomp) >380°C. MS (EI at 70 eV) $C_{28}H_{20}N_4F_{12}$ 640 Da. Detected, 640 (M+ 4%), 360 (M+ –F 1%), 360 (15%), CF_3+, 69 (8%), 319 (6%), 307 (5%), 280 (5%), 36 (100%). The dihydrochloride (100mg) was suspended in chloroform (100 ml) to which was added conc. NH_3 (100 ml) and stirred then left for one week. The solution slowly deposited a mass of clear crystals. These were isolated by filtration then slowly crystallized from a methanol chloroform mixture. Free base: m.p. 243.4 –245.2°C by DSC: 0 to 300°C at 10°C min^{-1}).

12. (±)-*trans*-N^1,N^2-*bis*(2-phenylquinazolin-4-yl)cyclohexane-l,-2 diamine, 7chloro-2-phenylquinazoline, compound **41**.

4-Chloro-2-phenylquinazoline (4.81 g, 0.02 mol), the (±)-1,2- diaminocyclohexane (1.14 g, 0.01 mol) and triethylamine (2.02 g, 0.02 mol) were heated under reflux in *N*-methyl-2-pyrrolidone (25 ml) for 3 days to give a black-brown liquid that was worked up using process II to give a white crystalline solid, m.p. 274°C (Figure 2.36).

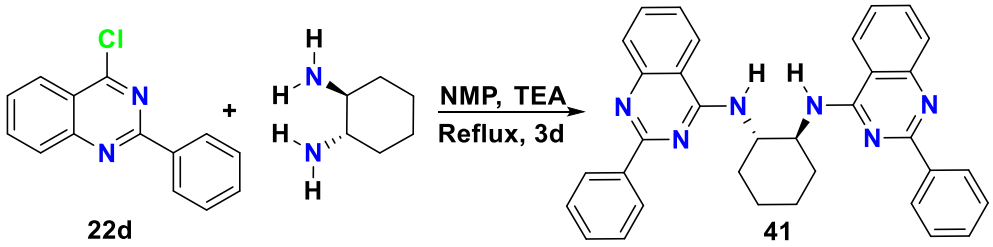

Figure 2.36. Scheme 12, S_NAr displacement, (±)-1,2-diaminocyclohexane, NMP, reflux.

The yield from a single synthesis of **41** was 2.98 g, 57%. Molecular Formula = $C_{34}H_{30}N_6$. ^{1}H NMR (DMSO-d_6) δ (PPM): 1.34-1.69 (4H', m), 1.7-1.91 (4H', m), 2.0-2.5 (2H', m), 7.3 (2H, dd, $J_{5,6}$ = 8.9 Hz, $J_{6,8}$ = 2.1 Hz), 7.5-8.4 (10H, m), 7.58-7.68 (2H, d, $J_{6,8}$ = 2.1 Hz), 8.02-8.18 (2H, d, $J_{5,6}$ = 8.9 Hz), 8.22-8.35 (2H'', d, $J_{2,3}$ = 5.7 Hz).

^{13}C NMR ($CDCl_3$) δ (ppm): 56.50 (Cl', CH), 32.63 (C2', CH_2), 24.98 (C3', CH_2), 154.12 (C2, quaternary), 150.05 (C4, quaternary), 121.18 (C5, CH), 125.43 (C6, CH), 130.31 (C7, CH), 132.62 (C8, CH), 160.03 (C9, quaternary), 121.18 (C10, quaternary), phenyl: 128.36 (C2", CH); 128.5 (C3",CH) 129.50 (C4",CH) 131.7, (C1",quaternary). MS m/z: 522.5 (M+), 222 (l00%), 301 (100%) base peak.

13. *N*^{1}*N*^{2}-*bis*(7chloroquiolin-4-yl) ethane-1,2-diamine, compound **42**.

4,7-Dichloroquinoline (**22**) (3.96 g, 0.02 mol), ethane-1,2-diamine (0.62 g, 0.01 mol) and triethylamine (2.02 g, 0.02 mol) were heated under reflux in *N*-methyl-2-pyrrolidone (25 ml) for 3 days to give a dark brown oily liquid that was worked up using process III. The yield from a single synthesis of **42** was 2.51 g crude yield, 77% (Figure 2.37). The cream-coloured powder obtained after purification was recrystallized from aqueous ethanol to give crystals (1.53 g, 61%), (m.p. 342-345°C (Lit. Pearson *et al.* (**1946**)) m.p. 334.5-337°C by DSC: 0 to 300°C at 10°C min^{-1}; IR 3460, 3230, 3065, 3020, 2970, 2890, 1610, 1580, 1535 cm^{-1}.

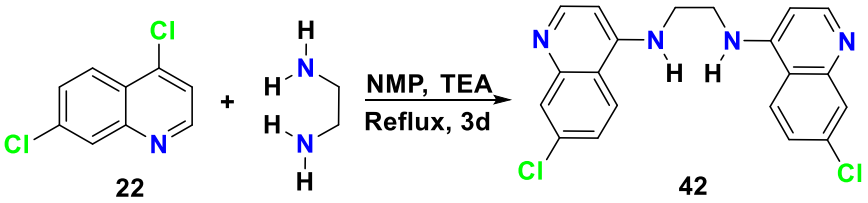

Figure 2.37. Scheme 13, S_NAr displacement, ethane-1,2-diamine, NMP, reflux.

Molecular Formula = $C_{20}H_{16}Cl_2N_4$. ^{1}H NMR: δH (DMSO-d_6): 3.62 (4H', m), 6.58 (2H, H3, d, J = 5.4 Hz), 7.47 (2H, H6, dd, J = 9.0, 2.4 Hz), 7.79 (2H, H9, d, J = 2.4 Hz, 2H), 8.23 (2H, H7, d, J = 9.0 Hz), 8.41 (2H, H2, d, J = 5.4 Hz).

^{13}C NMR: (DMSO-d_6) δ (ppm): 49.34, 98.91, 118.5, 121.16, 124.34, 129.14, 134.29, 149.34, 152.17, 154.29.

14. N^1,N^3-*bis*(7-chloroquinolin-4-yl)propane-l,3-diamine, compound **43**.

4,7-Dichloroquinoline (**22**) (3.96 g, 0.02 mol), propane-1,3-diamine (0.88 g, 0.01 mol) and triethylamine (2.02 g, 0.02 mol) were heated under reflux in *N*-methyl-2-pyrrolidone (25 ml) for 3 days to give an oily liquid that was worked up using process III (Figure 2.38). The yield was 0.98 g, 50%), m.p. 315-317°C; ((Vennerstrom *et al*., **1992**) m.p. 312-314°C, 0.70g, 37%), IR 3450, 3240, 3070, 2960, 2880, 1610 1580, 1535 cm^{-1}.

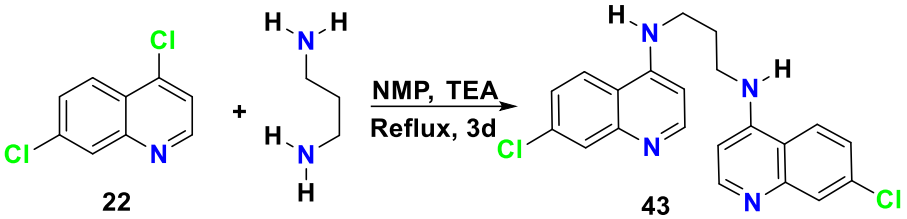

Figure 2.38. Scheme 14, S_NAr displacement, propane-1,3-diamine, NMP, reflux.

Molecular Formula = $C_{21}H_{18}Cl_2N_4$. ^{1}H NMR δH: 2.07 (2H, H2′, m), 3.43 (4H, H1′, m), 6.51 (2H, H3, d, J = 5.4 Hz), 7.45 (2H, H6, dd, J = 9.0 Hz, J = 2.4 Hz); 7.78 (2H, H9, d, J = 2.4 Hz), 8.29 (2H, H5, d, J = 9.0 Hz), 8.37 (2H, H2, d, J = 5.4 Hz). ^{13}C NMR: (DMSO-d_6) δ (ppm): 28.49, 41.12, 98.92, 118.50, 121.16, 124.28, 129.41, 139.34, 149.31, 152.17, 154.25.

15. N^1,N^4-*bis*(7-chloroquinolin-4-yl)butane-l,4-diamine, compound **44**.

4,7-Dichloroquinoline (**22**) (3.96 g, 0.02 mol), butane-1,4-diamine (0.88 g, 0.01 mol) and triethylamine (2.02 g, 0.02 mol) were heated under reflux in *N*-methyl-2-pyrrolidone (25 ml) for 3 days to give an oily liquid that was worked up using process III (Figure 2.39). 2.05 g, 50%, m.p. 360°C; (lit, Vennerstrom *et al* (**1992**) m.p. 339-341°C, 1.11g, 54%); IR 3215, 3065, 2960, 1610, 1580, 1550 cm^{-1}.

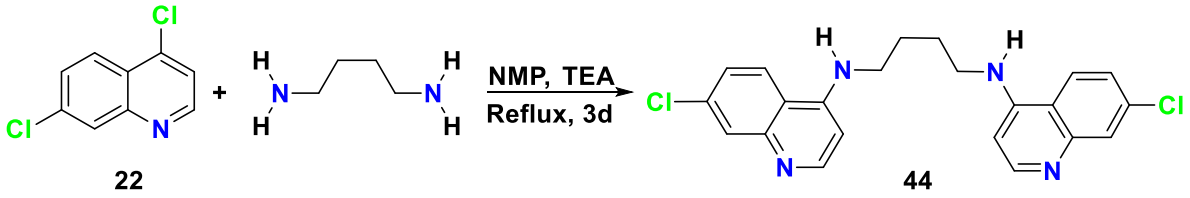

Figure 2.39. Scheme 15, S_NAr displacement, butane-1,4-diamine, NMP, reflux.

Molecular Formula = $C_{22}H_{20}Cl_2N_4$. ^{1}H NMR δH 1.74-1.87 (m, 4H'), 3.21-3.54 (4H', m), 6.50 (2H, d, J = 5.3 Hz), 7.40-7.47 (2H, m), 7.74-7.77 (2H, m), 8.26 (2H, d, J = 9.1Hz), 8.37(2H, d, J = 5.1 Hz).

^{13}C NMR: (DMSO-d_6) δ (ppm): 26.34, 51.72, 98.90, 118.51, 121.62, 124.8, 129.34, 139.41, 149.23, 152.71, 154.35.

16. N^1,N^5-*bis*(7-chloroquinolin-4-yl)pentane-l,5-diamine, compound **45**.

4,7-Dichloroquinoline (**22**) (3.96 g, 0.02 mol), pentane-1,5-diamine (1.021 g, 0.01 mol) and triethylamine (2.02 g, 0.02 mol) were heated under reflux in *N*-methyl-2-pyrrolidone (25 ml) for 3 days to give an oily liquid that was worked up using process III (Figure 2.40). The yield was 2.08g, 49%. m.p. 269-271°C, (lit: Vennerstrom *et al* (**1992**) m.p. 272-274°C, 0.50g, 23%): IR 3450, 3250, 3070, 2950, 2880, 1610, 1585,1535 cm^{-1}.

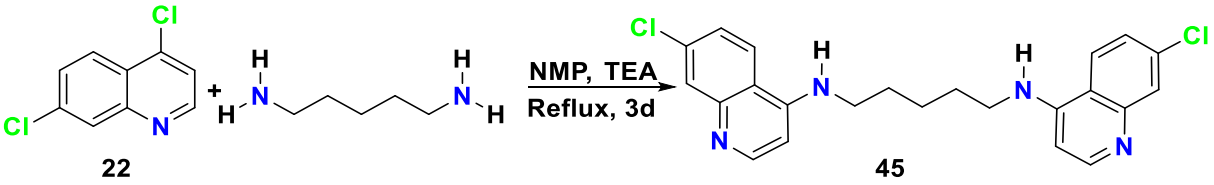

Figure 2.40. Scheme 16, S_NAr displacement, pentane-1,5-diamine, NMP, reflux.

Molecular Formula = $C_{23}H_{22}Cl_2N_4$. ^1H NMR δ 1.49-1.56 (2H', m), 1.69-1.78 (4H', m), 3.25-3.32 (4H', m), 6.46 (2H, H3, d, J = 5.4 Hz), 7.44 (2H, H6, dd, J = 9.0, 2.4 Hz), 7.78 (2H, H9, d, J = 2.4 Hz), 8.28 (2H, H7, d, J = 9.0 Hz), 8.38 (2H, H2, d, J = 5.4 Hz);

^{13}C NMR: (DMSO-d_6) δ (ppm): 24.25, 27.55, 42.33, 98.56, 117.42, 123.88, 124.04, 127.45, 133.28, 149.08, 150.03, 151.85.

17. N^1,N^6-*bis*(7-chloroquinolin-4-yl)hexane-l,6-diamine, compound **46**.

4,7-Dichloroquinoline (**22**) (3.96 g, 0.02 mol), hexane-1,6-diamine (1.11 g, 0.01 mol) and triethylamine (2.02 g, 0.02 mol) were heated under reflux in *N*-methyl-2-pyrrolidone (25 ml) for 3 days to give an oily liquid that was worked up using process III (Figure 2.41). The yield was 1.74g, 80%), (lit Vennerstrom *et al* (**1992**), m.p. 282-283, 1.55g, 70%); m.p. 284-286°C; IR 3450, 3300, 3105, 3065, 3010, 2930, 2830, 1610, 1570, 1535 cm^{-1}.

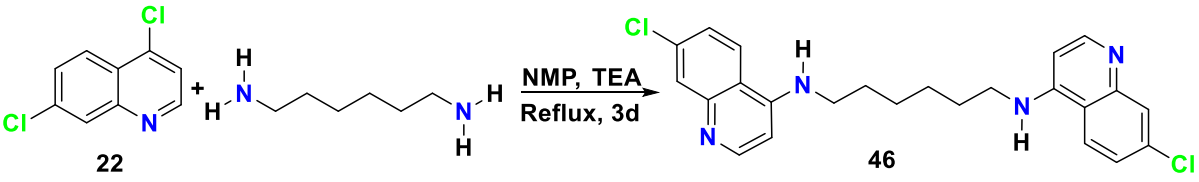

Figure 2.41. Scheme 17, S_NAr displacement, hexane-1,6-diamine, NMP, reflux.

Molecular Formula = $C_{24}H_{24}Cl_2N_4$. ^1H NMR δ 1.42-1.53 (4H', m), 1.63-1.74 (4H', m), 3.23-3.29 (4H', m), 6.45 (2H, H3, d, J = 5.4 Hz), 7.43 (2H, H6, dd, J = 9.0, 2.1 Hz), 7.77 (2H, H9, d, J = 2.1 Hz), 8.27 (2H, H7, d, J = 9.0 Hz), 8.37 (2H, H2, d, J = 5.4 Hz).

^{13}C NMR: (DMSO-d_6) δ (ppm): 26.37, 27.71, 42.29, 98.52, 117.39, 123.86, 124.02, 127.41, 133.25, 149.06, 150.01, 151.83.

18. N^1,N^7-bis(7-chloroquinolin-4-yl)heptane-l,7-diamine, compound **47**.

4,7-Dichloroquinoline (**22**) (3.96 g, 0.02 mol), heptane-1,7-diamine (1.30 g, 0.01 mol) and triethylamine (2.02 g, 0.02 mol) were heated under reflux in *N*-methyl-2-pyrrolidone (25 ml) (1.98 g, 80%; NMP) for 3 days to give a dark brown semi-solid that was worked up using process III (Figure 2.42). 2.27 g, 50%; m.p. 222-223°C; (lit Vennerstrom *et al* (**1992**) m.p. 218-220°C); IR 3450, 3060, 2935, 2860, 1610, 1580, 1535 cm^{-1}.

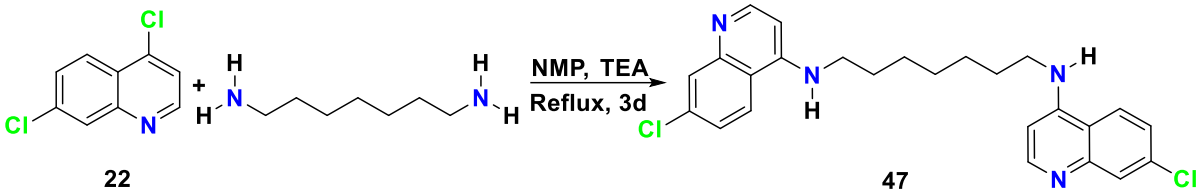

Figure 2.42. Scheme 18, S_NAr displacement, heptane-1,7-diamine, NMP, reflux.

Molecular Formula = $C_{25}H_{26}Cl_2N_4$. ^1H NMR δH: 1.39 (6H, H3′, H4′, br s), 1.53-1.77 (4H, H2′, m), 3.16-3.32 (4H, H1′, m), 6.44 (2H, H3, d, J = 5.5 Hz), 7.44 (2H, H6, dd, J = 9.0, 2.2 Hz), 7.79 (2H, H9, d, J = 2.2 Hz), 8.29 (2H, H7, d, J = 9.1 Hz), 8.39 (2H, H2, d, J = 5.4 Hz).

^{13}C NMR: (DMSO-d_6) δ (ppm): 27.73, 28.64, 42.35, 98.54, 117.43, 123.91, 124.08, 127.46, 133.30,149.09,150.04, 151.87.

19. N^1,N^8-*bis*(7-chloroquinolin-4-yl)Octane-l,8-diamine, compound **48**.

4,7-Dichloroquinoline (**22**) (3.96 g, 0.02 mol), octane-1,8-diamine (1.44 g, 0.01 mol) and triethylamine (2.02 g, 0.02 mol) were heated under reflux in *N*-methyl-2-pyrrolidone (25 ml) for 3 days to give a brown solid that was worked up using process III (Figure 2.43). Yield: 3.27 g, 70%, m.p. 219-220°C (lit. Vennerstrom *et al* (**1992**) m.p. 216-219°C, 3.60 g, 77%); IR 3450, 3350, 3070, 2940, 2865, 1610,1580, 1540 cm^{-1}.

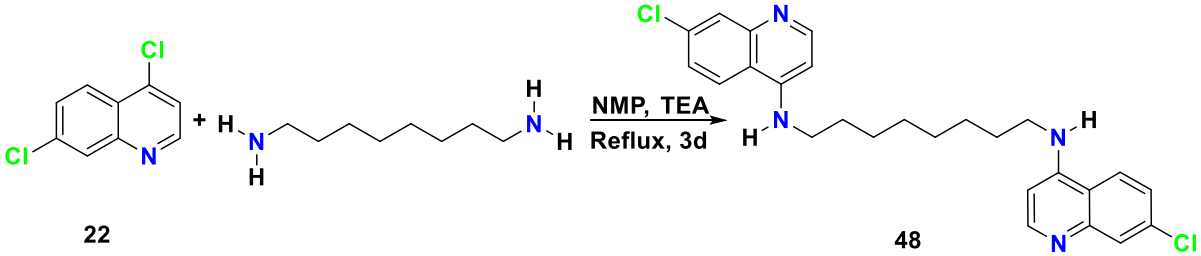

Figure 2.43. Scheme 19, S_NAr displacement, octane-1,8-diamine, NMP, reflux.

Molecular Formula = $C_{26}H_{28}Cl_2N_4$. ^1H NMR δH: 1.35 (8H, H3′, H4′, br s), 1.57-1.75 (4H, H2′, m), 3.15-3.31 (4H, H1′, m), 6.44 (2H, H3, d, J = 5.5 Hz), 7.43 (2H, H6, dd, J = 9.0,2.3 Hz), 7.77 (2H, H9, d, J = 2.2 Hz), 8.27 (2H, H7, d, J = 9.1 Hz), 8.38 (2H, H2, d, J =

5.4 Hz);

^{13}C NMR: (DMSO-d_6) δ (ppm): 26.58, 27.73, 28.79, 42.36, 98.55, 117.42, 123.92, 124.08, 127.44, 137.4, 147.7, 149.3 152.3.

20. N^1,N^9-*bis*(7-chloroquinolin-4-yl)nonane-l,9-diamine, compound **49**.

4,7-Dichloroquinoline (**22**) (3.96 g, 0.02 mol), nonane-1,9-diamine (1.58 g, 0.01 mol) and triethylamine (2.02 g, 0.02 mol) were heated under reflux in *N*-methyl-2-pyrrolidone (25 ml) for 3 days to give a grey semi-solid that was worked up using process III (Figure 2.44). Yield: 3.56 g, 85% ((3.64 g 74%), m.p. 163-164°C, lit Vennerstrom *et al* (**1992**))161-164°C; IR 3455,3370,3065, 2930,2860, 1610, 1575, 1540, 1535 cm^{-1}.

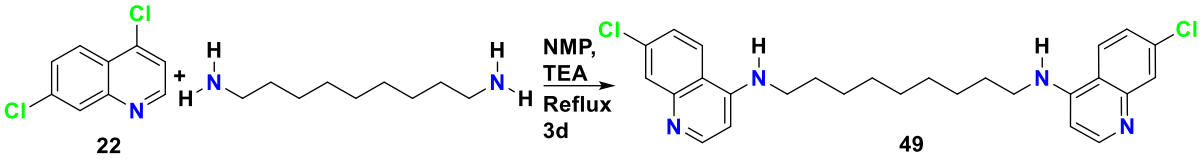

Figure 2.44. Scheme 20, S_NAr displacement, nonane-1,9-diamine, NMP, reflux.

Molecular Formula = $C_{27}H_{30}Cl_2N_4$. ^{1}H NMR δH 1.14-1.50 (10H, H3′, H4′, H5′, br s), 1.54-1.73 (4H, H2′, m), 3.13-3.32 (4H, H1′, m),6.44 (2H, H3, d, J = 5.5 Hz), 7.43 (2H, H6, dd, J = 9.0, 2.3 Hz), 7.77 (2H, H9, d, J = 2.2 Hz), 8.28 (2H, H7, d, J = 9.0 Hz), 8.38 (2H, H2, d, J = 5.4 Hz).

^{13}C NMR: (DMSO-d_6) δ (ppm): 26.61, 27.74, 28.78, 28.98, 42.37, 98.53, 117.43, 123.90, 124.08, 127.46, 133.30, 149.09, 150.04, 151.87.

21. N^1,N^{10}-*bis*(7-chloroquinolin-4-yl)decane-l,10-diamine, compound **50**.

4,7-Dichloroquinoline (**22**) (3.96 g, 0.02 mol), decane-l,10-diamine (1.58 g, 0.01 mol) and triethylamine (2.02 g, 0.02 mol) were heated under reflux in *N*-methyl-2-pyrrolidone (25 ml) for 3 days to give a grey semi-solid that was worked up using process III (Figure 2.45). Yield: 3.56 g, 85% ((3.64 g 74%); m.p. 163-164°C, lit Vennerstrom *et al* (**1992**))161-164°C; IR 3455,3370,3065, 2930,2860, 1610, 1575, 1540, 1535 cm^{-1}.

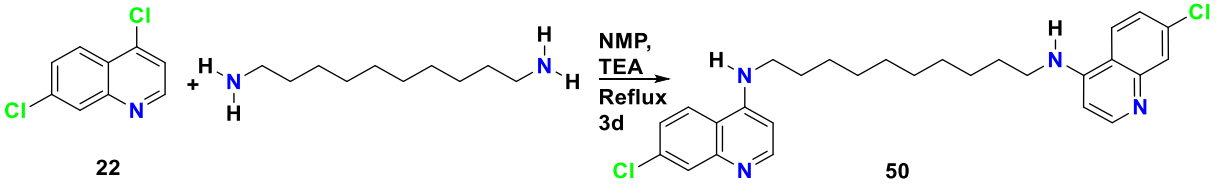

Figure 2.45. Scheme 21, S_NAr displacement, decane-l,10-diamine, NMP, reflux.

Molecular Formula = $C_{27}H_{30}Cl_2N_4$. ^{1}H NMR δH 1.14-1.50 (10H, H3′, H4′, H5′, br s),

1.54-1.73 (4H, H2′, m), 3.13-3.32 (4H, H1′, m),6.44 (2H, H3, d, J = 5.5 Hz), 7.43 (2H, H6, dd, J = 9.0, 2.3 Hz), 7.77 (2H, H9, d, J = 2.2 Hz), 8.28 (2H, H7, d, J = 9.0 Hz), 8.38 (2H, H2, d, J = 5.4 Hz).

^{13}C NMR: (DMSO-d_6) δ (ppm): 26.61, 27.74, 28.78, 28.98, 42.37, 98.53, 117.43, 123.90, 124.08, 127.46, 133.30, 149.09, 150.04, 151.87.

22. N^1,N^{12}-*bis*(7-chloroquinolin-4-yl)dodecane-l,12-diamine, compound **51**.

4,7-Dichloroquinoline (**22**) (3.96 g, 0.02 mol), dodecane-1,12-diamine (2.00g, 0.01 mol) and triethylamine (2.02 g, 0.02 mol) were heated under reflux in *N*-methyl-2-pyrrolidone (25 ml) for 3 days to give a white liquid that was worked up using process III (Figure 2.46). Yield: 2.61g, 65% (2nd extraction yield: 1.57g, 50%); m.p. 188-190°C; IR 3460, 3070, 2930, 2860, 1610, 1580, 1540 cm^{-1}.

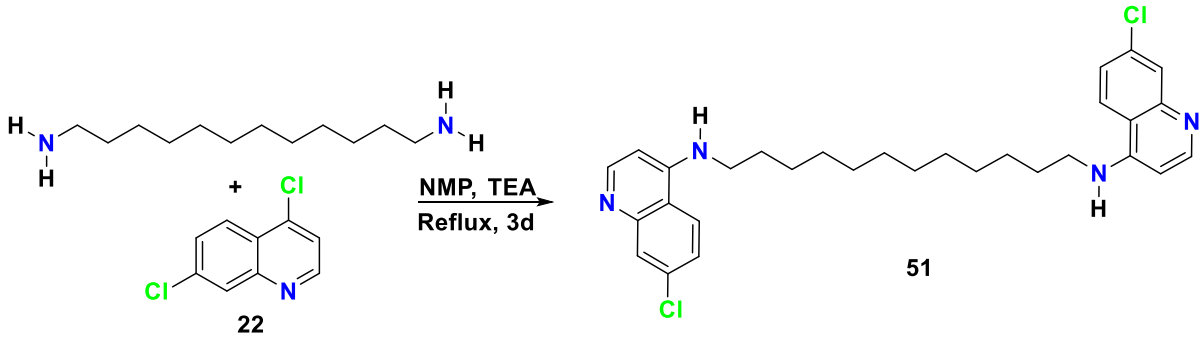

Figure 2.46. Scheme 22, S_NAr displacement, dodecane-1,12-diamine, NMP, reflux.

Molecular Formula = $C_{30}H_{36}Cl_2N_4$. ^{1}H NMR δ 1.24-1.35 (16H, H3′, H4′, H5′, H6′, br m), 1.59-1.69 (4H, H2′, m), 3.22-3.28 (4H, H1′, m), 6.46 (2H, H3, d, J = 5.7 Hz), 7.44 (2H, H6, dd, J = 9.0, 2.1 Hz), 7.78 (2H, H9, d, J = 2.1 Hz), 8.29 (2H, H7, d, J = 9.0 Hz), 8.39 (2H, H2, d, J = 5.7 Hz).

^{13}C NMR: (DMSO-d_6) δ (ppm): 18.49, 25.42, 26.55, 27.69, 28.4, 48.91, 93.34, 117.97, 121.52, 123.86, 124.05, 137.41, 149.07,150.03, 151.83.

2.6.3. Synthesis of dibenzyl-amine bridged *bis*quinolines.

23. (7-chloroquinolin-4-yl)-(4-(7-chloroquinolin-4-yl-aminomethyl)-benzyl)-amine, compound **52**.

4,7-Dichloroquinoline (2.90 g 0.0156 moles) was added to α,α'-diamino-*p*-xylene (1,4-phenylenedimethanamine (136)) (1 g, 0.009 moles) and triethylamine (1.3 g, 0.013 moles)

were reacted at 120°C in Ethoxyethanol (10 ml) under Argon for 16 hrs.

After cooling, water (50 ml) and ethyl acetate (50 ml) were added and the mixture was adjusted to pH 1 (conc. HCl). Precipitated product was filtered off and was triturated in 2N NaOH (150 ml). Extraction with ethyl acetate (100 ml), aqueous solution was evaporated and filtered. Crystalline amine (0.8 g) was obtained. Then reflux in 1N HCl (15 ml) and ethanol (10 ml) producing Crystalline dihydrochloride (0.84 g), (m.p. :>>250°C) (Figure 2.47).

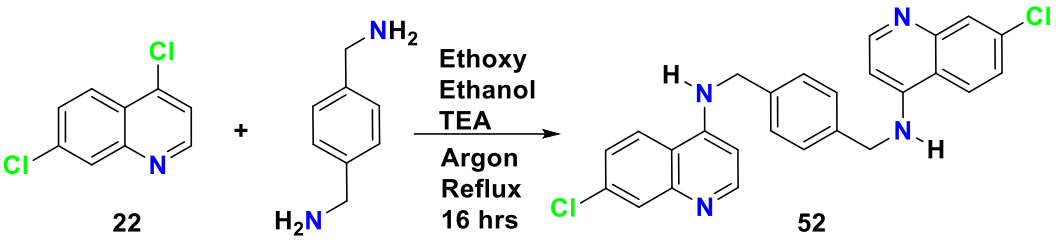

Figure 2.47. Scheme 23, S_NAr displacement, argon, ethoxyethanol, reflux.

Molecular Formula = $C_{26}H_{20}Cl_2N_4$. ^{1}H-NMR (DMSO-d_6/ D_2O) δ (PPM): 4.57(4H, s), 5.54(2H, d, J=7.5 Hz), 7.26(2H, s), 7.56(4H, m, J=2 and 9Hz). 7.75(2H, d, J=2Hz), 8.15(2H, d, J=7.5 Hz), 8.23(2H, d, J=9Hz).

2.6.4. Synthesis of aromatic bridged *bis*quinolines.

24. N^1,N^2-*bis*(7-chloroquinolin-4-l)phenylene-1,2- diamine.2HCl (*ortho*-quine), compound. **24a** (I)

4,7-Dichloroquinoline (1.05 g, 0.005 moles) and freshly recrystallized 1,2-phenylenediamine (0.31 g, 0.003 moles) were refluxed in methanol-water (3: 1, v/v, 40 ml adjusted to pH 4.7 with 2M HCl) for 2 days to give a cream precipitate, then washed with water (3 x 50 ml) and acetone (3 x 50 ml, Analar) respectively. The solid was triturated with and filtered from acetone (3 x 50 ml) before drying (120°C) (Figure 2.48).

Yields from three syntheses of *ortho-quine* were on average 53%; the product was a white powder (decomposition point at around 320°C determined by differential scanning calorimetry (DSC).

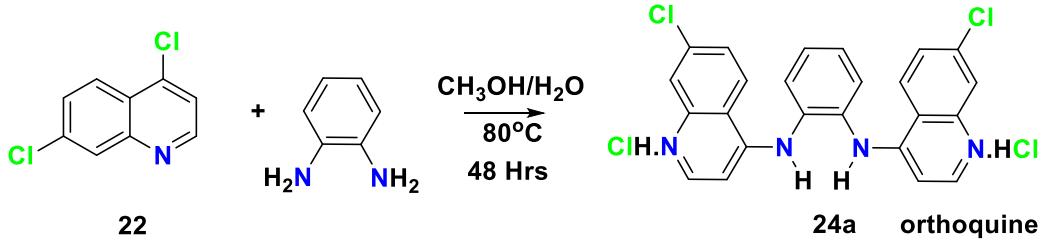

Figure 2.48. Scheme 24, S_NAr displacement, methanol-water (3:1), reflux.

FTIR (cm^{-1}): 3446 (N-H stretch, quinoline), 3442, 3257 (N-H stretch, secondary amine), 3233 (secondary amine), 2930 (C-H aromatic stretch), 1571 (N-H bend, secondary amine), 1416 (C=C stretch), 859 (C-H bend),767, 643 (C-Cl stretch).

Molecular Formula = $C_{24}H_{16}Cl_2N_4$. ^1H NMR (D_20-TFA-*d*): δ (± 0.305 Hz): 6.98 (2H, d, $J_{2,3}$= 7.11 Hz, H_3), 7.76 (2H, dd, $J_{5`,6`}$ = 9.15 Hz, $J_{6,8}$ = 1.69 Hz, H_6), 7.45-7.85 (4H, $H_{2'}$, $H_{3'}$, $H_{4'}$, $H_{5'}$), 8.00 (2H, d, $J_{6,8}$= 1.62Hz, H_8), 8.37 (2H, d, $J_{5,6}$ = 9.14Hz, H_5), 8.39 (2H, d, $J_{2,3}$ = 7.09 Hz, H_2).

^{13}C NMR (TFA-*d*): 158.0 (CH, C2), 118.0 (CH, C3), 144.3 (CH, C1'), 122.0 (CH, C2'), 133.3 (CH, C3'), 144.0 (quaternary C4), 132.7 (CH, C5), 130.1 (CH, C6), 133.7 (quaternary C7), 133.2 (CH, C8), 140.1 (quaternary C9), 122.9 (quaternary C10).

The electron-impact (EI) mass spectrum of purified compound *ortho*-quine contained the ions m/z = 430/432 (100%) confirming $C_{24}H_{16}N_4Cl_2$, 395 (12%) loss of HCl, 268 (18%)monomer, 252 (12%) - NH_2 from monomer, 215 (100%) mass ion and parent ion, 523, mass ion + glycerol + H, 269 (35%), 253 (12%), 218 (6%) 397 (10%). (16%), 178 (4%), 163 (9%), 128 (6%). FAB: 431 (100%) mass ion and parent ion, 523, mass ion + glycerol + H, 269 (35%), 253 (12%), 218 (6%) 397 (10%).

25. N^1, N^3-*bis* (7-chloroquinolin-4-yl)phenylene-1,3-diamine.2HCl (*meta*-quine), compound **21a**.

4,7-Dichloroquinoline (5.12 g, 0.027 moles) and freshly sublimed 1,3-phenylenediamine (1.41 g, 0.013 moles) and copper (2.7 mg, 0.00042 moles) were under reflux for 12 hrs (at 68°C) in acidified (pH 4.7) methanol-water (100: 30, v/v). Product was filtered and triturated three times with Analar acetone and filtered again. Yields of two syntheses were 80% and 85%. m.p. 295-296°C determined by DSC (Figure 2.49).

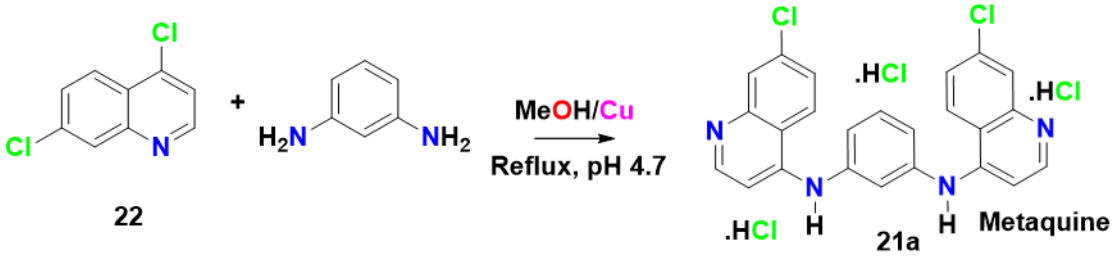

Figure 2.49. Scheme 25, S_NAr displacement, methanol-water (10:3), Cu, reflux.

FTIR (cm^{-1}): 3446 (N-H stretch, quinoline), 3442, 3257 (N-H stretch, secondary amine), 3233 (secondary amine), 2930 (C-H aromatic stretch), 1571 (N-H bend, secondary amine), 1416 (C=C stretch), 859 (C-H bend), 767, 643 (C-C stretch).

Molecular Formula = $C_{24}H_{16}Cl_2N_4$. ^1H NMR (DMSO-d_6) assuming first-order system: δ 6.93 (2H, d, H3),7.09 (1H, s, H6'), 7.22 (2H, dd, $J_{4,6}$= $J_{2,3}$ = 7.94 Hz, H2', H4'), 7.44 (2H, d, $J_{2,6}$=$J_{2,4}$= 1.70, H2), 7.50 (1H, t, $J_{4,5}$=8.01 Hz, H3'), 7.62 (2H, d, $J_{5,6}$= 9.05 Hz, $J_{6',8'}$=2.09 Hz, H6), 7.96 (2H, d, $J_{6,8}$= 2.05 Hz, H8), 8.55 (2H, d, $J_{5,6}$=4.84 Hz, H5).

^{13}C NMR: (DMSO-d_6), δ (ppm): 151.5 (CH, C2), 115.2 (CH, C3), 141.05 (quaternary C1'), 115.7 (CH, C2'), 117.8 (CH, C3'), 102.3 (CH, C6'), 148.4 (quaternary C4), 125.2 (CH, C5), 122.5 (CH, C6), 134.3 (quaternary C7), 128.2 (CH, C8), 148.2 (quaternary C9), 118.2 (quaternary C10).

The chemical ionization (CI) mass spectrum contained the ions m/z = 431/433 confirming $C_{24}H_{16}N_4Cl_2$, 432 (64%), 430 (100%), 394 (7%), 252 (19%), 217 (6%), 215 (9%), 197/198 (10%), 43 (10%).

26. (1S,2S)-*N*^{1},*N*^{2}-*bis*(6-chloro-2-methoxyacridin-9-yl)cyclohexane-1,2-diamine, an acridine hybrid, compound **40**(II).

6,9-Dichloro-2-methoxyacridine (3.56 g, 0.02 moles), (±)-1,2 diaminocyclohexane (1.14 g, 0.01 mol) and triethylamine (2.02 g, 0.02 mol) were heated under reflux in 1-methyl-2-pyrrolidone (25 ml) for 3 days. The mixture was worked up using process I and then process II to give a yellow solid (Figure 2.50). This highly insoluble compound had m.p. of approximately 380°C (yield: 1.75g, 49%) FTIR (cm^{-1}): 3268.95, 3237.61, 3168, 3137, 3 107 (N-H stretch, secondary amine), 3030.77 (C-H aromatic stretch), 1570 (N-H bend, secondary amine), 1223 (C-N stretch, aliphatic), 684.17 (C-Cl stretch). It had similar spectra as last experiment, when run under the same conditions. MS confirmed a molecular ion at m/z = 596, 598 together with the base ion at m/z = 258.

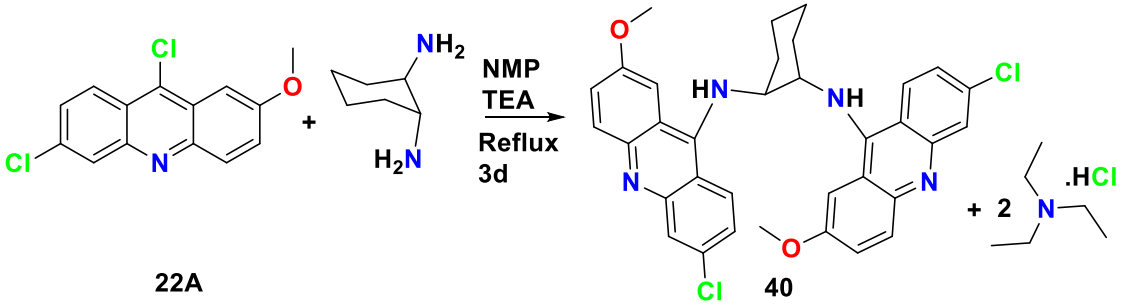

Figure 2.50. Scheme 26. S_NAr displacement, acidified methanol-water (10:3), reflux.

2.6.5. Microwave synthesis (MS).

Microwave synthesis was developed as opposed to thermal synthesis.

27. *N*^{1},*N*^{2}-*bis*(7-chloroquinolin-4-l)phenylene-1,2- diamine.2HCl (*ortho*-quine) compound **24a** (II).

4,7-Dichloroquinoline (1.99 g, 0.01 moles) was added to *ortho*-phenylene-diamine (benzene 1,2 diamine) (0.54 g, 0.005 moles) and copper (2.7 mg, 0.00042 moles) then finely ground (mortar and pestle) until homogenous, With Cu and NaCl. It was then irradiated for 10 minutes at 180°C and 100W (Figure 2.51).

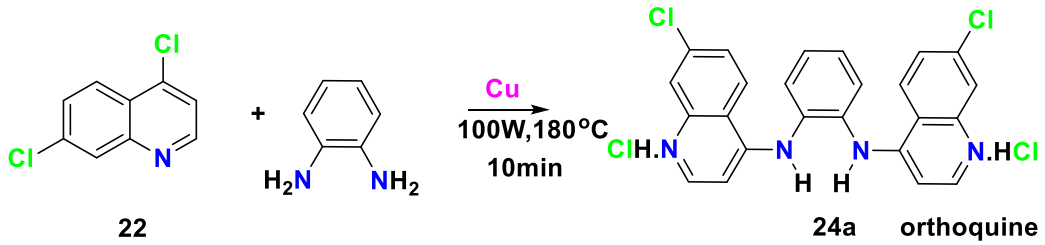

Figure 2.51. Scheme 27, S_NAr displacement, Cu, NaCl, trituration, irradiation.

28. N^1,N^2-*bis*(7-chloroquinolin-4-l)phenylene-1,2- diamine.2HCl (*ortho*-quine) compound **24a** (III).

4,7-Dichloroquinoline (1.97 g, 0.01 moles) was added to of *ortho*-phenylenediamine (0.53 g, 0.005 moles) with copper (4mg, 0.0006 moles) and sodium chloride (6.77 g, 0.12 moles). This was ground with a mortar and pestle until homogenous. It was then irradiated for 30 minutes at 180°C and 100W. Methanol (2.72 g) was added before vortexing. The solution was irradiated for a further 30 minutes at 180°C and 100W (Figure 2.52).

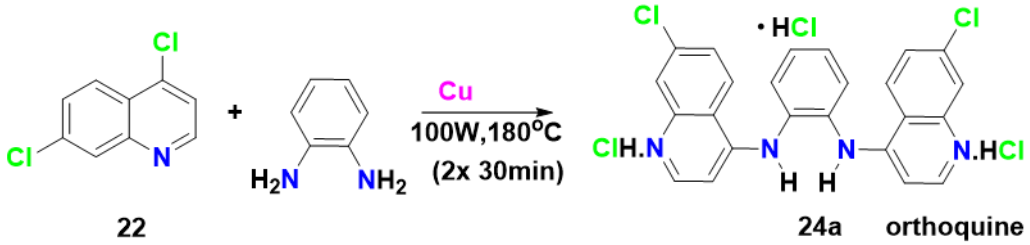

Figure 2.52. Scheme 28, S_NAr displacement, Cu, NaCl, trituration, irradiation.

29. N^1,N^2-*bis*(7-chloroquinolin-4-l)phenylene-1,2- diamine.2HCl (*ortho*-quine) compound **24a** (IV).

4,7-dichloroquinoline (1.00g, 0.005 moles) was added to *ortho*-phenylenediamine (0.27 g, 0.0025 moles). Potassium iodide (0.19 g, 0.012 moles) was added. This was ground with a mortar and pestle until homogenous. This mixture was then split into five equal fractions of approximately 0.29g (Figure 2.53).

Phenol was added five times, approximately 1 gram. Each mixture was then irradiated for 30 minutes at 100W from 125-225°C (Table 2-1). After microwaving, a dark brown solution formed which was yellow and thin at first. 4.5g of acetone was then added to each and irradiated further. The products were filtered, washed with acetone (10 ml) and dried. Products were measured in moles. Optimum results were given at 175°C (Table 2-1).

Table 2-1 Optimisation of *Ortho*-quine Synthesis.

Temp (°C)	Mass of reactants (g)	Mass of phenol (g)	mmoles	Equiv
125	0.29	0.99	10.54	2.077
150	0.29	1.07	11.40	2.248
175	0.29	1.09	11.60	2.287
200	0.29	0.89	9.508	1.874
225	0.28	0.91	9.668	1.905

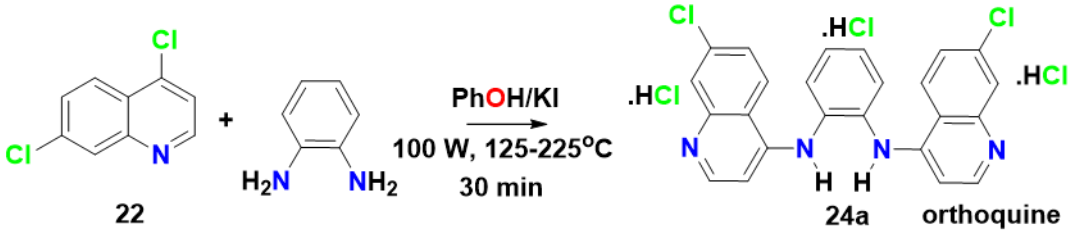

Figure 2.53. Scheme 29, S_NAr displacement, KI, phenol, trituration, irradiation.

30. *N*[1],*N*[2]-*bis*(7-chloroquinolin-4-l)phenylene-1,2- diamine.2HCl (*ortho*-quine) compound **24a** (V).

4,7-dichloroquinoline (1.05g, 0.0053 moles) was added to (0.27g, 0025 moles) of *ortho*-phenylenediamine. Methanol (5g) was added along with phenol (0.96g, 0.01 moles). The mixture was sealed and vortexed, producing a yellow solution (95 minutes, 100W 180°C). As HCl gas was formed, and absorbed, oscillations in the pressure profile were observed, resulting a red solution (Figure 2.54).

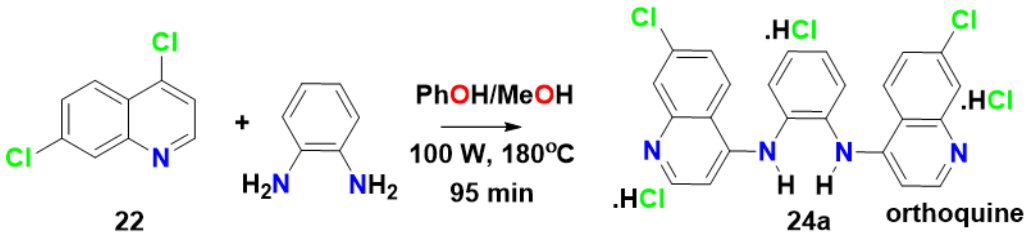

Figure 2.54. Scheme 30, S_NAr displacement, phenol, methanol, trituration, irradiation.

31. *N*[1],*N*[2]-*bis*(7-chloroquinolin-4-l)phenylene-1,2- diamine.2HCl (*ortho*-quine) compound **24a** (VI).

4,7-Dichloroquinoline (1.03 g, 0.0052 moles) was added to *ortho*-phenylenediamine (0.29 g 0.0027 moles), which was dissolved in methanol (4.4 g) before *ortho*phosphoric acid was added (1.73 g, 0.0177 moles). The mixture was sealed and vortexing produced an orange solution that was irradiated (200 minutes, 100W, 150°C). Post irradiation the black solution was poured onto ice-water (Figure 2.55).

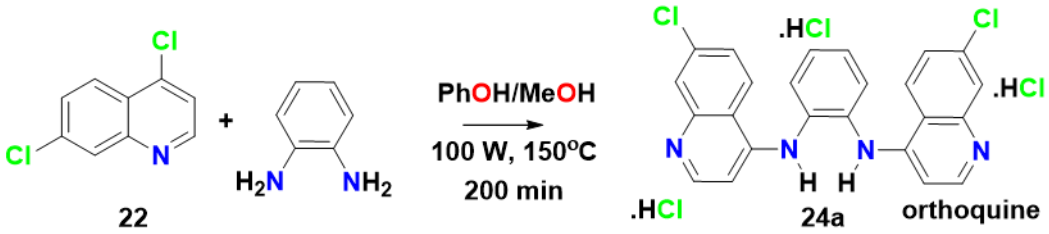

Figure 2.55. Scheme 31, S_NAr displacement, methanol, *ortho*phosphoric acid trituration, irradiation.

Scratching the side of the glass beaker with a Pasteur pipette produced a white material which became dense after15 minutes. The suspension had an apparent pH of 3 (Universal indicator paper). The white solid was then filtered off at the pump and dried in vacuo (12hrs). Ammonia was added to the brown solution producing a yellow solid (pH 5) which was filtered at the pump. Mass Spectrometry showed this to be partly the target product, but mainly the monomer.

32. N^1,N^2-*bis*(7-chloroquinolin-4-l)phenylene-1,2- diamine.2HCl (*ortho*-quine) compound **24a** (VII).

4,7-dichloroquinoline (1g, 0.005 moles) was added to *ortho*-phenylene-diamine (0.26 g, 0.0025 moles) dissolved in methanol (3.76 g) to which *ortho*phosphoric acid (3.17 g, 0.032 moles) was added dropwise with stirring. The mixture was sealed and vortexed to give an orange solution. Irradiation of the mixture (185 minutes, 100W, 150°C). Producing a black solution. (Scheme 32)

33. N^1,N^2-*bis*(7-chloroquinolin-4-l)phenylene-1,2- diamine.2HCl (*ortho*-quine) compound **24a** (VIII).

4,7-dichloroquinoline (1g, 0.005 moles) was added to *ortho*-phenylenediamine (0.26 g, 0.0025 moles), dissolved in methanol (4g) before *ortho*phosphoric acid (1.95 g, 0.02 moles, 3.9 equivalents) was added dropwise. The mixture was sealed and vortexed producing an orange solution which was irradiated (200 minutes, 100W, 150°C) to give a black solution (Scheme 33).

34. N^1,N^2-*bis*(7-chloroquinolin-4-l)phenylene-1,2- diamine.2HCl (*ortho*-quine) compound **24a** (IX).

4,7-dichloroquinoline (0.99 g, 0.005 moles) was added to *ortho*-phenylenediamine (0.29 g, 0.0027 moles), then dissolved in methanol (4.52g). Capping and vortexing produced a pale-yellow solution with a white precipitate. It was irradiated for 60 minutes at 180°C and

100W and post irradiation a black solution was formed (Figure 2.56).

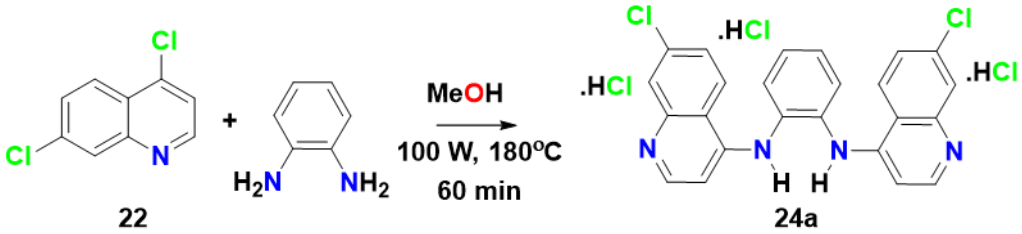

Figure 2.56. Scheme 34, S_NAr displacement, methanol, *ortho*phosphoric acid, trituration, irradiation.

35. Crystallisation of N^1,N^2-*bis*(7-chloroquinolin-4-l)phenylene-1,2- diamine.2HCl (*ortho*-quine).

Attempts were made to crystallise the *ortho*-quine synthesised, compound **24a** (VI) (fraction #1) *ortho*-quine (0.039 g, 0.0091 moles) was dissolved in methanol (2.19 g). This left a clear solution – all had dissolved without the need for vortexing. It was irradiated for 7 minutes at 180˚C and 100W. Microwaving left a clear solution. This was left for a day to cool before being placed in the fridge and formed crystals after 2 years. Previously synthesised compound **24a** (VI) (fraction #2) – *ortho*-quine (0.022 g, 0.0051 moles) - was dissolved in methanol (2.55 g). This left a clear solution, all had dissolved without the need for vortexing. It was irradiated for 7 minutes at 180°C and 100W. Microwaving left a clear solution. This was left for a day to cool before being placed in the fridge (Scheme 35).

36. N^1, N^3-*bis* (7-chloroquinolin-4-yl)phenylene-1,3-diamine.2HCl (*meta*-quine) compound **21a** (II).

4,7-Dichloroquinoline (1.95 g, 0.0098 moles) was added to *meta*-phenylenediamine (0.53 g, 0.0049 moles) with a trace of copper (9.4mg, 0.0015 moles). This was ground with a mortar and pestle until homogenous. It was then irradiated for 30 minutes at 180°C and 100W. After microwaving, coloured solids formed. Brown at the bottom changing to orange and then to yellow at the top. Methanol (4g) was then added before vortexing. The solution was then irradiated for a further 30 minutes at 180°C and 100W. After reflux with methanol, a solvated orange solid formed in a red solution.

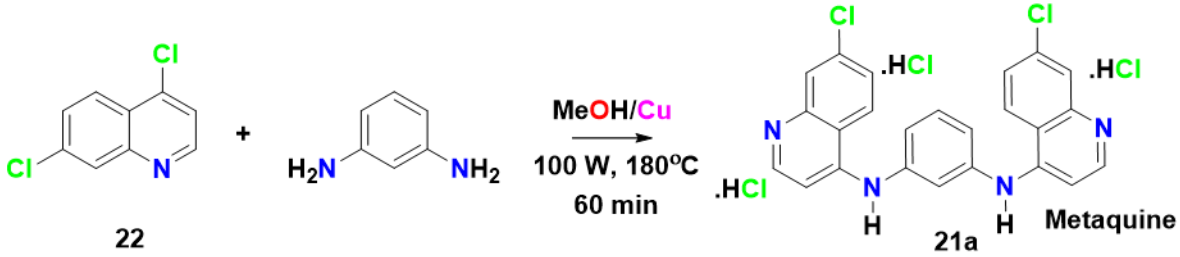

Figure 2.57. Scheme 36, SNAr displacement, methanol, copper, trituration, irradiation.

37. N^1,N^4-*bis*(7-chloroquinolin-4-1)phenylene-1,4-diamine.2HCl (*para*-quine) compound **25a**.

4,7-Dichloroquinoline (10.24 g, 0.052 moles) and freshly recrystallized 1,4-phenylenediamine (2.79g, 0.026 moles) were heated under reflux in acidified (pH 4.7) methanol-water (180: 50, v/v) for 10 h on a steam bath (Figure 2.58). Yields from three syntheses were 8.80g (79%), 10.03g (90%) and 10.13g (91%). Purification was achieved by repeated trituration with Analar acetone and recovery of the insoluble pale-yellow product at the pump (m.p. 295°C-296°C determined by DSC; thermometer > 330°C). FTIR (cm^{-1}): 3446 (N-H stretch, quinoline), 3257 (N-H stretch, secondary amine), 3233 (secondary amine), 2930 (C-H aromatic stretch), 1571 (N-H bend, secondary amine, 1416 (C=C stretch), 859 (C-H bend), 767, 643.

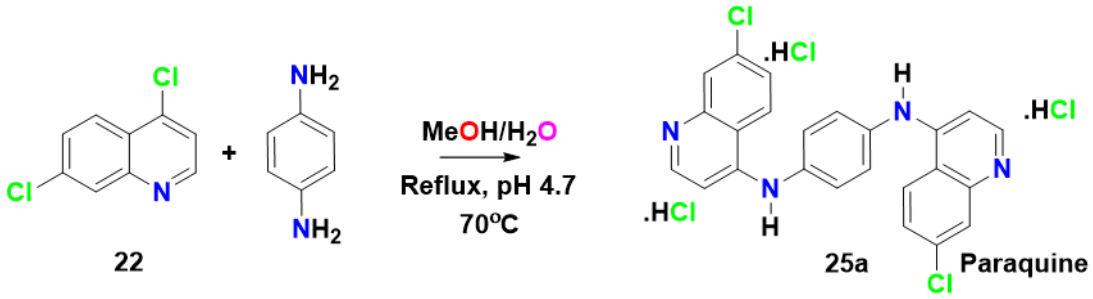

Figure 2.58. Scheme 37. S_NAr displacement, acidified methanol-water (10:3), reflux.

Molecular Formula = $C_{24}H_{16}Cl_2N_4$. ^1H NMR (DMSO-d_6) ^1H NMR (DMSO-d_6) spectra run at 360K with digital resolution ± 0.984Hz: δ 6.95 (2H, d, $J_{2,3=}$ 5.92 Hz, H3), 7.57 (4H, H2', H3', H5', H6'), 7.62 (2H, dd, $J_{5,6}$= 9.05 Hz, $J_{6,8}$= 2.09 Hz, H6), 8.06 (2H, d, $J_{6,8}$= 1.99Hz, H8), 8.55 (2H, d, $J_{2,3}$ = 6.69 Hz, H2), 8.66 (2H, d, $J_{5,6}$ = 9.19 Hz, H5).

^1H NMR: (TFA-D_20) δ 7.04 (2H, d, $J_{2,3}$ = 7.00 Hz, H3), 7.72 (2H, d, H2', H3'), 7.85 (2H, dd, $J_{5,6}$=9.06Hz, $J_{6,8}$= 1.49Hz, H6), 8.02 (2H, s, $J_{6,8}$= 1.58 Hz, H8), 8.33 (2H, d, $J_{2,3}$ = 6.98 Hz, H2), 8.43 (2H, d, $J_{5,6}$ = 9.11 Hz, H5).

^{13}C NMR: (DMSO-d_6), δ (ppm): 141.05 (quaternary C1'), 102.3 (C2', C3'), 151.5 (C2), 124.6 (C3), 148.2 (quaternary C4), 126.7 (C5), 125.2 (C6), 134.3 (quaternary C7), 130.3 (C8), 148.4 (quaternary C9), 118.2 (quaternary C10).

CI MS: m/z = 431/433, 432 (63%), 431 (30%), 430 (100%), 394 (5%), 268 (5%), 252 (12%), 215 (5%), 218 (10%).

A microwave method was also developed for making the *para*-quine molecule.

38. (N^1,N^4-*bis*-(7-chloro-quinolin-4-yl)-benzene-1, 4-diamine)dihydrochloride (*Para*-quine) compound **25a** (II).

4,7-Dichloroquinoline (1.98 g, 0.01 moles) was added to *para*-phenylenediamine (0.54 g,

0.005 moles) with a trace of copper (20 mg, 0.00032 moles). This was ground with a pestle and mortar until homogenous. It was then irradiated for 10 minutes at 180°C and 100W. Coloured solids formed. Orange at the bottom changing to yellow and white at the top. Methanol (2g) was then added before vortexing. It was further microwaved for 25 minutes at 180°C and 100W. A brown solid formed in a darker-brown solution. it had similar spectra as last compound, when run under the same conditions. The experiment was repeated again with similar results (Figure 2.59).

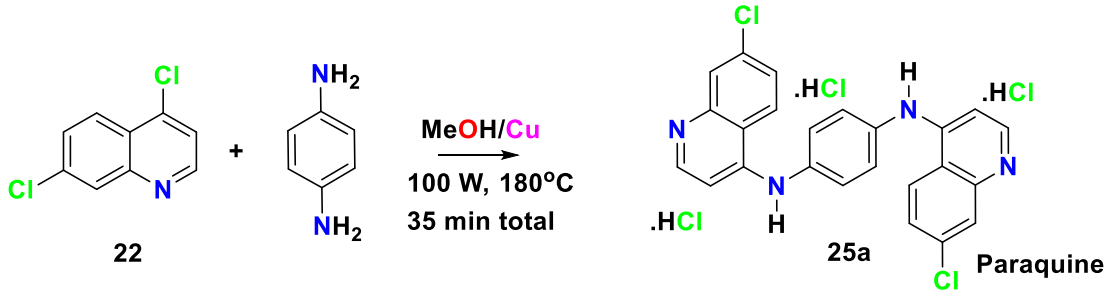

Figure 2.59. Scheme 38, SNAr displacement, methanol, copper, trituration, irradiation.

39. (N^1,N^4-*bis*-(7-chloro-quinolin-4-yl)-benzene-1, 4-diamine)dihydrochloride (*Para*-quine) compound **25a** (III).

4,7-dichloroquinoline (1.98g, 0.01 moles) was added to *para*-phenylenedia-mine (0.54g, 0.005 moles) with a trace of copper (17mg, 0.00027 moles). This was ground with a mortar and pestle until homogenous. It was then irradiated for 10 minutes at 180°C and 100W, forming a yellow solid. Methanol (2g) was then added before vortexing. The solution was then irradiated for a further 30 minutes at 180°C and 100W. Some yellow solid remained but most of the solid turned to a dark orange colour (scheme 39).

2.7. Conclusion.

The synthesis of various *bis*quinolines, was successfully investigated. Aliphatic bridge *bis*quinelines were synthesised comprehensively, Scheme 1 to 22.

Dibenzyl-amine bridged bisquinoline, using ethoxy ethanol was synthesised and analysed (scheme 22).

Aromatic bridged *bis*quinolines, mainly *ortho, meta, para*-quine were synthesised using thermal method and microwave synthesis (scheme 23 to 39). They were subject of full analytical and biological testing.

The development of a potent, soluble, orally bioavailable antimalarial *bis*quinoline, *meta*-quine (*N,N-bis*(7-chloroquinolin-4-yl)benzene-1,3-diamine) (dihydrochloride) was achieved, which is active against *Plasmodium berghei in-vivo* (oral ID_{50} of 25 μmol/kg) and multidrug-resistant *Plasmodium falciparum* K1 *in-vitro* (0.17 μM).

2.8. References.

Adams, J. T., Bradsher, C. K., Breslow, D. S., Amore, T. S., Hause, C. R. 1946. Synthesis of antimalarials; synthesis of certain 1,5- and 1,8-naphthyridine derivatives. *J Am Chem Soc.* 68, 1317-1319.

Andersag, H. 1939. Manufacture of Z-methyl-Z-alkoxy 3-halogen tetrahydrofurans. 2,286,884. *German Patent*.

Anft, B. 1955. Friedlieb Ferinand Runge: A forgotten chemist of the nineteenth century. *J. Chem. Educ.* 32, 566.

Baciocchi, E., Illuminati, G., Marino, G. 1958. Electronic Transmission Through Condensed Ring Systems. III. The Evaluation of epi and cata Sigma Constants from Dissociation and Methoxydechlorination Data on Substituted 1-*Aza*-4-chloronaphthalenes. *J. Am. Chem. Soc.* 80, 2270-2273.

Bandrowski, E. 1886. Oxidation of Diphenylamine. *Montash Chem, 7*, 375-382.

Barlin, G., Jiravinyu, C., YAN, J. 1991. Potential Antimalarials. XIV. Mono-Mannich Bases of 4-(7'-Bromo (and trifluoromethyl)-1',5'-naphthyridin-4'-yl-amino)-5,6,7, 8-tetrahydronaphthalen-1-ols. *Aust. J. Chem.* 44, 677.

Barlin, G., Tan, W. 1985. Potential Antimalarials. III N 4 -Substituted 7-Bromo-1,5-naphthyridin-4-amines. *Aust. J. Chem.* 38, 459.

Basco, L. K., Anderson, S., Milhous, W., Le Bras, J., Vennerstrom, J. 1994. *In vitro* activity of *bis*quinoline WR268,668 against African clones and isolates of *Plasmodium falciparum*. *Am J Trop Med Hyg.* 50, 200-205.

Beak, P., Chaffin, T. L. 1970. Geminal substitution via steroidal 2- and 4-cyano-3-ones. *J Org Chem.* 35, 2275-2282.

Belli, M., Illuminati, G., Marino, G. 1963. Meta-substituent effects on the kinetics of methoxydechlorination of some 2- and 4-chloroquinolines. *Tetrahedron. 19(2)*, 345-355.

Bisby, R. H. 1990. Reactions of a free radical intermediate in the oxidation of amodiaquine. *Biochem Pharmacol*. 39, 2051-2055.

Blanksby, S. J., Ellison, G. B. 2003. Bond dissociation energies of organic molecules. *Acc Chem Res.* 36, 255-263.

Bunnett, J. F., Zahler, R. E. 1951. Aromatic Nucleophilic Substitution Reactions.*Chem. Rev.* 49, 273-412.

BunnetT, J. F., Hermann, D. H. 1970. Kinetics of dinitrophenylation of amino acids. *Biochemistry*. 9, 816-822.

Burckhalter, J. H., Tendick, F. H., Jones, E. M., Holcomb. W. F., Rawlins, A. L. 1948. Aminoalkylphenols as antimalarials (heterocyclicamino)-alpha-amino-o-cresols; the synthesis of camoquin. *J Am Chem Soc*. 70, 1363-1373.

Burckhalter, J. H. 1949. The Mannich Reaction with *o*-Phenylphenol. *Journal of the American Chemical Society*. 72 (2), 5309-5310.

Cain, B. F., Baguley, B. C., Denny, W. A. 1978. Potenial antitumor agents. 28. Deoxyribonucleic acid polyintercalating agents. *J Med Chem.* 21, 658-668.

Chapman, N. B., Russell-Hill, D. Q. 1956. Nucleophilic displacement reactions in aromatic systems. Part V. Kinetics of the reactions of some chloroazanaphthalenes and related compounds with ethoxide ions and with piperidine. *Journal of the Chemical Society.* 1563.

Cheruku, S. R., Maiti, S., Dorn, A., Scorneaux, B., Bhattacharjee, A. K., Ellis, W. Y., Vennerstrom, J. L. 2003. Carbon isosteres of the 4-aminopyridine substructure of chloroquine: effects on pKa, hematin binding, inhibition of hemozoin formation, and parasite growth. *J Med Chem.* 46, 3166-3169.

Cook, G. C. 1995. Adverse effects of chemotherapeutic agents used in tropical medicine. *Drug Safety.* 13, 31-45.

Dascombe, M., Drew, M., Evans, P., Ismail, F. 2007. Rational Design Strategies for the Development of Synthetic Quinoline and Acridine Based Antimalarials. *Frontiers in Drug Design & Discovery*. 3, 559-609.

Dascombe, M. J., Drew, M. G., Morris, H., Wilairat, P., Auparakkitanon, S., Moule, W. A., Alizadeh-Shekalgourabi, S., Evans, P. G., Lloyd, M., Dyas, A. M., Carr, P., Ismail, F. M. 2005. Mapping antimalarial pharmacophores as a useful tool for the rapid discovery of drugs effective *in-vivo*: design, construction, characterization, and pharmacology of *meta*-quine. *J Med Chem.* 48, 5423-5436.

Dearden, J. C., Cronin, M. T., Kaiser, K. L. 2009. How not to develop a quantitative structure-activity or structure-property relationship (QSAR/QSPR). *SAR QSAR Environ Res.* 20, 241-266.

Doubleday, C., Suhrada, C. P., Houk, K. N. 2006. Dynamics of the degenerate rearrangement of bicyclo[3.1.0]hex-2-ene. *J Am Chem Soc.* 128, 90-94.

Eisner, T., Morgan, R. C., Attygalle, A. B., Smedley, S. R., Herath, K. B., Meinwald, J. 1997. Defensive production of quinoline by a *phasmid* insect (Oreophoetes peruana). *The Journal of experimental biology.* 200, 2493-2500.

Elslager, E. F., Thompson, P.E., Olszewski, B. J., Worth, D. F. 1964. Repository Antimalarial Drug. *American Journal of Tropical Medicine and Hygiene*. 12(4), 481-493.

Elslager, E, F., Hess, C., Johnson, J., Ortwine, D., Chu, V., Werbel, L, M. 1981. Synthesis and Antimalarial Effects of W-Aryl-N^4-(dialky1amino)alkyll- and N^4-Aryl*N*- 2(-dialkylamino)alkyl)-2,4-quinazolinediamine. *J.Med.Chem*. 24, 127-140.

Farrell, J., Jenkinson, C., Lavergne, S. N., Maggs, J. L., Park, K. B., Naisbitt, D. J. 2009. Investigation of the immunogenicity of *p*-phenylenediamine and Bandrowski's base in the mouse. *Toxicol Lett.* 185, 153-159.

Forrest, T, P., Dauphinee, G, A., Deraniyag, A., 1984. The mechanism of disproportionation reactions of 1,2-dihydroquinoline. *Can. J. Chem.* Vol 63, 1985, 412-417.

Haigh, C.W., Palmer, M.H., Semple, B. 1965. Preparation and nuclear magnetic resonance

spectra of some halogenoquinolines. Nearly degenerate ABX spectra. *Journal of the chemical society.* Issue 0.

Harrison, A. C., Kitteringham, N. R., Clarke, J. B., Park, B. K. 1992. The mechanism of bioactivation and antigen formation of amodiaquine in the rat. *Biochem Pharmacol.* 43, 1421-1430.

Hassan, J., Sevignon, M., Gozzi, C., Schulz, E., Lemaire, M. 2002. Aryl-aryl bond formation one century after the discovery of the Ullmann reaction. *Chem Rev.* 102, 1359-1470.

Hofheinz, W., Leupin, W. 1998. *N,N-bis*(Quinolin-4-yl)-Diamine Derivatives, their Preparation and their use as Antimalarials. *US Patent.* 5,736,557.

Hu, M. K. 2001. Synthesis and *in-vitro* anticancer evaluation of *bis*-tacrine congeners. *J Pharm Pharmacol. 2001 Jan,* 53, 83-88.

Illuminati, G. 1964. Nucleophilic heteroaromatic substitution Quick View Other Sources. From Advan. *Heterocyclic Chem.* 3,285-371.

Illuminati, G., Marino, G. 1965. The substituent effects on the α and γ reactivity of the quinoline system: Piperidinodechlorination in piperidine. *Ricerca Scientifica. Parte 2: Rendiconti, Sezione A: Abiologica*.

Iseminger, P. W., Gregory, M., Weakley, T. J., Caple, G., Sykes, A. G. 1997. Characterization of 3-Aminophenazin-2-ol Isolated from the Chemical Oxidation of o-Phenylenediamine. *J Org Chem.* 62, 2643-2645.

Ismail, F. 2002. Important Fluorinated Drugs in Experimental and Clinical Use. *Journal of Fluorine Chemistry.* 118, 27-33.

Ismail, F. M., Alizadeh-Shekalgourabi, S., Dascombe, M. J., Carr, P., Wilairat, P., Sutcliffe, L. J., Auparakkitanon, S., Evans, P. 2010. Synthesis, Pharmacology and Molecular Modelling of Novel Antimalarials with Activity *in-vivo*. *Liverpool John Moore university conference*.

Ismail, F. M., Dascombe, M. J., Carr, P., Merette, S. A., Rouault, P. 1998. Novel aryl-*bis*quinolines with antimalarial activity *in-vivo*. *J Pharm Pharmacol.* 50, 483-492.

Ismail, F. M., Dascombe, M. J., Carr, P., North, S. E. 1996. An exploration of the structure-activity relationships of 4-aminoquinolines: novel antimalarials with activity in-vivo. *J Pharm Pharmacol.* 48, 841-850.

Kami, H., Watanabe, T., Takemura, S., Kameda, Y., Hirayama, T. 2000. Isolation and chemical--structural identification of a novel aromatic amine mutagen in an ozonized solution of m-phenylenediamine. *Chem Res Toxicol.* 13, 165-169.

Kermack, K. A., Haldane, J. B. 1950. Attempts to find new antimalarials. Part XXIX. The synthesis of various derivatives of 2: 3-benz-γ-carboline. *J. Chem. Soc.* 607-612.

Kgokong, J. L., Matsabisa, G. M., Smithand, P. P., Breytenbach, J. C. 2008. *N,N-bis*(trifluoromethylquinolin-4-yl)diamino alkanes: synthesis and antimalarial activity. *Med Chem.* 4, 438-445.

Lutz, R. E., Ohnmacht, C. J., Patel, A. R. 1971. Antimalarials. 7. *Bis*(trifluoromethyl)-(2-piperidyl)-4- quinolinemethanols. *J Med Chem.* 14, 926-928.

Maggs, J. L., Tingle, M. D., Kitteringham, N. R., Park, B. K. 1988. Drug-protein conjugates--XIV. Mechanisms of formation of protein-arylating intermediates from amodiaquine, a myelotoxin and hepatotoxin in man. *Biochem Pharmacol.* 37, 303-311.

Magidson, O. J., Grigorovskii, A. M. 1933. Formation of meso-chloroacridines, and the mobility of chlorine in the mesoposition. Berichte der Deutschen Chemischen Gesellschaft. *Berichte der Deutschen Chemischen Gesellschaft, (Abteilung) B: Abhandlungen.* 66B, 866-872.

Magidson, O. J., Grigorovskii, A. M. 1936. Acridin-Verbindungen und ihre Antimalaria-Wirkung (I. Mittail.). Aus d. Synthet. Abteil. d. Chem.-pharmazeut. Forschungs-Instituts N. I. Moskau. *Eingegangen*. 396-400.

March, J. 1985. Advanced organic chemistry. mechanisms and structure 3ed. New York, *Wiley*.

Mc Caustland, D., Cheng, C. P. 1970. 1,5-naphthyridines. Synthesis of 7-chloro-4-(4- diethylamino-1-methylbutylamino)-2-methoxy-1,5-naphthyridine and related compounds. *Journal of Heterocyclic Chemistry.* 7, 467-473.

Mital, A., Singh, V., Ramachandran, U. 2006. Synthesis and antimycobacterial activities of certain trifluoromethyl-aminoquinoline derivatives. *Arkivoc.* (10), 220-227.

Motiwala, H., Kumar, R., Chakraborti, A. 2007. Microwave-Accelerated Solvent- and Catalyst-Free Synthesis of 4-Aminoaryl/alkyl-7-chloroquinolines and 2-Aminoaryl/alkylbenzothiazoles. *Aust. J. Chem.* 60, 269.

Muller, P., Siegfried, B. 1972. Nucleophilic Substitution in Dipolar Aprotic Solvents: Hexamethylphosphoric triamide. *Helvetica*. Volume 55, issue 8. https://doi.org/10.1002/hlca.19720550829.

Muller, O., Van Hensbroek, M. B., Jaffar, S., Drakeley, C., Okorie, C., Joof, D., Pinder, M., Greenwood, B. 1996. A randomized trial of chloroquine (1), amodiaquine and pyrimethamine-sulphadoxine in Gambian children with uncomplicated malaria. *Trop Med Int Health.* 1, 124-132.

Neftel, K. A., Woodtly, W., Schmid, M., Frick, P. G., Fehr, J. 1986. Amodiaquine induced agranulocytosis and liver damage. *Br Med J (Clin Res Ed).* 292, 721-723.

Nogueira, F., Rosario, V, E., 2010. Methods for assessment of antimalarial activity in the different phases of the *Plasmodium* life cycle. *Rev Pan-Amaz Saude* [online]. vol.1, n.3, pp.109-124. ISSN 2176-6215.

Olah, G. 2009. Superacid chemistry. *Hoboken, N.J. Wiley*.

Olliaro, P., Nevill, C., Lebras, J., Ringwald, P., Mussano, P., Garner, P., Brasseur, P. 1996. Systematic review of amodiaquine treatment in uncomplicated malaria. *Lancet.* 348, 1196-1201.

O'neill, P. M., Mukhtar, A., Stocks, P. A., Randle, L. E., Hindley, S., Ward, S. A., Storr, R.

C., Bickley, J. F., O'neil, I. A., Maggs, J. L., Hughes, R. H., Winstanley, P. A., Bray, P. G., Park, B. K. 2003. Isoquine and related amodiaquine analogues: a new generation of improved 4-aminoquinoline antimalarials. *J Med Chem.* 46, 4933-4945.

O'neill, P. M., Park, B. K., Ward, S. A. 2000. Synthesis, antimalarial activity, and molecular modeling of tebuquine analogues. *PCT*/GB1999/002812.

O'neill, P. M., Willock, D. J., Hawley, S. R., Bray, P. G., Storr, R. C., Ward, S. A., Park, B. K. 1997. Synthesis, antimalarial activity, and molecular modeling of tebuquine analogues. *J Med Chem.* 40, 437-448.

Osborne, A., Buley, J., Clarke, H., Dakin, R., Price, P. 1993. 2,4-Dihalogenoquinolines. Synthesis, orientation effects and ^{1}H and ^{13}C NMR spectral studies. *Journal of the Chemical Society, Perkin Transactions. 1, (22)*, 2747-2755.

Patel, H. D., Prajapati, S. M., Patel, K. D., Vekariya, R. H., Panchal, S. N. 2014. Recent advances in the synthesis of quinolines: a review. *RSC Adv*. 2014, 4, 24463. DOI: 10.1039/c4ra01814a.

Pearson, D. E., Jones, W. H., Cope, A. C. 1946. Synthesis of monoalkyl-substituted diamines and their condensation products with 4,7-dichloroquinoline. *J Am Chem Soc.* 68, 1225-1229.

Perrin, D. D., Armarego, W. L. F. 1988. Purification of laboratory chemicals, Oxford; New York, *Pergamon Press*.

Peters, W., Portus, H., Robinson, L. 1975. The four-day suppressive *in vivo* antimalarial test. *Ann Trop Med Parasitol*. 69:155–71.

Peters, W. 1975. The chemotherapy of rodent malaria, XXII. The value of drug-resistant strains of P. berghei in screening for blood schizontocidal activity. *Annals of tropical medicine and parasitology*. 69 (2), 155–171.

Price, C., Roberts, R. 1946. The Synthesis of 4-Hydroxyquinolines. 1. Through Ethoxymethylenemalonic Ester. *J. Am. Chem. Soc.* 68, 1204-1208.

Ramon, G., Davies, k., Nassimbeni. L. R. 2014. Structures of benzoic acids with substituted pyridines and quinolines: salt versus co-crystal formation. *CrystEngComm*. 16, 5802-5810. DOI: 10.1039/C3CE41963K.

Ridley, R. 1997. Haemoglobin Degradation and Haem Polymerization as Antimalarial Drug Targets. *Journal of Pharmacy and Pharmacology.* 49, 43-48.

Ridley, R. G., Matile, H., Jaquet, C., Dorn, A., Hofheinz, W., Leupin, W., Masciadri, R., Theil, F. P., Richter, W. F., Girometta, M. A., Guenzi, A., Urwyler, H., Gocke, E., Potthast, J. M., Csato, M., Thomas, A., Peters, W. 1997. Antimalarial activity of the *bis*quinoline trans-N^1,N^2-*bis* (7-chloroquinolin-4-yl)cyclohexane-1,2-diamine: comparison of two stereoisomers and detailed evaluation of the S,S enantiomer, Ro 47-7737. *Antimicrob Agents Chemother.* 41, 677-686.

Ruscoe, J. E., Jewell, H., Maggs, J. L., O'neill, P. M., Storr, R. C., Ward, S. A., Park, B. K.

1995. The effect of chemical substitution on the metabolic activation, metabolic detoxication, and pharmacological activity of amodiaquine in the mouse. *J Pharmacol Exp Ther.* 273, 393-404.

Sample, H. C., Senge, M, O. 2021, Nucleophilic Aromatic Substitution (S_NAr) and Related Reactions of Porphyrinoids: Mechanistic and Regiochemical Aspects. *Eur. J. Org. Chem*. 2021: 7-42. https://doi.org/10.1002/ejoc.202001183.

Schock, R. 1957. The Preparation of Some *N,N'-bis*-(4-quinaldyl)-α,ω -diaminoalkanes as Potential Trypanocides *J. Am. Chem. Soc.* 79, 1672-1675.

Sebestik, J., Safarik, M., Stibor, I., Hlavacek, J. 2006. Acridin-9-yl exchange: a proposal for the action of some 9-aminoacridine drugs. *Biopolymers.* 84, 605-614.

Singh, T., Hoops, J. F., Biel, J. H., Hoya, W. K., Stein, R. G., Cruz, D. R. 1971. Antimalarials. "Distal" hydrazine derivatives of 7-chloroquinoline. *J Med Chem.* 14, 532-535.

Sinha, B. K., Philen, R. M., Sato, R., Cysyk, R. L. 1977. Synthsis and antitumor properties of *bis*(quinaldine) derivatives. *J Med Chem.* 20, 1528-1531.

Slater, R. 1930. CLII.-Quinoline compounds containing arsenic. Part I. Synthesis of 6-methoxyquinoline derivatives of aminophenylarsinic acids. *Journal of the Chemical Society (Resumed).* 1209-1215.

Slater, R. 1931. XVII.—Quinoline compounds containing arsenic. Part II. Synthesis of 6-methoxyquinoline derivatives of aminophenylarsinic acids by the use of 4-bromo-6-methoxy-2-methylquinoline. *Journal of the Chemical Society (Resumed).* 107-118.

Smalley, R, K. 1977. Chapter 3 Haloquinolines. "The Chemistry of heterocyclic compounds: Quinolines Part I" Volume 32, p 319-786, Ed. by Gurnos Jones. *J.Wiley*, N.Y.

Socrates, G. 2004. Infrared and Raman Characteristic Group Frequencies: Tables and Charts, 3rd Edition, *J.Wiley*. N.Y.

Staderini, M., Cabezas, N., Bolognesi, M. L., Menendez, J. C. 2013. Solvent- and chromatography-free amination of π-deficient nitrogen heterocycles under microwave irradiation. A fast, efficient and green route to 9-aminoacridines, 4-aminoquinolines and 4-aminoquinazolines and its application to the synthesis of the drugs amsacrine and bistacrine. *Tetrahedron. 69(3),* 1024-1030.

Surrey, A, R., Cutler, R. 1951. The role of phenol in the reaction of 4,7-dichloroquinoline with Novol diamine. *J. Am. Chem. Soc*. 73, 2623-2626.

Surrey, A, R., Hammer, H, F. 1946. The Preparation of Bz-Dichloro-4-aminoquinoline Derivatives. *J. Am. Chem. Soc*. 68, 1244–1246.

Sveinbjornsson, A., Vanderwerf, C. A. 1951. Synthesis of 2-Diethylaminomethyl-4-(7 -chloro-4-quinolyl)-aminofluorobenzene Dihydrobromide. *J. Am. Chem. Soc.* 73, 1378-1379.

Terrier, F., Buncel, E., Crampton, M, R., Strauss, M, J. 1984. Electron Deficient Aromatic- and Heteroaromatic-Base Interactions. The Chemistry of Anionic Sigma Complexes, *Elsevier*. Amsterdam.

Tyman, J., Ghorbanian, S., Muir, M., Tychopoulous., V., B., I., Fisher, I. 1989. Improved Nucleophilic Displacements in *N*-Methyl Pyrrolidinone as a Solvent. *Synthetic Communications.* 19(1-2), 179-188.

Vennerstrom, J. L., Ager, A. L., Dorn, A., Andersen, S. L., Gerena, L., Ridley, R. G., Milhous, W. K. 1998. *Bis*quinolines. 2. Antimalarial *N,N-bis*(7-chloroquinolin-4-yl)heteroalkanediamines. *J Med Chem.* 41, 4360-4364.

Vennerstrom, J. L., Ellis, W. Y., Ager, A. L., Andersen, S. L., Gerena, L., Milhous, W. K. 1992. *Bis*quinolines. 1. *N,N-bis*(7-chloroquinolin-4-yl)alkanediamines with potential against chloroquine (1)-resistant malaria. *J Med Chem.* 35, 2129-2134.

Vippagunta, S. R., Dorn, A., Matile, H., Bhattacharjee, A. K., Karle, J. M., Ellis, W. Y., Ridley, R. G., Vennerstrom, J. L. 1999. Structural specificity of chloroquine (1)-hematin binding related to inhibition of hematin polymerization and parasite growth. *J Med Chem.* 42, 4630-4639.

Watanabe, T., Hirayama, T., Fukui, S. 1989. Phenazine derivatives as the mutagenic reaction product from *o*- or *m*-phenylenediamine derivatives with hydrogen peroxide. *Mutat Res.* 227, 135-145.

Werbel, L. M., Cook, P. D., Elslager, E. F., Hung, J. H., Johnson, J. L., Kesten, S. J., Mcnamara, D. J., Ortwine, D. F., Worth, D. F. 1986. Synthesis, antimalarial activity, and quantitative structure-activity relationships of tebuquine and a series of related 5-((7-chloro-4-quinolinyl)amino)-3-((alkylamino)methyl) (1,1'-biphenyl)-2-ols and N omega-oxides. *J Med Chem.* 29, 924-939.

Werbel, L. M., Thompson, P. E. 1972. Antimalarial agents: chemistry and pharmacology, New York, *Academic Press*.

Zhu, Y., Zhao, G., Zhou, Y. 2002. A novel synthetic method of di-9-acridinyl derivatives of amines. *Chinese Journal of Synthetic Chemistry.* 10, 65-67.

Ziegler, J., Linck, R., Wright, D. W. 2001. Heme Aggregation inhibitors: antimalarial drugs targeting an essential biomineralization process. *Curr Med Chem.* 8, 171-189.

Chapter 3

Modulation of antimalarial activity at a putative *bis*quinoline receptor *in-vivo* using fluorinated *bis*quinolines.

Index of contents chapter 3.

Figure of contents chapter 3.

Table of contents chapter 3.

Aim.

Antimalarials interact with Haem covalently, π..π or by hydrogen bonding. This study investigates prototropy of quinoline methanols using quantum mechanics. Theoretical calculations (DFT calculations: B3LYP/BS1) and crystal structure of (±)-*trans*- N^1, N^2-*bis*-(2,8-ditrifluoromethyl-quinolin-4-yl) cyclo-hexane-1, 2-diamine (**26f**) are used to investigate the protonation sites and hence the preferred mode of interaction with haematin.

A new hydrogen bonding pattern involving trifluoromethyl groups and propionic side chains in hematin has been found that may explain the high antimalarial activity found in 2,8-*bis*-trifluorinated quinoline methanols such as mefloquine (**13**).

3.1. Introduction.

One currently effective, but expensive, antimalarial drug is the fluorinated quinoline methanol, mefloquine (**13**) (Page 22), Lariam^{TM}, (*R, S)*-(±)-α-2-piperidinyl-2,8-(*bis*-trifluoromethyl)-4-quinolinyl methanol). Despite limited clinical use, the incidence of drug resistance to (**13**) continues to increase world-wide (Cravo *et al.,* **2013**). Also, of great concern, especially to travelers from wealthy countries where malaria is non endemic, is the occurrence of adverse neuropsychiatric reactions to (**13**) (Van Riemsdijk *et al.,* **1997**). In order to better understand the molecular mechanism(s) of antimalarial action, the effect of trifluoromethylation has been examined in several *mono*quinolines (Ismail *et al.,* **2002**).

Previously, characterization of a putative *bis*quinoline receptor encoded with features desirable within 4-aminoquinolines and, perhaps, quinoline methanol antimalarials with activity *in-vivo* have proven useful in exploring the mechanism of antimalarial drug action (Ismail *et al.,* **1996**, **1998**).

One important factor is determining the sites of proton acceptance and donation within these drugs as they contain both aliphatic and aromatic nitrogen groups. Certain biochemical and pharmacological evidence suggests that 4-aminoquinolines such as (**26b**) (Figure 3.2) interfere with haem processing (Gabay *et al.,* **1994**; Egan *et al.,* **1997**; Chou *et al.,* **1980**) although this hypothesis has been challenged (Meshnick *et al.,* **1997**). The poor solubility of these *bis*quinolines in common solvents necessitates that quantum mechanical methods are used to predict sites of protonation and lipophilicity. Despite the exact molecular sequence of events that lead to *Plasmodial* death not being known, it is currently accepted that processes leading up to and involving the formation of haemozoin can be disrupted *in-vitro* by 4-amino quinolines and by a different binding geometry, quinoline methanols (Chou *et al*., **1980**).

The absence of fluorine in mammalian systems as well as the high natural abundance of this NMR active isotope (^{19}F) (Ismail *et al.,* **2002**) has been previously exploited as a sensitive probe for quinoline receptor binding in solution (Hooper *et al.,* **1993**). Mass spectrometry based cartographic analysis (Pacholski and Winograd, **1999**) of mefloquine distribution within *Plasmodia* has revealed its accumulation profile (Guerquin-Kern *et al.,* **1997**). In order to refine our model further, we examined factors modulating antimalarial activity and explored possible homology with mefloquine-type compounds.

Reports in the literature can be subdivided into studies involving interactions with the quinoline ring and those involving side chain substituents. Interestingly, Andersag (Andersag *et al.,* **1941**) found that the trifluoromethyl bioisostere (**1a**) (Figure 3.2) failed to confer advantages over chloroquine (**1**) (Figure 3.2), a result subsequently confirmed against sensitive and resistant strains *in-vitro* (De *et al.,* **1998**).

VanderWerf *et al* pioneered bioisosteric replacement of the hydroxyl group of amodiaquine (**9**) (Figure 3.3) with fluorine, which resulted in less activity than amodiaquine (**9**) *in-vivo* (O'Neill *et al.,* **1994**)

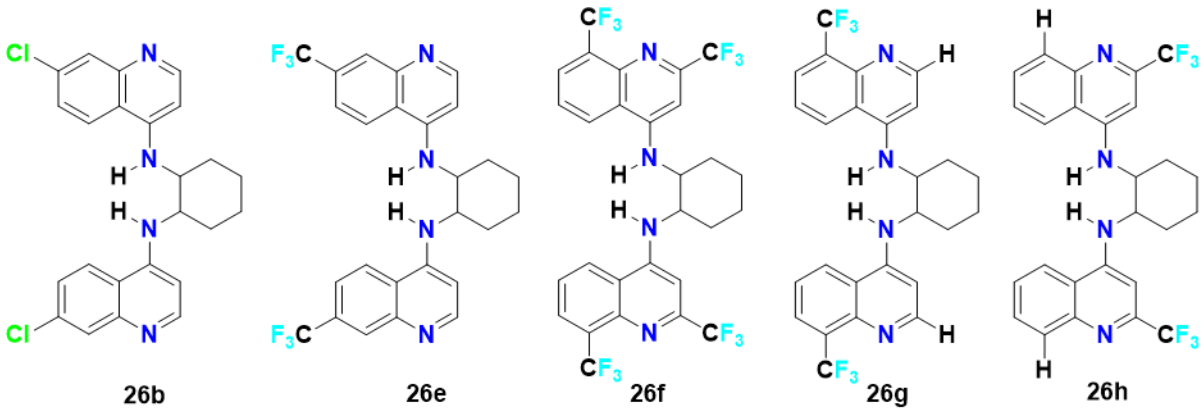

Figure 3.1. (±)-*trans*- and *cis*-N^1,N^2-*bis*(7-chloroquinolin-4-yl)cyclohexane-1,2-diamine is (**26**). (**26b**) (**26e**) (**26f**) (**26g**) and (**26h**) without additional letters are used generically to describe any isomer. They can exist in different isomeric forms. i.e.There are two isomers for these compounds named as **A** (R-R) with *trans* geometry, and **B** (R,S) with *cis* geometry, with the identifiers equatorial (eq) and axial (ax) respectively referring to the position of the substituent amino nitrogen atoms relative to the cyclohexane ring. (Dascombe *et al*., 2005)

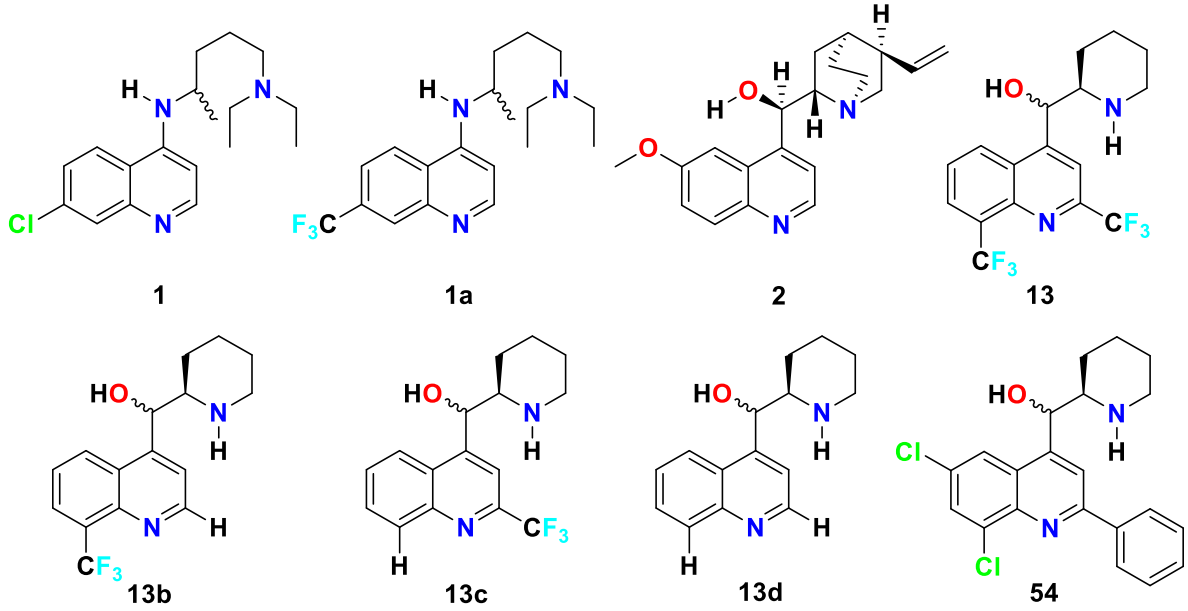

Figure 3.2. Structural formulae chloroquine (**1**) and its derivative (**1a**), Quinine (**2**), Mefloquine (**13**) and its derivatives, (6, 8-Dichloro-2-phenyl-quinolin-4-yl)-piperidin-2-yl-methanol (WR7930) (**54**) (Eynde *et al*., 2019).

Although this compound (**9a**) (Figure 3.3) showed a corresponding loss of antimalarial potency when compared to amodiaquine *in-vitro*, the need for new antimalarials is such that it was successfully patented (Park *et al.*, **2002**). A greater degree of success has been achieved in the 8-aminoquinoline class of compounds, such as WR 238, 605 (Tafenoquine, Krintafel) (**55**), which benefit from judicious introduction of trifluoromethyl substituents into the side chain. (McIntyre *et al.*, **2002**; Eynde *et al.*, **2019**).

The synthesis and pharmacological profile of (**13**) (Figure 3.2) resulted from the antimalarial program initiated by the US Army during World War II; the drug came into use after the end of the US-Vietnam conflict (Clyde *et al.*, **1973**; Kitchener, **2003**; Lim *et al.*, **1985**; Ohnmacht *et al.*, **1971**; Pullman *et al.*, **1948**; Rieckmann *et al.*, **1975**; Wiselogle, **1946**).

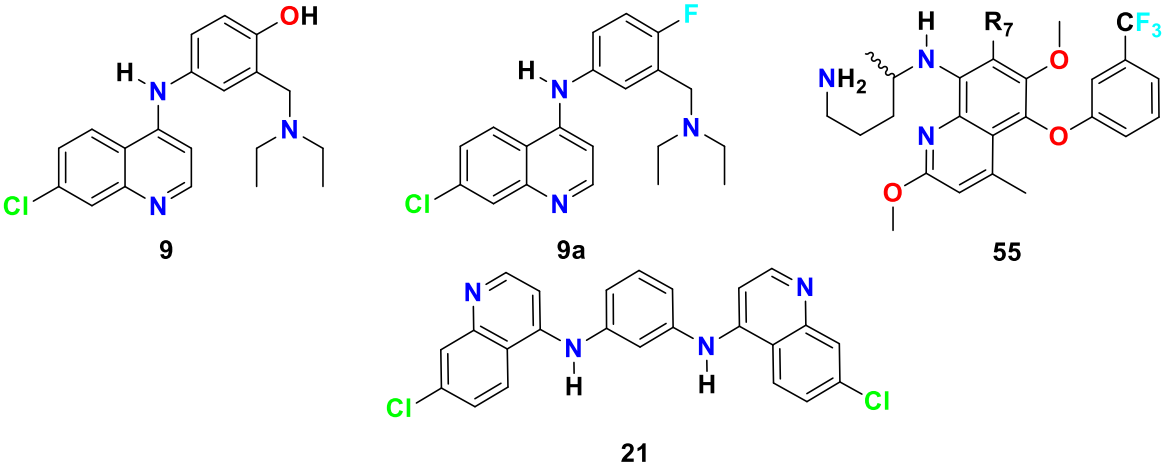

Figure 3.3. Amodiaquine (**9**) and its derivative (**9a**) WR 238,605 (CAS 106635-81-8) (Tafenoquine, Krintafel) (**55**) (Eynde *et al.*, 2019) (R7 = H); *meta*-quine (**21**) (Dascombe *et al.*, 2005).

A mefloquine progenitor, (**54**) (Figure 3.2) was first disclosed in a comprehensive survey of antimalarials by Wiselogle (Wiselogle, **1946**), which also showed that in quinine (**2**) the quinuclidine ring could be simplified and also that the methoxy group could be replaced by halogens (consequently enhancing overall drug lipophilicity). The resulting compound showed an 80-fold greater activity than (**2**) (Figure 3.2) (Pullman *et al.*, **1948**), initially in a duck (*Plasmodium cathaemrium*) (Ohnmacht *et al.*, **1971**) and, subsequently, a murine model of malaria (*Plasmodium berghei*). Introduction of the lipophilic groups into position 2 of both (**13**) and (**54**) effectively delay premature metabolic inactivation at this position by oxidation, an assumed weakness of Quinine (**2**) (Figure 3.2) (Mirghani, **2002**; Sarma *et al.*, **2005**).

The prolonged photosensitizing action of (**54**) (Figure 3.2) prevented further development of this *seco*-derivative into a clinically useful drug (Pullman *et al.*, **1948**). In contrast, the introduction of trifluoromethyl (CF_3) groups into positions 2 and 8 were dictated by bioassay-guided antimalarial screening. This provided a compound with an improved antimalarial/ pharmacological profile against *Plasmodium berghei in-vivo* (Clyde *et al.*, **1973**; Ohnmacht *et al.*, **1971**). Similarly, the exact role of substituent positioning, especially chlorine on position 7 in 4-aminoquinoline antimalarials (**1** and **26b**) (Figure 3.1) has never been adequately clarified. Presumably the chlorine atoms in (**26b**) (Figure 3.1) impart improved lipophilic and/or pharmacokinetic properties (We can use software such as Chemdraw to determine the Log P (ClogP value other software can also be used determine pharmacokinetic profile)), but they may also serve a yet undefined pharmacodynamic role such as reduction of

metabolism. The structural significance of halogenated substituents, whether it is chlorine or trifluoromethyl remains unknown. However, halogens alter and retard premature metabolism of a drug (so called obstructive halogenation) and for this reason, chloroquine may possess a halogen at the 7-position (Ismail *et al.,* **2005**). Studies of chloro and *di*-chloro analogues in a haem binding assay suggest that this group in the 7- position enhances binding of chloroquine-like drugs to the monomeric haem drug target *in-vitro* (Egan *et al*., **2000**)**.** The work described in this chapter allows some suggestions as to their role when binding to the haem receptor.

One enantiomer of chloroquine (**1**) (Figure 3.2) (dextrorotary (+) and thus assigned as the S-CQ) demonstrates greater antimalarial (Haberkorn *et al.,* **1979)** and anti-covid efficacy than the other (Li *et al*., **2020**). Similarly, enantiomers of mefloquine possess differing pharmacodynamic and pharmacokinetic profiles (Lima *et al.,* **2002**; Pham *et al.,* **1999**; Tajerzadeh & Cutler, **1993**). Our most potent compounds developed using this receptor model include individual enantiomers of (±)-*trans*-N^1, N^2-*bis*-(7-chloroquinolin-4-yl)cyclohexane-1,2-diamine (**26b**, ID_{50} < 2.5 mg/kg, 0.0057 mol/kg) as well as its structural isomer. (Ismail *et al.*, **1996**, **1998**).

Dascombe *et al.*, reported a molecular mechanics study detailing the binding geometry of *meta*-quine (Figure 3.3) to haematin (Pham *et al.,* **1999**). In this earlier report, a number of close contacts with the receptor were revealed, including hydrogen bonds. Such observations, together with our previous study, prompted the construction of a lead compound incorporating bulky CF_3 groups (Ismail *et al.,* **2002**; Robinson *et al.*, **1997**) in positions 2 and 8 of the quinoline ring and bridged at position 4 with (±)-*trans*-1, 2-diaminocyclohexane to make a *bis*-(mefloquine/4-aminoquinoline) hybrid. In addition, one or more suitably positioned CF_3 groups may modulate, either favourably or unfavourably, lipophilicity (Yale, **1958**), as well as protect various antimalarials from metabolism (Ismail *et al.,* **2002**).

In this part of the study, a mefloquine/*bis*quinoline hybrid was constructed to ascertain:

(i) what effect this would have on antimalarial activity *in-vivo;*
(ii) to elucidate hydrogen bonding sites within these drugs and their site of CF_3 substitution;
(iii) to explore the potential sites of protonation through quantum mechanical calculations (Dascombe *et al.,* **2005**) and
(iv) to examine these interactions using x-ray crystallography and molecular mechanics.

3.2 Results and discussion.

3.2.1. Synthesis.

The target substance (±)-*trans*- N^1, N^2-*bis*-(2,8-ditrifluoromethyl-quinolin-4-yl) cyclohexane-1, 2-diamine (**26f**) was constructed by refluxing freshly distilled (±)-*trans*-1, 2-diaminocyclohexane with two equivalents of the corresponding 4-halo-2,8-*bis*-trifluoromethyl substituted quinolines under atmosphere of argon. Use of anhydrous *N*-methylpyrollidinone (NMP) with triethylamine under reflux (forcing conditions) encouraged dimer formation (Ismail *et al.*, **1996**, **1998**).

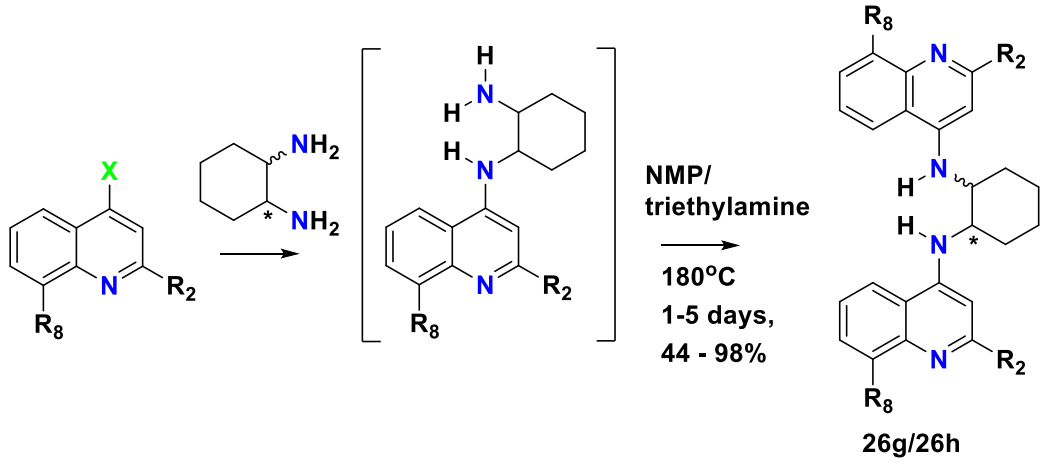

Figure 3.4. Stepwise de-halogenoamination and S_NAr reaction. *bis*quinoline formation where (R_2 = H or CF_3; R_8 = H or CF_3). When 4-bromo (or 4-chloro)-2,8-trifluoro methyl quinoline was used for the S_NAr reaction, the reaction mixtures always became blue-black despite the presence of a protective atmosphere of argon.

It is possible that the reactants or products were photosensitive, hence all further experiments were conducted in aluminum foil covered reactors. For instance, 4-bromo-2, 8-(*bis*-trifluoromethyl)-quinoline reacted with (±)-*trans*-1,2-diaminocyclohexane, triethylamine/NMP (180°C, 5 days, sand bath) to provide the required product (**26f**) in 88% crude yield (Ismail *et al.*, **1996**, **1998**). Repeated recrystallization of the crude brown/black reaction mixture from acetone/HCl gave a 44% overall purified yield of the required grey dimer (**26f**). The (±)-*trans*-N^1-(2, 8-di-trifluoromethylquinolin-4-yl) cyclohexane-1, 2-diamine intermediate (*mono*-quinoline) was not detected (Figure 3.4), presumably a consequence of the long reaction times employed. The poor solubility profile, typical of such salts e.g. (**26b**) (Ismail *et al.*, **1996**, **1998**), prevented the acquisition of NMR spectra of the salt necessitating conversion to the free base for such experiments. Nevertheless, the solubility of (**26f**) in DMSO was still inadequate, requiring long spectral acquisition times and the use of a sensitive inverse probe NMR instrument equipped with gradient detection facility.

EI-mass spectra (m/z = 640 Da), revealed loss of a fluorine radical from the mass ion leading onto complex fragmentation and rearrangement phenomena (not shown). Since the base ion was m/z =36 (with the expected chlorine isotope patterns), this verified the (unexpected) presence of (**26f**) as a hydrochloride salt. Additional evidence from accurate positive-ion high-resolution electrospray-mass spectrometry of the free base confirmed the identity of the compounds (see below). Compounds (**26b**) and (**26e**) were constructed using anhydrous NMP/Triethylamine as reported previously and in chapter **2**. (Ismail *et al.,* **1996**, **1998**).

HPLC-MS analysis showed monomeric impurities such as starting materials, were absent from purified compounds used in the studies reported here. Positive-ion electrospray high resolution mass spectrometry was performed to confirm whether compounds (**26e**A) and (**26f**A) were singly or doubly protonated (A stands for (R,R) isomer with *trans* geometry). Results indicate that both compounds were exclusively *mono*-protonated. The resultant accurate mass positive-ion spectra indicate good agreement between predicted and observed mass spectra (Table 3-3). Only the 4-aminoquinoline compound formed complexes with haem in electrospray experiments using methanol as the solvent. Both the interaction of (**26e**A) and (**26f**A) with haem, as well as their protonated species, were studied further using molecular modeling methods (see below).

3.2.2. Spectroscopic studies.

The state of ionization of antimalarial drugs is influenced by the environmental pH. For example, whether or not the drug is present in the acidic feeding vacuole of *Plasmodium*. In order to determine the effect of protonation on (**26e**A and **26f**A) the UV spectra were determined in DMSO and in trifluoroacetic acid (TFA). The two compounds exhibited similar UV spectra with two maxima in DMSO, but three maxima in TFA (Table 3-2) with a bathochromic shift reflecting conformational changes upon protonation which were subsequently investigated using quantum mechanics. Similarly, fluorescence spectra of (**26e**A) and (**26f**A) were determined in DMSO and TFA solutions (Table 3.2). Shifts in UV and fluorescence maxima may be used to establish the state of protonation of these compounds in biological systems.

Table 3-1 Fluorescence-spectroscopic data for (**26e**A) and (**26f**A).

COMPOUND	SOLVENT	Excitation Maxima (nm)	Emission Maxima (nm)
(26eA**)**	DMSO	265.46, 346.46	408.46
(26eA**)**	TFA	301.56, 357.01	373.07
(26fA**)**	DMSO	267.03, 348.46, 363.43	418.93
(26fA**)**	TFA	316.00, 347.53, 366.56	387.53

Table 3-2 UV-spectroscopic data for (**26e**A) and (**26f**A) indicating bathochromic shifts upon ionization (A stands for (R-R) isomer with *trans* geometry).

COMPOUND	SOLVENT	MAXIMA	MINIMA
(26eA**)**	DMSO	262nm (ε ≅36,088) 346nm (ε ≅ 38,313)	286nm
(26eA**)**	TFA	256nm (ε≅ 16,931) 334nm (ε ≅ 42,395) 350nm (ε ≅ 43,142)	280nm 340nm
(26fA**)**	DMSO	260nm (ε ≅ 32,425) 354nm (ε ≅ 32,700)	286nm
(26fA**)**	TFA	256nm (ε ≅ 12,954) 338nm (ε ≅ 30,332) 362nm (ε ≅ 34,184)	294nm 352nm

Table 3-3 Observed and predicted masses for (**26e**A) and (**26f**A).

COMPOUND	PREDICTED	OBSERVED	DISCREPANCY
(26eA**)**	505.1821	505.1805	3 ppm
(26fA**)**	641.1575	641.1491	13 ppm

3.2.3. NMR experiments.

Our projected receptor binding experiments require unequivocal identification of both quaternary centers associated with the trifluoromethyl group, because they are sensitive probes for the drug-binding environment. Using the free base, both trifluoromethyl groups were identified by the magnitude of the $^{1}J_{C\text{-}F}$ and $^{2}J_{C\text{-}F}$ coupling constants.

Assuming that the quaternary carbons attached to C-8' are the most deshielded (Proton test experiment/spectral prediction methods are attached), the resonant positions of the remaining peaks were deduced. Partial analysis of vicinal coupling constants ascribed to the (±)-*trans*-1, 2-diamino-cyclohexane bridging unit suggests that the axial-axial conformer predominates in DMSO-d_6 solution, at room temperature, an observation consistent with the situation detected in the solid state (Figure 3.10).

This condition remained unchanged in the presence of both strongly and weakly coordinating solvents such as NMP and methanol. The latter reveals the desired position of hydrogen bonding, the NH proton being split into a doublet by one of two of the eight protons found in this complex, a result confirmed by COSY experiments (Figure 3.5).
This result confirms that the exocyclic secondary amino group participates in hydrogen bonding interactions confirming its role as a donor group and probably acts with haem in a similar fashion (See modelling section) (Ismail *et al*., **1996**, **1998**; Dascombe *et al*., **2005**).

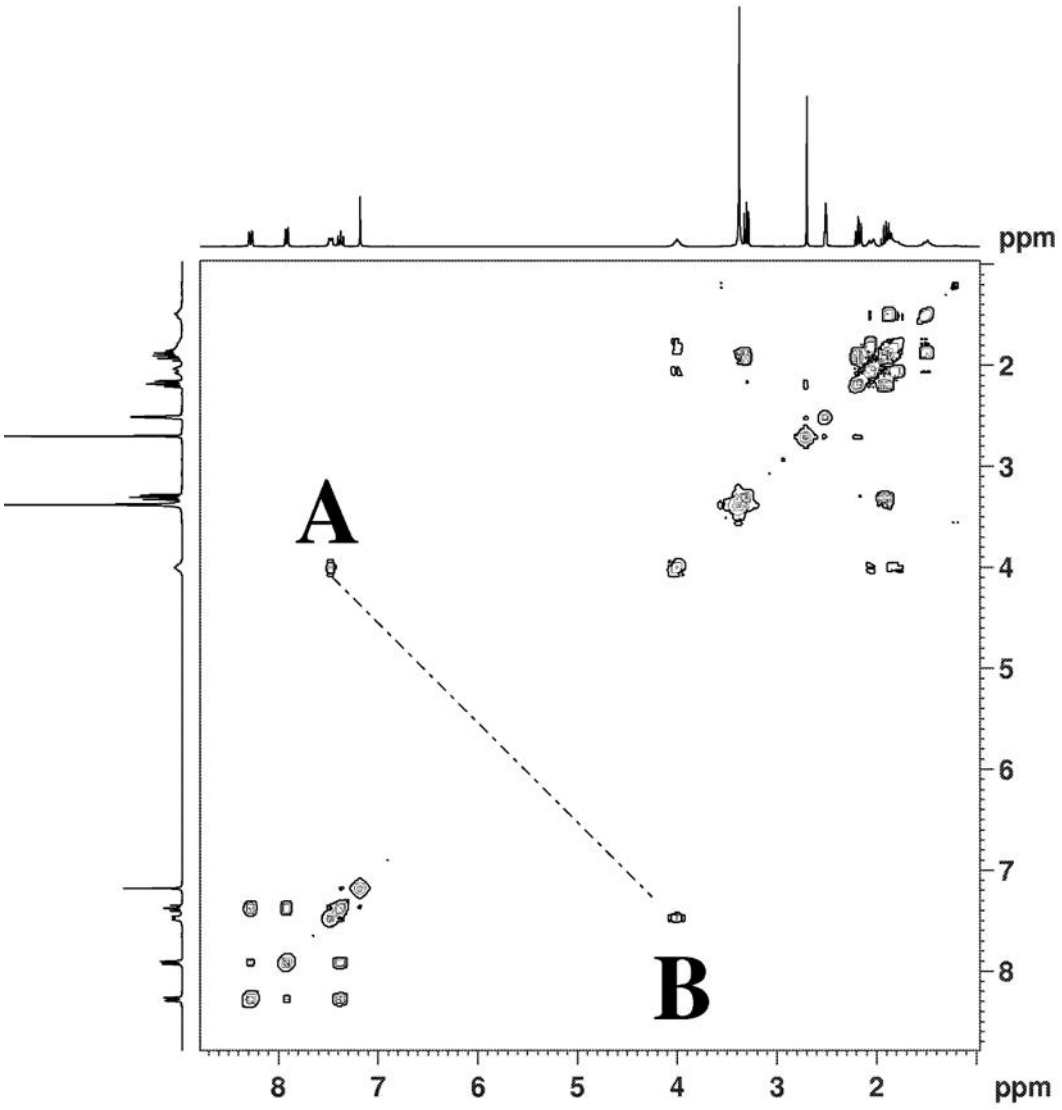

Figure 3.5. COSY spectrum of (**26f**A): Note cross peak between NH and a molecule of water at B.

3.2.4. Pharmacology.

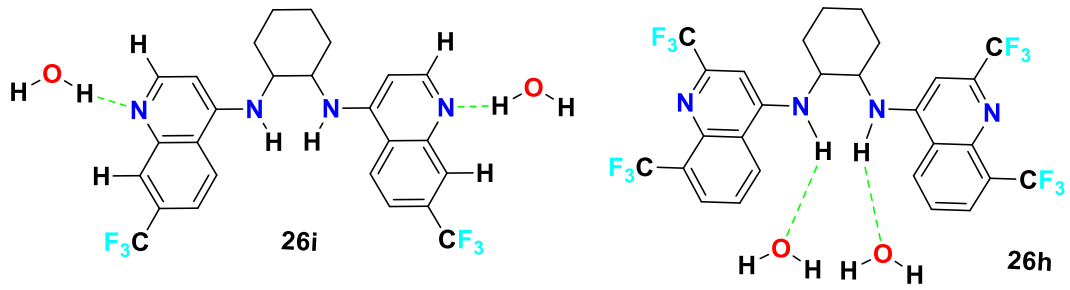

Figure 3.6. Possible hydrogen bonding sites.

Compound (**26f**) (Figure 3.1) injected subcutaneously (s.c.) twice daily in mice infected with chloroquine-sensitive *P. berghei* (dose levels 10 and 50 mg/kg, 23.6 and 0.1178 mol kg^{-1} respectively; n = 5) had no effect on parasitaemia 72hrs after inoculation with

Plasmodium, when compared with vehicle-treated animals (control 64.8 ± s.e.m. 2.1%, (**26f**) 10 mg/kg (0.0236 mol kg^{-1}) 61.6 ± 1.55 %, (**26f**) (Figure 3.1) 50 mg/kg (117.8 μmol kg^{-1}) 66.1 ± 2.7% erythrocytes contained Leishman-positive bodies, $P > 0.05$, (Mann-Whitney U) (Ismail *et al.,* **1996, 1998**). Repeated administration of (**26f**) (Figure 3.1) in these doses over the 3 day period was also without effect on body weight gain, colonic temperature, locomotor activity or, by visual inspection, the general autonomic state of mice when compared with control animals receiving vehicle (Olive oil/DMSO 24:1, injection volume 10 ml kg^{-1} subcutaneously).

In contrast, (**26e**) (Figure 3.1) we previously tested in this murine model of malaria (ID_{50} 5.9 mg kg^{-1} ; 14.9 μmol kg^{-1}) (Ismail *et al.*, **1996**) and found it to have less antimalarial activity than the compound (**26b**) (Figure 3.1), suggesting its interaction with the target receptor is sterically unfavourable. A similar loss of antimalarial potency in the trifluoromethyl analogue of chloroquine (**1**) may explain why it was not developed further (Andersag, **1942**). Compound (**26e**) injected s.c. in mice infected with *P. berghei* (dose range 6.3-252.2 μmol kg^{-1}, 5 doses in 72 hours) produced no observable adverse effects. Chloroquine diphosphate in this model had an ID_{50} of 4.3 mg kg^{-1} (8.3 μmol kg^{-1}).

Comparison of the data for putative 4-aminoquinoline antimalarials containing CF_3 groups in both the 2^{nd} and 8^{th} position, indicates that they, all derivatives, decreased antimalarial activity compared to their 7- CF_3 counterparts either *in-vitro* or *in-vivo* (Adovelande, **1994**; Barlin, **1985**, **1991**, **1992**, **1993**, **1994**; De *et al*., **1998**; Hawley, **1996**; O'Neill *et al*., **1994**; Park *et al.*, **2002**; Ruscoe, **1995**; Stocks, **2002**; Sveinbjornsson *et al*., **1951**).

3.2.5. Quantum mechanical Investigations: comparison of quinoline methanol behaviour versus 4-aminoquinolines.

Conformational analyses were carried out on mefloquine (**13**) and its progenitor (**54**). A comparison of the crystal structures of different forms of mefloquine, namely (±) mefloquine methylsulfonate monohydrate, (±) mefloquine hydrochloride methanol solvate (Karle *et al.,* **1991**), (±) mefloquine free base, and (-) mefloquine hydrochloride hydrate (Karle *et al.,* **2002**), shows that all four structures contain short N...O contacts of 2.73-2.94 Å, which can be considered as hydrogen bond interactions (H...A distances: Weak (2.2-3.2 Å); medium (1.5-2.2 Å); strong (1.2-1.5 Å).

In figure 3.7, Open circles, medium carbon, small hydrogen, hashed circles, large oxygen, medium nitrogen, small fluorine. The intramolecular hydrogen bond is shown as a dotted line. We have carried out conformational analysis on (**13**) using molecular dynamics. The simulations were carried out at 3000K with step sizes of 1 fs. 1000 structures were saved at 1 ps intervals and geometry optimized by molecular mechanics using the Dreiding force field

within Cerius2. Two low energy conformations were obtained in this study, which differed only in the O-C-C-N torsion angle (Dihedral angle, eclipsed/gauche molecular conformations).

The protonation preferences of (**13**) (Figure 3.7) were investigated because they may assist in defining electrostatic interactions with the haem receptor. The crystal structures of the protonated mefloquine all show that the aliphatic nitrogen is protonated in preference to the aromatic nitrogen. This result is consistent with observed crystal structures for both quinine and quinidine salts. The energies of the protonated mefloquine ions were calculated as -9.27019 a.u. with N (aromatic) protonated and -9.26237 a.u with N (aliphatic) protonated, an energy difference of 20.51 kJ mol^{-1}.

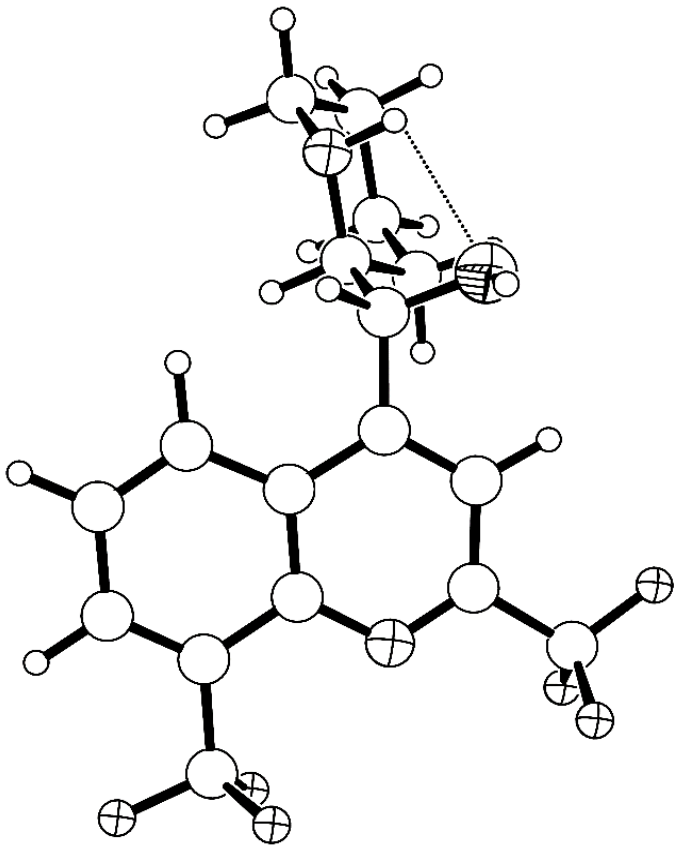

Figure 3.7. This confirms the lowest energy conformation of (**13**), contains an intramolecular hydrogen bond, a result consistent with the experimental crystal structures.

These were subsequently geometry optimized using the ADF program at the TZP level: energies obtained were -9.36493 a.u. with a torsion angle of -69.0^{o} with a hydrogen bond, and -9.35898 a.u. with a torsion angle of 71.8^{o} without a hydrogen bond, a difference of 15.61

kJmol^{-1}. These calculations were repeated using the COSMO (Klamt *et al.*, **1995**) continuum solvent method with a dielectric constant of 78.8, a value appropriate to water. The two energies were -9.41908 and -9.41685 a.u. respectively, thus the difference in energy has decreased by 5.85 kJmol^{-1} which is still significant.

Implementation of the COSMO method increases the energy difference to a much larger value i.e. 124.63 kJ mol^{-1}. This preference of aliphatic protonation is also consistent with the fact that similar molecules, such as quinine and quinidine, are also protonated on the aliphatic nitrogen rather than the aromatic nitrogen atom. The pKa values of quinine have been measured as 9.7 for the aliphatic and 5.1 for the quinoline nitrogen atoms, respectively.

We were also interested to establish the effect of the substituent CF_3 groups and possible interactions. Accordingly, model compounds (**13b**) (mefloquine with the CF_3 group in position 2 removed), (**13c**) (mefloquine with the CF_3 group in position 8 removed) and (**13d**) (mefloquine with both CF_3 groups removed) were created (*in silico*). The structures of these compounds were optimized with protonation at either type of nitrogen. The resulting energies, given in Table 3-4, show that the presence of the CF_3 group in position 2 decreases the likelihood of the adjacent aromatic nitrogen being protonated in preference to the aliphatic nitrogen atom, whereas the presence of the CF_3 in position 8 has a much smaller effect.

The two CF_3 groups allow, in principle, the formation of an internal bifurcated hydrogen bond to the adjacent protonated aromatic nitrogen.

Table 3-4 The energies /a.u. of mefloquine calculated at the TZP level with either the aliphatic or aromatic nitrogen protonated. Also included are values of various models created from mefloquine by omitting CF_3 groups.

Energies/a.u.			**Energies/kjmol^{-1}**			
	Aliphatic N protonated		**Aromatic N protonated**		**Energy difference**	
	gas phase	in water	gas phase	in water	gas phase	in water
Mefloquine (13)	-9.27019	-9.44485	-9.26237	-9.41908	-20.51	-67.59
13b	-8.63745	-8.81023	-8.63937	-8.78007	5.03	-79.11
13c	-9.26983	-9.44332	-9.26157	-9.39583	-21.66	-124.56
13d	-8.01129	-8.17570	-8.01351	-8.15826	5.82	-45.74

This could occur either from the CF_3 group in the 2nd or 8th position. From the CF_3 group in the 2nd position, the fluorine would be in the plane of the quinoline ring and the F...H distance would be 2.14 Å with a N-H...F angle of 104.6^{o}. From the CF_3 group in the 8th position, a fluorine in the plane of the aromatic ring would be 1.60 Å with an angle of 129.6^{o}. There are, however, no examples in the Cambridge Crystallographic database (Allen *et al.*, **1987**) of either type of hydrogen bond formation, an observation that suggests that the formation of such hydrogen bond is not likely to occur.

However, what is clear is that the introduction of CF_3 groups in both positions 2 and 8 of

the quinoline ring causes steric crowding around the aromatic nitrogen (whether protonated or not) that will modulate efficient interaction of this atom with the haem receptor (Dascombe *et al.,* **2005**). Calculations for (**54**) were repeated after geometry optimization showed an inter-ring angle of 6.4^{o} between the phenyl ring in position 2 and the aromatic system. The energies for the conformation without a hydrogen bond were -10.44535 a.u. with a torsion angle for O-C-C-N of 68.7^{o} and, with a hydrogen bond, -10.45070 a.u. with a torsion angle of -70.6^{o}, a difference of 14.03 kJ mol^{-1} (Figure 3.8).

When the calculations were repeated in a water environment, the difference was reduced to 9.97 kJmol^{-1}. The lowest energy conformation shown in table 3-4.

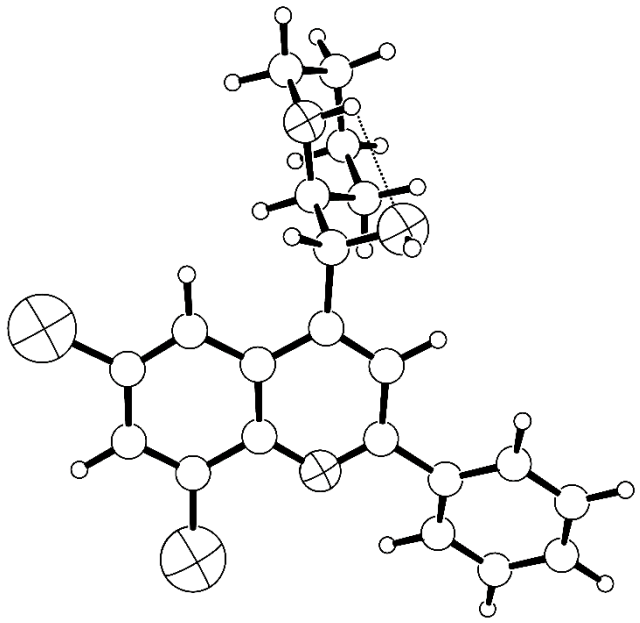

Figure 3.8. The lowest energy conformation of (**54**): Open circles, medium carbon, small hydrogen, hashed circles, very large chlorine, large oxygen, medium nitrogen, small fluorine. The intramolecular hydrogen bond is shown as a dotted line.

The energies of the protonated compounds were next calculated for the conformations with a hydrogen bond. These showed a preference for the aromatic nitrogen (-10.37209 a.u.) rather than the aliphatic nitrogen (-10.36365 a.u); thus, the reverse situation to (**13**), with an energy difference of 22.1 kJ mol^{-1}(gas phase).

The phenyl ring substituent in position 2 clearly has the opposite effect to that of the CF_3 groups in (**54**). The energies in solvent water were -10.50778, -10.53787 a.u. respectively, showing that in high dielectric constants, protonation at the aliphatic nitrogen is more favoured.

A similar calculation was carried out for chloroquine (**1**), using the crystal structure of the diprotonated diphosphate monohydrate (Furuseth *et al.,* **1990**) as the starting model.

There are three possible nitrogens to be protonated: the aromatic nitrogen, the exocyclic

nitrogen and the diethyl aliphatic nitrogen. The energies were calculated as -10.21321, -10.16489, -10.19848 a.u. respectively, a result consistent with the crystallographic results. Repeating the calculations in water gave energies of -10.35673, -10.33175, -10.36646 a.u indicating that the protonation at the aliphatic nitrogen becomes more favoured than the aromatic nitrogen at high dielectric constants.

These theoretical values are consistent with experimental data (Ferrari & Cutler., **1987**) that confirm that the mono-cation resides almost exclusively in the alkyl amino protonated form (pK_{a1} = 7.94 +/- 0.02; pK_{a2} = 10.03 +/- 0.02) whereby ionization of chloroquine is controlled mainly by the change in enthalpy.

Subsequently, the structure of (**26b**), Ro 47-7737 was investigated. There are two chiral carbon atoms, the two carbon atoms in the cyclohexane ring that are bonded to nitrogen. These give rise to two different isomers *trans* (*R,R*) and its mirror image *trans* (*S,S*). Their structural *cis* isomer, (*R,S*) can also possess a mirror images (*S,R*). All of these enantiomers and structural isomers will have equivalent theoretical energies. The possible conformations of the *trans* isomer (**26b**) (*R,R*) and (**26b)** cis isomer (*R,S*) structures were investigated with molecular dynamics and subsequent molecular mechanics energy minimization, which was followed by geometry minimization on the lowest energy conformations with the ADF program.

Utilizing molecular mechanics calculations, two low energy conformations were established for the (*R,R*) conformation with the two nitrogen atoms in equatorial positions (eq,eq) relative to the cyclohexane ring in the chair conformation but with ADF, these two converged to an equivalent geometry. In addition, a conformation with the two nitrogen atoms in axial positions (ax,ax) was established. The eq,eq conformation has a significantly lower energy by 15.61 $kJmol^{-1}$ at -12.05545 a.u. compared to -12.04950 a.u for the ax,ax conformation. These results compare with an energy difference found by Karle *et al.,* at the HF/6-311G level (ADF program) of 11.3 kcal mol^{-1} (47.2 $kJmol^{-1}$) in favour of the (eq,eq) configuration over the (ax,ax) configuration for the diprotonated compound.(Ismail *et al.,* **1996**)(Karle *et al.,* **2002**) (courtesy of Prof Drew).

The conformations can be characterized by the central torsion angles in the C-N-C(cy)-C-(cy)-N-C where C(cy) indicates the adjacent carbon atoms in the cyclohexane ring, which were respectively -12.2, 169.2, -57.9, 169.8, -11.8^{o} for the eq,eq conformation and 12.6, -165.7, 167.5, -165.9, 11.2^{o} for the ax,ax conformation. The first conformation is similar to that observed in the crystal structure of (**26g**).

A slightly different eq,eq conformation was observed in the crystal structure of the diprotonated dimethylsulfonate salt (Karle *et al.,* **2002)** where the torsion angles were 8.9, 103.3, -62.0, 104.2 -11.0^{o}.

Although this conformation was established as distinct in molecular mechanics calculations, as stated above, it converged to the aforementioned eq,eq structure on energy minimization with the ADF program.

In the *R,S* conformation only one conformation was established with an energy of -12.05545 a.u. and torsion angles (starting at the axial substituents) of 22.7, -161.1, 56.9, 156.6, -0.5°. With the COSMO system the energies were for *R,R* (eq,eq) -12.13941, *R,R* (ax,ax) -12.13096 a.u. and for *R,S* -12.13285 a.u. respectively. The lowest energy conformations for the *trans* **26b**A (R,R) configuration and for the *cis* **26b**B (*R,S*) configuration are shown in figure 3.9 (courtesy of Prof Drew).

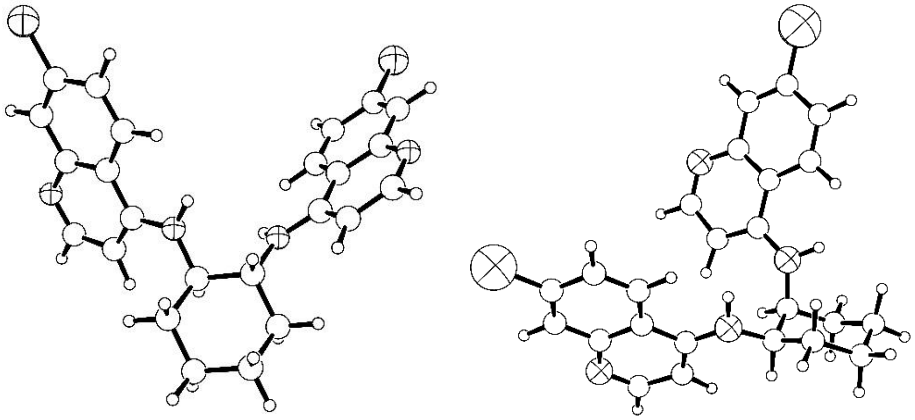

(a) (b)

Figure 3.9. (a) Lowest energy conformer *trans* (**26b**A) (R-R) (eq-eq), (b) Lowest energy conformer of *cis* (**26b**B) (R-S) (ax,eq).

In order to investigate the protonation pattern of the ligand, we chose the lowest energy eq,eq conformation of (**26b**A**)** (Figure 3.1) and the crystal structure of the related (**26f**A) has been determined (REF). This ligand was first protonated via one aliphatic nitrogen and then via one aromatic nitrogen atom to give energies of -11.94119 and -11.98577 a.u respectively, an energy difference of 116.93 kJmol^{-1}. Similar differences were obtained with the (*R,S*) configuration. In solvent water, however, the two energies were -12.15536 and -12.12881 a.u. respectively, which gave a reduced energy difference of 14.0 kJmol^{-1}. When two equivalent nitrogen atoms were protonated, the resulting energies in the (eq,eq) configuration in the gas phase were -11.69675 a.u. for two aliphatic nitrogen atoms compared to -11.84168 a.u. for two aromatic nitrogen atoms. Thus, the difference in energy of 380.44 kJmol^{-1} was more than twice that for the *mono*-protonated compounds, presumably because of the close proximity of the protonated aliphatic nitrogen atoms to each other (Figure 38).

Although the difference in solvent is much reduced (-12.11039, -12.17308 a.u. which represents 164.43 kJmol^{-1}), the results suggest that only the endocyclic quinoline nitrogen atoms are likely to be protonated. This observation is in agreement with the crystal structure of the (*R,R*) configuration, where the hydrogen atoms were located on the two endocyclic

quinoline nitrogen atoms in the diprotonated compound. (Karle *et al.*, **2002**).

These observations are consistent with our published biophore in which the endocyclic nitrogens are proton acceptors whereas the secondary 4-aminoquinoline groups are donors. (Ismail *et al.*, **1996**, **1998**; Dascombe *et al.*, **2005**).

In this study, the structures of (**26e**) and (**26f**A) constructing starting models from the lowest energy (eq,eq) conformation of the *trans* (**26b)** (*R,R*) configuration were obtained previously. CF_3 groups were subsequently added into positions seven for (**26e**) and both two and eight for **(26f**A) and results are compared to those for (**26b**, Table 3-1).

Table 3-5 Gas phase the protonation preferences for the *bis*quinolines (**26b**A), (**26e**A) and (**26f**A).

	Energies/a.u.			**Difference in Energy (kjmol^{-1})**		
State	**Free Molecule**	**Npy protonated**	**Nali protonated**	**Npy-free**	**Nali-free**	**Nali-Npy**
(26bA) gas	-12.05545	-11.98577	-11.94119	-182.8	-299.7	-116.9
solvent	-12.13941	-12.15536	-12.12881	-41.8	-27.8	14.0
(26eA) gas	-13.45049	-13.37306	-13.33267	-203.1	-309.0	-105.9
solvent	-13.53904	-13.50957	-13.52505	-77.3	-36.7	40.6
(26fA) gas	-14.71345	-14.62535	-14.58369	-231.1	-340.3	-109.3
solvent	-14.80106	-14.79041	-14.78282	-27.9	-47.8	-19.9

The results shown Table 3-5, allow investigators to draw several significant conclusions. First, in the gas phase the protonation preferences for the *bis*quinolines (**26b**A)**,** (**26e**A) and (**26f**A) are the opposite of those observed in mefloquine (**13**) with the *bis*quinolines favoring aromatic protonation and mefloquine aliphatic protonation in the gas phase. Protonation at the bridging nitrogen is very unfavorable for all conformations for (**26b**A), (**26e**A) and (**26f**A), the energy differences for all three molecules being over 105 kJmol^{-1}. Comparison of the protonation energies of (**26b**A) and **(26e**A)**,** shows that the replacement of Cl with CF_3 in the 7th position or the inclusion of CF_3 groups in the 2nd and 8th positions has had only a small effect of ca 10 kJmol^{-1} upon the preferences (gas phase differences). The effect of solvent on these values is very striking. In all cases, the difference between protonation preferences is very much reduced and indeed for (**26e**A) it is reversed, protonation at the aliphatic nitrogen being favoured by 40.6 kJmol^{-1} and indeed for 26**b**A by kJmol^{-1} (courtesy of Prof Drew). However, for (**26b**A) and (**26f**A) protonation at the aromatic nitrogen is still favoured by 14.0 and 19.9 kJmol^{-1} respectively. Egan and Ncozaki (Egan *et al.*, **2004**) have highlighted the critical role of water in studying drug receptor interactions and we have also shown that in the absence of water, these interactions diminish to the point where complex formation with haematin is weak (but not altogether abolished) (Ismail *et al.*, **2004**).

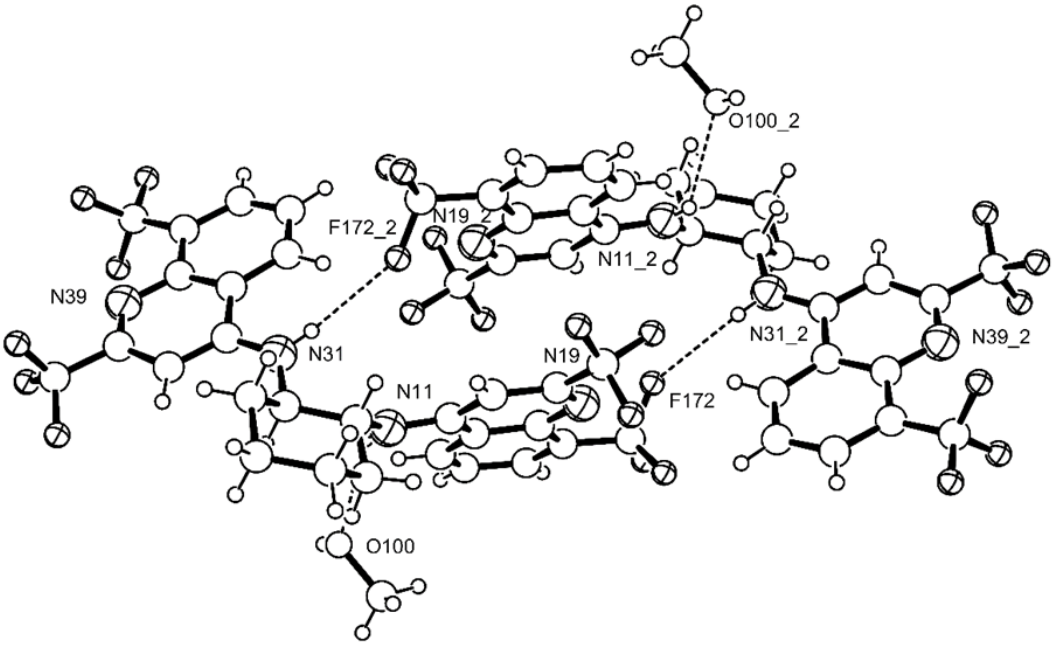

Figure 3.10. The structure of (**26f**A) as determined by X-ray Crystallography. Hydrogen bonds are shown as dotted lines between i) NH and CF and ii) N-H and methanol. _2 refers to symmetry element 1-x,1-y,-z.

The five torsion angles in the link are 1.7, 164.0, -52.2, 154.6, -5.5^{o} so the conformation is very similar to that obtained from conformational analysis of (**26b**A) (Figure 3.1) where the angles were -11.7, 160.4, -55.8, 155.6, and 7.9^{o}. The minimal difference indicate that the crystal packing which involves the formation of a centrosymmetric dimer in which N(11) in each molecule forms a hydrogen bond to a methanol solvent molecule (N(11)-H…O(100) N…O 2.93, H…O 2.37A, N-H…O angle 123.0^{o}) (as also seen in the COSY spectrum (Figure 3.4). In contrast, N(31) forms a hydrogen bond to F172(1-x,1-y,-z) at 3.29Å and these two hydrogen bonds create a dimer shown in (Figure 3.10). Here the aromatic rings stack but the distance between them is too long at 4.0Å so does not indicate a significant interaction.

In addition, the solvent methanol forms close contacts to F(374), F(404), F(372) (all -x,-y,-z-1) with O…F at 2.97, 3.14, 3.32Å (Figure 3.10). The vibrational spectrum showed a peak (3436 cm^{-1}) normally assigned to inter or intra-molecular hydrogen bonding (compare with data from a related structure confirmed by crystallography which vibrates at 3455/ 3415 and 3400 cm^{-1}; for two 12 membered macrocycles: 4-aminobenzo-12-crown-4 and mono*aza*-12-crown-4 ligand respectively (Gelmboldt *et al.*, **2007**), significance of such behaviour with the receptor is considered in the next section (courtesy of Prof Drew) (Figure 310).

3.2.6. Binding of drugs to haem.

Neither the exact binding mode of *bis*quinolines to their putative receptor (i.e. haem) nor the maximum volume within the binding site is available, but we have previously suggested an upper limit for the latter by measuring the antimalarial effectiveness of an acridine/quinoline and acridine/acridine hybrid compound (Ismail *et al.,* **1996**, **1998**; Dascombe *et al.,* **2005**). In previous work, Ismail group have postulated that *meta*-quine (**21**) (Figure 3.3) is complexed to haematin via several non-bonded contacts including two intramolecular hydrogen bonds, one from an exocyclic N-H in *meta*-quine to the axial hydroxyl group in haematin and the second from the associated endocyclic quinoline nitrogen atom to the carboxyl group in haematin.

This is dubbed this an "above-face" interaction (i.e. that containing the axial hydroxyl group) as opposed to binding on the obverse (below) face which favours π - π interactions with suitable drugs. A previous modeling study (Ismail, *et al.*, **2004**) on chloroquine concentrated on this obverse binding and found significant π-π interactions but above-face interactions were not considered. In the present work, compounds (**26b**)**,** (**26e**) and (**26f**) all contain a cyclohexane bridge between two aromatic moieties which creates a very different shape for the molecule (however, other geometric interactions are also possible, and they are beyond scope of this thesis).

Consequently, interactions with the receptor are likely to be different from those involving *meta*-quine. One major change is that in the *trans* A isomer it is possible for both exocyclic N-H groups to hydrogen bond to the hydroxyl group. In addition, the existence of the CF_3 groups in (**26e**) and its isomers permit alternative hydrogen bonding from the CF_3 groups rather than the endocyclic nitrogen atom to the carboxylic acid group. In *meta*-quine, the N...H-O hydrogen bond is somewhat strained (N...H-O) being 140^o and therefore the F...H-O hydrogen bond seemed a preferable alternative.

These possibilities were investigated by molecular mechanics using the Cerius2 software with the Universal Force Field. Atoms were given partial charges by the Charge equilibration (**Qeq**) method and the system was given a total charge of +1, assuming that the ligands were unprotonated. In the starting model, the ligands were given their lowest energy conformations and haematin its crystal structure. The proposed hydrogen bonds were fixed at appropriate distances and the structure (haematin and ligand) were then geometry optimized. Models of (**26b**A), (**26e**A) and (**26f**A) were all minimized with two hydrogen bonds in place from the exocyclic N-H bonds to the axial hydroxyl group in the haem.

For example, in (**26e**) with the CF_3 in the 7th position, and the F...H-O angle optimized to 159^o rather than 142^o for N...H-O with an energy lower by 30.9 $kJmol^{-1}$ (Figure 3.11). The chlorine atoms in the 7th position in (**26b**), in theory, provide an alternative hydrogen bond with the carboxylic acid group, but modeling showed that such hydrogen bonds could not be formed.

The resulting energy being about 60.5 kJmol^{-1} greater than when the hydrogen bond was formed to the endocyclic nitrogen atom (Comparing **26e**A and **26f**A) (Table 3-1; Figure 3.2; Figure 3.3). At first, we only considered (**26f**A) and the possibility of hydrogen bonds to the CF_3 in the 2nd or 8th positions as well as to the endocyclic nitrogen atom. Four models were optimized with no O-H…F hydrogen bonds, with two such bonds, with one hydrogen bond to the CF_3 in position 2 and to position 8. Relative energies were 0.0, 43.5, -29.3 and -23.0 kJmol^{-1} respectively indicating that one hydrogen bond to either CF_3 is favoured over no hydrogen bonds. The formation of two hydrogen bonds is unlikely. The structure with the hydrogen bond to the position 2 is shown in figure 3.2 and figure 3.3.

With Mefloquine (**13**) however, the possibility of two O-H…F hydrogen bonds can be considered. We can assume two hydrogen bonds can be formed from the secondary hydroxyl group and piperidine NH group to the hydroxyl group in haematin. Four models were optimized with no O-H…F hydrogen bonds, with two such bonds, with one hydrogen bond to the CF_3 in position 2 and to position 8. A fifth model was included which contained an O-H…N hydrogen bond to the endocyclic nitrogen atom but no O-H…F hydrogen bonds. Relative energies were 0.0, -0.8, -10.4, 6.7 and 69.7 kJmol^{-1} respectively indicating that the most favoured model contains one hydrogen bond to the CF_3 in position 2. Our calculations also show endocyclic nitrogen is sterically crowded by the two adjacent CF_3 groups so that it cannot readily form a hydrogen bond with haematin.

The structure with 2O-H…F is relatively low in energy in this case, (Figure 3.11). Structures in which the molecule is attached to the obverse face were also considered but, in general, these had energies of ca 8-10 KJmol^{-1} higher than those reported for the above face interaction. An example of (**26h**) bound in this way is shown in figure 3.11(e). It is, of course, possible for two molecules to sandwich one haematin molecule and an example with (**26h**) is shown in figure 3.11(f).

It has been argued that in some circumstances, the parasite may/will actively or passively import the drug into the vacuole such that a high enough concentration is accumulated for a 2:1 complex to be formed. This (Figure 3.11) (f) shows the different interactions on the two sites of the haematin, primarily π-π interactions on the obverse side and hydrogen bonds on the alternative side. However, whether such interactions exist within the parasite vacuole are yet to be determined. The introduction of CF_3 groups into position 2 and 8 in (**26f**) agrees with previously reported structure-activity correlations,(Chou *et al.,* **1980**; Dascombe *et al.,* **2005**; Egan *et al.,* **1997**; Gabay *et al.,* **1994**; Guerquin-Kern *et al.,* **1997**; Hooper *et al.,* **1993**; Ismail *et al.,* **2002**; Meshnik *et al.,* **1997**; Pacholski, **1999**; Robinson *et al.,* **1997**; Tajerzadeh *et al.,* **1993**) where introduction of a CF_3 group in position 7 is superior in antimalarial activity over 2,7-*bis*-trifluoromethyl substitution, which in turn is more active than 2,8 *bis*-trifluromethylated-*mono*-4-aminoquinolines analogues (Figure 3.11).

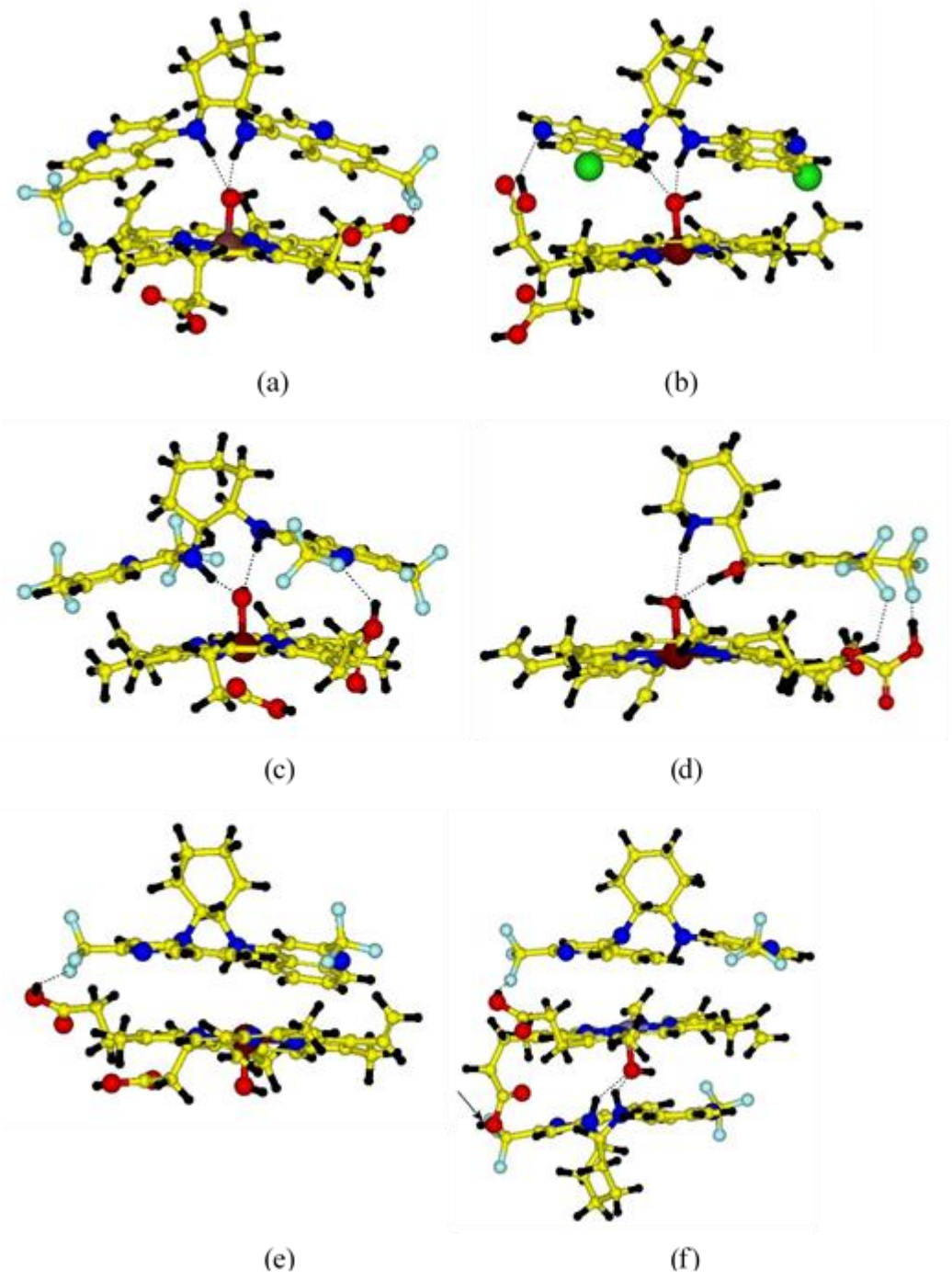

Figure 3.11. Structures showing possible hydrogen bond interactions with haematin. Fe brown, N blue, F pale blue, O red, C yellow, Cl green, hydrogen black. Hydrogen bonds shown as dotted lines. (**a**)(**26e**A) showing hydrogen bond to the CF_3 in the position 7; (**b**)(**26b**A) showing hydrogen bond to endocyclic nitrogen atom; (**c**)(**26f**A) showing hydrogen bond to CF_3 in position 2; (**d**) mefloquine, showing hydrogen bonds to CF_3 in both positions 2 and 8; (**e**) (**26h**A) bound on the obverse face with a O-H…F hydrogen bond; (**f**) 2 molecules of (**26h**A) forming a sandwich around haematin. An additional hydrogen bond from O-H to F is indicated by the arrow.

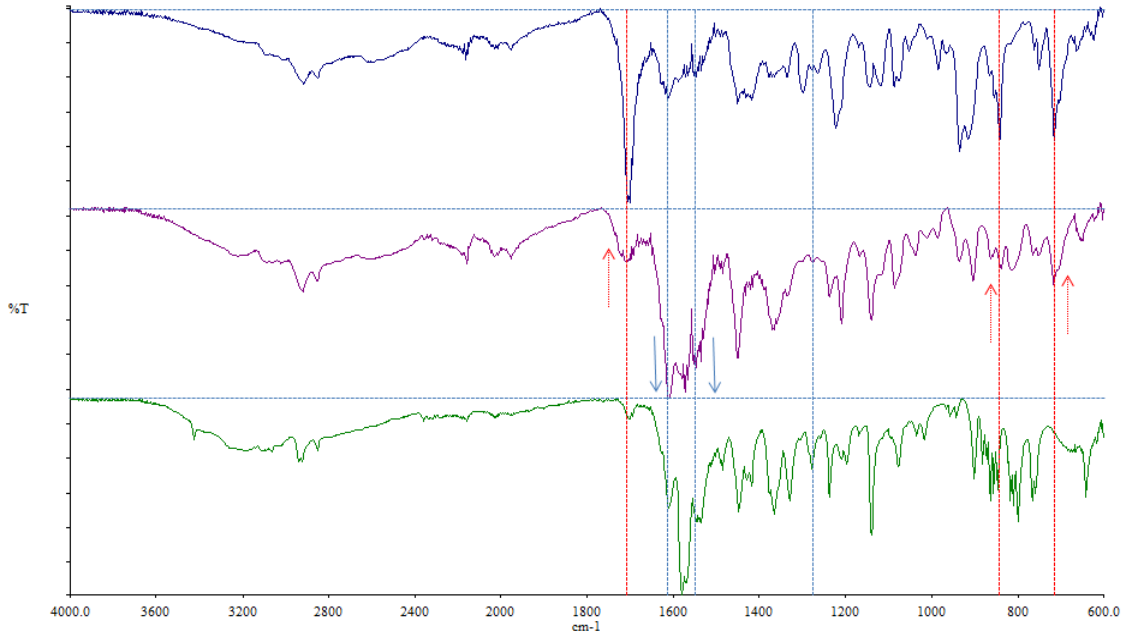

Figure 3.12. Haem interactions: a) **26b** freebase; b) Haem-**26b** complex (middle) c) Haemin Chloride at the top. All compounds that efficiently interact with haem show quenching of the peak at 1700 cm^{-1}.

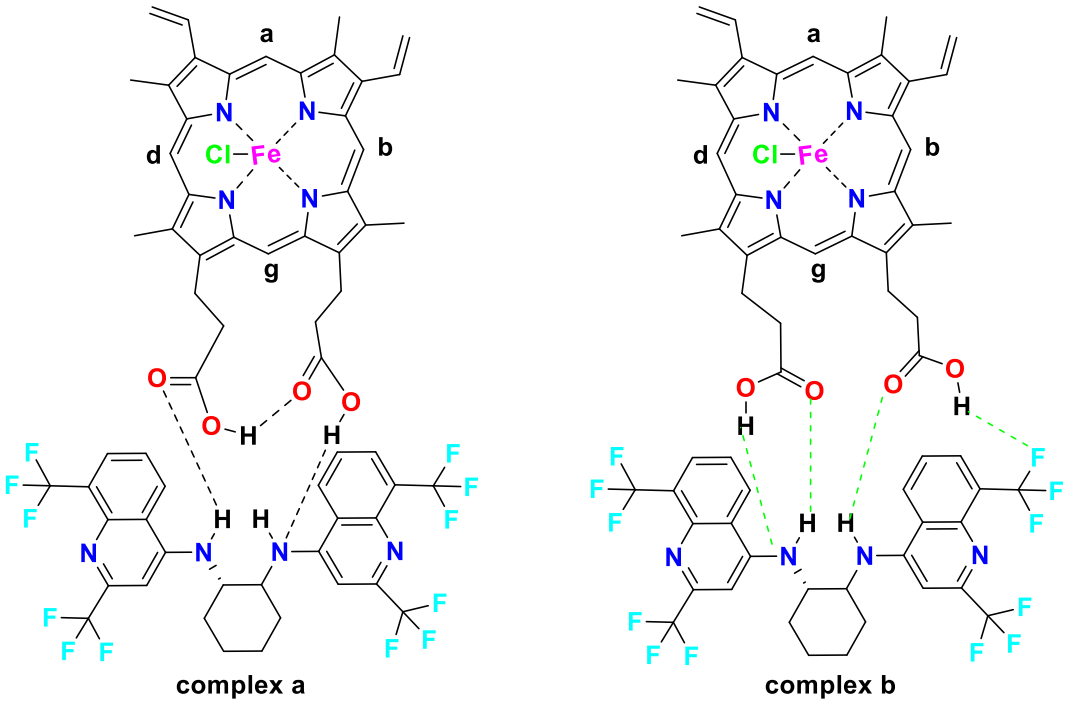

Figure 3.13. Haem-drug complex. Complex A supported by data, Complex B unlikely by calculations.

In conclusion, these results show that the inclusion of CF_3 substituents has a major impact on the interaction of the drug with the antimalarial haem receptor.

This may explain why the substituent pattern present in mefloquine is optimized for antimalarial activity in the quinoline methanol class. This type of molecule can be coordinated to the central haem atom in quinine type compounds but whether this occurs in mefloquine has yet to be proven.

Consequently, not only do the substituents affect the electronic properties of the molecule, they also offer alternative, preferential hydrogen bonding sites, and their steric bulk will reduce the possibility of interactions from adjacent endocyclic nitrogen atom (Figure 3.13).

3.3. Experimental.

Solvents used in the reactions were purified according to standard methods. All starting materials were of the highest purity available and were obtained from either the Aldrich Chemical Co., Lancaster Synthesis or Fluka. Chloroquine diphosphate was purchased from Sigma. Microanalyses were performed by MEDAC LTD, Brunel Science Centre, Egham, Surrey, UK and The Chemistry Department, University of Liverpool. Synthetic experiments were conducted using oven-dried glassware on a double vacuum manifold glass line under a protective atmosphere of dry argon.

All materials, whether synthesised in our laboratory, or purchased, were continuously purified until they demonstrated a single peak by GC-NMR and NMR spectroscopy (^{19}F and ^{1}H) to ensure that spectroscopic, physiochemical and pharmacological results were valid. Melting points were determined using a Gallenkamp melting point apparatus and are reported uncorrected but were verified by DSC.

Thin Layer Chromatography (TLC) was carried out on silica gel 60 glass backed plates using chloroform as eluent. Visualization was carried out either at 254 nm under UV light or in an iodine tank. Medium pressure chromatography was carried out using a custom made, on piece, all glass apparatus, foil covered packed with silica or neutral alumina (argon 1-15 bar).

3.3.1. Spectroscopy.

NMR spectra were recorded on a Brucker AC-250 and Brucker Avance 300 (5 mm BBO probe head) nuclear magnetic resonance spectrometer. Spectrometer frequencies (and internal standards) were: ^{1}H: 250 MHz (TMS); ^{13}C: 62.89 MHz ^{19}F: 235.36 MHz ($CFC1_3$) or ^{1}H: 300.13 MHz (TMS); ^{13}C: 75.46. Peak multiplicity and partial connectivity were deduced using a combination of DEPT, APT, HMQC and ^{1}H- NMR experiments. Attached proton test experiment (10,000 scans) were used to identify quaternary centers. Mass spectrometry experiments were performed using a VG MICROMASS 7070H, operated at 70 eV electron energy (Source temperature 200-250°C; Scan speed of 1 to 3 Hz). For chemical ionization

(CI) experiments, the instrument was operated at 50 eV, and ammonia was used as the ionizing reagent. FT-IR spectroscopy was carried out using KBr discs on a GALAXY series 5000 FT-IR spectrometer GL-7020.

Electrospray experiments: Positive-ion electrospray mass spectrometry was performed using a Micromass model LCT TOF-MS with nitrogen as a nebulization gas (Micromass Limited, Wythenshawe, Manchester, UK). UV spectra were measured using a Hewlett Packard HP8452A diode array spectrophotometer fitted with a 2 mm path-length quartz cell.

Fluorescence spectra were determined using a Varian Cary Eclipse® fluorescence spectrophotometer operating Cary Eclipse® software. HPLC: Chromatography was performed using a system comprising a Perkin Elmer PE250 isocratic pump, PE ISS200 autosampler and PE 235C diode-array detector. Chromatograms were collected, stored and processed using the Labsystems Ltd X-Chrom® chromatography data system (Eswaran, *et al.*, **2010**).

3.3.1.1. 40. Synthesis of 2,8-*bis*(trifluoromethyl)quinolin-4-ol, Compound 58.

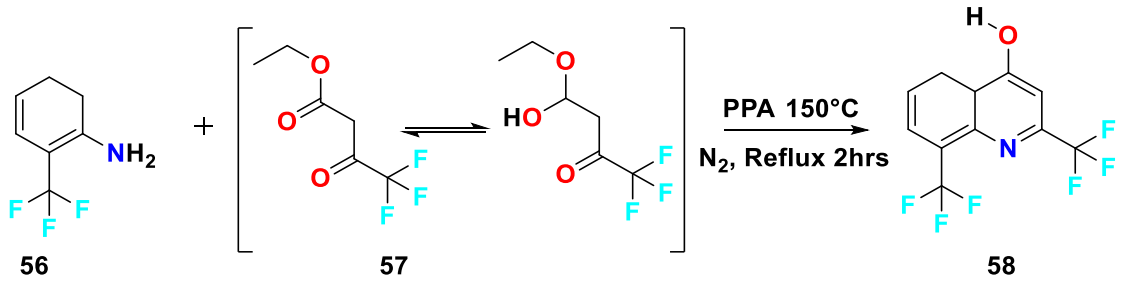

Figure 3.14. Scheme 40. addition, elimination. nitrogen, PPA, reflux.

To a mixture of 2-trifluoromethylaniline (**56**) (25 g, 0.1553 mol) and ethyl-4,4,4-trifluoroacetoacetate (**57**) (28.6 g, 0.1553 mol, from Lancaster synthesis) in a 500 ml flask, equipped with a reflux condenser and a blanket of nitrogen, was added polyphosphoric acid (125 g, 5 w/w). The reaction mixture was magnetically stirred at 150-155°C for 2hrs (Reaction progress was monitored by silica gel) (Figure 3.14). The crude reaction mixture was gradually poured into cracked ice water (500 mL) with vigorous stirring (glass rod). The resulting precipitate was filtered at the pump and dried *in vacuo* (oven, 24 h) yielding a white solid sufficiently pure and was used in the next step. Yield 76 %. ^{1}H NMR (300 MHz, DMSO-d_6) δ_H; 7.27(1H, s, CH), 7.78 (1H, t, CH, J = 7.8Hz), 8.28(1H, d, CH, J =7 .2Hz), 8.52(1H, d, CH, J = 8.4 Hz), 12.78 (1H, brs, OH, absent upon D_2O exchange).

3.3.1.2. 41. Bromo-2,8-*bis*(trifluoromethyl)-4a,5-dihydroquinoline, compound **59**.

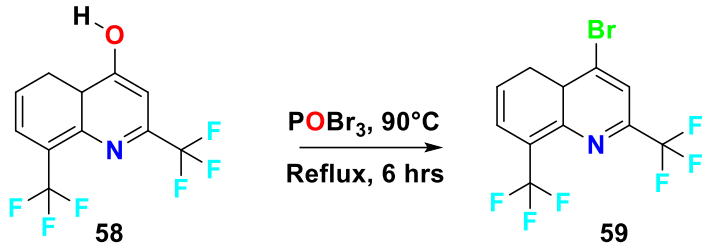

Figure 3.15. Scheme 41. bromination, $POBr_3$, argon, reflux.

Phosphorous oxybromide (4 g, 0.142 mol), under an argon atmosphere, was heated to 90°C until complete dissolution of the solid. Compound **58** (4.08 g, 0.014 mol) was added to this hot solution and the bath temperature was increased to 150°C. After 6 hrs, the resulting mixture was allowed to cool to room temperature (Figure 3.15).

The reaction mixture was quenched by addition of ice-cold water and the precipitate formed was filtered and washed with water to afford as a white solid **(**4.70 g, 96%). R_f 0.79 (cyclohexane/Et_2O 5:1); m.p.: 60°C; ^{1}H NMR (300 MHz, $CDCl_3$) δ_H; 7.82 (1H, t, J = 7.9 Hz), 8.11 (s, 1H), 8.22 (1H, d, J = 7.3 Hz), 8.46 (1H, d, J = 8.6 Hz), NMR data were in agreement with the lit (Jonet *et al*., **2011**; Jayaprakash *et al.*, **2006**). ^{13}C NMR (125 MHz, $CDCl_3$) δ_C; 120.9 (C2', q, J = 276.0 Hz), 122.0 (C8', q, J = 2.0 Hz), 123.6 (C3, J = 273.8 Hz), 128.9, 129.4, 129.8 (C6, C7, C5, J = 30.8 Hz), 130.5 (q, J = 5.3 Hz), 131.5, 138.5, 144.5, 148.6 (C4, C8, C2, C9, q, J = 36.1 Hz); IR ν_{max} = 1577, 1422, 1302, 1136, 1098, 1010, 876, 824 cm^{-1}. Molecular Formula = $C_{11}H_4BrF_6NNa$ $(M+Na)^+$ 365.93, found 365.93.

3.3.1.3. 42. (±) *trans*-N^1,N^2-*bis*-(2,8-*bis*-trifluoromethyl-quinolin-4-yl) cyclohexane-1,2-diamine (**26f**).

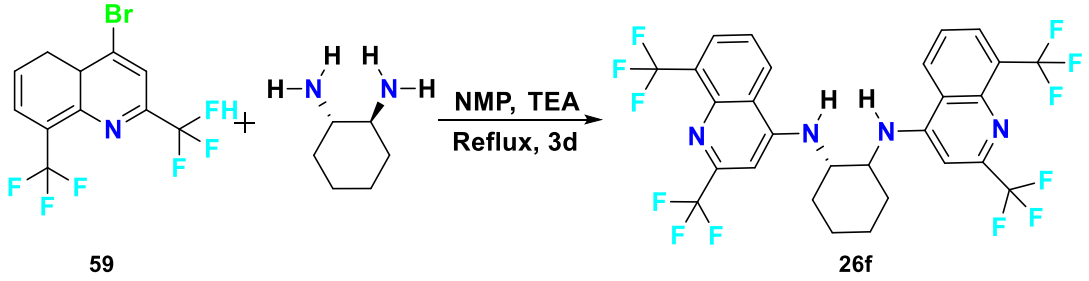

Figure 3.16. Scheme 42. S_NAr displacement, NMP, TEA, reflux.

Preparation using similar method outlined in Chapter **2** (Page 88) produced a brown compound. Suspension and vortexing in chloroform/ conc. NH_3 for one hour, filtering at the pump and washing with chloroform (5 x 25 ml) at the pump produced a tan solid, free base: m.p. 350.8°C, DSC scan: 25 to 400°C at 5.00°C min^{-1}). FT-IR cm^{-1}: 3436 (medium intensity, broadened N-H stretch);1327 Amine γ (C-N) aromatic stretch (Figure 3.16).

3.3.1.4. 43. (±) *trans*-N^1,N^2-*bis*-(2,8-*bis*-trifluoromethyl-quinolin-4-yl) cyclohexane-1,2-diamine (**26f**).

The dihydrochloride was a gray solid: m.p. >380ºC (decomposition). MS: (EI at 70 eV)) $C_{25}H_{20}N_4F_{12}$ 640 Da. Detected, 640 ($M^{+\cdot}$, 4%), 360 ($M^{+\cdot}$ -$F^{\cdot}$,1%), 360 (15%), CF_3^+, 69 (8%), 319 (6%), 307 (5%), 280 (5%), 36 (100%). The dihydrochloride (100mg), was suspended in chloroform (100ml) to which was added concentrated NH_3 (33% solution in water, 100 ml) and stirred then left for one week. The solution slowly deposited a mass of clear crystals. These were isolated by filtration then slowly crystallized by diffusion of methanol into chloroform. Free base: m.p. 243.4 –245.2°C DSC: 0° to 300°C at 10°C min^{-1}).

^{1}H NMR: δ_H (DMSO-d_6): 1.49-1.51 (4H', m, ^3J H_{ax}-H_{ax} = 9.48 Hz), 1.77-1.89 (4H', m), 2.06 (2H', d, ^3J H_{ax}-H_{ax} = 12.64 Hz), 4.00 (2H, m), 7.16 (2H, s, H3), 7.37 (2H, broad, d, 2NH), 7.89 (2H, d, H5, $^3J_{H\text{-}H}$ = 7.20 Hz), 8.27 (2H, d, $^3J_{H\text{-}H}$ = 8.49 Hz). Methanol peak at 3.33 ppm (24H).

^{13}C NMR: APT (75.5 MHz): δC (DMSO-d_6); 24.6 (C3', CH_2), 31.2 (C2', CH_2), 56.8 (C1', CH), 145.3 (C2, quaternary, distorted), 95.1 (C3, CH), 114.6 (C2", quartet, $^2J_{C\text{-}F}$ = 33 Hz), 152.0 (C4, quaternary), 123.7 (C5, CH), 128.5 (C6, CH), 125.8 (C7, CH), 129.2 (C8", quartet, $^2J_{C\text{-}F}$ = 29 Hz), 143.5 (C8, quaternary), 147.3 (C9, quaternary), 126.3 (C10, quaternary).

FT-IR cm^{-1}: 3436 (medium intensity, Sharp N-H stretch; intermolecular hydrogen bond); 1315, 1292 (strong 2°Amine γ (C-N), aromatic stretching vibration).

Compounds (**26b**, **26e**, **26f**, **26g** and **26h**) were also constructed (Ismail *et al.*, **1998**).

3.3.2. Crystallography.

(**26f**A), $C_{25}H_{20}F_{12}N_4O$, M = 620.46, triclinic, a = 11.026(14), b = 11.043(14), c = 12.808(14)Å, α=93.63(1), β= 108.99(1), γ = 92.59(1)º, U = 1467Å^3, spacegroup P-1, d_{calc} = 1.404 gcm^{-3}, Z=2. Data were measured with MoKα radiation using the MARresearch Image Plate System The crystal was positioned at 70 mm from the Image Plate. 100 frames were measured at 2º intervals with a counting time of 2 mins. Data analysis was carried out with the XDS program (Kabsch, **1988**) to provide 4216 independent reflections respectively. The structure was solved using direct methods with the Shelx86 (Shelx86, **1990**) program. Non-hydrogen atoms were refined with anisotropic thermal parameters. The hydrogen atoms bonded to carbon were included in geometric positions and given thermal parameters equivalent to 1.2 times those of the atom to which they were attached. The structure was refined on F^2 using Shelxl (Shelxl97, **1997**) to R1 0.0958, wR2 0.1716 for 1825 reflections respectively with I>2σ(I). The data have been deposited at the Cambridge Crystallographic Data Centre with reference number CCDC 223083 (courtesy of Prof Drew).

3.3.3. UV spectroscopic studies.

The UV spectra of the two compounds were determined over the range 190 – 800 nm. The samples were prepared as follows: (**26e**A) (i) DMSO Solution. 3.04 mg of material was transferred to a 10 ml volumetric, DMSO added and the flask shaken to disperse the material before being made to volume using DMSO (= 304 μg/ml). This solution was diluted with an equal volume of DMSO and the spectrum determined on the resultant solution (= 152 μg/ml). (ii) TFA Solution. 2.03 mg of material was transferred to a 10 ml volumetric, TFA added and the flask shaken to disperse the material before being made to volume using TFA (= 203 μg/ml).

This solution was diluted with an equal volume of TFA and the spectrum determined on the resultant solution (= 102 μg/ml). (**26f**A) (i) DMSO Solution 1.08 mg of material was transferred to a 10 ml volumetric, DMSO added and the flask shaken to disperse the material before being made to volume using DMSO (= 108 μg/ml). (ii) TFA Solution 2.14 mg of material was transferred to a 10 ml volumetric, TFA added and the flask shaken to disperse the material before being made to volume using TFA. (= 214 μg/ml).

3.3.3.1. Fluorescence spectroscopic studies.

Fluorescence spectra of the DMSO and TFA solutions of the two analytes were determined in a 10mm mirrored, 90º cuvette was used for the measurements and the instrument blanked with the appropriate solvent prior to determination of the excitation and emission spectra of the various solutions. The samples were prepared as follows: (**26e**A) (i) DMSO Solution. The 304 μg/ml solution prepared for the UV spectroscopic was used to determine the excitation spectrum whilst a 20-fold dilution of this in DMSO was used to determine the emission spectrum. (ii) TFA Solution. The 203 μg/ml solution prepared for the UV spectroscopic studies was used to determine both the excitation and emission spectra. (**26f**A): (i) DMSO Solution. The 108 μg/ml solution prepared for the UV spectroscopic studies was diluted 100-fold with DMSO and the resultant solution used to determine both the excitation and emission spectra; (ii) TFA Solution. The 214 μg/ml solution prepared for the UV spectroscopic studies was used to determine both the excitation and emission spectra.

3.3.3.2. Mass spectrometric studies.

Samples were dissolved in a 1:1 (v/v) mixture of water and acetonitrile containing 0.1% v/v of formic acid and diluted so as to yield approximately 3 μg/ml solutions. These were then each infused into the mass spectrometer at a rate of 3 μl/min, using a 250 μl glass syringe fitted into a Harvard Apparatus Model II syringe driver. Spectra were collected at a rate of 1 per second over a three-minute period. For accurate mass determinations, a reference solution containing 10 μg/ml of Leucine-Enkephalin in acetonitrile/water/formic acid was

infused at a rate of 3 μl/min into the Lockspray™ attachment using a second syringe. The analyte and reference streams were sampled at a rate of one spectrum per second over a three-minute period and the spectra averaged. The MassLynx® software was used to adjust the average analyte spectrum on the basis of the observed base-peak mass of the average leucine-enkaphalin spectrum, which has a nominal mass of 556.2771 Da. Instrumental operating conditions were factory standard with the following variable settings: Capillary: 2250V; Sample cone: 30V; Extraction cone: 10V; RF Lens: 1000V; Desolvation gas flow: 638 L/min; Desolvation temperature: 150ºC; Source temperature: 100ºC.

3.3.3.3. High performance liquid chromatographic studies.

Approximately 1.5 mg samples were shaken with 1.5 ml aliquots of the HPLC eluent and left to stand for several minutes before being centrifuged at 14,000 rpm for 1 minute. A 1ml aliquot of the supernatant was then transferred to a 2 ml autosampler vial which was sealed and placed in the autosampler. The following instrumental conditions were employed: eluent: 0.1M KH_2PO_4/0.1M $NaClO_4$ adjusted to pH 2.0 ($HClO_4$): Acetonitrile (87:13 $^{v}/_{v}$) flow rate: 1.0 ml/min (approx. 1650 psi); Injection 10 μl; Column Phenomenex Lichrosphere 5CN, 4.6 x 150mm; Detection 254 nm.

3.3.3.4. Antimalarial Efficacy.

P. berghei N/13 (2×10^7 parasitized erythrocytes) was inoculated intravenously (i.v.) in MF1 mice supplied by the Biological Services Unit, The University of Manchester, UK. Mice were housed in groups within plastic cages (length 38 cm × width 22 cm × height 11cm) at room temperature (19-22°C), on a 12hrs light (08:00-20:00) and 12hrs dark (20:00-08:00) cycle, with unlimited access to food (CRM feeding pellets, SDS) and water. Experiments were licensed under the Animals (Scientific Procedures) Act 1986. In compliance with the conditions of the licence, infected mice were humanely killed when humane endpoints were reached. Parasitemia was measured by counting Leishman-positive cells 72 h following infection using tail blood smears stained with Leishman's reagent (Sigma Chemical Co., USA) 2 mg/ml methanol. Parasitemia was calculated as the mean percentage (%) ± SEM of erythrocytes containing Leishman-positive bodies for groups of 4 – 8 mice for each dose tested. Drugs were delivered by the subcutaneous (s.c., 5 injections over 72 h), intraperitoneal (i.p., 5 injections over 72 h) as described previously (Pacholski *et al., Rev.* **1999**).

(Guerquin-Kern *et al.,* **1997)** An appropriate number of dose levels (2-8) were investigated for each compound, in order to determine the dose of drug (ID_{50}) required to inhibit parasitaemia by 50% compared with parasitaemia in concurrent vehicle-treated mice. (±)-*trans*-N^1, N^2-*bis*-(7-chloroquinolin-4-yl)cyclohexane-1,2-diamine (**26b**) (ID_{50} = 3.0

mg/kg; 0.0083 mol/kg) and the 7-trifluoromethyl analogue (**26e**A), (ID_{50} = 5.9 mg/kg; 0.0149 mol/kg) was active. However, the *bis*trifluoromethyl analogue (**26f**A) was inactive *in-vivo*: there was no reduction in parasitaemia following 5 x doses of 10 and 50 mg/kg, compare with treated with vehicle treated animals (control parasitaemia: 65%) chloroquine diphosphate was used as the control compound (ID_{50} = 4.3 mg/kg; 0.0083 mol/kg).

3.4. Conclusion.

This study demonstrates the presence of CF_3 substituents and the impact it has on the geometry of drug interaction with the antimalarial haem receptor. This may explain the pattern present in mefloquine (**13**) (Figure 3.1.) as it induces axial attack on the porphyrin as verified recently by crystal structure (Gildenhuys, **2015**).

Mefloquine (**13**) is protonated preferentially at the piperidine side chain. In gas phase calculations, 7-substituted *mono*- and *bis*-4-aminoquinolines are protonated at the endocyclic quinoline nitrogen. By contrast, compounds with a trifluoromethyl substituent on the 7th position, reverse the order of protonation which now favours the exocyclic secondary, aliphatic nitrogen at the 4th position. Trifluromethyl groups buttressing the endocyclic quinolinyl nitrogen are shown by molecular mechanics calculations to modulate the binding of antimalarials to haematin.

CF_3 substituents affect the electronic properties of the molecule, and they also offer alternative, preferential hydrogen-bonding sites, and their steric bulk will reduce the possiblity of interactions from the adjacent endocyclic nitrogen atom. Also, both changes in redox state and geometry of binding to haem, may lead to the design of outstanding antimalarial drugs both *in-vivo* and *in-vitro*.

3.5. References.

ADF Modeling, P. 2000. Amsterdam Density Functional (ADF): DFT for molecules, Band: 1D, 2D, 3D *periodic DFT*. Amsterdam.

Andersag, H., Breitner, S. 1941. *N*-Basically substituted compounds of the heterocyclic series. *U.S. Patent*. US2231444.

Adovelande, J., Boulard, Y., Berry, J. P., Galle, P., Slodzian, G., Schrevel, J. 1994. Detection and cartography of the fluorinated antimalarial drug mefloquine in normal and *Plasmodium falciparum* infected red blood cells by scanning ion microscopy and mass spectrometry. *Biol Cell.* 81, 185-192.

Allen, F., Kennard, O., Watson, D., Brammer, L., Orpen, A., Taylor, R. 1987. Tables of bond lengths determined by X-ray and neutron diffraction. Part 1. Bond lengths in organic compounds. *J. Chem. Soc., Perkin Trans.* 2, S1-S19.

Barlin, G., Jiravinyu, C., Yan, J. 1991. Potential Antimalarials. XIV. *Mono*-Mannich Bases of 4-[7'-Bromo (and trifluoromethyl)-1',5'-naphthyridin-4'-yl-amino]-5,6,7, 8-tetrahydronaphthalen-1-ols. *Aust. J. Chem.* 44, 677.

Barlin, G., Tan, W. 1985. Potential Antimalarials. III N^4 -Substituted 7-Bromo-1,5-naphthyridin-4-amines. *Aust. J. Chem.* 38, 459.

Barlin, G. B., Ireland, S., Jiravinyu, C., Nguyen, T., Kotecka, B., Rieckmann, K. 1993. Potential Antimalarials. XIX. Syntheses and Testing of-α-(Piperidin-2-yl)-α- (7′ -trifluoromethylquinolin-4′-yl)methanol and-α-(7-Bromo-1,5-naphthyridin-4-yl) -α-(piperidin-2′-yl)methanol. *Aust. J. Chem.* 46, 1695.

Barlin, G. B., Ireland, S., Nguyen, T., Kotecka, B., Rieckmann, K. 1994. Potential Antimalarials. XX. Mannich Base Derivatives of 2-[7-Chloroquinolin-4-ylamino and 7-Bromo(and 7-trifluoromethyl)-1,5-naphthyridin-4-ylamino]-4-chloro(or 4- or 6-t-Butyl or 4- or 5-fluoro)phenols and 4(or 6)-t-Butyl-2-(7-trifluoromethylquinolin-4-ylamino)phenol. *Aust. J. Chem.* 47, 1143-1154.

Barlin, G. B., Ireland, S. J., Nguyen, T., Kotecka, B., Rieckmann, K. 1993. Potential Antimalarials. XVIII. Some *Mono*- and Di-Mannich Bases of 3-[7-Chloro(and trifluoromethyl)quinolin-4-ylamino]phenol. *Aust. J. Chem.* 46, 1685-1693.

Barlin, G. B., Jiravinyu, C., Butcher, G. A., Kotecka, B., Rieckmann, K. 1992. The *in vitro* and *in vivo* antimalarial activity of some Mannich bases derived from 4-(7'-trifluoromethyl-1',5'-naphthyridin-4'-ylamino)phenol, 2-(7'-trifluoromethyl-quinolin-4'-ylamino)phenol, and 4'-chloro-5-(7''-trifluoromethylquinolin-4''-ylamino)biphenyl -2-ols. *Ann Trop Med Parasitol.* 86, 323-331.

Barlin, G. B., Nguyen, T., Kotecka, B., Rieckmann, K. 1992. Potential Antimalarials. XV. Di-Mannich Bases of 2-(7'-Chloroquinolin-4'-ylamino)phenol and 2-[7'-Bromo(and trifluoromethyl)-1',5'-naphthyridin-4'-ylamino]phenol. *Aust. J. Chem.* 45(10), 1651-1662.

Bowman, G. D., Nodelman, I. M., Hong, Y., Chua, N. H., Lindberg, U., Schutt, C. E. 2000. A comparative structural analysis of the ADF/cofilin family. *Proteins.* 41, 374-384.

Chou, A. C., Chevli, R., Fitch, C. D. 1980. Ferriprotoporphyrin IX fulfills the criteria for identification as the chloroquine receptor of malaria parasites. *Biochemistry.* 19, 1543-1549.

Clyde, D. F., McCarthy, V. C., Rebert, C. C., Miller, R. M. 1973. Prophylactic activity of a phenanthrene methanol (WR 33063) and a quinoline methanol (WR 30090) in human malaria. *Antimicrobial agents and chemotherapy*. 3(2), 220–223.

Cravo, P., Rodrigues, L., Hernrique, G. 2013. MDR1-associated resistance to artesunate +mefloquine does not impair blood-stage parasite fitness in a rodent malaria model. *Infection, Genetics and Evolution*. March 2013, Volume 14, Pages 340-346.

Dascombe, M. J., Drew, M. G., Morris, H., Wilairat, P., Auparakkitanon, S., Moule, W. A., Alizadeh-Shekalgourabi, S., Evans, P. G., Lloyd, M., Dyas, A. M., Carr, P., Ismail, F. M. 2005. Mapping antimalarial pharmacophores as a useful tool for the rapid discovery of drugs effective *in-vivo*: design, construction, characterization, and pharmacology of *meta*-quine. *J Med Chem*. 48, 5423-5436.

De, D., Krogstad, F., Byers, L., Krogstad, D. 1998. Structure-Activity Relationships for Antiplasmodial Activity among 7-Substituted 4-Aminoquinolines. *J. Med. Chem.* 41, 4918-4926.

Egan, T. J., Hunter, R., Kaschula, C. H., Marques, H. M., Misplon, A., Walden, J. 2000. Structure-function relationships in aminoquinolines: effect of amino and chloro groups on quinoline-haematin complex formation, inhibition of beta-haematin formation, and antiplasmodial activity. *J Med Chem.* 43, 283-91.

Egan, T. J., Mavuso, W. W., Ross, D. C., Marques, H. M. 1997. Thermodynamic factors controlling the interaction of quinoline antimalarial drugs with ferriprotoporphyrin IX. *J Inorg Biochem.* 68, 137-145.

Egan, T. J., Ncokazi, K. K. 2004. Effects of solvent composition and ionic strength on the interaction of quinoline antimalarials with ferriprotoporphyrin IX. *J Inorg Biochem.* 98, 144-152.

El Benna, J., Hakim, J., Labro, M. T. 1992. Inhibition of human neutrophil protein kinase C activity by the antimalarial drug mefloquine. *Biochem Pharmacol.* 43, 527-532.

Eswaran, S., Adhikari, A. V., Chowdhury, I. H., Pal, N. K., Thomas, K. D. 2010. New quinoline derivatives: synthesis and investigation of antibacterial and antituberculosis properties. *Eur J Med Chem.* 45, 3374-83.

Eynde, J.J.V., Mayence, A., 2019. Tafenoquine: A 2018 Novel FDA-Approved Prodrug for the Radical Cure of *Plasmodium vivax* Malaria and Prophylaxis of Malaria. *Pharmaceuticals.* 12, 115; doi:10.3390/ph12030115.2

Ferrari, V., Cutler, D. J. 1987. Temperature dependence of the acid dissociation constants of chloroquine. *J Pharm Sci.* 76, 554-556.

Florey, K. G., Brewer, G. A., Lim, P. 1972. Analytical profiles of drug substances. New York*: Academic Press*.

Furuseth, K., Karlsen, J., Mostad, A., Romming, C., Salmen, R., Tonnesen, H., Tokii, T. 1990. N^4-(7-Chloro-4-quinolinyl)-N^1,N^1-diethyl-1,4-pentanediamine. An X-Ray Diffraction Study of chloroquine Diphosphate Hydrate. *Acta Chemica Scandinavica.* 44, 741-745

Gabay, T., Krugliak, M., Shalmiev, G., Ginsburg, H. 1994. Inhibition by antimalarial drugs of haemoglobin denaturation and iron release in acidified red blood cell lysates-a possible mechanism of their anti-malarial effect? *Parasitology.* 108 (Pt 4), 371-381.

Gelmboldt, V. O., Ganin, E. V., Fonari, M. S., Simonov, Y. A., Koroeva, L. V., Ennan, A. A., Basok, S. S., Shova, S., Kahlig, H., Arion, V. B., Keppler, B. K. 2007. Two new "onium" fluorosilicates, the products of interaction of fluorosilicic acid with 12-membered macrocycles: structures and spectroscopic properties. *Dalton Trans*. 2915-2924.

Gildenhuys, J., Sammy, C, J., Muller, R., Streltsov, V. A., Le Roex, T., Kutter, D., De Villiers, K. A. 2015. *Dalton Trans*. 44, 16767-16777.

Guerquin-Kern, J. L., Coppey, M., Carrez, D., Brunet, A. C., Nguyen, C. H., Rivalle, C., Slodzian, G., Croisy, A. 1997. Complementary advantages of fluorescence and SIMS microscopies in the study of cellular localization of two new antitumor drugs. *Microsc Res Tech.* 36, 287-295.

Haberkorn, A., Kraft, H. P., Blaschke, G. 1979. Antimalarial activity of the optical isomers of chloroquine diphosphate. *Tropenmed Parasitol.* 30, 308-312.

Hawley, S. R., Bray, P. G., O'neill, P. M., Naisbitt, D. J., Park, B. K., Ward, S. A. 1996. Manipulation of the *N*-alkyl substituent in amodiaquine to overcome the verapamil-sensitive chloroquine resistance component. *Antimicrob Agents Chemother.* 40, 2345-2349.

Hooper, D. C., Soussy, C. J., Wolfson, J. S., NG, E. Y. 1993. Limitations of plasmid complementation test for determination of quinolone resistance due to changes in the gyrase A protein and identification of conditional quinolone resistance locus. *Antimicrob Agents Chemother.* 37, 2588-2592.

Ismail, F. 2002. Important Fluorinated Drugs in Experimental and Clinical Use. *Journal of Fluorine Chemistry.* 118, 27-33.

Ismail, F., Dascombe, M., Drew, M. 2009. Modulation of drug pharmacokinetics and pharmacodynamics by fluorine substitution. *Chimica Oggi: Chemistry Today.* 27, 18-22.

Ismail, F., Drew, M., Dascombe, M., Clark, I. P., I., Parker, A. W. 2004. Unraveling the mechanism of 4-aminoquinoline antimalarial action. *CCLRC Annual Report,Central Laser Facility*. Chilton, U.K.

Ismail, F. M., Dascombe, M. J., Carr, P., Merette, S. A., Rouault, P. 1998. Novel aryl-*bis*quinolines with antimalarial activity *in-vivo*. *J Pharm Pharmacol.* 50, 483-492.

Ismail, F. M., Dascombe, M. J., Carr, P., North, S. E. 1996. An exploration of the structure-

activity relationships of 4-aminoquinolines: novel antimalarials with activity *in-vivo*. *J Pharm Pharmacol.* 48, 841-850.

Jayaprakash, S., Iso, Y., Wan, B., Franzblau, S. G., Kozikowski, A. P. 2006. Design, synthesis, and SAR studies of mefloquine-based ligands as potential antituberculosis agents. *ChemMedChem.* 1, 593-597.

Jonet, A., Dassonvilt-Klimpt, A., Da Nasciment S., Leger J.-M., Guillon J., Sonnet P. 2011. First enantioselective synthesis of 4-aminoalcohol quinoline derivatives through a regioselective S_N2 epoxide opening mechanism. *Tetrahedron Asymmetry*. 22 (2), pp. 138-148.

Karle, J. M., Karle, I. L. 2002. Crystal structure of (-)-mefloquine hydrochloride reveals consistency of configuration with biological activity. *Antimicrob Agents Chemother.* 46, 1529-1534.

Kitchener, S. J., L Navshed, P. E., Edstein, M. D., Brennan, L., Harris, I. E., Leggat, P. A., Pickford, P., Kerr. C., Ohrt. C., Prescott, W., and the Tafenoquine Study Team. 2010. Randomized, Double-Blind Study of the Safety, Tolerability, and Efficacy of Tafenoquine versus Mefloquine for Malaria Prophylaxis in Nonimmune Subjects. *Antimicrob Agents Chemother*. 54, 792–798

Klamt, A. 1995. Conductor-like Screening Model for Real Solvents: A New Approach to the Quantitative Calculation of Solvation Phenomena. *The Journal of Physical Chemistry.* 99, 2224-2235.

Li, G., Sun, J., Li, Y., Huang, Y. Y., Shi, Y., Li, Z., Li, X., Yang, F. H., Zhao, J., Luo, H., Zhang, T., Zhang, X. 2020. Enantiomers of chloroquine and Hydroxy chloroquine Exhibit Different Activities Against SARS-CoV-2 *in vitro*, Evidencing S-Hydroxy chloroquine as a Potentially Superior Drug for COVID-19. *bioRxiv.*

Lim, P. Florey, K. G., Brewer, G. A. 1972. Analytical profiles of drug substances. New York: *Academic Press*.

Lima, P. C., Avery, M. A., Tekwani, B. L., De Alves, H. M., Barreiro, E. J., Fraga, C. A. 2002. Synthesis and biological evaluation of new imidazo[1,2-a]pyridine derivatives designed as mefloquine analogues. *Farmaco.* 57, 825-832.

Mcintyre, J., Castaner, J., Bayes, M. 2003. Tafenoquine Succinate. *Drugs of the Future,* 28, 859-869.

Meshnick, S. R. 1997. Is haemozoin a target for antimalarial drugs? *Ann Trop Med Parasitol. 90(4):367-72.,* 90, 367-372.

Mietzsch, F. 1951. [Trends of progress in chemotherapy]. *Klin Wochenschr.* 29, 125-35.

Mirghani, R. A., Yasar, U., Zheng, T., Cook, J. M., Gustafsson, L. L., Tybring, G., Ericsson, O. 2002. Enzyme kinetics for the formation of 3-hydroxyquinine and three new metabolites of quinine *in vitro*; 3-hydroxylation by CYP3A4 is indeed the major metabolic pathway. *Drug Metab Dispos.* 30, 1368-71.

Ohnmacht, C. J., Patel, A. R., Lutz, R. E. 1971. Antimalarials. 7. *Bis*(trifluoromethyl)- -(2-

piperidyl)-4-quinolinemethanols. *J Med Chem.* 14, 926-928.

O'neill, P. M., Harrison, A. C., Storr, R. C., Hawley, S. R., Ward, S. A., Park, B. K. 1994. The effect of fluorine substitution on the metabolism and antimalarial activity of amodiaquine. *J Med Chem.* 37, 1362-1370.

O'neill, P. M., Mukhtar, A., Stocks, P. A., Randle, L. E., Hindley, S., Ward, S. A., Storr, R. C., Bickley, J. F., O'neil, I. A., Maggs, J. L., Hughes, R. H., Winstanley, P. A., Bray, P. G., Park, B. K. 2003. Isoquine and related amodiaquine analogues: a new generation of improved 4-aminoquinoline antimalarials. *J Med Chem.* 46, 4933-4945.

O'neill, P. M., Willock, D. J., Hawley, S. R., Bray, P. G., Storr, R. C., Ward, S. A., Park, B. K. 1997. Synthesis, antimalarial activity, and molecular modeling of tebuquine analogues. *J Med Chem.* 40, 437-48.

Pacholski, M. L., Winograd, N. 1999. Imaging with mass spectrometry. *Chem Rev.* 99, 2977-3006.

Park, S., Jeong, Y., Pradeep, K. (2009). Synthesis of [2H]-and [13C]-labeled pyronaridine tetraphosphate: an antimalarial drug. *Journal of Labelled Compounds and Radiopharmaceuticals*. 52, 56-62.

Pham, Y. T., Nosten, F., Farinotti, R., White, N. J., Gimenez, F. 1999. Cerebral uptake of mefloquine enantiomers in fatal cerebral malaria. *Int J Clin Pharmacol Ther.* 37, 58-61.

Program, C. 2002. Cerius2.

Pullman T.N., Alving, A.S., Craige, B., Jones, R., Whorton, C.M., Eichelberger, L. 1948. The clinical trial of eighteen analogues of pamaquin (*plasmochin*) in *vivax* malaria (chesson strain). *J Clin Invest*. 27(3 Pt 2):34-45. doi:10.1172/JCI101963

Robinson, E. A., Johnson, S. A., Tang, T. H., Gillespie, R. J. 1997. Reinterpretation of the Lengths of Bonds to Fluorine in Terms of an Almost Ionic Model. *Inorg Chem.* 36, 3022-3030.

Ruscoe, J. E., Jewell, H., Maggs, J. L., O'neill, P. M., Storr, R. C., Ward, S. A., Park, B. K. 1995. The effect of chemical substitution on the metabolic activation, metabolic detoxication, and pharmacological activity of amodiaquine in the mouse. *J Pharmacol Exp Ther.* 273, 393-404.

Sheldrick, G. M. 1997. Shelx 86: high-resolution refinement. *Shelx Workshops.*

Sheldrick, G. M., Schneider, T. R. 1997. Shelxl: high-resolution refinement. *Methods Enzymol.* 277, 319-343.

Sarma, P. V., Han, D., Deschamps, J. R., Cook, J. M. 2005. Confirmation of the structure of (3S)-3-hydroxyquinine: synthesis and X-ray crystal structure of its 9-aceto analogue. *J Nat Prod.* 68, 942-4.

Stocks, P. A., Raynes, K. J., Bray, P. G., Park, B. K., O'neill, P. M., Ward, S. A. 2002. Novel short chain chloroquine analogues retain activity against chloroquine resistant K1 *Plasmodium falciparum*. *J Med Chem.* 45, 4975-4983.

Sveinbjornsson, A., Vanderwerf, C. A. 1951. Some Fluorine Containing Isoesteres of Sulfa Drugs. *J. Am. Chem. Soc.* 73, 869-870.

Tajerzadeh, H., Cutler, D. J. 1993. Blood to plasma ratio of mefloquine: interpretation and pharmacokinetic implications. *Biopharm Drug Dispos.* 14, 87-91.

Trenholme, C. M., Williams, R. L., Desjardins, R. E., Frischer, H., Carson, P. E., Rieckmann, K. H., Canfield, C. J. 1975. Mefloquine (WR 142,490) in the treatment of human malaria. *Science.* 190, 792-794.

Van Riemsdijk, M. M., Van Der Klauw, M. M., Van Heest, J. A., Reedeker, F. R., Ligthelm, R. J., Herings, R. M. & Stricker, B. H. 1997. Neuro-psychiatric effects of antimalarials. *Eur J Clin Pharmacol.* 52, 1-6.

Wiselogle, F. Y., National Research Council (U.S.) 1946. *A survey of antimalarial drugs, 1941-1945,* Ann Arbor, Mich. *Edwards.*

Yale, H. L. 1958. The Trifluoromethyl Group in Medical Chemistry. *Journal of Medicinal Chemistry.* 1, 121–133.

Chapter 4

Synthesis of naphthyridines rapid one-pot synthesis of 4-hydroxy-1,5-naphthyridine (SN 13,639) via sequential gould-Jacobs cyclization-retro-fries rearrangement under thermal and focused microwave irradiation.

Index of Contents chapter 4.

Figure of contents chapter 4.

Aim.

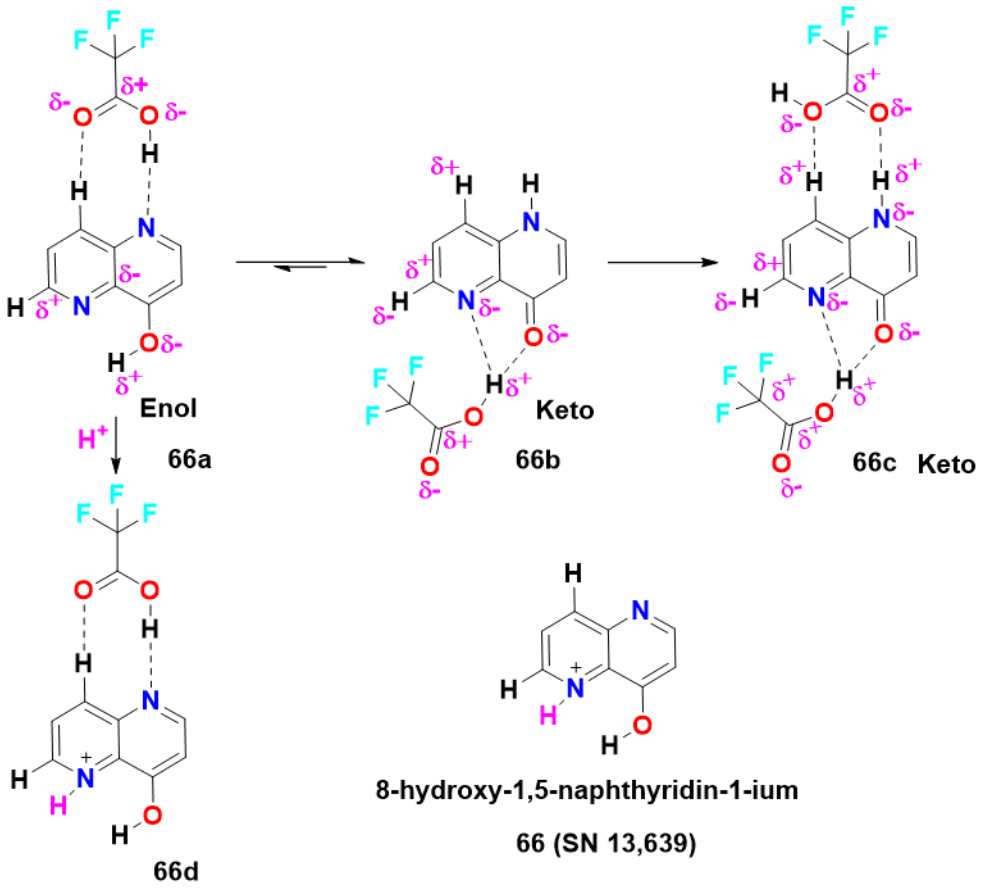

Figure 4.1. 4-Hydroxy-1,5-naphthyridine (SN 13,639).

4-Hydroxy-1,5-naphthyridine (SN 13,639), a key intermediate in the production of certain *aza*-substituted antimalarials, is normally synthesised by a multistep route comprising cyclization, de-esterification and decarboxylation. In this study it was noted, the unexpected and direct formation of 4-hydroxy-1,5-naphthyridine from (Z)-diethyl 2-((pyridin-3-ylimino)methyl) malonate by Gould-Jacob cyclization in refluxing diphenyl ether under thermal and focused microwave conditions, to produce ethyl 4-hydroxy-1,5-naphthyridine-3-carboxylate, which spontaneously undergoes the rare retro-Fries rearrangement to form 4-hydroxy-1,5-naphthyridine. This mechanism is supported by computational investigations, DFT with the B3LYP/6-31+G* methodology (Courtesy of Prof Drew, Reading University), who also identified the transition state reported here (Figure 4.1).

4.1. Introduction.

Quinolines have an antimalarial action which has so far resisted elucidation in over a century of research (Romanowsky in 1891 by Sneader, **2005)** an omission which has delayed the rational design of antimalarial drugs *de novo* (Dascombe *et al.,* **2007**). The inability to crystallize alkaloidal drug-haem receptor complexes (the currently favoured antimalarial drug target) (Egan *et al*., **2006**; Solomonov *et al*., **2007**; Vippagunta *et al*., **1999**, **2000**) has contributed to this slow progress and necessitated the use of computational and spectroscopic methods to study possible pharmacodynamic mechanisms (Casabianca *et al*., **2006**; de Dios *et al*., **2003**, **2004**; de Villiers *et al*., **2008**; Frosch *et al*., **2007**; Leed *et al*., **2002**; O'Neill *et al.,* **1997**).

The crystal structure of halofantrine-ferriprotoporphyrin, shows a covalent interaction through the oxygen atom of the drug to the iron with a bond length of 1.840(4)Å concomitant with π-π stacking and an intermolecular hydrogen bond between drug and porphyrin, but this combination of interactions is not possible with 4-hydroxy1,5-naphthyridine. This may indicate that the π-π stacking may only occur with covalent and/or intermolecular hydrogen bonds. Construction of biophoric maps, perhaps essential for unravelling both the mechanism(s) of action of antimalarial 4-aminoquinolines (Ismail *et al*., **1996**, **1998**; Kurosawa *et al*., **2000**; Dascombe *et al*., **2005**; Acharya *et al*., **2007**; Gemma *et al*., **2008**; Fattorusso *et al*., **2008**) and the induction of resistance to compounds such as chloroquine (SN 7,618; Figure 4.2.Figure 4.2.) (Wiselogle, **1945**) V2 part II (Figure 4.2., **1b**)(The designation SN identifies a compound in the monograph entitled A Survey of Antimalarial Drugs **1941-1945,** published in **1946**). Our previous mapping study suggests biosteric *aza*-substitution at close contact points between *meta*-quine (Figure 4.2, **21**); at position 5) and haematin could modulate the pharmacodynamic interactions of this antimalarial molecule (Dascombe *et al*., **2005**) thereby helping to understand the antimalarial action of quinolines. Constraining the conformational flexibility of ligands can facilitate binding by decreasing the entropic cost required to adopt a preferred binding orientation and so we have investigated putative drugs that possess aromatic rather than aliphatic side chains and bridging groups. Azalogues of chloroquine, (±)-4-(4-diethylamino-1-methylbutylamino)-1,5-naphthyridine (SN 7,618, Figure 4-2, **1b**) (Wiselogle, **1945**; Adams *et al*., **1946**) and pyronaridine (Figure 4.2., **15**) (Auparakkitanon *et al*., **2006**; Fu *et al*., **1991**; Zheng *et al*., **1982**), also form complexes with haematin (and haemozoin), the currently favoured antimalarial drug target(s) (Egan *et al*., **2006**; Pagola *et al*., **2000**; Solomonov *et al*., **2007**; Vippagunta *et al*., **1999**, **2000**). This may do so by reinforcing these intimate non-bonding interactions. For instance, incorporation of *aza*-substitution in certain drugs e.g. chloroquine (**1b**), and *meta*-quine, (Figure 4.2, **21**) at position 5 is superior to positions 2, 3 or 7 (Dascombe *et al*., **2005**).

The presence of a nitrogen substituent at the 5th position may promote preferential accumulation within *Plasmodia* through the weak base effect, i.e. entrapping the drug in the

acidic food vacuole that catabolises haemoglobin, thereby overcoming drug resistance and helping to explain how quinoline containing drugs bind to their receptor.

The synthesis of an azalogue of dichloro-*meta*-quine 2 (Figure 4.2, **21b**) (Ismail *et al*., **1999**) requires multi-gram quantities of a key intermediate, 4-hydroxy-1,5-naphthyridine (SN 7,618) (Figure 4.2, **1b**) (Adams *et al*., **1946**; Eck *et al*., **1966**; Hart *et al*., **1954**). In our experience procedure cannot be scaled up in the solution phase, (Chandrasekhar *et al*., **2002**; Johns *et al*., **2001**; Kirabo-Wamimbi *et al*., **1993**).

These particular 1,5-naphthyridines also serve as a vital precursor for the first orexin-1 receptor SB-334867 (a human protein that is expressed in projections from the lateral hypothalamus and is involved in the regulation of feeding behaviour, **61**) (Johns *et al*., **2001**; Kirabo-Wamimbi *et al*., **1993**). It has excellent selectivity for the orexin-1 receptor and shows activity *in-vivo*. Consequently, the efficient synthesis and analysis of naphthyridines was pursued. Since compound (**66a**) exists in a tautomeric equilibrium (**66a**/**66b**) (Figure 4.1) that shifts depending on the polarity of the solvent and the physical state (solid or in solution) it is collectively referred to as (**66**) (Figure 4.1).

Synthesis of (**66**) has been achieved by a variety of routes: including the Skraup (Price and Roberts., **1946**) and Gould-Jacobs reactions (Adams *et al*., **1946**; Eck *et al*., **1966**), degradation from quinoline, as well by thermolysis of Meldrum's acid derivatives (**65a**) (Figure 4.1) (Eck *et al*., **1966**).

Securing multi-gram quantities of (**66**) by the Gould-Jacobs reaction (Adams *et al*., **1946**; Eck *et al*., **1966**), which involves apparent regiospecific cyclization to 3-carbethoxy-4-hydroxy-l,5-naphthyridine (Figure 4.4, **70**a), was difficult (Adams *et al*., **1946**). Furthermore, it is commonly believed that only 1,5-naphthyridines are formed in this reaction (Johns *et al*., **2001**; Kirabo-Wamimbi *et al*., **1993**) but this has been shown to be untrue by Morgentin *et al* (**2008**) who found a mixture of the two products, 1,7 and 1,5-naphthyridin-4-ols, that they were unable to separate and, as a consequence, resorted to a different and unambiguous synthetic route to provide each isomer (Morgentin *et al*., **2008**).

A hypothesis that suggested tautomerism was an important property for antimalarial action within 4-aminoacridines and 9-aminoacridines was advanced by Schönhöfer in **1942** (Fig. 4.2.), (Hirai *et al*., **2003**; Hoeppli, **1959**; Jang *et al*., **1946**; Jiang *et al*., **2005**; Kikuchi *et al*., **2002**) and so it was important to establish which tautomer was present in any given situation. Infrared spectroscopy alone proved uninformative as to the position of the *keto-enol* equilibrium (Jiang *et al*., **2005**), but in conjunction with MO studies proved only useful in assigning bands.

This chapter reports a rapid one pot method using thermal heating, as well as focused microwaves in a sealed vessel to produce 1,5-naphthyridin-4(1H)-one (**66**). In addition, we investigate the likely mechanism of direct formation using DFT (DFT Calculations are Courtesy of Prof Drew, Reading University).

X-ray crystallography and NMR established where the tautomeric equilibrium is positioned both in the solid and solution state respectively (Figure 4.11). Finally, the antimalarial activity of 4-hydroxy-1,5-naphthyridine was measured against a multi-drug resistant *K1* strain of *Plasmodia in-vitro* to investigate claimed activity against *Plasmodia* (Screening of biological activity, Courtesy of Prof. Prapon Wilairat, Mahidol University).

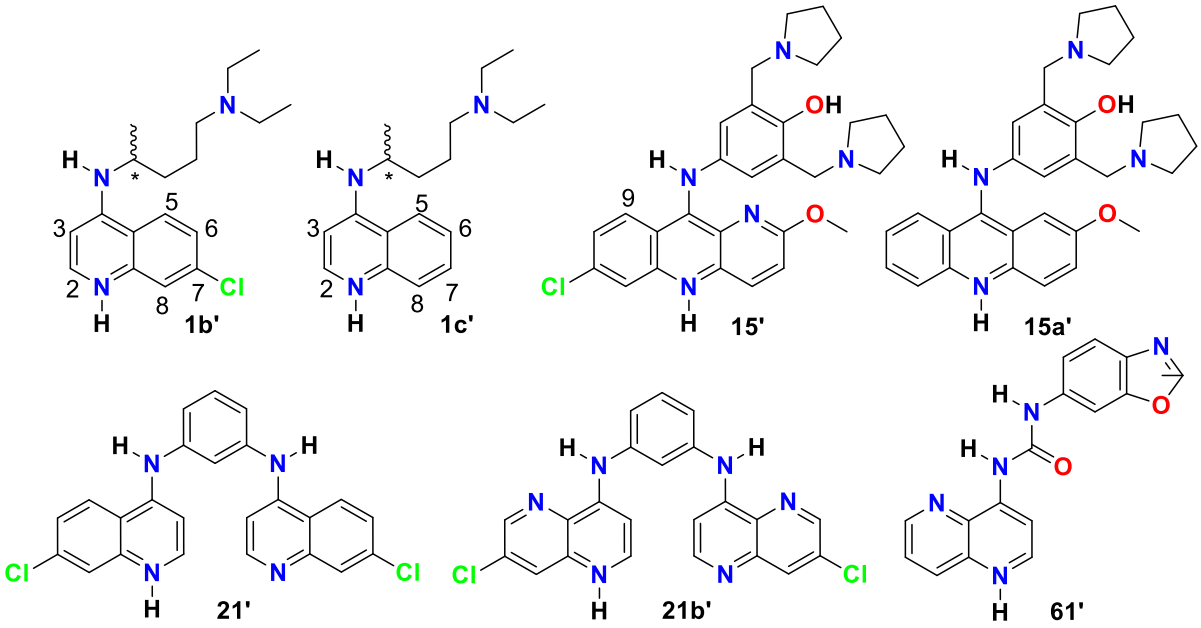

Figure 4.2. Chloroquine (**1b**) Resochin, SN 7,618(**1c**); (Dascombe *et al*., 2007); Pyronaridine (**15**) its analogue, Pyracrine (**15a**) (Zheng *et al*., 1982) (Fu *et al*., 1991); *meta*-quine (**21**) and its analogue, Metazaquine (**21b**)(Dascombe, *et al*., 2007), (Ismail *et al*., 1998), where Cl can be replaced by Br (Ismail *et al*., 1999); 1-(2-methylbenzo[d] oxazol-6-yl)-3-(1,5-naphthyridin-4-yl)urea (**61**)(SB-334867, Orexin antagonist, (*E*)-1-(2-methylbenzo[*d*]oxazol-6-yl)-3-(1,5-naphthyridin-4(*1H*)-ylidene)urea). And below is the imine form of the same compounds.

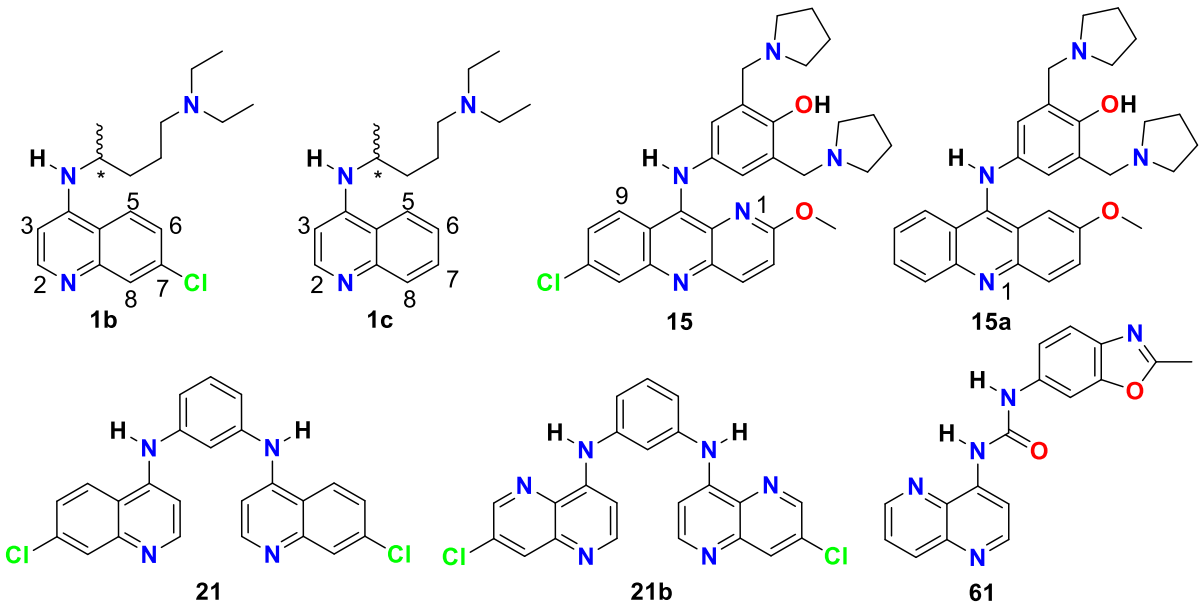

4.2. Results and discussion.

Various preparations of 1,5-hydroxynapthyridine are available (Albert *et al*., **1952**; Albert *et al*., **1960**; Allen, **1950**). We chose the route of Adams (Figure 4.4) (Adams, *et al*., **1946**). As emphasised by Eck (Eck *et al*., **1966**), we also found it vital to use pure starting materials and intermediates before attempting either condensations or cyclizations to any type of naphthyridine in either diphenyl ether or Dowtherm A™. Failure to use pure starting material results in products that cannot be subsequently purified. The external pressure recorded by the CEM™ focused microwave suggests the onset of small molecule (or gas) evolution only occurs when an internal temperature of 220°C is achieved; Eck *et al* (**1966**) also observed this phenomenon but at 150°C in a Claisen flask (Bohn *et al*., **1994**) (Figure 4.3). This reaction was monitored carefully over numerous occasions and we could not replicate their observations. It is now known, that only around 30% of literature experiments can be replicated (Baker, **2016**).

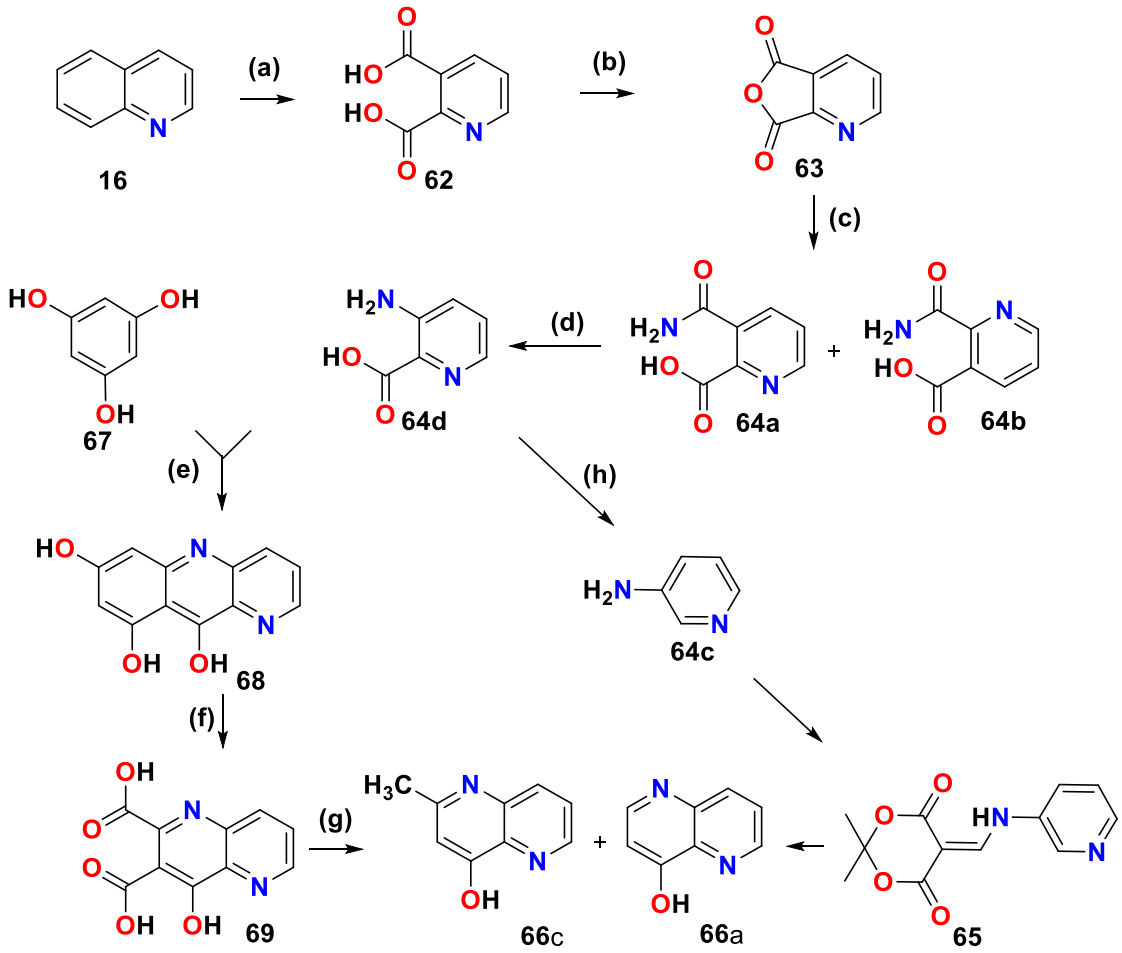

Figure 4.3. Scheme 43. (a) HNO_3, forming pyridine-2,3-dicarboxylic acid (**62**) 77% (b) Ac_2O, forming furo[3,4-b]pyridine-5,7-dione (**63**) 86% (Drummond *et al*., 1989); (c) $SOCl_2$, $CHCl_3$/0°C then NH_3, mixture of (**64a**) 3-carbamoylpicolinic acid and (**64b**) 2-carbamoyl nicotinic acid, 99%; (d) NaOH/Br2, 0-70°C, (**64d**) 3-aminopicolinic acid, 71% ;(e) Fusion

with (**67**), 205°C, neat 30 min, (**68**) benzo[b][1,5] naphthyridine-7,9,10-triol, 2-12% ; (f) HNO_3, 4-hydroxy-1,5-naphthyridine-2,3-dicarboxylic acid, (**69**) 5-12% ; (g) refluxing quinoline, -CO_2, (**66**) (SN 13,639), 98%; (h) Ethylacetoacetate, heat. (**66a**), 11%. Overall yield = 0.023−0.33 % from initial charge of (**62**) (Full calculation is given in ESI)

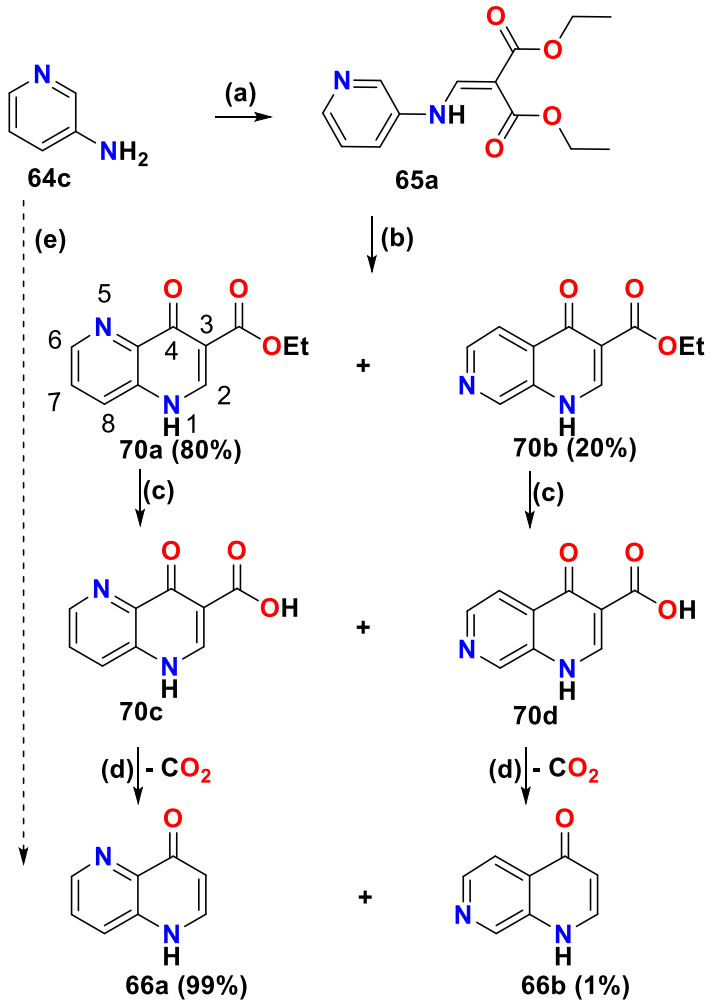

Figure 4.4. Scheme 44. In situ condensation of 3-aminopyridine and diethylEthoxymethylene malonate (EMME) produces diethyl 2-((pyridin-3-ylamino)methylene)malonate which can either cyclise to (**70a**) 1,5-naphthyridine and (**70b**) 1,7-naphthyridine: (a) heat, loss of EtOH, (110°C) produces (**65a**) 99%; (b) reflux, diphenyl ether, 150-220˚C (**70a**) 84-85% ; alternatively Dowtherm A™ 150-270˚C (Eck, *et al.*, 1966) or focused microwaves (Ismail *et al.*, Unpublished data) 45%; (c) Hydrolysis: NaOH/H_2O, (**70a**) 80% (this study). (d) mineral oil 325-330°C, (**66**) (90%; this study) refluxing quinoline (89%) or focused microwaves (85%; this study); The 1,7-naphthyridine isomer was always formed in 11-20% yield which was most easily identified in the subsequent *de*-esterification step, Heating the reaction mixture above 250°C causes large amounts of impurities to be formed and increases the danger of igniting the Dowtherm).

The visual changes during the course of the reaction are illustrated (Figure 4.4). On every occasion, we observed efficient cyclization only at temperatures around 200-220°C.

Unusually, this supposedly exclusive Regio cyclisation to 3-carbethoxy-4-hydroxy-l,5-

naphthyridine (Figure 4.4, **70a**) has never been fully investigated by NMR (either in DMSO–d_6 or TFA-*d*), despite its recent utility during synthesis of orexin receptor agonists (Johns *et al*., **2001**; Kirabo-Wamimbi *et al*., **1993**). The progress of reactions was monitored by HPLC-positive ion electrospray mass spectrometry (Figure 4.6) proving the presence of isomeric species. ^{1}H NMR spectroscopy of the crude cyclized product (DMSO–d_6) reveals that the corresponding 1,7-naphthyridine regio-isomer dominates the spectrum (Figure 4.4. Figure 4.4 **70b**), an observation inconsistent with previous investigations. It was not possible to separate crude reaction mixtures by HPLC.

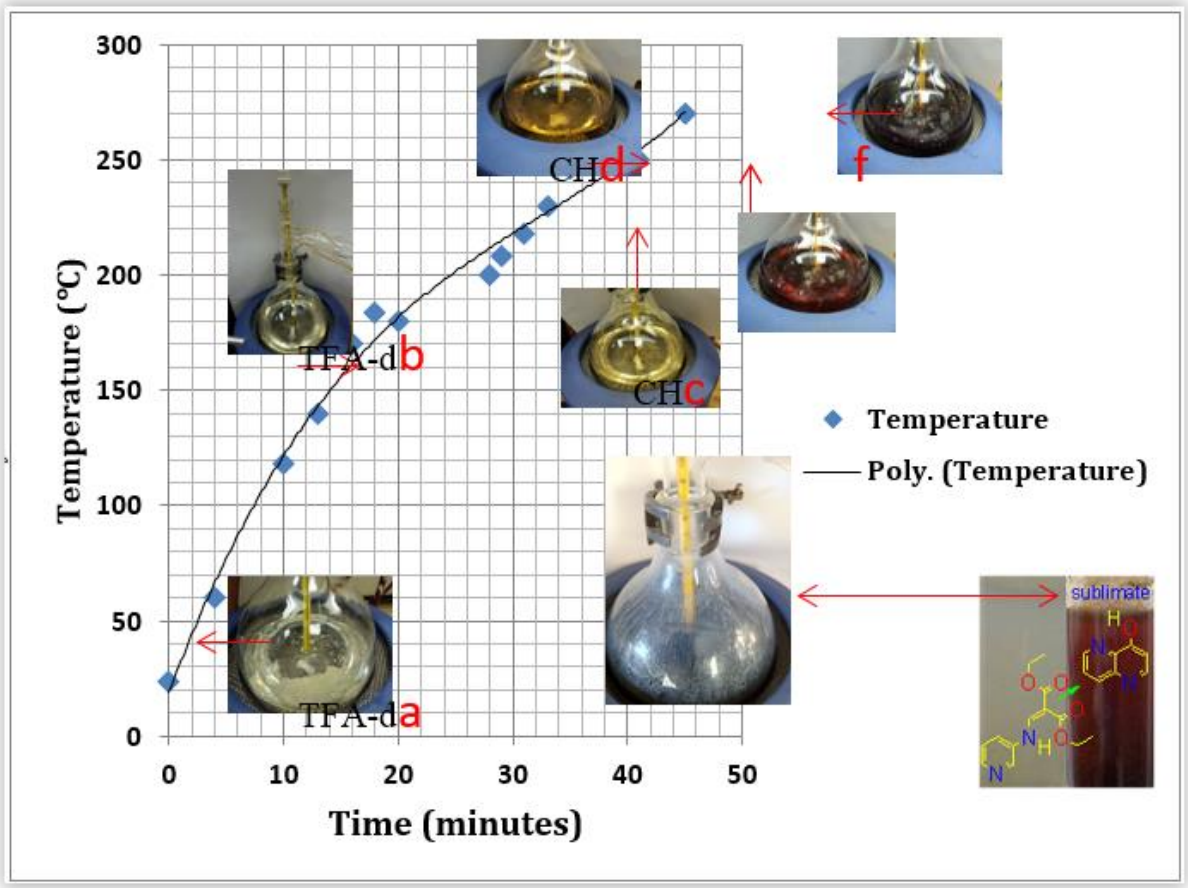

Figure 4.5. Time vs. Temperature Profile illustrating visual changes in the bulk solution(**65a**) (diethyl 2-((pyridin-3-ylamino)methylene)malonate) refluxing in Dowtherm A^{TM} to produce crude cyclized **70a**/**70b** (a-f) Temperature relates to inner core temperature of the reaction mixture; (g) Sublimate on the upper, internal part of the round bottomed flask at termination of the reaction; (h) before focused microwave irradiation; (i) post irradiation showing formation of sublimate. Reaction kinetics were monitored by ^{1}H-NMR and ^{13}C-NMR (APT) and speciated with positive-ion electrospray mass spectrometry. (Poly refers to polynomial equation)

The 1,5-isomer has poor solubility in DMSO–d_6 and neither its concentration nor position of the tautomeric equilibrium could be inferred from previous data, so investigations took place using complex reaction mixtures (Figure 4.6). Furthermore, the presence of the diphenyl ether overlapped with key diagnostic peaks and caused some peaks to shift downfield (Figure 4.6). Initially, the crude material was purified by precipitation using

petroleum ether as commonly practiced for isolating such materials (Adams, *et al.*, **1946**).

Elimination of the diphenyl ether and the subsequent re-acquisition of NMR spectra on the crude compound indicated that DMSO–d_6 indeed mostly solubilized the 1,7 isomer but we found that careful expansion of regions of interest also allowed other major constituents with partial solubility to be identified. (Figure 4.7).

Regions downfield (δ11-13 ppm) showed the presence of several exchangeable protons which suggested the presence of various naphthyridin-4-one and naphthyridin-4-ol species (Figure 4.5). Although the aliphatic portion of the ^{1}H-NMR spectrum (petroleum ether or hexane washed) crude material is unremarkable, in the ^{13}C-NMR spectrum, it is most surprising to note two methylene peaks resonating at δ59.78 and 59.71 ppm.

This suggests it is possible to distinguish within the mixture a coupling extending over seven bonds ascribed to the 1,7- and 1,5- naphthyridines. This fact subsequently proved useful as a rapid test for purity when considering compounds for further structural and pharmacological investigations.

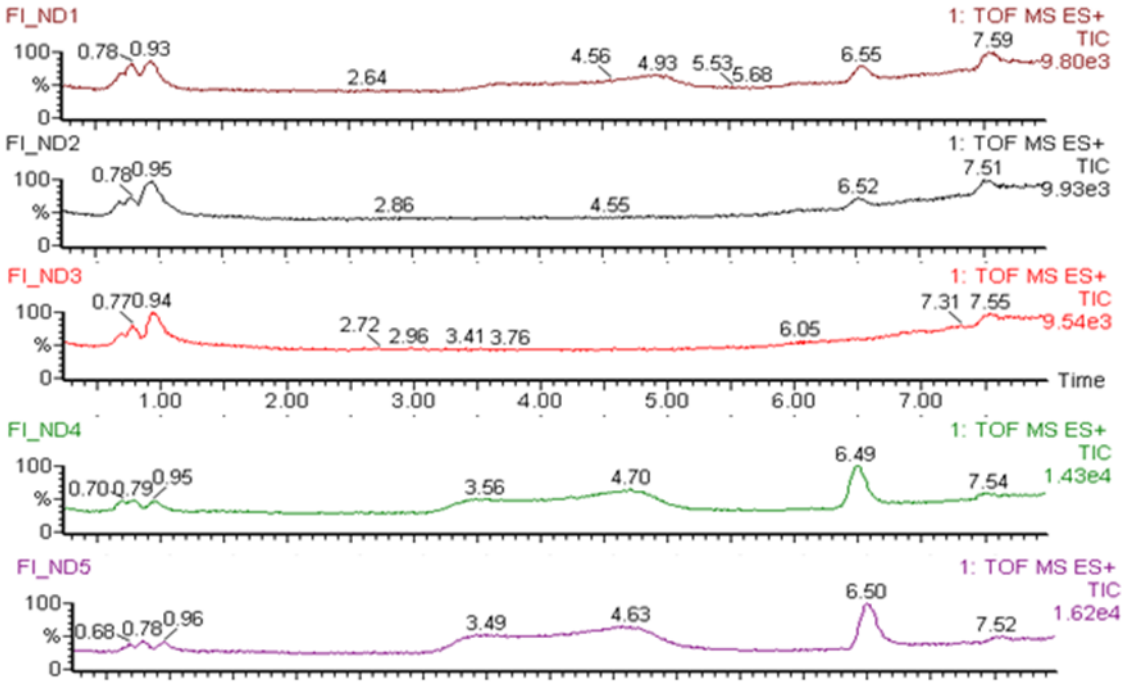

Figure 4.6. HPLC-MS of crude cyclized **70a**/**70b** (gradient separation in acetonitrile water; Diluted 1:20 acetonitrile:water (v/v); 30V after optimisation). Positive-ion mass total ion chromatograms shown. ND1: DMSO insoluble material crude reaction mixture hexane washed to remove Dowtherm A^{TM}. ND2: DMSO soluble material (ethyl 4-hydroxy-1,7-naphthyridine-3-carboxylate at 6.52 min); ND3: purified 4-hydroxy-1,5-naphthyridine (0.95 min); ND4: crude methanol washed to remove Dowtherm A^{TM}; ND5: crude pet ether washed to remove Dowtherm A^{TM} (includes ethyl 4-hydroxy-1,5-naphthyridine-3-carboxylate and an isomeric species ethyl 4-oxo-1,4-dihydro-1,5-naphthyridine-3-carboxylate). Peaks assigned by detection of various ions especially 219 Da: $C_{11}H_{11}N_2O_3^+$ and 241 Da (ESI).

On large scale (250-1000g), precipitation of the cyclized naphthyridine **70** (or **66**) as hydrochloride salts, using anhydrous HCl gas *in situ* by Kipps apparatus followed by Buchner

filtration, replaced tedious precipitation with ligroin (Adams *et al*., **1946**; Eck *et al*., **1966**) and centrifugation. Saponification of ethyl 4-hydroxy-1,5-naphthyridine-3-carboxylate (Figure 4.4, **70**a) using a literature method (Adams *et al* **1946**) gave the carboxylic acid (Figure 4.4,**70**c). Subsequent decarboxylation of the free base in boiling quinoline (Barlin *et al*., **1985**) (rather than Dowtherm ATM or diphenyl ether) followed by acid precipitation gave grey coloured material, when recrystallized from hot water (decolourizing charcoal), yielded yellow compound **66** (crude material 31%).

Laborious alternate recrystallization and vacuum sublimation (seven times) at 300-325°C provided pure **66** albeit on a small scale (approximately 100 mg; 5% overall yield). All mixtures and isolated compounds were further characterized by HPLC positive-ion electrospray mass spectrometry.

All mixtures and isolated compounds were further characterized by HPLC-positive ion electrospray mass spectrometry (Figure 4.6). Retention times are flagged and of all the HPLC columns investigated, a Waters X-bridge reverse phase, using a water-acetonitrile gradient, proved most useful in separating the various components within crude mixtures but like Morgentin (Morgentin *et al*., **2008**), Complete separation of peaks seems impossible. One explanation is that the compounds hydrogen bond to one another denying efficient resolution; electrospray-mass spectrometry of each region confirms the presence of several isomers.

The collected Dowtherm^{TM} was washed with cold aq. H_2SO_4, then NaCl saturated water and could be purified for reuse. Also, in order to further optimize production of SN 13, 639 (**66**), various solvents and reaction conditions were investigated but none of the procedures could be scaled up to provide kg quantities in good yield.

Extended reflux of the malonate ester (**65**a) in diphenyl ether, the transient presence of white sublimate in the neck of the condenser or the inner upper surface of the round bottom flask was observed (Figure 4.5, (a-f)). A slow stream of water was used to trap this material using a heavy walled double surface condenser (Bailey *et al.*, **1967**).

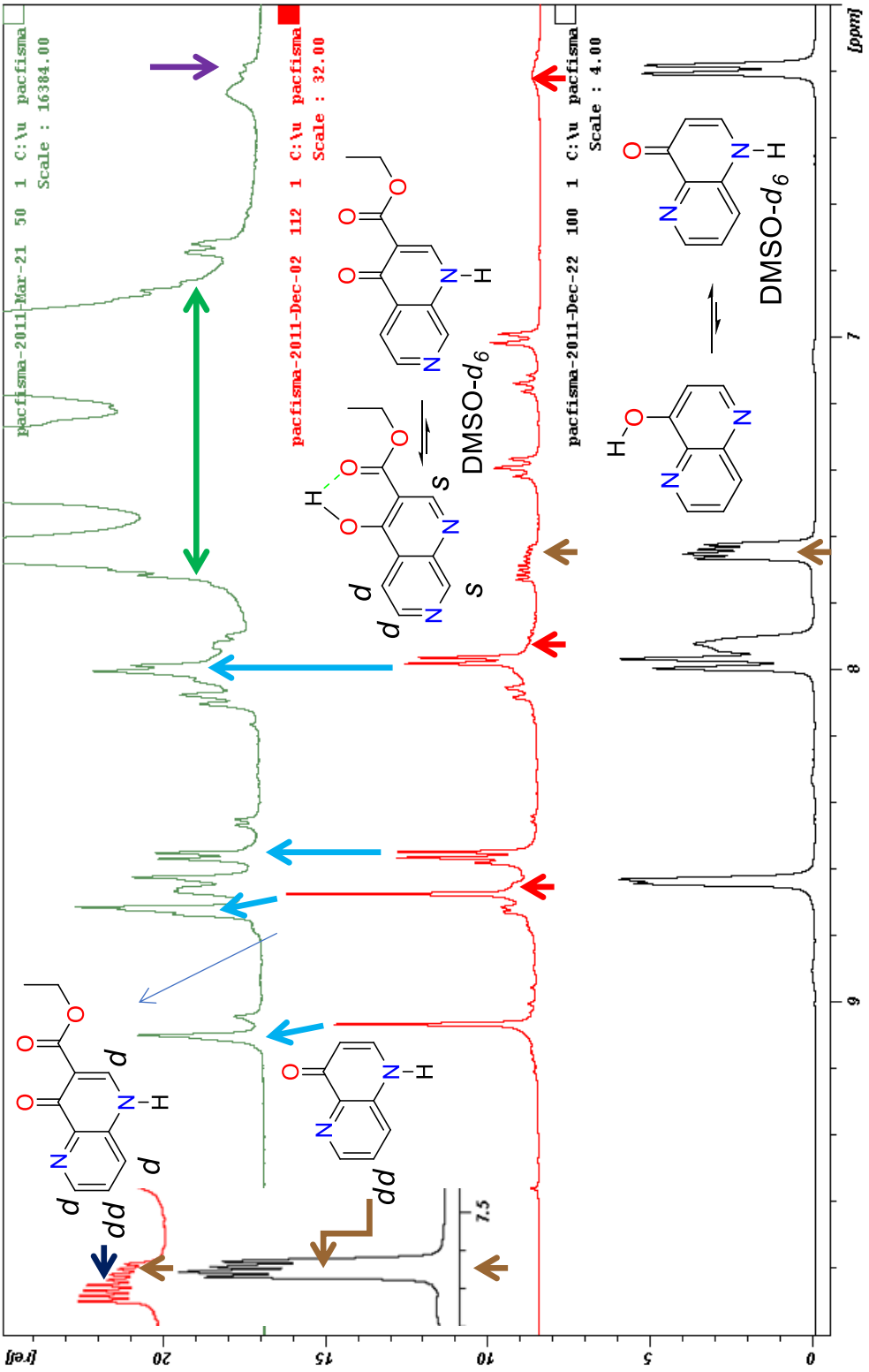

Figure 4.7. ^{1}H-NMR spectral region illustrating NH/OH peaks of a) crude cyclized **70a**/**70b** product before work up to ascertain product distribution in Dowtherm A™ (green); b) After washing with petroleum ether (red); c) pure 1,5-naphthyridin-4(1H)-one tautomer (**66**). Inset shows expansion of δ7.5-7.8 ppm region of petroleum ether washed crude mixture showing both **66a**/**66a'** with a diagnostic doublet of doublets (2:1 ratio), internally hydrogen bonded in ethyl 4-hydroxy-1,5-naphthyridine-3-carboxylate. A is assigned to the corresponding 4-oxo-1,4-dihydro-1,7-naphthyridine-3-carboxylate isomer (by integration); B is assigned to ethyl 4-hydroxy-1,5-naphthyridine-3-carboxylate.

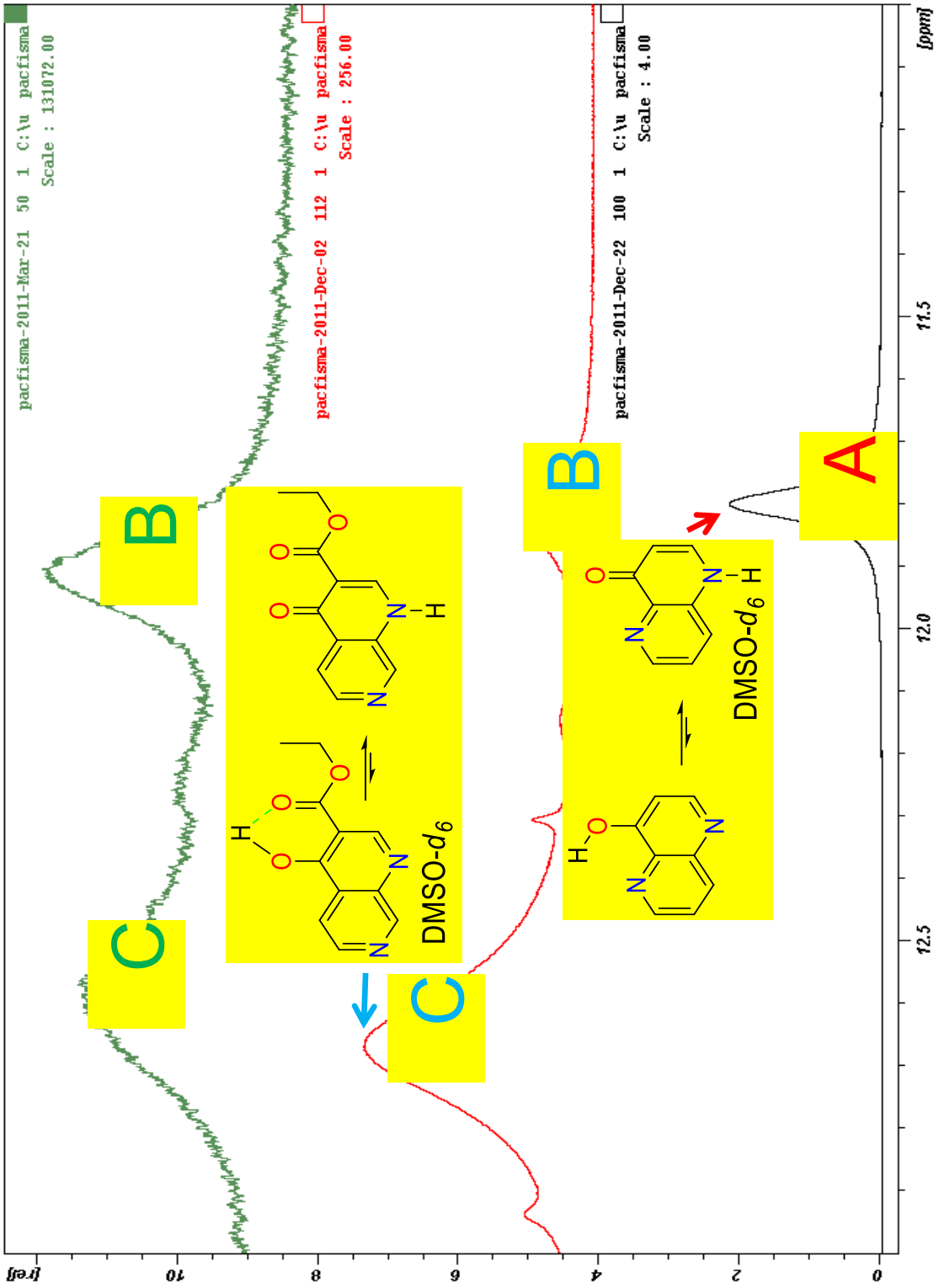

Figure 4.8. ^{1}H-NMR spectrum in DMSO-d_6 of crude cyclized **70a**/ **70a'** product before work up to ascertain product distribution in Dowtherm A^{TM} (green) using the exchangeable hydrogens. The red spectrum is the product washed with petroleum (see peaks marked B& C), whereas the black spectrum is authentic 4-hydroxy-1,5-naphthyridine. Note the broad (δ 11.9 ppm), diffuse (δ12.1-12.40 ppm), and quite broad peaks (δ 12.60 ppm) suggesting the presence of three species (**70a**, **70a'** and **66**; green spectrum).

The following points need to be considered when performing this operation to make sure it is undertaken in a safe fashion:

i) Apparatus needs to be re-annealed regularly, ii) If care is not taken, condenser can crack and mixing cold water with boiling diphenyl ether is extremely dangerous, iii) experiments should be conducted behind a sturdy shield. iv) The plug of naphthyridine can easily fall back into the dark reaction mixture when the condenser is removed.

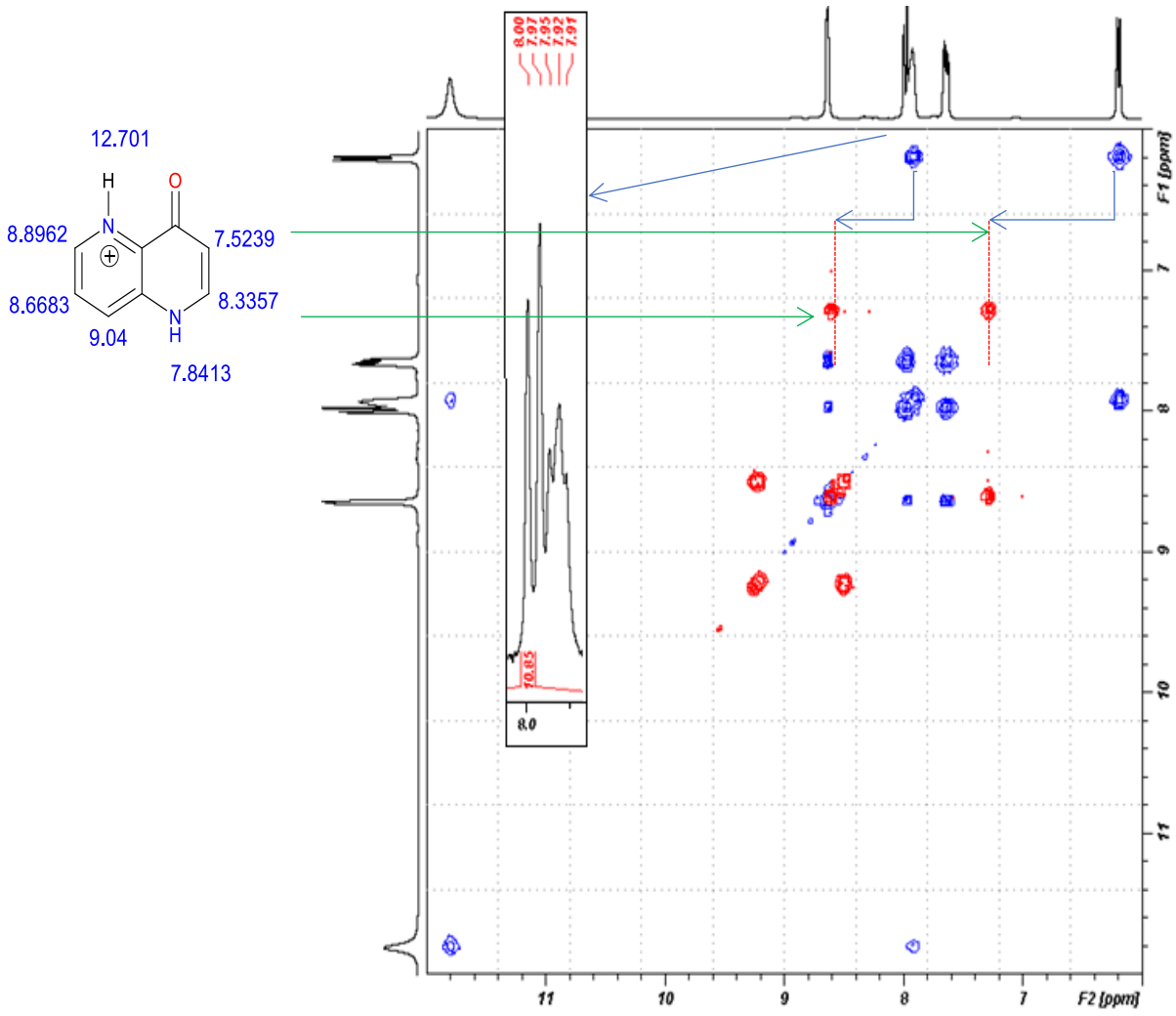

Figure 4.9. Blue projection: ^{1}H-^{1}H (Through bond correlation) COSYGPSW NMR spectrum of pure 1,5-naphthyridin-4(1H)-one in a) DMSO-d_6 suspension (**66**), showing connectivity between the proton on N-1 (11.80 ppm) and H-2 triplet (7.92 ppm, See expansion); b) Red projection: TFA-*d* solution, proton. Inset (Top left) shows predicted values from DFT calculations (Courtesy of Proff MGB Drew, Reading university).

A white sublimate depositing above the refluxing reaction mixture was also observed (Figure 4.5, (g)). This material rapidly deposits itself on the inner unlagged walls of the reaction vessel. Repetition of this experiment under focused microwave irradiation, in a sealed tube, trapped the sublimate more efficiently as a band of material (Figure 4.5, (h,i)).

The sublimate was identified as 4-hydroxy-1,5-napthyridine (SN 13,639, **66**) from NMR

analysis, (TFA-*d*) position of the peaks was shifted far from anticipated positions, and we assume to be due to halogen and hydrogen bonding with the solvent (Figure 4.7).

Note the presence of broad diffuse and quite broad peaks at 10.9, 12.0-12.25 and 12.30 ppm respectively suggesting the presence of the three species **70**a, **70**a' and **66** (Figure 4.8, (green)).

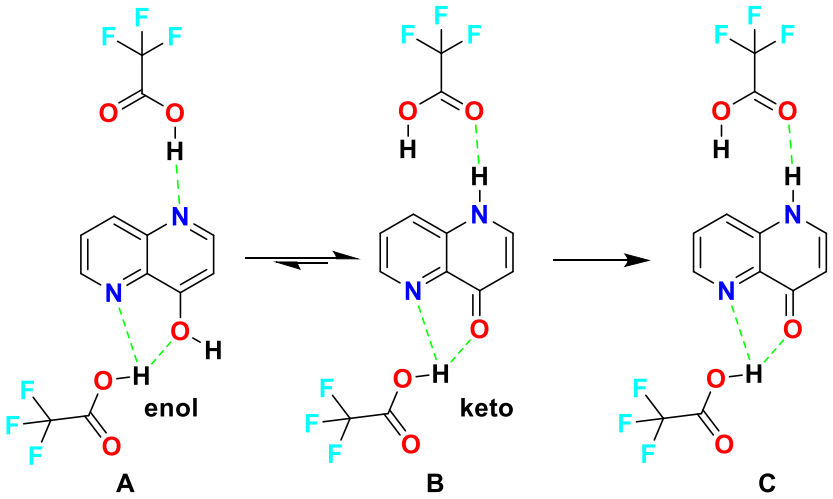

Figure 4.10. Keto-Enol Tautomerism (**66**).

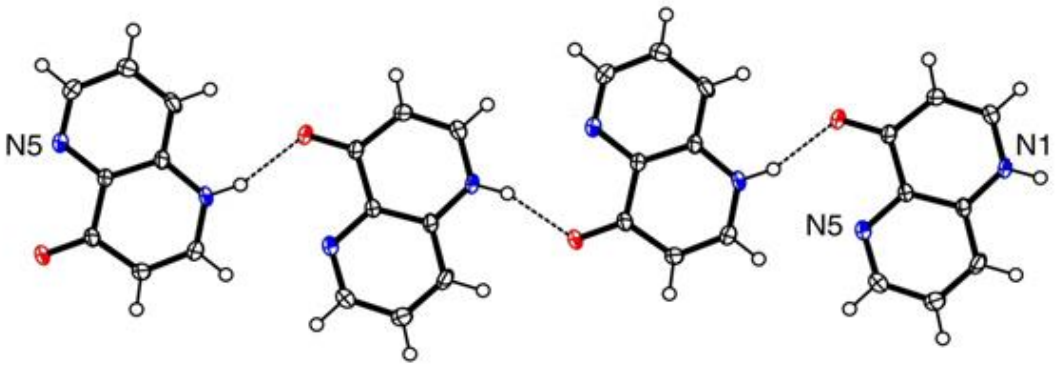

Figure 4.11. The structure of (**66a**) with ellipsoids at 50 % probability. Hydrogen bonds along the c axis shown as dotted lines.

The carbonyl peak of the compound, dissolved in DMSO-d_6 (176.31 ppm) resonates in similar position to that in TFA-*d* (173.21 ppm) suggesting both possess the enone form. The large downfield shifts shown by protons suggest structure similar to C exist in the later solution.

(Liao *et al*., **2009**) suggest that 1,5-naphthyridin-4(1H)-one (**66**) (Figure 4.1) is found to exhibit keto-enol tautomerism in polar solvents, but deuterium exchange of the NH signal in

this protic solvent will not show the connectivity with the proton residing on N1. Most deshielded ^{13}C APT (^{13}C chemical shift, C and CH_2 have the opposite phase from CH and CH_3) assigned quaternary carbon atom resonates at 176.31 ppm whereas that given by Liao (Liao *et al*., **2009**) (148.37 ppm in CD_3OD) does not appear to support their assignment of the 1,5-naphthyridin-4(1H)-one(**66b**).

Various NMR experiments in DMSO-d_6 using multi-dimensional NMR (COSY, HSQC, HMBC) indicated that our sublimate was strongly suspected of being the desired 4-hydroxy-1,5-naphthyridine (**66a**), final product and this was subsequently unambiguously confirmed by X-ray crystallography (Figure 4.11).

Filtration of the undissolved material and acquisition of NMR spectrum in TFA-*d* proved that the insoluble fraction was the anticipated 1,5-naphthyridine ester (**70**a), and the residual was unsublimed 4-hydroxy-1,5-naphthyridine as its tautomer (**66a**). 4-hydrox-1,5-naphthyridine can hydrogen bond inter molecularly in hydrocarbon solvents explaining why it sublimes from diphenyl ether and Dowtherm A™.

Efficient acquisition of the NMR spectrum of the 4-hydroxy-1,5-naphthyride in DMSO–d_6 proved difficult due to poor solubility but an extended number of scans (100,000) showed that the tautomeric 1,5-naphthyridin-4(1H)-one (**66a**) (Figure 4.1)was present in DMSO–d_6 with all COSY spectra showing connectivity between the proton on N-1 and the triplet found for H-2 (Figure 4.9), consistent with inferences from a solution and solid state spectroscopy study (Liao *et al*., **2009**).

Substances that sublime may regularly escape undetected, because air condensers are commonly used in Gould-Jacobs reactions (Brown *et al*., **2008**; Czuba *et al*., **1979**; Gould *et al*., **1939**; Hermecz *et al*., **1992**; Litvinov *et al*., **2000**, **2006**; McNab, **2005**; Milata *et al*., **2001**; Noravyan *et al*., **1985**; Reitsema, **1948**; Weiss *et al*., **1967**) so our observations may have wider significance, especially for the industrial production of chloroquine. Porter (Porter *et al*., **2001**) report the production of 1,5-naphthyridin-4(1H)-one (**66a**) in 43% overall yield following the method of (Adams *et al*., **1946**) but at unspecified purity. Although our procedure provided the desired 4-hydroxy-1,5-naphthyridine in variable yield (17-54%), depending on the scale of the reaction (i.e. 15g-1kg initial charge of **65**). We note that Porter *et al*. limit the amount of **70c**, decarboxylated to **66a**. In accordance with earlier observations Eck *et al*., the exceptional purity of our sublimate rendered it suitable for pharmacological evaluation, because it only required a simple acetone wash to remove traces of diphenyl ether or Dowtherm A^{TM} (Ismail *et al*., Unpublished data) and did not require zone refining under argon as preferred by Liao (Liao *et al*., **2009**). Considering the difficulty that we and all others have had in securing this compound and the unaffordability of commercially available material for investigators in the malaria field, we suggest our route is by far the most convenient reported to date.

4.3. X-ray Analysis of 4-hydroxy-1,5-naphthyridine

The tris-(4-hydroxy-1,5-naphthyridine) aluminium chelate has been characterized by a diffraction study but the free ligand remained unsolved until the current study (Liao *et al*., **2009**). The structure of **66a** is shown in (Figure 4.11). Surprisingly the hydrogen atom was found bonded to N1 rather than the oxygen. Indeed, the C-O bond length is 1.246(3) Å indicating a carbonyl group. It is interesting to note that calculations using Gaussian software at the B3LYP/6-31+G* level show that the enol form has an energy 7.84 kcalmol^{-1} less than this carbonyl form. Protonation of N-5 is however 2.79 kcalmol^{-1} higher in energy (Prof Drew, Reading university). However, the reason for the unexpected structure is likely to be found in the formation of strong hydrogen bonds in the crystal which can more than compensate for this difference in energy. As shown in figure 4.1, there are strong intermolecular hydrogen bonds along the c axis connecting molecules, thus forming a chain. Dimensions of the hydrogen bond are N-H…O (x-1/2, ½-y, z+1/2) with N…O 2.773(3) Å, N-H…O 160º and H…O 1.95Å.(Courtesy of Prof Drew, Reading University).

4.3.1. NMR Analysis of 4-hydroxy-1,5-naphthyridine

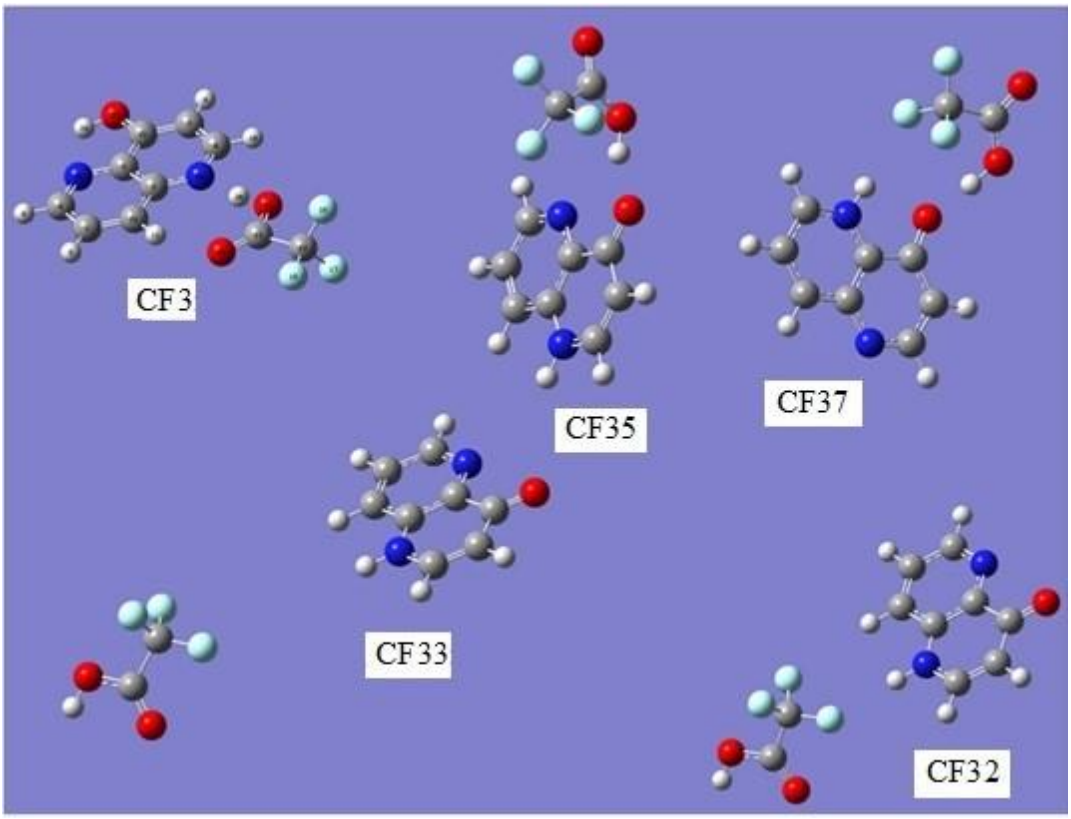

Figure 4.12. Relative energies of **66a**, 1:1 complexes of 4-hydroxy-1,5-naphthyridine , where CF3: -22; CF32: -1; CF33: 0; CF35: -14; CF37: -8 kcal/mol respectively.

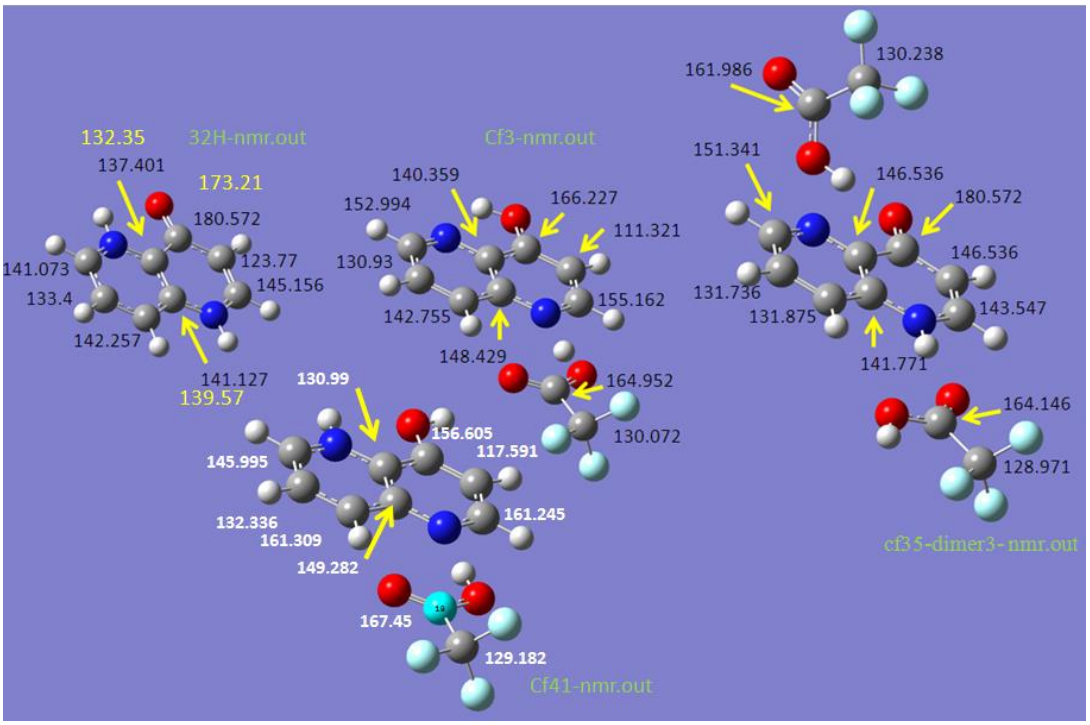

Figure 4.13. Relative energies of 4-hydroxy-1,5-naphthyridine complexes. The hydrogen bonded motif in CF_3 is clearly the most thermodynamically favoured and was subsequently incorporated in NMR shifts which are shown in black and white colour. Yellow data show values measured in TFA-*d*.

The poor solubility of the crude complex mixtures required a medium that allowed analysis of the reaction mixture *in toto* which necessitated the use of TFA-*d*. We noted that 4-hydroxy-1,5-naphthyridine (**66a**) (Figure 4.1) exhibited unusual chemical shifts both in the ^{1}H and ^{13}C spectra. Using a combination of COSY, HMBC and HMQC spectra in conjunction with APT (Attached Proton Test) and DEPTQ experiments it was established that the most deshielded carbon (and the proton attached to it) was surprisingly at position 8.

Consequently, we performed computational investigations involving one molecule of TFA and 4-hydroxy-1,5-naphthyridine (**66a**) allowing identification of a novel structural motif depicted in (structure CF_3). Geometry optimisation on models were performed involving one molecule of TFA hydrogen bonded with (**66a**) (Figure 4.1), considering all three proton positions on N1, N5 and O. The resulting structures with the lowest energy are shown in (Figure 4.11) (Courtesy of Prof Drew, Reading university) (Figure 4.12 and 4.13).

The hydrogen bonding to the naphthyridine N1 positions the carbonyl of the TFA towards CH8 deshielding more than the nitrogen adjacent to CH6. Based on chrystalographic data and DFT calculations, the carbon oxygen bond also shows some double bond character (Courtesy of Prof Drew, Reading university).

In particular, possible structures were computationally filtered on the basis of fine structure and splitting of peaks at H-5, H-6 and H-8 in ^{1}H-NMR spectra, and three likely low

energy structures were established (Figure 4.13). Calculated ^{13}C-NMR shifts of low energy structures (**66a**) (Figure 4.1) at 164.952 in the top middle, (**66a**) with 2 TFA 161.986, 164.146. (**66a**) 130.99, 149.282.

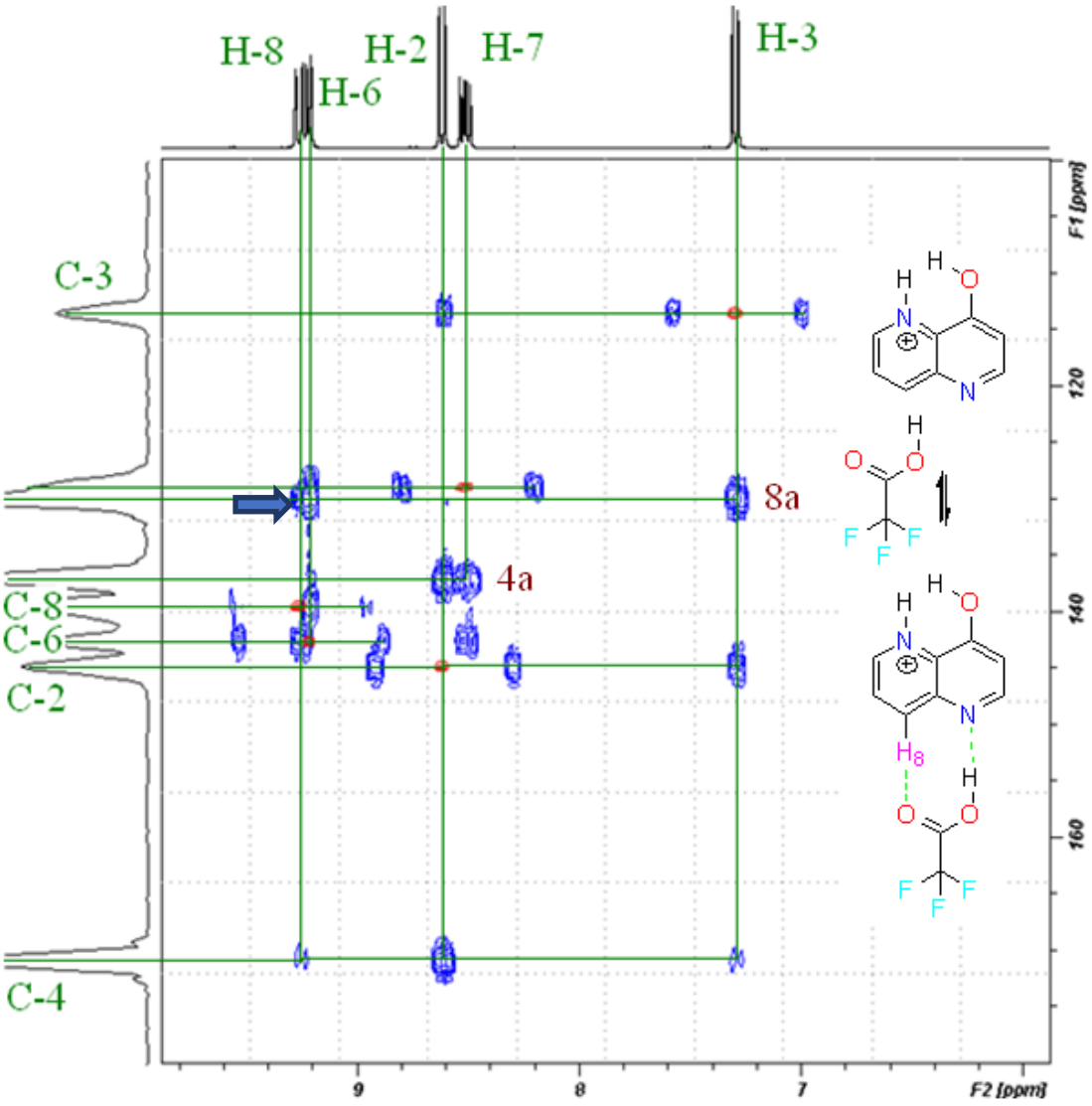

Figure 4.14. Blue projection: ^{1}H-^{13}C HMBC NMR spectrum of pure 1,5-naphthyridin-4(1H)-one in a) TFA-*d*; (66) b) Red projection: ^{1}H-^{13}C HMQC spectrum. A reliable cross peak can be seen between the H8 and C8. Consequently, the remaining quaternary is assigned as C4.

4.3.2. Mechanism of 1,5-naphthyridine Formation.

Direct one step production of naphthyridin-4-ols from malonate esters is unprecedented. One pot synthesis of naphthyridine-4-ols has previously been possible only when using flash vacuum thermolysis of Meldrum's acid derivatives and is almost unknown in solution (Chandrasekhar *et al.*, **2002**; Czuba, **1979**; Hermecz *et al.*, **1992**; Litvinov *et al.*, **2000**; Litvinov *et al.*, **2006**; McNab, **2005**; Milata *et al.*, **2001**; Noravyan *et al.*, **1985**) a notable exception being work reported by (Morgentin *et al.*, **2008**).

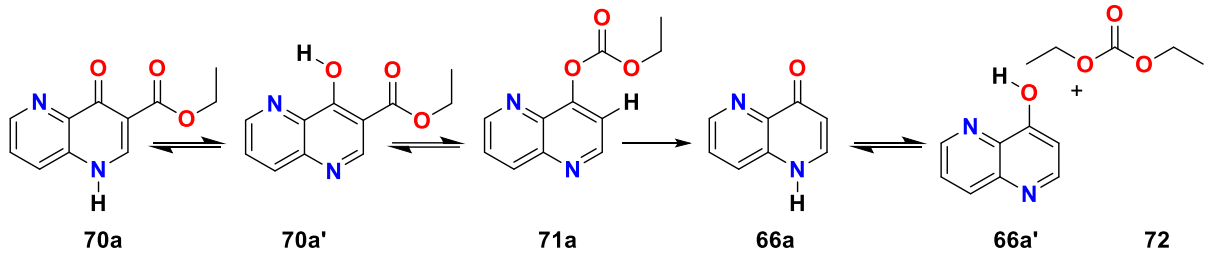

Figure 4.15. Possible mechanism of Retro-Fries reaction of ethyl 4-hydroxy-1,5-naphthyridine-3-carboxylate to ethyl 1,5-naphthyridin-4-yl carbonate (**71a**), which thermally ethanolyses to 1,5-naphthyridin-4-ol (**66a'**), diethyl carbonate (**72**).

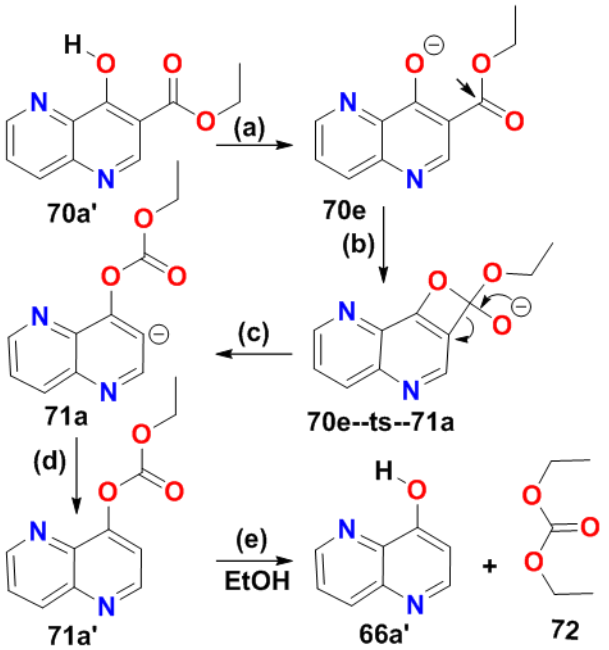

Figure 4.16. Scheme 45. Mechanism of retro-Fries reaction of ethyl 4-hydroxy-1,5-naphthyridine-3- carboxylate(**70a'**) to form 1,5-naphthyridin-4-ol and diethyl carbonate (**70e**): 3-(ethoxycarbonyl)-1,5-naphthyridin-4-olate; (**70e**--ts --**71a**): 2-ethoxy-2H-oxeto[3,2-c][1,5]naphthyridin-2-olate.

Spontaneous de-esterification and decarboxylation has never been reported during the Gould-Jacobs reaction. However, during the modified Niementowski type condensation of 3-aminopicolinic acid with excess ethylacetoacetate, 2-methyl-1,5-naphthyridine-4-(1H)-one was produced serendipitously in 11% isolated yield (Figure 4.3, **66**c), although this event was not satisfactorily explained (Baumgarten *et al.*, **1966**) (Figure 4.15).

It is, however, conceivable that both this study and that of Baumgarten (Baumgarten *et al.*, **1966**) generate naphthyridines through a two-step process, as the absence of either significant quantities of water to initiate hydrolysis or the isolation of the intermediate carboxylic acid (Figure 4.4,**70c**) suggests that the products arise through other means.

Analysis suggested formation of a novel retro-Fries product (Effenberger *et al.*, **1973**; Jackson *et al.*, **1990**).

Equilibrium occurs between ethyl 4-hydroxy-1,5-naphthyridine-3-carboxylate **70a'** which deprotonates to **70e**, then cyclizes to give **71a**, which re-protonates and solvolyses to 1,5-naphthyridin-4-ol **66a'** and diethyl carbonate **72** (Figure 4.16).

A possible mechanism could involve autocatalysed deprotonation to establish a retro-Fries equilibrium reaction (Figure 4.16); this was investigated by computational methods using Gaussian 03 (Frisch *et al.*, **2004**). The transition state **70e**-ts--**71a** was located from a quadratic synchronous transit (QST2) calculation involving **70a** and **71a**. The C1-C2 open bond has a length of 2.121Å (Figure 4.16).

Intrinsic reaction coordinate (IRC) calculations (Gonzalez *et al.*, **1989**) were then carried out on **70e**--ts--**71a**- and these confirmed that the structure was a transition state between **70e** and **71a** (Figure 4.15). At one point on the energy curve, the O2-C1 bond length increased and the C1-C2 bond length shortened to form a distorted four-membered ring, but this did not prove to be a stationary state. Crossover experiments under focused microwave irradiation (Ismail & Kirabo-Wamimbi., **1993**) confirm that the reaction proceeds through this novel concerted, autocatalysed and reversible inter-molecular retro-Fries reaction (Effenberger *et al.*, **1973**; Jackson *et al.*, **1990**).

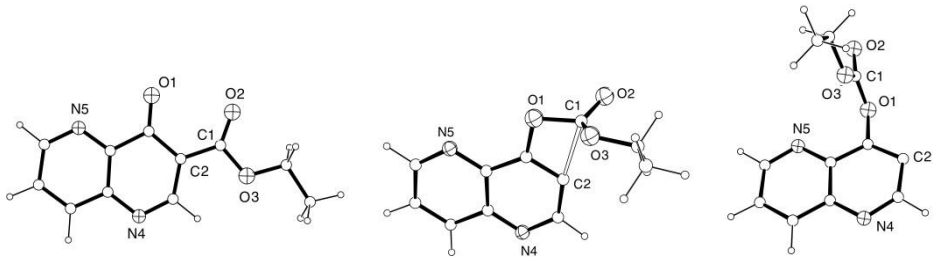

70a- 70a--ts -71a-. 71a-

Figure 4.17. Conversion of the anion **70a**- to **71a**- via the transition state **70a**--ts –**71a**-. Relative energies kcal.mol^{-1}. **70a**-: 0.00; **70a**--ts -**71a**-: 57.28 and **71a**-: 51.31.

Calculations involving the reaction of **71a** (Figure 4.17) with EtOH inducing scission of the ester side chain generating **66a'** and **72**, is exothermic with ΔH = -9.49 kcalmol^{-1}, thereby driving the reaction forward (Figure). Further experiments are being conducted both to optimize this one pot reaction of 1,5-naphthyridines using focused microwaves, and to define the mechanistic pathways (involving classic Gould-Jacobs pathways) using a combination of kinetic, spectroscopic, computational methods and fluorescence in the Solid State (Ismail *et al.*, **2004**)(DFT Calculations are Courtesy of Prof Drew, Reading University) (Figure 4.17).

4.4. Antimalarial Activity *in-vitro*.

SN 13,639, **66**, has been previously evaluated for antimalarial activity *in-vivo* against two avian models of malaria (Wiselogle *et al.,* **1946**). The published data claims that it is perhaps twice as effective as quinine against *P. gallinaceum* in chicks or *P. lophurae* in ducks (Wiselogle, *et al.,* **1946**).

In the present study, the antimalarial activity of **66a**, produced by the rapid process detailed here, was measured against synchronized human *P. falciparum* strain K1 parasites *in -vitro* (Cheng, **1974**). Activity against the human *P. falciparum* K1 clone was EC_{50} = 320 μM compared with chloroquine EC_{50} = 0.23 μM. The related *de-aza* compound 8-hydroxquinoline (oxine) has interesting antibacterial activity, whose mechanism of action involves chelating metal ions such as iron (Chobot *et al*., **2011**). This transition metal is present in parasites during erythrocyte invasion but the exact concentrations are a measure of debate (Allen *et al.,* **1963**). Egan *et al* have speciated the total elemental iron content of unparasitized red cells, parasitized red cells, isolated trophozoites, food vacuoles and haemozoin and have shown that the vacuole contains the majority of iron deposited as haemozoin and the amount entering the so-called haem 'pool of iron' is less than previously thought (Drew *et al.,* **2005**; Egan *et al.,* **2002**). Consequently, one explanation for poor activity of this naphthyridine is the concentration of free iron within parasites is indeed negligible but haem's availability explains the activity of artemisinin and related compounds (Drew *et al.,* **2004**; Drew *et al.,* **2005**; Drew *et al.,* **2007**)

By contrast with the structure of SN 13,639, **66**, which has low antimalarial activity, SN 12,017 (**1c**) contains the side chain present in chloroquine and is claimed to be approximately equipotent with quinine against avian malaria (Wiselogle *et al.,* **1946**). SN 12,017 (**1c**) with its pentanediamine side chain is also reported (Wiselogle *et al.,* **1946**) to be less toxic to the host than **66a**, which is consistent with previous suggestions that *aza*-substitution at the 5-positon of quinolines increases the therapeutic index (Dascombe *et al*., **2005**). When the mass spectrum of the naphthyridine was examined, it clearly binds with haem but additional evidence shows that the haemozoin formed during the process had additional and unexpected species present.

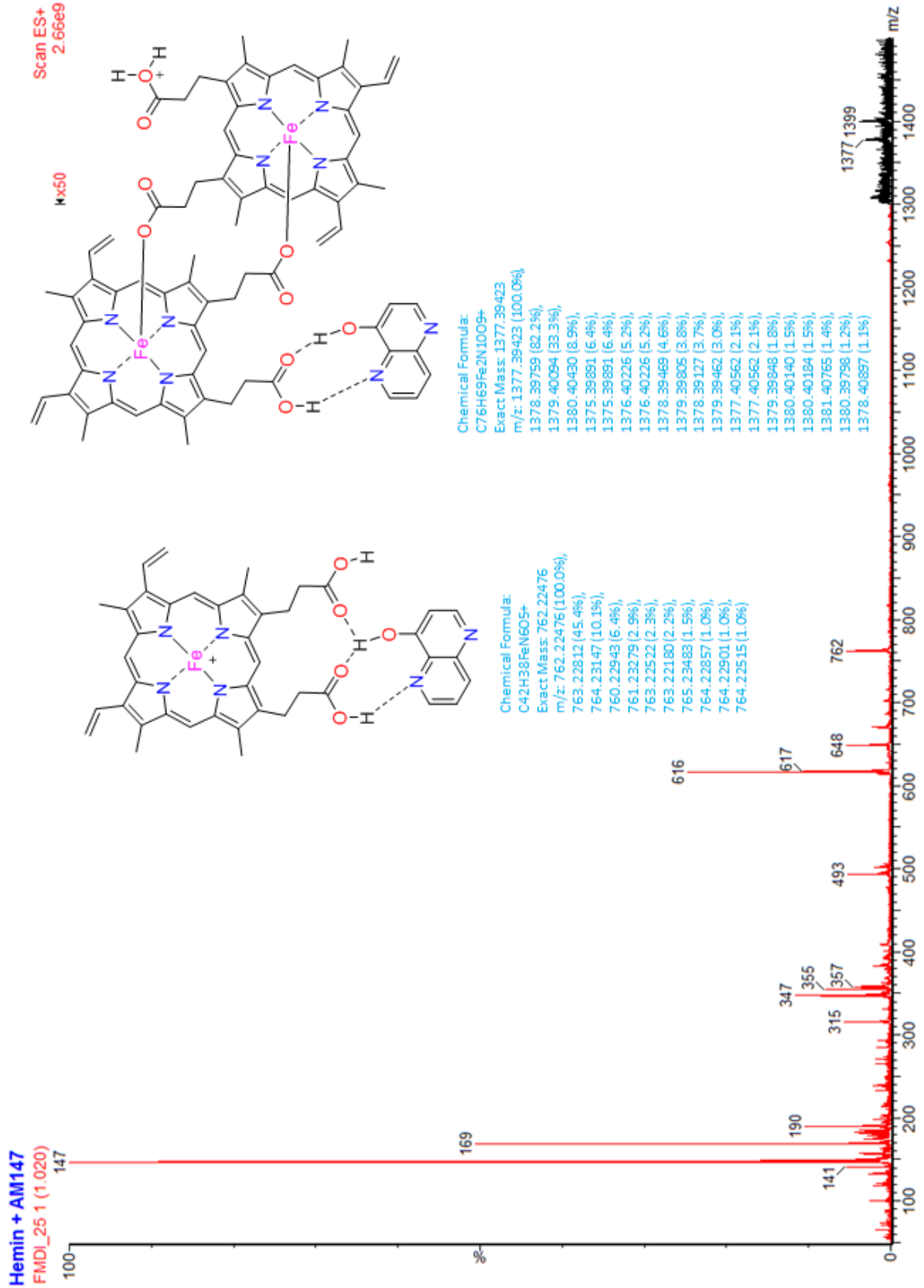

Figure 4.18. Mass spectrum of the naphthyridine, it clearly binds with haem but also points to haemozoin presence.

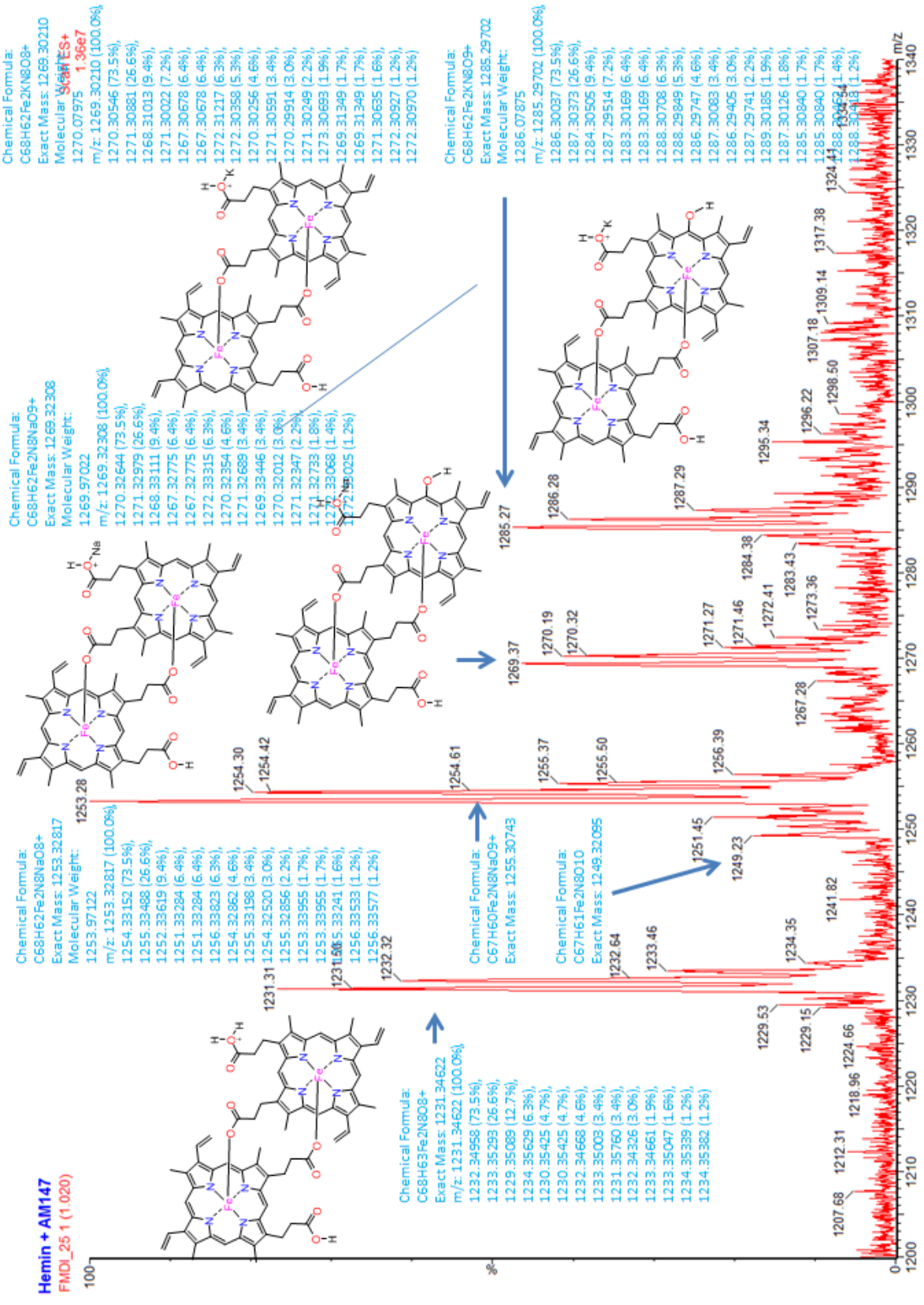

Figure 4.19. Mass spectrum of haem and haem binding.

Haemozoin can protonate either at a suitable heteroatom (of undefined position) or attack a vinyl group to form a stable secondary carbocation. Sodiation or potassiation is also seen, in the presence of 4-hydoroxy-1,5-naphthyridine (Figure 4.19), with sodiated species also forming the corresponding mesohydroxylated haemozoin (i.e. oxophlorins or α-hydroxyhaem) analogues akin to the known biochemical degradation pathways for the formation of α-verdohaem which can undergo ring scission to form the corresponding α-vilverdin haemozoin analogue. A review detailing how haem oxygenase catalyzes the three step-wise oxidation of hemin to α-biliverdin, via α-*meso*-hydroxyhemin, verdohaem, and ferric iron–biliverdin complex has been published (Yoshida & Migita, **2000**). An active species of oxygen i.e. Fe-OOH, which self-hydroxylates haem to form α-*meso*-hydroxyhemin is considered the critical step. Consequently, it is suggested by us that the peak seen at 648 Da previously ascribed to a methanol adduct of protonated haem (Pashynska *et al*., **2004**) could also be the isobaric species described in the formation of oxophlorins published (Yoshida & Migita, **2000**). The various reduction and oxidation steps are summarised.

The significance of detecting compounds in which the primary reciprocal sub-unit of haemozoin being oxidised (in the presence of antimalarial drugs) and releasing some free iron (Egan *et al*., **2002**). It may also provide an additional source of free radical stress to the parasite since the decomposition pathway can proceed to demetallation to α-bilverdin and then α-bilirubin haemozoin analogues (Yoshida & Migita, **2000**). To our knowledge, destabilising the principal redox inert storage form of iron within parasites i.e. haemozoin, has not previously been suggested as a mechanism of (additional) drug action. How much such species contribute to the overall mechanism of action of quinoline-drugs remains unknown and will be the subject of future investigations.

In conclusion, this study reports a cheap, efficient, reliable and simple synthetic method allowing for the rapid production of extremely pure 1,5-naphthyridin-4-ol in a one-pot retro-Fries method. The compound also exhibits complexation behaviour with TFA which is indicative of interactions occurring with compounds of biological importance. The intrinsic florescence of 1,5-naphthyridin-4-ol may be a useful probe for monitoring intracellular concentrations of metals within cells. Our study provides a reliable and convenient method of producing naphthyridines which will make additional compounds available for further pharmacological testing. For instance, this method could accelerate access of key intermediates for producing novel azalogues of important *mono*quinolines such as chloroquine (SN 7,618) (**1b**) and *bis*quinolines such as *meta*-quine, which efficiently interact with haem (Dascombe *et al*., **2005**; Ismail *et al*., **1999**) (Figure 4.20).

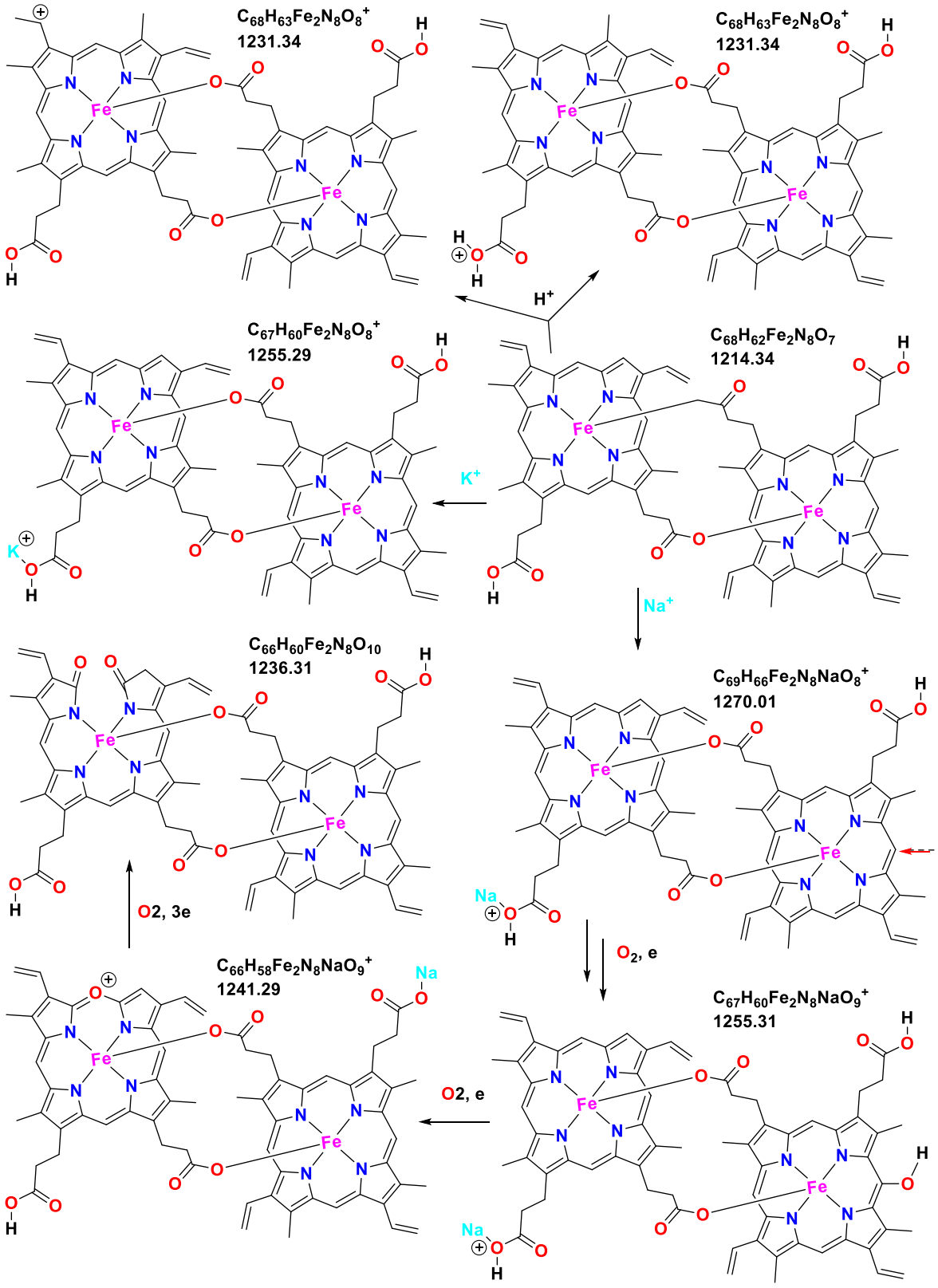

Figure 4.20. Haemozoin protonating either at a suitable heteroatom [of undefined position] or attacking a vinyl group, forming a stable secondary carbocation. Sodiation or potassiation is also seen, in the presence of 4-hydoroxy-1,5-naphthyridine, with sodiated species also forming the corresponding mesohydroxylated haemozoin (i.e. oxophlorins or α-hydroxyhaem) (Yoshida & Migita, 2000**).**

4.4.1. Synthesis.

Diethyl ethoxymethylenemalonate (EMME or diethyl 2-(ethoxymethylene)malonate) and diphenyl ether, Dowtherm A™ were all purchased from the Aldrich Chemical Co. 3-Amino pyridine was recrystallized from a benzene-ligroine mixture according to the procedure of Allen & Wolf (Allen, **1963**)(m.p. 63-64°C). EMME was vacuum distilled immediately before use and stored under dry argon. 4-Hydroxy-l,5-naphthyridine was prepared by modifying the procedures of Adams (Adams *et al.,* **1946**; Eck *et al.,***1966)**.

We concur with the observations of (Eck *et al.,* **1966**) in that price and roberts (Moh *et al.,* **1999**) provided insufficient detail for their synthesis to be followed and that the method of Adams *et al*. **1946**, gave low yields of 4-hydroxy naphtyridine. Contamination with Dowtherm A™ was monitored using the procedure outlined below (Drummond *et al.,* **1989**) using NMR.

Crude (Z)-diethyl 2-((pyridin-3-ylimino)methyl)malonate (aka ethyl-β-(3-pyridylamino)-α-carbethoxyacrylate (10.413g) (Eck *et al.,***1966)** was heated in ethyl acetate/hexane (1:1); 250 ml was heated to 60°C, cooled and filtered to remove brown impurities as well as unreacted 3-aminopyridine. The solution was filtered through a pad of silica, and the colourless material was evaporated at reduced pressure, then suspended in diphenyl ether (500ml) to and made alkaline (pH 12) with 2M aqueous ammonia. Whilst stirring magnetically, the suspension was heated to 245-250°C under a slow stream of argon for 95 minutes until ethanol ceased to evolve using downward distillation (Figure 4.5); higher temperatures were avoided as they could cause solvent ignition and risk of fire. After completion of the reaction, a crude sample was withdrawn, filtered at 70°C and directly analysed by NMR in DMSO-d_6 (Figure 4.21). In some experiments using an upright reflux condenser, a thin stream of water was maintained in the double surface water condenser to trap the sublimate. If the flow rate of water through the condenser is high, it can cause the condenser to crack. The sublimate was removed from the condenser and analysed for impurities using HPLC (Vogel *et al.,* **1989**). After allowing the product to cool to 70°C with stirring, the reaction mixture was diluted with ligroine or petroleum ether (40-60°C), inducing an ultra-fine brown precipitate of the naphthyridine esters. The product could be separated by ultra-centrifugation at 17,700 x g (JA-10 rotor @ 10,000 rpm; Avanti® J-HC High-Capacity Centrifuge) or slowly filtered at the pump (12 hrs) using a copper jacketed funnel held at 60°C. It was necessary to use a glass filter paper, which had to be replaced periodically (Buchner, Whatman® Glass Microfiber GS Filter Paper, Grade GF/A 1.6μm). Combined brown solids, which when washed with ligroine (2 L), produced a light tan amorphous powder (17-54%). Ligroine could be replaced with ethylacetate hexane (1:1); one litre and the solution filtered at 70°C (Figure 4.21).

A second step involving filtration of material through a pad of silica removed residual yellow impurities producing an almost colourless solution. Subsequent filtration of solution through a pad of silica shows retention of remaining impurities on the base line. The clear filtrate appears pure (99%) by HPLC.

The solid product was washed with chloroform (3 x 125 ml) to yield a grey product. This was analysed by NMR, Electron Ionisation-MS and Positive-Ion High Resolution ElectroSpray-MS (PIHRESMS) and found to be a mixture of 1,5 and 1,7-naphthyridine esters **70**a/**70**b (80:20) by integration of the peaks (Figure 4.21).

Figure 4.21. Filtration of crude (Z)-diethyl 2-((pyridin-3-ylimino)methyl)malonate (aka ethyl-β-(3-pyridylamino)-α-carbethoxyacrylate suspended in n-hexane/ethyl acetate removes most coloured material (see brown disc in upper right of picture).

4.4.2. Fries-Equilibrium Experiments.

Purified **70a** (100 mg) was suspended in diphenyl ether (3 ml) or Dowtherm A™ (3 ml) and irradiated using a focused microwave robot (CEM Corporation) programmed to conduct a series of runs between 180-270°C and 25 and 250 Watts. In a second set of experiments, 0.25 ml anhydrous ethanol was added under argon to each tube and the experiments repeated. The irradiated reaction was automatically cooled using compressed air, filtered at the pump, washed with acetone, dried under vacuum and analysed by ^{1}H NMR and PIHRESMS (Positive ion high-resolution electrospray mass spectrometry). NMR spectra are provided.

4.4.3. Spectroscopic data.

All spectral shifts are relative to added tetramethylsilane unless indicated otherwise; ^{1}H NMR 250.134 MHz; ^{13}C NMR 62.896 MHz; 297 K. Common contaminants in crude preparations: diphenyl ether (non-first order distorted spectrum) ^{1}H NMR 250.132 MHz (CF_3CO_2-D).

4.4.3.1. 43. 3-(pyridylamino-methylene)malonic acid diethyl ester, Compound **65a**.

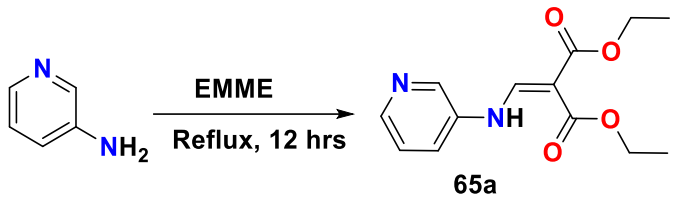

Figure 4.22. Scheme 46. condensation reaction, EMME, reflux.

Reaction procedure in page 178, under synthesis (Figure 4.22). This reaction was repeated several times. **65**(i) and **65**(ii) are two examples. Compound **65a**(i): 3-(pyridylamino-methylene) malonic acid diethyl ester, m.p. 70°C; EI-MS (70eV; source temp = 260 °C: 264 (55%), $M^{+\cdot}$ = $C_{13}H_{16}N_2O_4$+.; 218 (100%), $C_{11}H_{10}N_2O_3^{+\cdot}$; 162 (88%); 145 (75%); 78 (43%); 29 (46%).

^{1}H NMR 250 MHz (DMSO-*d*$_6$): 10.70 (IH, NH, d, 13.8 Hz; D_2O exchangeable), 8.67 (1H, d, 2.57 Hz), 13.76 (1H, d, 8.40 Hz), 8.36 (1H, d, 1.07 Hz), 7.85 (1H, ddd, 1.3, 2.8, 8.4 Hz), 7.43 (1H, d, 8.33 Hz), 7.41 (1H, d, 8.32 Hz), 4.14 (4H, septet (2 overlapped quartets), 7.08 Hz), 1.27 (2 overlapped triplets, 7.08 Hz).

^{13}C NMR (DMSO-*d*$_6$): 167.05 (4°C); 164.79 (4°C), 151.08 (CH), 145.38 (CH), 140.21 (CH), 136.25 (4°C), 124.53 (CH); 124.01 (CH), 94.63 (4°C), 59.70 (CH_2), 59.532 (CH_2), 14.1 (CH_3); 14.13 (CH_3).

Compound **65a**(ii), ($CDCl_3$): ^{1}H NMR 250.133 MHz ($CDCl_3$): 11.05 (IH, NH, d, 13.8 Hz; D_2O exchangeable), 8.67 (1H, d, 2.57 Hz), 13.76 (1H, d, 8.40 Hz), 8.36 (1H, d, 1.07 Hz), 7.85 (1H, ddd, 1.3, 2.8, 8.4 Hz), 7.43 (1H, d, 8.33 Hz), 7.41 (1H, d, 8.32 Hz), 4.14 (4H, septet (2 overlapped quartets); 4.14 Hz), 1.27 (2 overlapped triplets).

Compound **65a**(ii), ^{13}C NMR ($CDCl_3$): 168.85 (4°C), 165.32 (4°C), 151.38 (CH), 145.96 (CH), 139.79 (CH), 135.92 (4°C), 124.22 (CH), 123.58 (CH), 94.44 (4°C), 60.65 (CH_2), 60.32 (CH_2), 14.39 (CH_3), 14.26 (CH_3).

4.4.3.2. 44. Mixture of compounds **70a**, **70b** and **70e**.

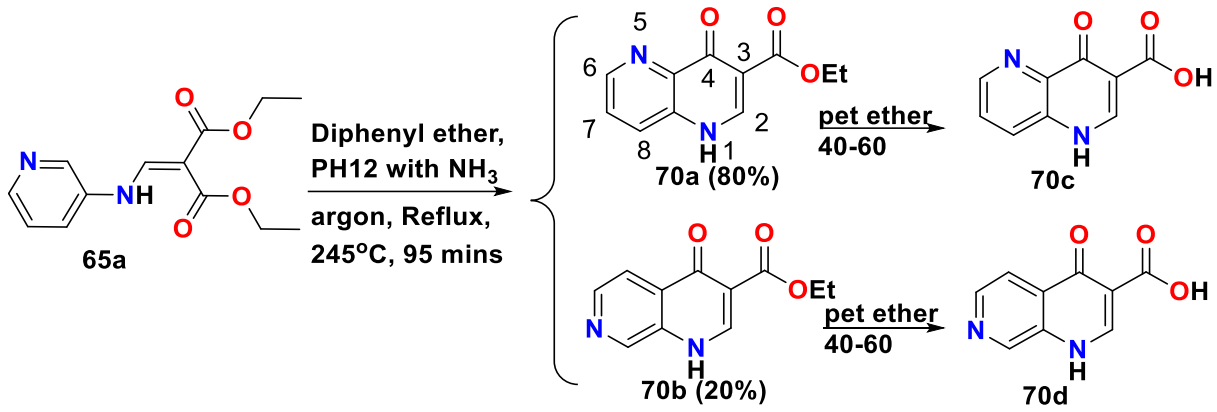

Figure 4.23. Scheme 47. Niementowski type cyclisation, diphenyl ether, NH_3, reflux.

Reaction procedure in page 178, under synthesis. This reaction was repeated several times. Isomers were seen. Reaction 1; mixture: ethyl 4-oxo-1,4-dihydro-1,5-naphthyridine-3-carboxylate(**70a**)/ ethyl 4-hydroxy-1,5-naphthyridine-3-carboxylate(**70e**); light tan solid 81% 1,5naphthyridine; 19% 1,7 naphthyridine by relative integration of methylene protons (Figure 4.23). Major isomer, ^{1}H NMR 250 MHz (TFA-*d*) 1.55 (3H, CH_3, t, 7.14 Hz (average)); 4.65 (2H, CH_2, q 7.14 Hz (average)); 8.55(1H, apparent dd, 5.35, 8.70 Hz); 9.24-9.33 (2H, m [2 overlapped doublets]); 9.39 (IH, H2, s); 250.134 MHz (TFA-*d*/D_2O) 1.52 (3H, CH_3, t, 7.05 Hz (average)); 4.60 (2H, CH_2, q 7.05 Hz); 8.52(1H, dd, 5.35, 8.70 Hz); 9.18 (8.88 Hz); 9.25(5.75 Hz); H-6/H-8; 9.34 (1H, H2, s); note H-5 intensity diminished due to exchange after 9 days at room temp. m.p. 270°C; EI-MS (70eV; source temp = 250 °C) 218 (29%), $M^{+\cdot}$ = $C_{11}H_9N_2O_3^{+\cdot}$; 173 (57%) [$M^{+\cdot}$ - OEt]; 172 (40%); 146 (100%), 173 - [HCN]; 145 (9%) $M^{+\cdot}$ – [.CO2Et]; 144 (8%) 172-CO; 117 (14%); 90 (11%).; c.f. reaction 2 [comments from MJF].

^{13}C NMR 62.896 Hz (TFA-*d*) reaction 1: 1,5-naphthyridine isomer: 11.44 (CH_3), 66.31 (CH_2), 116.02 (4°C), 132.36 (CH), 134.50 (4°C), 139.59 (CH), 141.55 (CH), 146.00 (CH), 151.20(CH), 167.18 (4°C), 171.25 (4°C). However, in reaction 1#1, peak seen at 174.56; 1,7 naphthyridine isomer: 14.34 (CH_3), 67.88 (CH_2), 113.16 (4°C), 125.78 (CH), 133.44 (4°C), 138.29 (4°C), 144.02 (CH), 154.39 (CH), 168.62 (4°C), 174.65 (4°C). Missing from DEPT 111.05 [present in ^{13}C spectrum; see reaction 2#2 DEPT; however, in reaction 1#1, peak seen at 174.563, absent at 111.05; comments from MJF]

4.4.3.3. 45. Reaction 1#1: 1,5-naphthyridin-4-ol: Compound **66**. (NMR in TFA)

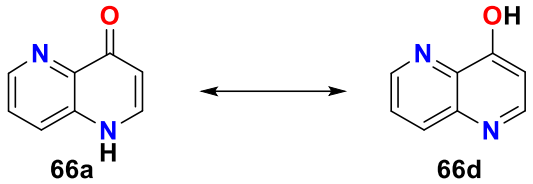

Figure 4.24. Keto-enol:1,5-naphthyridin-4(1H)-one (**66a**) 1,5-naphthyridin-4-ol (**66d**).

^{1}H NMR 250 MHz (DMSO-d_6): 3.35 (1H, OH), 7.10 (1H, d, 7.42 Hz), 7.14 (1H, apparent t, overlapped dd, 7.40, 7.40 Hz), 7.35-7.43 (2H, apparent triplet, tending towards non first order behaviour: 8.42 Hz, 9.99Hz). ^{13}C NMR 75 Hz (TFA-*d*) DEPTQ expt; 115.92 (4°C), 131.34 (CH), 132.35 (4°C), 139.57 (4°C), 141.93 (CH), 144.97 (CH), 147.26 (CH), 173.21 (4°C).

EI-MS (70eV; source temp = 250°C) M+. = $C_8H_6N_2O^{+\cdot}$= 146 (100%), 118 (60%); 91 (18%), 64 (12%), 47 (10%), 52 (9%), 63 (8%), 78 (6%). m.p. sublimation 332-335°C

4.4.3.4. 46. Reaction 1#2: 1,5-naphthyridin-4-ol: **66**. (NMR in DMSO-d_6)

1,5-naphthyridin-4-ol: **66**: ^{1}H NMR 250 MHz (TFA-d_6) 7.32 (1H, d, 7.75 Hz), 8.53 (1H, dd, 5.30, 8.88 Hz), 8.64 (1H, d, 7.10 Hz), 9.23 (1H, d, 5.58 Hz), 9.28 (1H, d, 8.88 Hz).

^{1}H NMR 250 MHz (DMSO-d_6): 3.35 (1H, OH), 7.10 (1H, d, 7.42 Hz), 7.14 (1H, apparent t, overlapped dd, 7.40, 7.40 Hz), 7.35-7.43 (2H, apparent triplet, tending towards non first order behaviour: 8.42 Hz, 9.99Hz).

^{13}C NMR 75 Hz (DMSO-d_6): 1,5-naphthyridine isomer: 176.31 (4°C), 145.95 (CH), 140.71 (4°C), 138.95 (CH), 136.84 (4°C), 127.06 (CH), 126.14 (CH).

EI-MS (70eV; source temp = 250°C) M+. = $C_8H_6N_2O^{+\cdot}$ = 146 (100%), 118 (60%), 91 (18%), 64 (12%), 47 (10%), 52 (9%), 63 (8%), 78 (6%) m.p. sublimation 332-335°C, lit: 340°C [10a]. 1,5-naphthyridin-4(1H)-one tautomer: **66a/66b**,

4.4.3.5. 47. Reaction 2: 1,5-naphthyridin-4-ol: Compound **66**.

Reaction 2#2 1,5-naphthyridin-4-ol: 250 MHz (TFA-d_6): 7.32 (1H, d, 7.75 Hz), 8.53 (1H, dd, 5.30, 8.88 Hz), 8.64 (1H, d, 7.10 Hz), 9.23 (1H, d, 5.58 Hz), 9.28 (1H, d, 8.88 Hz).

^{1}H NMR dilute solution: 250 MHz (DMSO-d_6) 3.35 (1H, OH), 7.10 (1H, d, 7.42 Hz),

7.14 (1H, apparent triplet, overlapped dd, 7.40, 7.40 Hz), 7.35-7.43 (2H, apparent triplet, tending towards non first order behaviour: 8.42 Hz, 9.99Hz).

^{13}C NMR 75 Hz (TFA-*d*) Reaction 2#3 APT: 111.91 (CH), 126.14 (CH), 127.06 (CH), 136.84 (4°C), 138.95 (CH), 140.71 (4°C), 145.95 (CH), 176.31 (4°C).

1,5-naphthyridin-4-ol: Reaction 2#3: 300 MHz (TFA-*d*): 7.32 (1H, d, 7.75 Hz), 8.53 (1H, dd, 5.30, 8.88 Hz), 8.64 (1H, d, 7.10 Hz), 9.23 (1H, d, 5.58 Hz), 9.28 (1H, d, 8.88 Hz), [present in ^{13}C spectrum; see reaction 2#2 DEPT; however, in reaction 1#1, peak seen at 174.56, absent at 111.05. [comments from MJF]

4.4.4. Crystal data.

Crystals were grown by refluxing 1.00 g of the 4-hydroxy,1-5-napthyridine in methanol and leaving to cool in a tube for two years by which time crystals had been deposited on the sides of the vessel. Crystal Data, 1, $C_8H_6N_2O$, M = 146.15, monoclinic, space group P21/n, Z = 4, a = 3.7776(6), b = 15.018(2), c = 11.495(2) Å, β = 97.213(16)o, U = 646.98(18)Å3, dcalc = 1.500 gcm-3. Independent reflection data were collected with MoKα radiation at 110K using the Oxford Diffraction XCalibur CCD System to be 1401. The crystal was positioned at 50 mm from the CCD. 321 frames were measured with a counting time of 10s. Data analysis was carried out with the CrysAlis program (CrysAlis, **2006**). The structure was solved using direct methods with the Shelxs97 program (Sheldrick, **2008**) The non-hydrogen atoms were refined with anisotropic thermal parameters. The hydrogen atoms bonded to carbon and nitrogen were included in geometric positions and given thermal parameters equivalent to 1.2 times those of the atom to which they were attached. The structure was refined on F2 to R1 0.0903; wR2 0.2269 for 1094 data with I>2σ(I). Details have been deposited at the Cambridge Crystallographic Data Centre (CCDC) number: 864110 (Courtesy of Prof Drew, Reading University).

4.4.5. Analytical methods.

FT-IR spectra were acquired with a Mattson Galaxy FT-IR 5000; 1 % compound KBr mixture was compressed into discs under pressure. Electron Ionisation mass spectra were determined using a VG Analytical (Floats Road, Altrincham, Manchester, UK) 70–250 MS, with a DEC PDP 11/24 data system, at 70eV and a source temperature of ~200°C; trap current 200 μAmps). Samples were admitted by a direct insertion probe heated to 250–300°C. Positive ion high resolution electrospray mass spectrometry (PIHRESMS) was conducted by direct infusion of the sample (20 µlmin-1) into a Micromass LCT orthogonal acceleration

time of flight (TOF) mass spectrometer (Waters, Micromass U.K. Ltd. Manchester UK). High resolution measurements were made (at a resolving power of ~ 10,000) using a Lockmass accessory with Leucine enkapholin reference. LC-MS analysis used a Waters Alliance 2695 separations module coupled to the Micromass LCT in ESI positive mode and Waters 486 UV detector at 246 nm. LCT calibration was performed using NaICsI solution. Leu-Enk 1 ngml-1 post column split for 0.2 mlmin-1 flow was 5:1 UV:LCT. The HPLC method used a C18 XBridge analytical column (2.1 x 50 mm, 3.5 μm particle size); column temperature 25°C, flow rate 0.2 mlmin-1; initial mobile phase 98% A (A: 0.1 % formic acid): 2% B (B: 0.1% formic acid in methanol). The final composition of 50% A: 50% B was attained using a linear gradient over a 10-minute analysis period. Operational settings for the LCT were: capillary voltage: 3000 V, sample cone voltage; 30 V, RF lens: 250 V, acceleration voltage: 200 V, desolvation temperature: 200°C, source temperature: 100°C, cone gas flow: 22 l/h and desolvation gas flow: 750 l/h.

4.5. Conclusion.

4-Hydroxy-1,5-naphthyridine (SN 13,639) was unambiguously characterised by X-ray crystallography and 2D-NMR and confirmed that tautomeric equilibrium favoured the 1,5-naphthyridin-4(1H)-one form both in the solid state and in solution (DMSO-d_6). The compound allows rapid, green, access to various naphthyridines, which are more active, and could act as fluorescent probes of drug action.

The unusual shifts of the proton spectrum upon dissolution in acid offer a simple model for interactions between haem and the drug. We have established the preferred site of protonation in the naphthyridines and validated them with the shifts seen in both ^{13}C and ^{1}H NMR and using predictions from DFT calculations, we speculate the nature of site of protonation. These observations are consistent with previous predictions generated from DFT calculations.

Calculating these torsion angles (dihedral angle) and vicinal hydrogen bonding (J3 couplings) enables us to use Karplus equation to find correlation between constituent atoms and bonds.

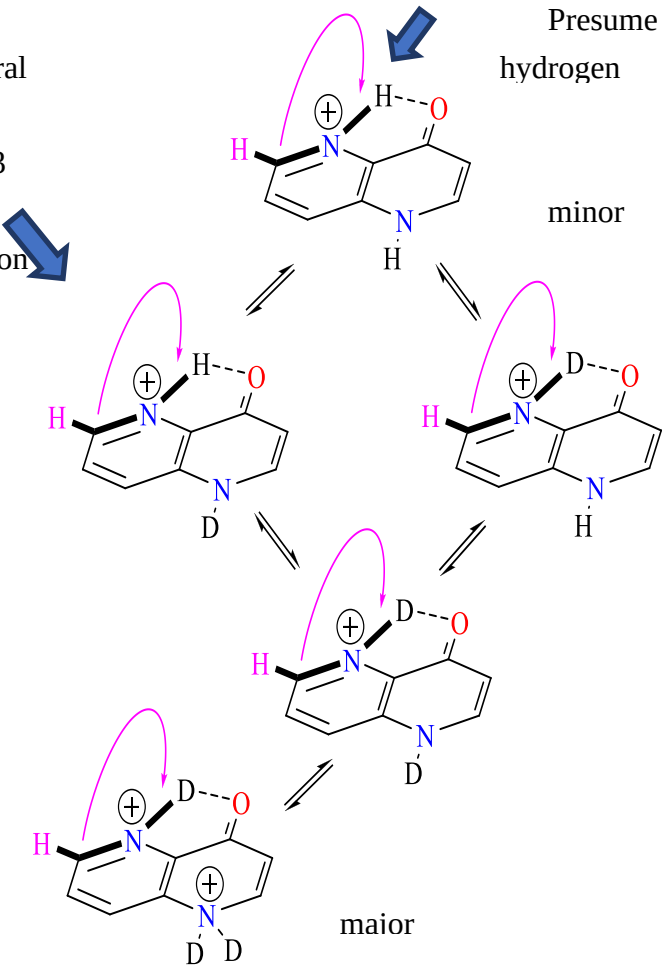

Figure 4.25. Possible Hydrogen bonding sites in 1,5 naphtyridines.

It appears that the 1 ppm shifts for certain protons can be explained by protonation and or deuteration at the 5 and/or 1 positon which will cause a shift in the ^{13}C and ^{1}H NMR peaks

within the spectrum but not necessarily show coupling to vicinal protons unless the small number of protons present exchange with existing deuterons. Absolute conformation will require growth of a suitable crystal and neutron diffraction since protons cannot be detected using X-rays and their positions are inferred. We predict that there may be a charge at the proton at N1.

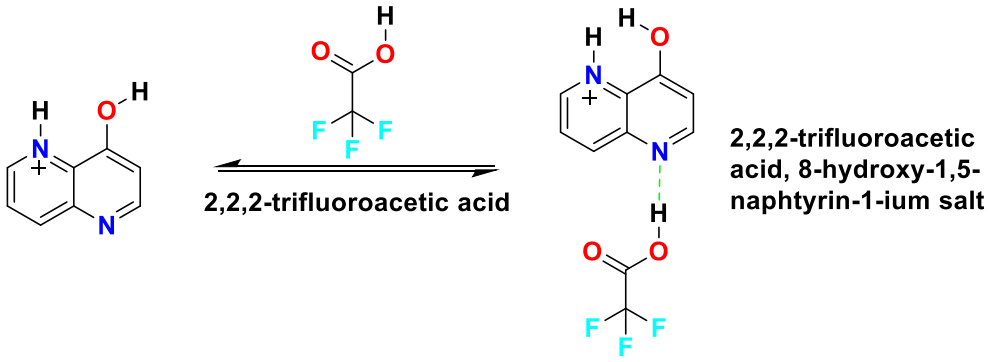

Figure 4.26. 8-hydroxy-1,5-naphthyridin-1-ium (**60**) and 2,2,2-trifluoroacetic acid forming 8-hydroxy-1,5-naphthyridin-1-ium salt (**60c**).

4.6. References.

Acharya, R., Gupta, M., Ramakumar, S., Ramagopal, U. A., Chauhan, V. S. 2007. Observation of glycine zipper and unanticipated occurrence of ambidextrous helices in the crystal structure of a chiral undecapeptide. *BMC Struct Biol*. 7, 51.

Adams, J. T., Bradsher, C. K. 1946. Synthesis of antimalarials; synthesis of certain 1,5- and 1,8-naphthyridine derivatives. *J Am Chem Soc*. 68, 1317-1319.

Albert, A. 1960. 355. Naphthyridines: ionization constants and spectra of four parent substances. *Journal of the Chemical Society (Resumed)*. 1790-1793.

Albert, A., Hampton, A. 1952. Analogues of 8-hydroxyquinoline having additional cyclic nitrogen atoms. Part I. Preparative. *Journal of the Chemical Society (Resumed)*. 4985.

Allen, C. F. 1950. The naphthyridines. *Chem Rev*. 47, 275-305.

Auparakkitanon, S., Chapoomram, S., Kuaha, K., Chirachariyavej, T., Wilairat, P. 2006. Targeting of haematin by the antimalarial pyronaridine. *Antimicrob Agents Chemother*. 50, 2197-2200.

Baker, M. 2016. 1,500 scientists lift the lid on reproducibility. *Nature*. 533, 452–454. https://doi.org/10.1038/533452a

Bailey, D. L., Hercules, D. Eck, T. 1967. Electronic spectra of 4-hydroxy-1,5-naphthyridine. *Analytical Chemistry*. 39, 877-880.

Barlin, G., Tan, W. 1985. Potential Antimalarials. III N 4 -Substituted 7-Bromo-1,5-naphthyridin-4-amines. *Aust. J. Chem*. 38, 459.

Bobranski, B., Sucharda, E. 1927. Uber eine Synthese des 1.5-Naphthyridins. Berichte der deutschen chemischen *Gesellschaft (A and B Series)*. 60, 1081-1084.

Bohn, B., Heinrich, N., Vorbrueggen, H. 1994. Hammick Cyclizations Studies on the Mechanism of the Hammick Reaction. *Heterocycles*. 37, 1731-1746.

Brown, D. J. 2008. The naphthyridines, Hoboken, N.J. *Wiley*.

Casabianca, L. B., De Dios, A. C. 2006. Relationship between NMR shielding and haem binding strength for a series of 7-substituted quinolines. *J Phys Chem* A. 110, 7787-7792.

Chobot, V., Drage, S., Hadacek, F. 2011. *Nat Prod Commun*. 6, 597-602

Chandrasekhar, S., Prasad, A., Eswaraiah, S., Venkateswaralu, A. 2002. Development of an Efficient Process for 4,5,7-Trichloroquinoline, A Key Intermediate for Agrochemical Synthesis. *Organic Process Research & Development*. 6, 242-245.

Cheng, C. C. 1974. Novel common structural feature among several classes of antimalarial agents. *J Pharm Sci*. 63, 307-310.

Czuba, W. 1979. Synthesis and reactions of naphthyridines (review). *Chemistry of Heterocyclic Compounds*. 15, 1-13.

Dascombe, M., Drew, M., Evans, P. Ismail, F. 2007. Rational Design Strategies for the Development of Synthetic Quinoline and Acridine Based Antimalarials. *Frontiers in Drug Design & Discovery*. 3, 559-609.

Dascombe, M. J., Drew, M. G., Morris, H., Wilairat, P., Auparakkitanon, S., Moule, W. A., Alizadeh-Shekalgourabi, S., Evans, P. G., Lloyd, M., Dyas, A. M., Carr, P., Ismail, F. M. 2005. Mapping antimalarial pharmacophores as a useful tool for the rapid

discovery of drugs effective *in-vivo*: design, construction, characterization, and pharmacology of *meta*-quine. *J Med Chem*. 48, 5423-5436.

De Dios, A. C., Casabianca, L. B., Kosar, A., Roepe, P. D. 2004. Structure of the amodiaquine-FPIX mu oxo dimer solution complex at atomic resolution. *Inorg Chem*. 43, 8078-8084.

De Dios, A. C., Tycko, R., Ursos, L., Roepe, P. 2003. NMR Studies of chloroquine-Ferriprotoporphyrin IX Complex. *J. Phys. Chem.* A. 107, 5821-5825.

De Villiers, K. A., Marques, H. M., Egan, T. J. 2008. The crystal structure of halofantrine-ferriprotoporphyrin IX and the mechanism of action of arylmethanol antimalarials. *J Inorg Biochem*. 102, 1660-1667.

Drew, M., Metcalfe, J., Dascombe, M., Ismail, F. 2007. De novo identification and stability of the artemisinin pharmacophore: Studies of the reductive decomposition of deoxyartemisinins and deoxyarteethers and the implications for the mode of antimalarial action. *Journal of Molecular Structure: THEOCHEM*. 823(1-3), 34-36.

Drew, M., Metcalfe, J., Ismail, F. 2005. Antimalarial drugs based on artemisinin: DFT calculations on the principal reactions. *Journal of Molecular Structure: THEOCHEM*. 756, 79-87.

Drew, M. D., Metcalfe, J., Ismail, F. 2004. A DFT study of free radicals formed from artemisinin and related compounds. *Journal of Molecular Structure: THEOCHEM*. 711, 95-105.

Drummond, J., Johnson, G., Nickell, D. G., Ortwine, D. F., Bruns, R. F., Welbaum, B. 1989. Evaluation and synthesis of aminohydroxyisoxazoles and pyrazoles as potential glycine agonists. *J Med Chem*. 32, 2116-2128.

Eck, T., Weary, E., Hercules, D. 1966. Some chelates of 4-hydroxy-1, 5-naphthyridine. *Journal of Inorganic and Nuclear Chemistry*. 28, 2439-2441.

Effenberger, F., Klenk, H., Reiter, P. 1973. New Aspects of the Fries Rearrangement. *Angewandte Chemie International Edition in English*. 12, 775-776.

Egan, T. J. 2006. Interactions of quinoline antimalarials with haematin in solution. *J Inorg Biochem*. 100, 916-926.

Egan, T. J., Chen, J. Y., De Villiers, K. A., Mabotha, T. E., Naidoo, K. J., Ncokazi, K. K., Langford, S. J., Mcnaughton, D., Pandiancherri, S., Wood, B. R. 2006. Haemozoin (beta-haematin) biomineralization occurs by self-assembly near the lipid/water interface. *FEBS Lett*. 580, 5105-5110.

Egan, T. J., Combrinck, J. M., Egan, J., Hearne, G. R., Marques, H. M., Ntenteni, S., Sewell, B. T., Smith, P. J., Taylor, D., Van Schalkwyk, D. A., Walden, J. C. 2002. Fate of haem iron in the malaria parasite *Plasmodium falciparum*. *Biochem J*. 365, 343-347.

Fattorusso, C., Campiani, G., Kukreja, G., Persico, M., Butini, S., Romano, M. P., Altarelli, M., Ros, S., Brindisi, M., Savini, L., Novellino, E., Nacci, V., Fattorusso, E., Parapini, S., Basilico, N., Taramelli, D., Yardley, V., Croft, S., Borriello, M., Gemma, S. 2008. Design, synthesis, and structure-activity relationship studies of 4-quinolinyl- and 9-acrydinylhydrazones as potent antimalarial agents. *J Med Chem*. 51, 1333-1343.

Fibel, L, R., Spoerri, P.E. 1948. The Synthesis and Investigation of Pyridine and Pyrazine Analogs of Salicylates. *J. Am. Chem. Soc.* 70, 11, 3908–3911

Frosch, T., Popp, J. 2010. Structural analysis of the antimalarial drug halofantrine by means

of Raman spectroscopy and density functional theory calculations. *J Biomed Opt*. 15, 041516.

Fu, S., Xiao, S. H. 1991. Pyronaridine: A new antimalarial drug. *Parasitol Today*, 7, 310-313.

Gaussian 2004. Gaussian 03, Wallingford, CT: *Gaussian, Inc*.

Gemma, S., Campiani, G., Butini, S., Kukreja, G., Coccone, S. S., Joshi, B. P., Persico, M., Nacci, V., Fiorini, I., Novellino, E., Fattorusso, E., Taglialatela-Scafati, O., Savini, L., Taramelli, D., Basilico, N., Parapini, S., Morace, G., Yardley, V., Croft, S., Coletta, M., Marini, S. Fattorusso, C. 2008. Clotrimazole scaffold as an innovative pharmacophore towards potent antimalarial agents: design, synthesis, and biological and structure-activity relationship studies. *J Med Chem*. 51, 1278-1294.

Gonzalez, C., Schlegel, H. 1989. An improved algorithm for reaction path following. *The Journal of Chemical Physics*. 90, 2154.

Gonzalez, C., Schlegel, H. 1990. Reaction path following in mass-weighted internal coordinates. *The Journal of Physical Chemistry*. 94, 5523-5527.

Gould, R., Jacobs, W. 1939. The Synthesis of Certain Substituted Quinolines and 5,6-Benzoquinolines. *J. Am. Chem. Soc*. 61, 2890-2895.

Gunther, F. A., Barkley, J. H. 1966. Conversion of a Dohrmann Microcoulometric Gas Chromatograph to a convenient and rapid "total chloride" unit. *Bull Environ Contam Toxicol*. 1, 39-45.

Handbook, D. 1971. Michigan, *Dow Chemical Company*.

Hart, E. P. 1954. Naphthyridines. Part I. The chemistry of 1,5-Naphthyridine. *Journal of the Chemical Society* (*Resumed*). 1879-1882.

Hermecz, I., Kereszturi, G., Vasvari-Debreczy, L. 1992. Aminomethylenemalonates and their use in heterocyclic synthesis, San Diego, *Academic Press*.

Hirai, S., Yamamoto, K., Kikuchi, H., Kim, H. S., Begum, K., Wataya, Y., Tasaka, H., Miyazawa, Y., Oshima, Y. 2003. Metabolites of febrifugine and its synthetic analogue by mouse liver S9 and their antimalarial activity against *Plasmodium* malaria parasite. *J Med Chem*. 46, 4351-4359.

Hoeppli, R. 1959. Parasites and parasitic infections in early medicine and science, Singapore, *University of Malaya Press*.

Ismail, F. A., K.-W., C. 1993. Reaction via autocatalysed and reversible inter-molecular retro-Fries reaction. *UH presentation*.

Ismail, F. M., Dascombe, M. J. 1999. The Rational Design, Synthesis and Pharmacological Evaluation of Novel Metazaquines. *UH conference presentation*.

Ismail, F. M., Dascombe, M. J., Carr, P., Merette, S. A., Rouault, P. 1998. Novel aryl-*bis*quinolines with antimalarial activity in-vivo. *J Pharm Pharmacol*, 50, 483-492.

Ismail, F. M., Dascombe, M. J., Carr, P., North, S. E. 1996. An exploration of the structure-activity relationships of 4-aminoquinolines: novel antimalarials with activity *in-vivo. J Pharm Pharmacol*. 48, 841-850.

Jackson, L., Waring, A. 1990. Reactions of 4-benzoyl-4-methylcyclohexa-2,5-dienone in acids: retro-Fries rearrangements. *J. Chem. Soc., Perkin Trans*. 2, 1893-1898.

Jang, C. S., Fu, F. Y., Wang, C. Y., Huang, K. C., Lu, G., Chou, T. C. 1946. Ch'ang Shan, a Chinese Antimalarial Herb. *Science*. 103, 59.

Jiang, S., Zeng, Q., Gettayacamin, M., Tungtaeng, A., Wannaying, S., Lim, A., Hansukjariya,

P., Okunji, C. O., Zhu, S., Fang, D. 2005. Antimalarial activities and therapeutic properties of febrifugine analogs. *Antimicrob Agents Chemother*. 49, 1169-1176.

Johns, A., Porter, R. 1999. Preparation of naphthyridinylureas and related compounds as orexin A receptor antagonists. *PCT/EP*1999/003100.

Johns, A., Porter, R. A., Chan, W. N., Coulton, S., Hadley, M. S., Widdowson, K., Jerman, J. C., Brough, S. J., Coldwell, M., Smart, D., Jewitt, F., Jeffrey, P., Austin, N. 2001. 1,3-Biarylureas as selective non-peptide antagonists of the orexin-1 receptor. *Bioorg Med Chem Lett. 11*, 1907-1910.

Kikuchi, H., Tasaka, H., Hirai, S., Takaya, Y., Iwabuchi, Y., Ooi, H., Hatakeyama, S., Kim, H. S., Wataya, Y., Oshima, Y. 2002. Potent antimalarial febrifugine analogues against the *Plasmodium* malaria parasite. *J Med Chem*. 45, 2563-2570.

Kurosawa, Y., Dorn, A., Kitsuji-Shirane, M., Shimada, H., Satoh, T., Matile, H., Hofheinz, W., Masciadri, R., Kansy, M., Ridley, R. G. 2000. Haematin polymerization assay as a high-throughput screen for identification of new antimalarial pharmacophores. *Antimicrob Agents Chemother*. 44, 2638-2644.

Leed, A., Dubay, K., Ursos, L. M., Sears, D., De Dios, A. C., Roepe, P. D. 2002. Solution structures of antimalarial drug-haem complexes. *Biochemistry*. 41, 10245-10255.

Liao, S. H., Shiu, J. R., Liu, S. W., Yeh, S. J., Chen, Y. H., Chen, C. T., Chow, T. J. Wu, C. I. 2009. Hydroxynaphthyridine-derived group III metal chelates: wide band gap and deep blue analogues of green Alq3 (tris(8-hydroxyquinolate) aluminum) and their versatile applications for organic light-emitting diodes. *J Am Chem Soc*. 131, 763-777.

Litvinov, V., Roman, S., Dyachenko, V. 2000. Naphthyridines. Structure, Physicochemical Properties, and General Methods of Synthesis. *Russian Chemical Reviews*. 31, 612-614.

Litvinov, V. P. 2006. Advances in the Chemistry of Naphthyridines. *Advances in Heterocyclic Chemistry*. 91, 189–300.

Mcnab, H. 2005. Chemistry Without Reagents: Synthetic Applications of Flash Vacuum Pyrolysis. *ChemInform.* 36(21, 36, 2766-2770.

Milata, V. 2001. Alkoxymethylenemalonates in Organic Synthesis. Aldrichimca Acta. 34, 20-27.

Moh, F. M., Tang, T. S. 1999. Liquid chromatographic detection of Dowtherm A contamination in oleochemicals and edible oils. *J Aoac Int*. 82, 893-896.

Morgentin, R., Pasquet, G., Boutron, P., Jung, F., Lamorlette, M., Maudet, M., Ple, P. 2008. Strategic studies in the syntheses of novel 6,7-substituted quinolones and 7- or 6-substituted 1,6- and 1,7-naphthyridones. *Tetrahedron*. 64, 2772-2782.

Noravyan, A. S., Paronikyan, E. G., Dashyan, S., Dzhagatspanyan, I. A., Paronikyan, R. G., Nazaryan, I. M., Akopyan, A. G. 2015. [Synthesis and Neurotropic Activity of 2,4-pyrano[4',3':4,5]pyrido[2,3-b]thieno[3,2-d] Pyrimidines]. *Bioorg Khim*. 41, 737-743.

O'neill, P. M., Willock, D. J., Hawley, S. R., Bray, P. G., Storr, R. C., Ward, S. A., Park, B. K. 1997. Synthesis, antimalarial activity, and molecular modeling of tebuquine analogues. *J Med Chem*. 40, 437-448.

Pagola, S., Stephens, P. W., Bohle, D. S., Kosar, A. D., Madsen, S. K. 2000. The structure of malaria pigment beta-haematin. *Nature*. 404, 307-310.

Paronikyan, E. G., Dashyan, S., Noravyan, A. S., Dzhagatspanyan, I. A., Paronikyan, R. G., Nazaryan, I. M., Akopyan, A. G. 2015. [Synthesis and Neurotropic Activity of 2,4-pyrano[4',3':4,5]pyrido[2,3-b]thieno[3,2-d] Pyrimidines]. *Bioorg Khim*. 41, 737-743.

Pashynska, V. A., Van Den Heuvel, H., Claeys, M., Kosevich, M. V. 2004. Characterization of noncovalent complexes of antimalarial agents of the artemisinin-type and FE(III)-haem by electrospray mass spectrometry and collisional activation tandem mass spectrometry. *J Am Soc Mass Spectrom*. 15, 1181-1190.

Porter, R. A., Smart, D., Sabido-David, C., Brough, S. J., Johns, A., Jerman, J. C. 2001. SB-334867-A: the first selective orexin-1 receptor antagonist. *British journal of pharmacology*. 132(6), 1179–1182. https://doi.org/10.1038/sj.bjp.0703953.

Price, C. C., Roberts, R. M. 1946. Synthesis of 4-hydroxyquinolines; a modified preparation through bis-(m-chlorophenyl)-formamidine. *J Am Chem Soc*. 68, 1255.

Reitsema, R. H. 1948. The chemistry of 4-hydroxyquinolines. *Chem Rev*. 43, 43-68.

Sheldrick, G. M. 2008. Programs for Crystallographic solution and refinement. *Acta Cryst*. 2008, A64 112. Shelxs97.

Sneader, W. 2005. Drug discovery: a history, Hoboken, N.J., *Wiley*.

Solomonov, I., Osipova, M., Feldman, Y., Baehtz, C., Kjaer, K., Robinson, I. K., Webster, G. T., Mcnaughton, D., Wood, B. R., Weissbuch, I., Leiserowitz, L. 2007. Crystal nucleation, growth, and morphology of the synthetic malaria pigment beta-haematin and the effect thereon by quinoline additives: the malaria pigment as a target of various antimalarial drugs. *J Am Chem Soc*. 129, 2615-2627.

Vippagunta, S. R., Dorn, A., Matile, H., Bhattacharjee, A. K., Karle, J. M., Ellis, W. Y., Ridley, R. G., Vennerstrom, J. L. 1999. Structural specificity of chloroquine (1)-hematin binding related to inhibition of hematin polymerization and parasite growth. *J Med Chem*. 42, 4630-4639.

Vippagunta, S. R., Dorn, A., Ridley, R. G., Vennerstrom, J. L. 2000. Characterization of chloroquine-haematin mu-oxo dimer binding by isothermal titration calorimetry. *Biochim Biophys Acta*. 1475, 133-40.

Vogel, A. I., Furniss, B. S., Vogel, A. I. 1989. Vogel's Textbook of practical organic chemistry, LondonNew York, Longman Scientific & Technical, *Wiley*.

Weiss, M., Elderfield, R. 1967. Naphthyridines, New York, *Wiley*.

Wiselogle, F. Y., National Research Council (U.S.) 1946. A survey of antimalarial drugs, 1941-1945, Ann Arbor, Mich. *Edwards*.

Yoshida, T., Migita, C. T. 2000. Mechanism of haem degradation by haem oxygenase. *J Inorg Biochem*. 82, 33-41.

Zheng, X. Y., Chen, C., Gao, F. H., Zhu, P. E., Guo, H. Z. 1982. [Synthesis of new antimalarial drug pyronaridine and its analogues (author's transl)]. *Yao Xue Xue Bao*. 17, 118-125.

Chapter 5

Pyronaridine.

Index of Contents chapter 5.

Figure of contents chapter 5.

Table of contents chapter 5.

Aim.

Pyronaridine (**15**), a highly efficacious antimalarial compound, first developed in China was notable for its efficacy against multi-drug resistant strains of *plasmodia.* At the time of this Pyronaridine, a highly efficacious antimalarial compound, first developed in China was notable for its efficacy against multi-drug resistant strains of *plasmodia*. At the time our study was initiated, the only synthesis described was in a short communication in Chinese and, consequently, we endeavoured to do structural determination of authentic samples gifted to us from both Professors Wallace Peters and David Warhurst (London School of Hygiene and Tropical medicine).

Again, it has been stated that only around 30% of literature experiments can be replicated (Baker, **2016**). This chapter details our efforts in synthesising pyronaridine (**15**) and improves upon the brief details in the literature and provides 2-D NMR spectra for the first time. In addition, the behaviour of pyronaridine was studied using NMR and High-resolution Electrospray Mass spectrometry and it was found that our synthesis replicated exactly the known compound in terms of spectroscopy, spectrometry and HPLC retention times.

There is a chance of protonation between a hydrogen and a strong electronegative element like nitrogen or oxygen and pyronaridine is abundant in these elements (Figure 5.1).

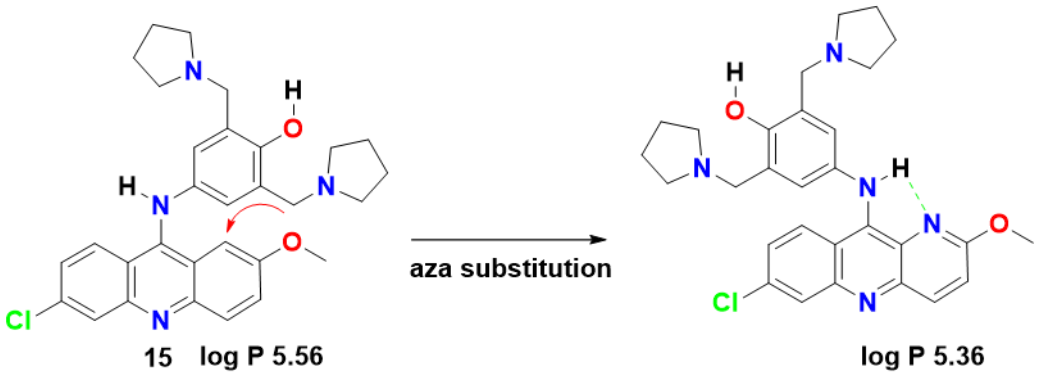

Figure 5.1. *Aza* isosteric substitution generates a hydrogen bond that then rotates the side chain.

5.1. Introduction.

Pyronaridine (PND) (**15**), a benzonaphthyridine derivative, was synthesised and suggested as a novel therapy for the treatment of malaria in **1970**s (Babalola *et al.*, **2003**). It is chemically similar to azacrine (Figure 5.4, **79**) (Park *et al.*, **2007**). Pyronaridine (**15**) has recently attracted much interest as a potential treatment in preventing SARS CoV2 infection in mice (Puhl *et al*., **2022**) and could have potential as a cheap treatment in man (if shown successful in randomised clinical trials). The anticancer potential of this compound has attracted renewed interest in cancer chemotherapy since it induces apoptosis in non-small cell lung cancer cells by upregulating Death Receptor 5 (DR5) expression and inhibiting epidermal growth factor receptor (Puhl *et al*., **2022**, Dai *et al*., **2018**, **2020**).

Pyronaridine-artesunate was put on clinical trial (Dabira *et al*., **2022**), and dihydroartemisinin-piperaquine combined with single low-dose primaquine (**6**) has been shown to prevent *Plasmodium falciparum* malaria transmission (Stone *et al*., **2022**).

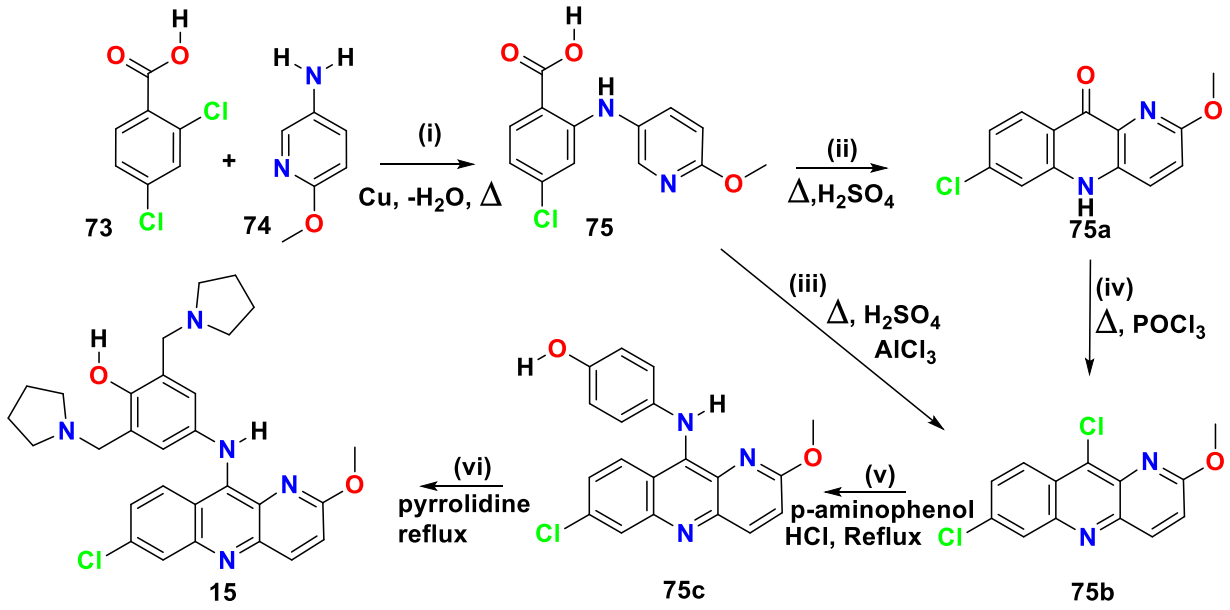

Figure 5.2. A preview of Pyronaridine (**15**) Synthesis discussed in this chapter.

Bulky cycloalkyl groups were placed around the phenolic moiety of amodiaquine (**9**) and replaced the chloroquine heterocycle frame with 7-chloro-2-methoxybenzo[*b*][1,5] naphthyridine group to produce PND (Zheng *et al.*, **1990**) (Figure 5.2). It is a blood schizontocidal agent with high efficacy against multi-drug resistant *P.falacipram* and *P.vivax* (Chang *et al.*, **1992**; Warsame *et al.*, **1991**). The triple combination of PND, sulfadoxine and pyrimethamine are used to treat chloroquine–resistant *falciparum*. This combination may reduce development of resistance to PND which now possesses high clinical efficacy and low

toxicity (Chang *et al.,* **1992**; Croft *et al.,* **2012**). Investigators had reported that PND acted similarly to chloroquine-*in-vitro* by targeting haematin formation (Auparakkitanon *et al.,* **2006**).

The Cl atom in pyronaridine (**15**) has been suggested to be beneficial in inhibiting *β*-haematin (Auparakkitanon *et al.,* **2006**). In contrast, Ismail *et al* have suggested, it acts as a "halogen block" to depress xenobiotic metabolism (Ismail *et al.,* **2001**, **2009**). Early studies reported that pyronaridine targeted the erythrocytic stages, specifically the food vacuole, of the parasite (Croft *et al.,* **2012**).

5.2. Synthesis of pyronaridine.

The first attempted preparation of 6-chloro-9-hydroxy-pyrido[3,2-*b*]quinoline (7,10-dichloro-benzo[*b*][1,5] naphthyridine)(**15**) was from 4-chloro-2-(3-pyridylamino)benzoic acid (**75)**, which in turn was prepared using an Ullmann coupling of 3-aminopyridine and 2,4-dichlorobenzoic acid (Price and Roberts, **1946**). 7-chlorobenzo[b][1,5]naphthyridin-10-ol was produced by sulphuric acid catalysed cyclisation. However, it could not be converted to the desired 10-halo compound **75f** and produced a tar. Hence, the synthesis of (±)N^3-(7-Chloro-benzo[*b*][1,5]naphthyridin-10-yl)-N^1,N^1-diethyl-butane-1,3-diamine (**76**) did not proceed due to the tarry substance. The strategy was the preparation of analogues of mepacrine (**78**) in which one of the benzene rings was replaced by a pyridine ring (Figure 5.3).

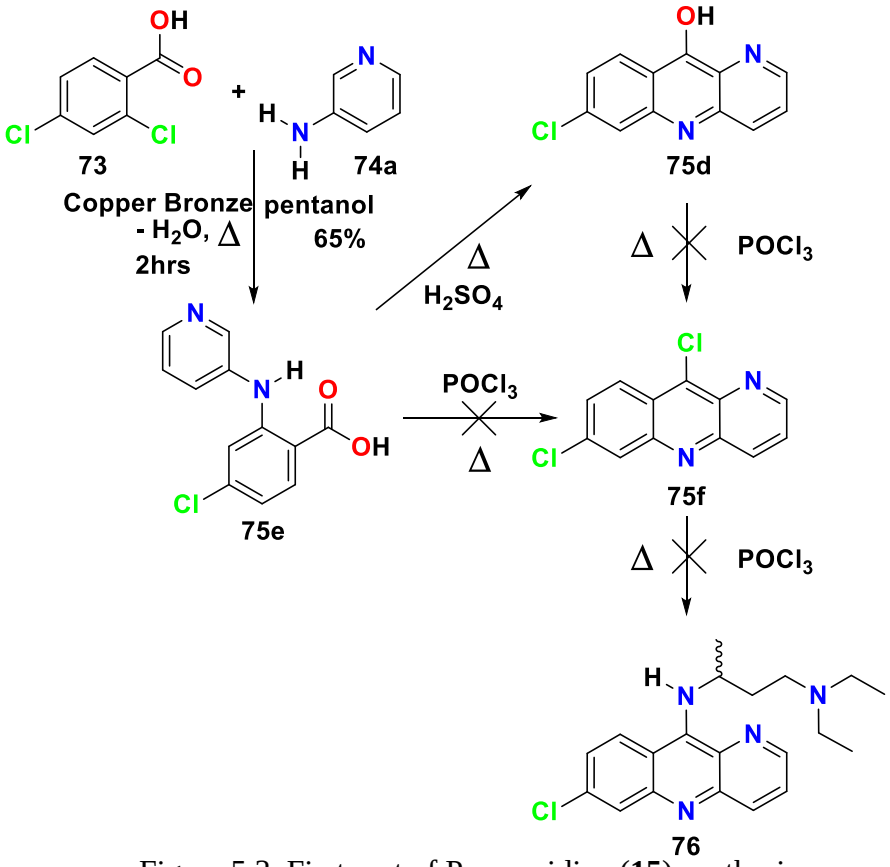

Figure 5.3. First part of Pyronaridine (**15**) synthesis.

The drug design processes that have led to the development of pyronaridine: 4-((7-chloro-2-methoxybenzo[b][1,5]naphthyridin-10-yl)amino)-2,6-bis(pyrrolidin-1-ylmethyl)phenol (**15**) can be traced back to some of the original hypotheses concerning the action of both 8-aminoquinoline and 4-aminoquinoline antimalarials.

One of the earliest design strategies led to the synthesis of 2-alkoxy-6-chloro-9-dialkylamino-1: 10-diaza-anthracenes structurally related to mepacrine (**78**) (N^4-(6-chloro-2-methoxy-acridin-9-yl)-N^1, N^1-diethyl-pentane-1,4-diamine) namely azacrine (**79**) (±) (N^4-(7-chloro-2-methoxy-benzo [*b*][1,5] naphthyridin-10-yl)-N^1, N^1-diethyl-pentane-1, 4-diamine).

Besly and Goldberg (**1954**) reasoned that the dialkylamino side chain was positioned *peri* to a ring nitrogen atom (see dotted red line, figure 5.4), as in pamaquine.

Superimposition of this common N^1, N^1-diethylpentane-1,4-diamine side chain onto compounds such as mepacrine (N^4-(6-chloro-2-methoxy-acridin-9-yl)-N^1, N^1-diethyl-pentane-1,4-diamine) (**78**) suggests that benzo [*b*][1,5]naphthyridines, such as azacrine (**79**), might possess both the schizonticidal activity of (**78**) (Bonse *et al.*, **1999**) as well as curative properties of pamaquine (**77**)(Besly and Goldberg, **1954**).

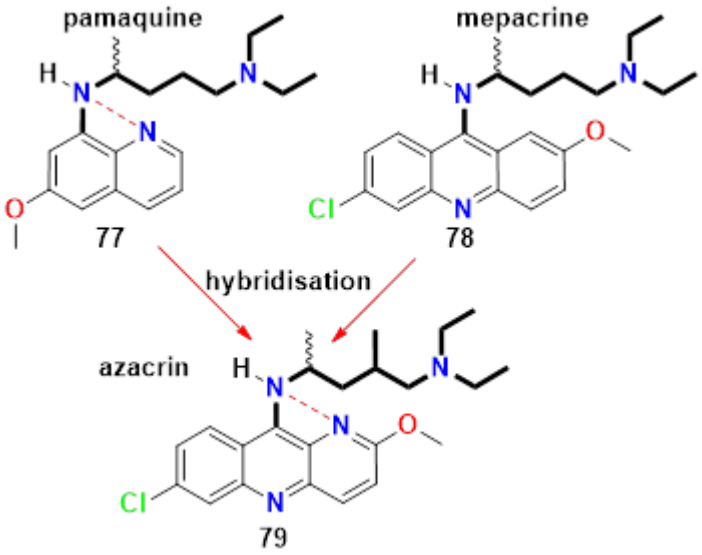

Figure 5.4. Drug hybridisation strategy.

It should, however, be noted that this compound (**79**) (Figure 5.4)had already been prepared independently by Takahashi (1945), using an Ullmann-Goldberg reaction as the key step. (Takahashi, **1945**, Chemical Abstracts, **1951**). Conversion of 4-chloro-2-((2-methoxypyridin-4-yl)amino)benzoic acid (77) using one equivalent of PCl_5 leads to 4-chloro-2-((2-methoxypyridin-4-yl)amino)benzoyl chloride and the $AlCl_3$ ensures completion of cyclisation to **75b**.

The successful patenting of azacrine (**79**) (Figure 5.4) by the Goldberg group (Ward *et al.*, **1956**), did not lead to widespread clinical use. Presumably due to its high cost of

production and lack of compelling advantage over chloroquine and amodiaquine (**9**) that had already become well established in the marketplace. Although it failed to show superior curative properties. Azacrine (**79**) (Figure 5.4) was claimed to be an effective schizonticide against human malaria caused by *P. falciparum*.

Also, shorter pyrexia and parasite clearance times as well as allowing fewer relapses than mepacrine (Besly and Goldberg, **1954**) (Figure 5.5) led Peters and Robinson (**1992**) to reinvestigate azacrine against drug resistant *Plasmodia in-vivo*.

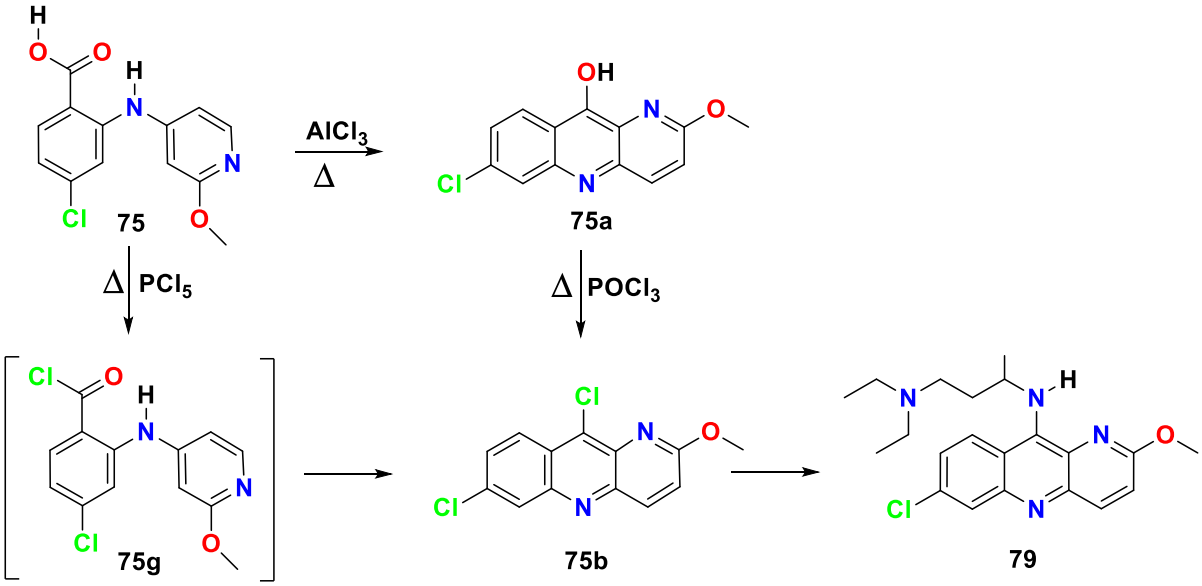

Figure 5.5. Azacrine synthesis overview (Besly and Goldberg, 1954).

To our knowledge, azacrine has not been evaluated against drug resistant malarias *in-vitro* unlike pyronaridine (Alin *et al.*, **1990**; Basco *et al.*, **1992**, **1994**; Childs *et al.*, **1988**; Elueze *et al.*, **1996**; Fu *et al.*, **1986**; Pradines *et al.*, **1998**; Ringwald *et al.*, **1996**). Its activity against *Plasmodial* topoisomerases was promising and could be used in future antimalarials design to target parasite DNA topoisomerase II (Auparakkitanon *et al.*, **2000**).

5.2.1. Origin of aromatic side chain or "head group".

Chemical evolution of the drug prototype amodiaquine (4-(7-chloro-2,3-dihydro-quinolin-4-ylamino)-2-diethylaminomethyl-phenol) highlighted the importance of an aromatic side group with a Mannich side chain (Rusco *et al.*, **1998**). Although 4-(7-chloro-2,3-dihydroquinolin-4-ylamino)-2,6-*bis*-diethylaminomethyl-phenol (7**9**) was a known compound, it did not replace chloroquine which, before the advent of resistance to this, had spearheaded the fight against malaria. It should also be noted that amodiaquine (**9**) had not previously produced liver failure or agranulocytosis when administered for short term

treatment of malaria, but was finally withdrawn because of these adverse effects when used prophylactically. As early as **1962**, Chinese research groups had synthesised a compound (which they named M6407, (**82**)) with (supposedly) metabolically inert pyrrolidine side chains namely; 4-(7-chloro-2,3-dihydro-quinolin-4-ylamino)-2,6-*bis*-pyrrolidin-1-ylmethyl-phenol (Zheng *et al.*, **1982**). In practice, many thousands of compounds were screened and rejected in the murine model of malaria *in-vivo*, until a final selection of compounds with a favourable toxicological and pharmacological profile, such as amopyraquine (**80**) and (**82**) were identified (Ismail *et al.*, **1996**).

These pyrrolidine rings resist successive *N*-dealkylation to eventually produce e.g. 2,6-*bis*-aminomethyl-4-(7-chloro-2-methoxy-benzo[*b*][1,5]naphthyridin-10-ylamino)-phenol, a process implicated in promoting drug resistance in *Plasmodia* by the corresponding Mannich base quinolines. Overall, this approach could be described as an "iterative bioassay guided drug hybridisation strategy" (Figure 5.6).

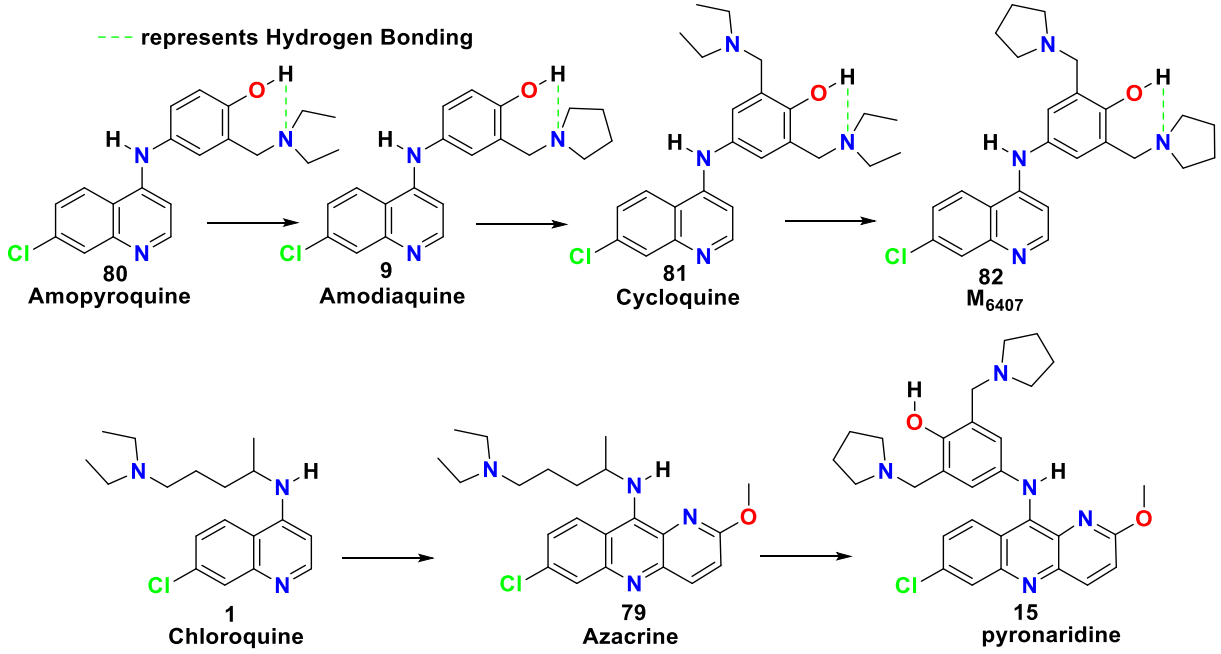

Figure 5.6. Amodiaquine evolution to pyronaridine. Drug hybridisation strategy leading to (M6407) (This is the Chinese designation of compound **15**). Chloroquine and azacrine leading to pyronaridine.

The drug metabolism-pharmacokinetic (DM-PK) profile of pyronaridine has been comprehensively investigated *in-vivo* whereas, to our knowledge, there has been only one detailed study exploring xenobiotic metabolism *in-vitro*, detecting pyronaridine quinone imine as major product (Lee *et al.*, **2004**).

Electrospray mass spectrometry proved vital in determining the identity of metabolites both *in-vitro* and *in-vivo*. The elimination half-life of pyronaridine in *Oryctolagus cuniculus* (European rabbit; 55 ± 5 hrs) was similar to that in malaria patients (*Homo sapiens*; 63 ± 5 hours), Feng *et al* (**1987**), which led (Ruscoe *et al.*, **1998**) to incorrectly suggest that

pyronaridine exhibited little metabolism and the long half-life was due to drug accumulation. Lee *et al* (**2004**) using nominal positive ion electrospray mass spectrometry showed that the pyrrolidinone side chains are metabolised (See figure 5.7). Potential toxicity ascribed to quinone-imine formation (similar to that seen for amodiaquine) was predicted since it was found in a metabolic study *in-vitro*; even though the drug has not been widely used prophylactically, Ismail *et al.,* (**2009**) urged caution since pulsed radiolysis showed the formation of potential toxic quinone imines. PK studies of pyronaridine in mouse (Zeng *et al.,* **2009**), rabbit (Feng *et al.,* **1986**) and humans (Feng *et al.,* **1987**, Wattanavijitkul, **2010**) were performed using microdosing studies.

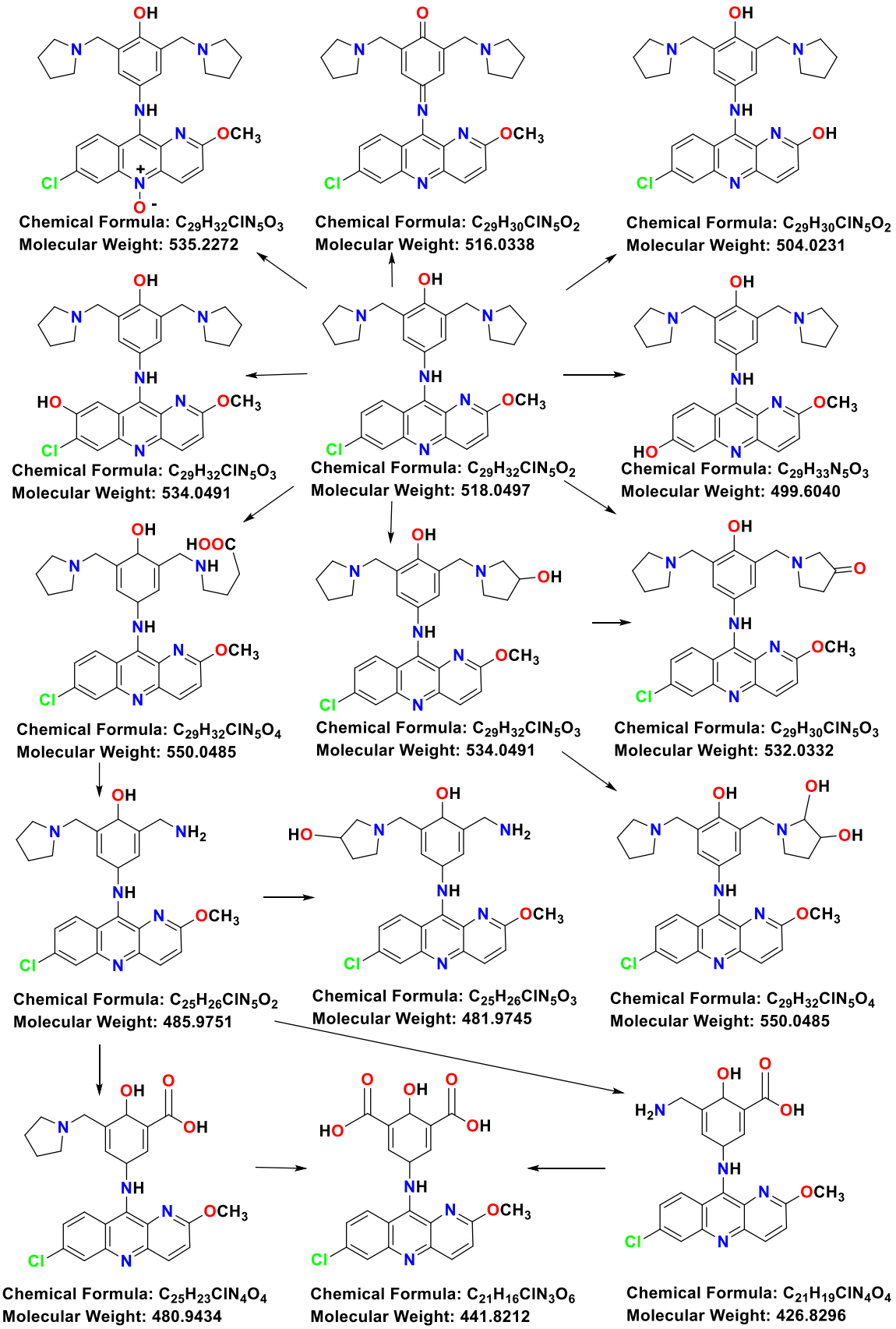

Figure 5.7. Reproduced from "An investigation/prediction of the metabolism of pyronaridine (**15**) and its analogues"; M. Pharm thesis, Liverpool john moores university, Hieu Truong Van, 2012 with permission.(the MWTs refer to structures deduced using CID-MS^n studies See: Lee *et al*., 2004).

Note that in this compound class (Pyronaridine (**15**) and its analogues) (Figure 5.7), the hydroxyl group can form an internal hydrogen bond with an adjacent pyrrolidine group and, since (H1) a sixth centre associates with itself, it can be considered an example of Newman's rule of six (Ingold, **1953**).

Supporting evidence from several molecular modelling studies, using Macromodel (Amber and MM2 forcefields) and DFT, suggests that those phenolic compounds with an *ortho* amino methylene group will form a hydrogen bond (Ismail *et al.*, **1992**; Gwizdek, **1997**) existing in low energy conformers (Figure 5.8).

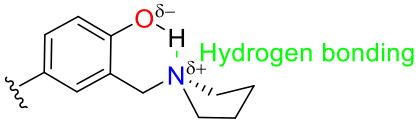

Figure 5.8. Internal hydrogen bonding showing Newman's rule of six.

The aromatic side chain has also been incorporated into changrolin (**82**), an anti-arrhythmic agent derived from febrifugine (**82A**) (Figure 5.9), an antimalarial natural product, isolated from Dichroa febrifuga (Chen *et al*., **2010**).

Subsequently, a series of investigations produced the antiarrhythmic agent (ACC-9358) (**84**) (Figure 5.9) which incorporated this as a fragment but was withdrawn from clinical trials due to side effects (Chorvat *et al.*, **1993**).

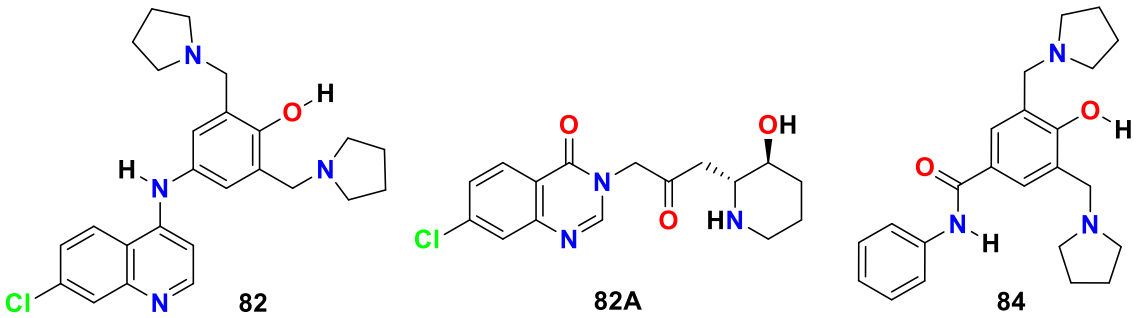

Figure 5.9. M6407 (**82**), febrifugine (**82A**) and ACC-9358 (**84**).

Interestingly, (Kotecka *et al*., **1997**) have suggested that the original lead compound for Pyronaridine, **(15)**, possesses a better profile than chloroquine in the Samiri monkey model of malaria (Huang *et al*., **1979**).

Huang *et al* had shown that M6407 (Figure 5.10) possessed both lower toxicity and greater potency against *Plasmodium berghei* in mice when compared to chloroquine. They compared the antimalarial activity of twelve new quinoline di-Mannich base compounds containing the 7-chloro- or 7-trifluoromethyl substituent in various naphthyridine and quinoline nuclei with amodiaquine (**9**), chloroquine (**1**), and pyronaridine (**15**) *ex-vivo*

(Huang *et al*., **1979**).

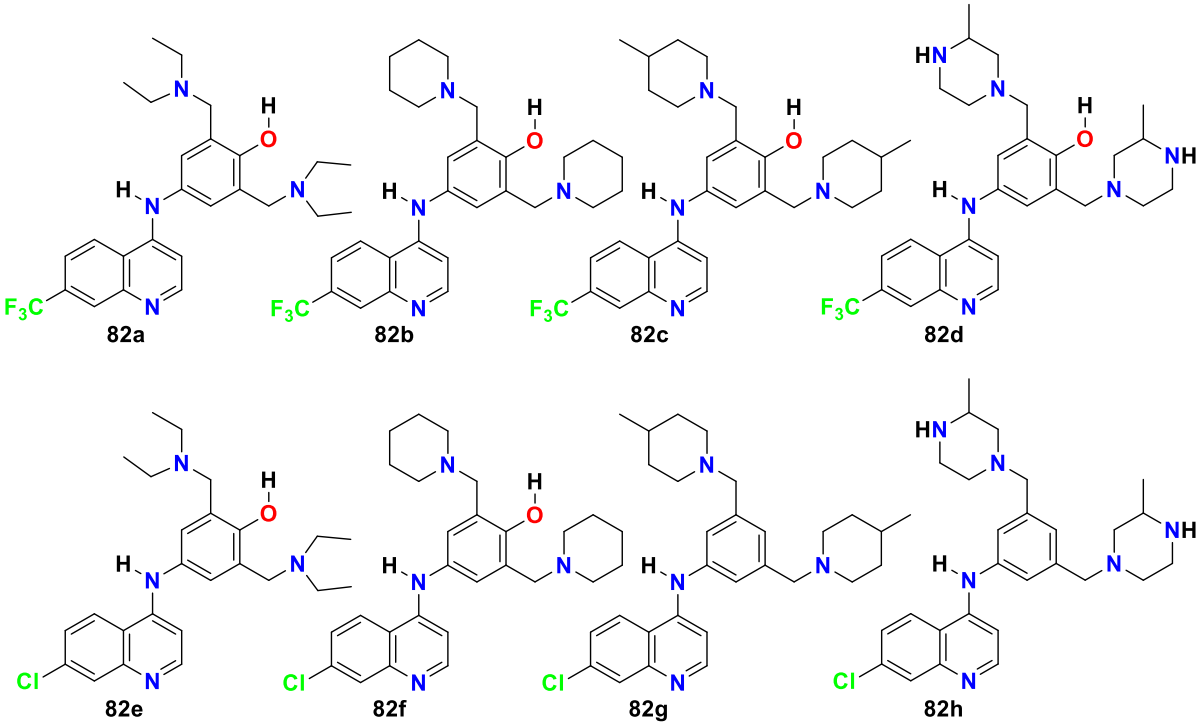

Figure 5.10. Adapted from: Kotecka *et al* (1997). Experimental antimalarial quinolone *di*-mannich bases. Based on variations of M6407 (**82**).

Each compound was administered orally (30 mg/kg of body weight) to three or more non-infected *Samiri sciureus* monkeys, and serum samples were collected at various times after drug administration and serially diluted with drug-free (control) serum.

Antimalarial activity against the multi-drug-resistant *K1* isolate of *Plasmodium falciparum* was determined in serum samples by measuring the maximum inhibitory dilution at which the treated monkey serum inhibited schizont maturation *in-vitro*. Of the twelve Mannich bases tested, eight were associated with levels of *ex vivo* antimalarial activity in serum greater than those of amodiaquine, chloroquine, or pyronaridine 1 to 7 days after drug administration. Nevertheless, these new compounds although patented (Barlin and Tan, **1986**) have not progressed to clinical use. Pyronaridine, in contrast, has been approved for human use (Croft *et al.*, **2012**), after Phase II and III clinical trials in Africa (Ringwald *et al.*, **1996**). The principal variation in the 7-chloro-benzo[*b*][1,5]naphthyridin-10-yl)-hydroxy-aryl-amine series has been the position of the hydroxyl group in the aryl side chain and, to a greater extent, the amine employed in the Mannich base (Zheng *et al.*, **1982**). But, since the IC_{50} values either *in-vitro* or *in-vivo* remain unpublished, it is not possible to construct any structure activity relationship nor perform receptor modelling.

5.2.2. Chemical reactions leading to the construction of pyronaridine.

The synthesis of pyronaridine can be disconnected into several known reaction types,

which are:

a) Ullmann Goldberg coupling whereby the copper mediated formation of an C-N bond produces a 4-chloro-2-(methoxy-3-pyridylamino)benzoic acid (Besly & Goldberg, **1954**) (Figure 5.11).
b) Lesnianski showed concurrent dehydration resulting in cyclisation and elimination of the hydroxyl group by a chlorine group by the action of $POCl_3$ to provide 7,10-di-chloro-2-methoxy-benzo[*b*][1,5]naphthyridine (Besly & Goldberg, **1954**; Magidson and Grigorovsky, **1933**, Ward *et al.*, **1956**).
c) S_NAr displacement of the 10-chloro substituent with fresh *p*-aminophenol yields 4-(7-chloro-2-methoxy-benzo[*b*][1,5]naphthyridin-10-ylamino)-phenol (Zheng *et al.*, **1982**).
d) Exposure to Mannich base conditions using pyrrolidine and aqueous formaldehyde produces pyronaridine (Zheng *et al.*, **1982**).

Each of these synthetic steps will be briefly reviewed so that the experimental findings can be placed in proper context.

5.2.3. Jourdan-Ullmann-Goldberg synthesis.

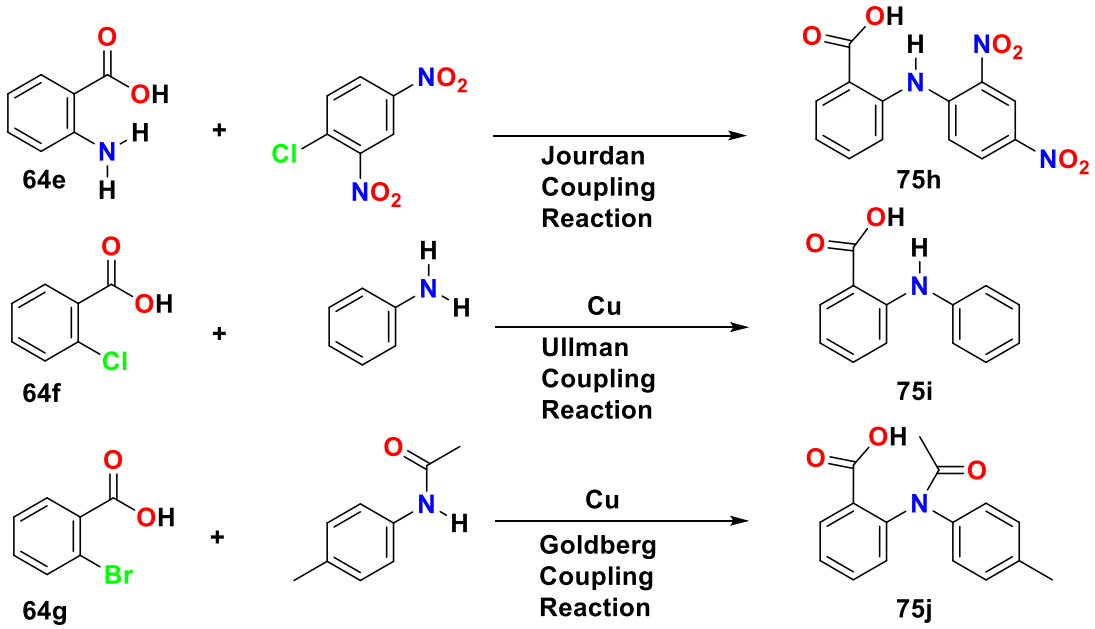

Figure 5.11. Comparison of Jourdan, Ullmann and Goldberg reactions.

These reactions involve the formation of *N*-phenylanthranilic acid derivatives. Activated halides, such as 2,4-dinitrochlorobenzene, undergo coupling without catalyst, a reaction first described by Friedrich Jourdan in 1885, which was further explored by Schroeter (Jourdan, **1885**; Schroeter, **1909**; Evano *et al*, **2008**) (Figure 5.11).

In 1903, Ullmann extended the usefulness of this reaction to unactivated anilines which

underwent condensation with an *ortho* chlorobenzoic acid by adding mechanically divided copper catalyst (Albert, **1966**). Three years later, Goldberg widened the scope of the reaction still further by producing *N*-phenyl-*N*-p-tolyl-acetamide from bromobenzene (Goldberg, **1906**, **1907)**. Diphenylamines can be produced by the substitution of a halogen atom in a benzene ring by a primary or secondary aryl amine, especially if it is activated by a suitable group such as an *ortho* substituted benzoic acid. Ullmann-Goldberg coupling was reviewed by Acheson (**1973**), Schulenberg & Archer (**1965**) and Albert (**1966**) and recently, it has been covered in a general fashion (Beletskaya & Cheprakov, **2004**).

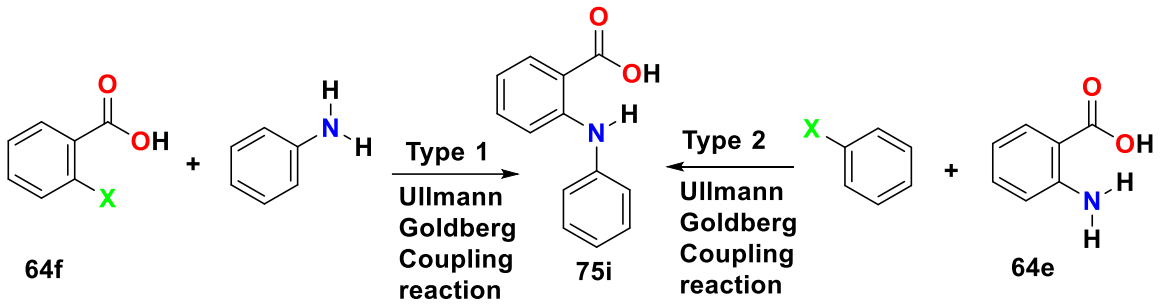

Figure 5.12. Type I and type II Ullmann coupling reaction.

Briefly, under copper catalysis, there are two methods whereby the desired diphenylamine-2-carboxylic acids can be produced (Figure 5.12), depending on if, in the starting materials, the carboxyl group is positioned *ortho* to the halogen or the amino group.

Amino and halobenzenes with *ortho* amide or ethoxycarbonyl groups may also be utilized where X represents a displaceable halogen such as chlorine, bromine or iodine.

The discovery by Ullmann that freshly prepared finely divided copper catalysed such reactions, removed the serious limitation to the scope of the reaction depressing the need for activating groups *ortho* or *para* to the halogen (Acheson, **1973**; Albert, **1966**; Bacon and Hill, **1965**; Elderfield, **1950**; Fanta, **1946**).

"Organic Syntheses" procedure describes a detailed protocol whereby *N*-phenyl anthranilic acid is prepared by condensing *o*-chlorobenzoic acid with aniline in the presence of copper bronze powder, promoting cyclisation by using hot conc sulphuric acid to the corresponding 9-acridinone (Allen and McKee, **1939**). The HCl generated during the reaction is normally scavenged by added base, preferably freshly fused potassium carbonate. This final is critical and Albert **(1951)** emphasised that "potassium carbonate should be carefully dried over a smal flame and finely powdered whilst still hot".

5.3. Aims of this study.

The synthesis of anti-malaria drug pyronaridine in four steps:
Step 1: Modified Ullmann-Goldberg reaction.
Step 2: Cyclisation and halogenations.
Step 3: S_NAr (substitution nucleophilic aromatic reaction).
Step 4: Mannich reaction.

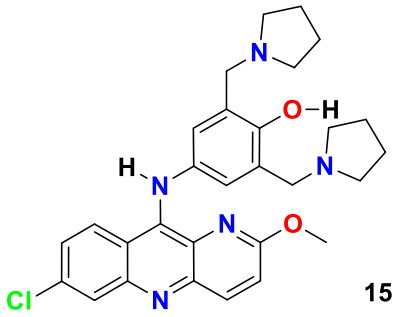

Figure 5.13. Pyronaridine (**15**).

Numerous attempts in our hands failed to reproduce these results, and also, importantly, disagreed with experimental yields quoted in a subsequent review article (Chen and Zheng, **1990**). Some difficulties were encountered, for instance, some of the intermediates, *p*-aminophenol or *o*-aminophenol substituents, would be sufficiently air sensitive under basic conditions that inert atmospheres were required to procure the intermediates and final product at the claimed yields. Since pyronaridine (Figure 5.13) contains the sensitive *p*-aminophenol group, it is liable to oxidation to make the corresponding quinone when in the free base form (Ismail *et al.*, **2009**)

5.3.1. Important sub-goals.

a) To construct the head group of pyronaridine (Figure 5.13) namely 4-(7-Chloro-2-methoxy-benzo[*b*][1,5]naphthyridin-10-ylamino)-2,6-bis-pyrrolidin-1-ylmethyl-phenol (**15**b) so that its antimalarial activity, could be evaluated against a drug sensitive strain of *Plasmodium in-vivo.* The acetate was used since the free amine is rapidly acetylated.
b) Phase II metabolism *in-vivo* following Chen method (Song & Chen, **2001**).
c) To construct 1-de-*aza* pyronaridine, i.e. pyracrine (4-(6-chloro-2-methoxy-acridin-9-ylamino)-2,6-bis-pyrrolidin-1-ylmethyl-phenol) (**15**a), the C-1 carba analogue of pyronaridine, dubbed pyracrine [which is reported to have reduced activity against drug

resistant *Plasmodia*. In this case the required 10-halo-acridine is commercially available since it is used for the construction of mepacrine (Burckhalter *et al.,* **1948**). Having synthesised the compound, its activity will be compared directly against pyronaridine (Figure 5.13) in drug sensitive *Plasmodium berghei* strain *in-vivo*. Such data are required to further develop the published functional pharmacophore for quinolines and *bis*quinolines (Ismail *et al.,* **1996**, **1998**) and structure activity relationships (Chavalitshewinkoon *et al.,* **1993**).

d) Finally I aim to obtain a full set of spectroscopic data, and fully characterise all stable intermediates, including those reported by Besly and Goldberg (1954), as well as those of subsequent compounds using both low and high field FT-NMR (250 & 600 MHz). Additionally electron impact mass spectrometry (EI-MS) would allow verification of previously described compounds (Figure 5.14).

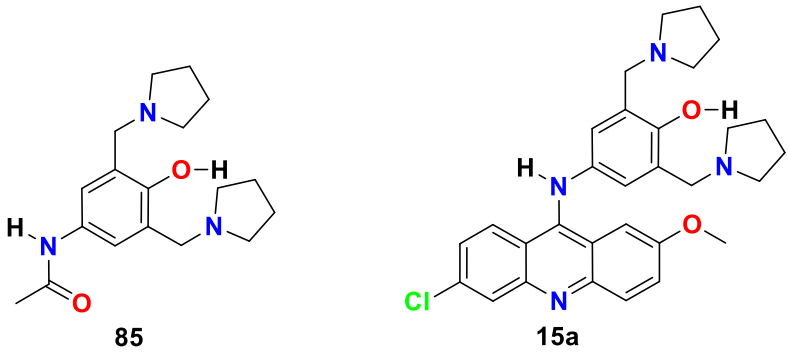

Figure 5.14. Head group and Pyracrine (**15a**).

5.4. Results and discussion.

Despite a large number of investigations into the mechanism involved during the Ullman-Goldberg coupling to form 2-(phenylamino)benzoic acid, referred to as *N*-phenyl anthranilic acid derivatives in the older literature, the mechanism of this reaction is still under investigations (Sperotto *et al.*, **2010**)

Investigations of the corresponding *N*-pyridyl anthranilic acid are rare and our literature survey did not reveal the mechanism or by-product distribution profile but only as a synthetic route. Other investigators attempt to prepare 9-dialkylaminoalkylamino-diaza-anthracenes from *o*-pyridylaminobenzoic acid and 3-phenylaminopicolinic acid were unsuccessful (Kermack, **1945**; Price and Roberts, **1946**; Bachmann, **1949**). In the few instances where ring closure was accomplished, it was suggested that *trans*-annular tautomerism of the central ring was inhibited, and that the 9-chlorodiaza-anthracene, essential for introduction of the dialkyl-aminoalkylamino-side-chain, was unobtainable.

Modifications were made by Besly & Goldberg, (Besly and Goldberg, **1954)**, apparently unaware of prior work by Takahashi who had managed to synthesise a pyridylanthranilic acid, a key precursor for pyronaridine production.

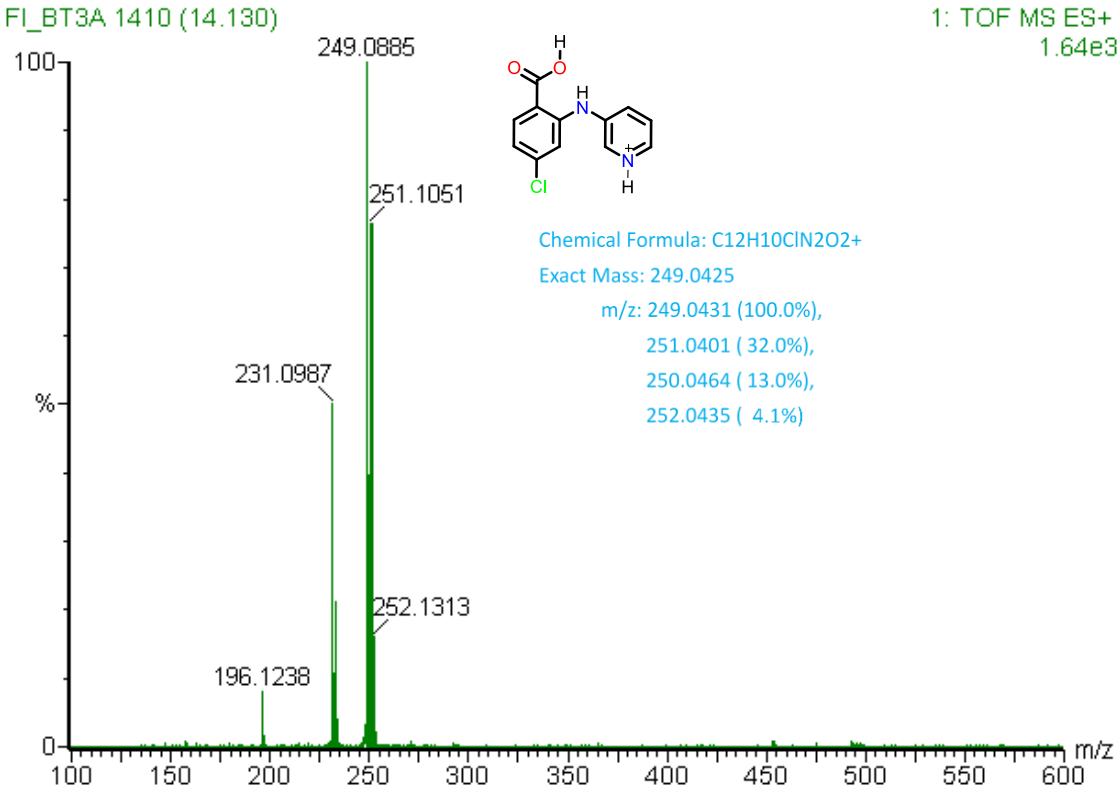

Figure 5.15. Using selected ion monitoring, the fastest eluting peak is identified using positive ion electrospray mass spectrometry as the 3-(2-carboxy-5-chlorophenylamino) pyridinium ion.

Working in parallel with Takahashi, American scientists attempts to find other antimalarials during World War II in part resulted in the combination of selected structural features of atabrine with pamaquine (*Plasmochin*) thus making benz-naphthyridines. the synthesis of such product was attempted following the work of Price & Roberts (**1946**), who had stated the difficulties in condensation of 2,4-dichlorobenzoic acid with 3-aminopyridine. The current study found that if sodium carbonate or potassium carbonate were not freshly fused and stored in the oven, reactions became sluggish and often failed. The materials produced were also rather dark in colour and analysis of the material using LC-MS indicated the presence of at least four compounds (Figure 5.15).

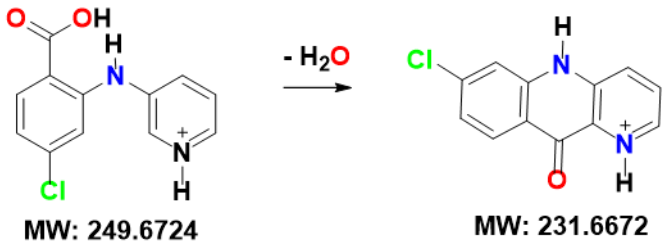

Figure 5.16. dehydration/cyclisation, $POCl_3$, reflux.

The loss of water shows that the mass ion, which is also the base peak forms an ion at 231 Daltons which corresponds with the desired naphthyridine. However, in our hands some of the reactions with $POCl_3$ failed and formed a large number of tarry products (which were not purified) (Figure 5.16).

The results indicate that the desired compound was successfully made, confirming that part of Price and Roberts study (**1946**).

5.4.1. Dehydration (cyclisation) of anthranilic and dehydroxy halogenation.

Benzo[*b*][1,5]naphthyridin-10(5H)-one in a mixture of dry DMF/dry CH_2Cl_2 (1:1) could be cyclised with oxalyl chloride at −10°C but attempted isolation of the product led to hydrolysis. This *aza*-acridone upon suspension and heating in $SOCl_2$, contained traces of DMF but could be isolated *in vacuo* by dissolution in EtOH-free $CHC1_3$. The solution was cooled to -5°C and then poured in a thin stream into a vigorously stirred mixture of chipped ice/cNH_4OH. Unless the $CHCl_3$ layer was separated in a prechilled separating funnel and immediately washed with ice-cold NH_4OH (2M), it rapidly hydrolysed. The chloro compound could not be obtained completely free of traces of acridone. Consequently, further work on this compound was abandoned and its extreme reactivity explains why price and roberts could not synthesise it. It was not until 2012 when a patent disclosed that the desired dihalo benzacridine could be used successfully, and was used in condensation reactions but

no synthetic details were provided (Mackeigan *et al.*, **2012**).

Hence it may be that the presence of the methoxy group decreased the reactivity of the adjacent halogen in pyronaridine precursors (Figure 5.17).

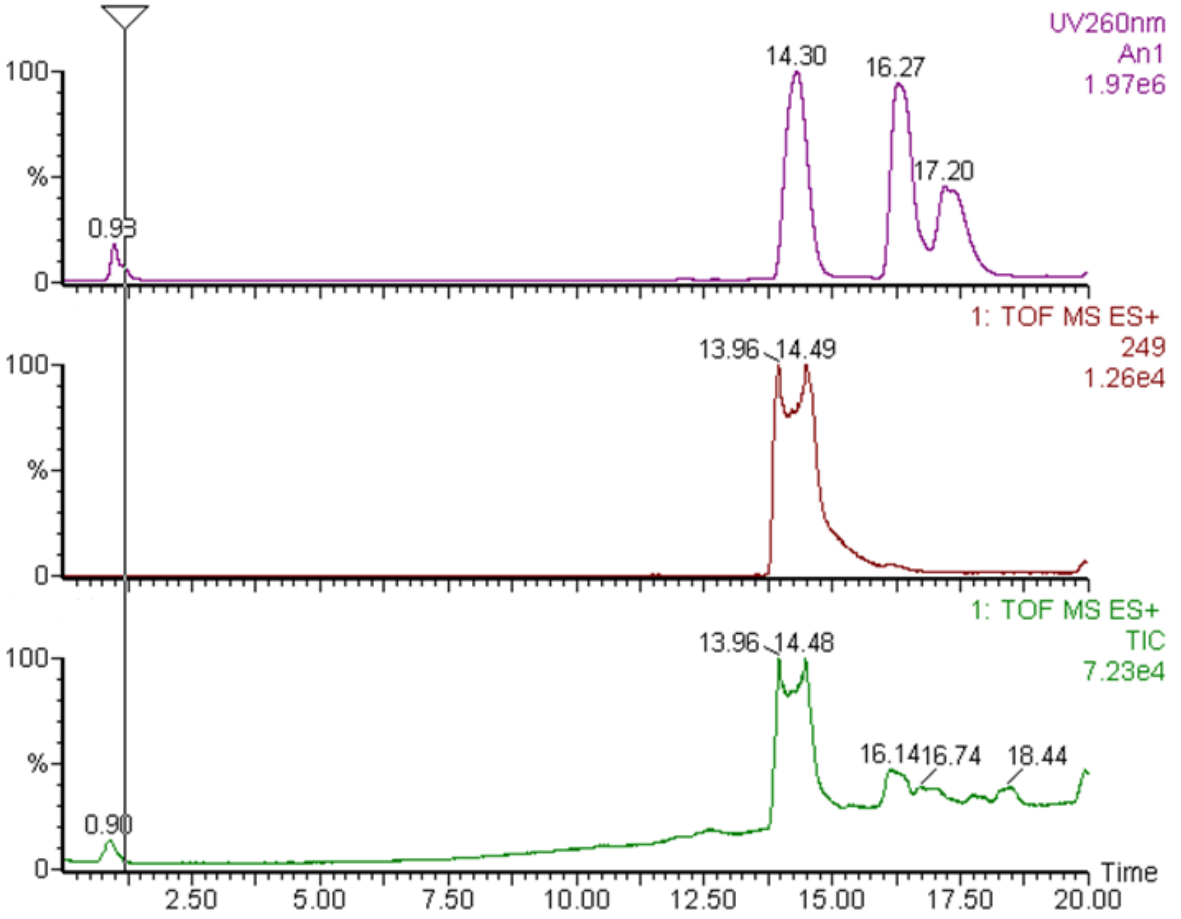

Figure 5.17. The lower figure (in green) showing the total ion current (TIC) showing a broad range of species eluting after 15 minutes of which 3 absorb strongly at 260 nm (top HPLC trace, magenta). the middle trace dark scarlet shows the desired ions 249 Mass units +ve ion electrospray.

5.4.2. Routes Leading to precursors for pyronaridine.

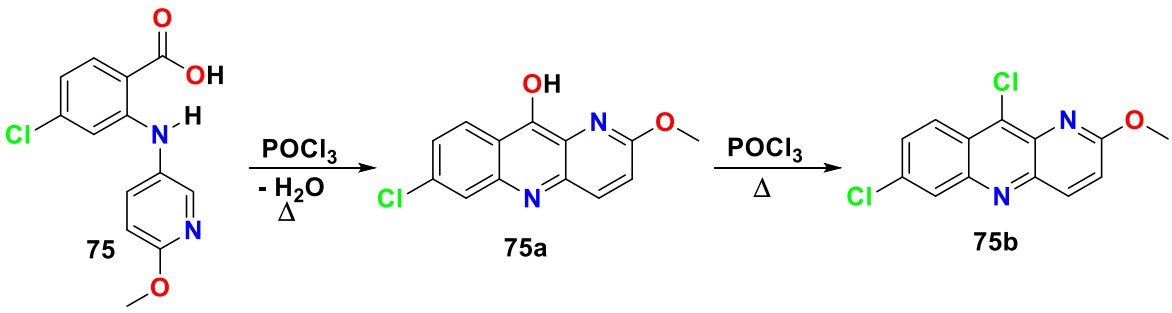

Figure 5.18. Besly and Goldberg cyclisation, $POCl_3$, reflux.

Takahashi reported successful production of benz-[*b*]naphthyridine bearing a methoxy group on the 2-position) (Takahashi, **1945**; Chemical abstracts, **1951**; Besly & Goldberg, **1954**).

On repetition of the work of Besly & Goldberg 1954 (Figure 5.18), it was noted early on that analysis of compounds constructed using pentanol as a solvent, were complex. Furthermore, the tar produced complicated analyses. Numerous TLC systems using silica plates were explored to determine a system that would successfully separate the complex mixture so it could be flash chromatographed and subsequently analysed by NMR.

Ethyl acetate: cyclohexane: acetic acid (60:30:10, v/v/v) was the best system (Figure 5.19) but when the mixture of individual components was present, the dichlorobenzoic acid co-eluted with the desired anthranilic acids most probably caused by ion pairing of the unreacted components with the product causing a change in R_f within mixtures (see lane 4).

Consequently, the traditional method of washing the anthranilic acid with boiling water was found to be the best method for purification since it is well known that the benzoic acid starting materials have appreciable solubility in hot water unlike the target compounds. Final purification was affected by recrystallization (Albert, Acridines, 1st Edition).

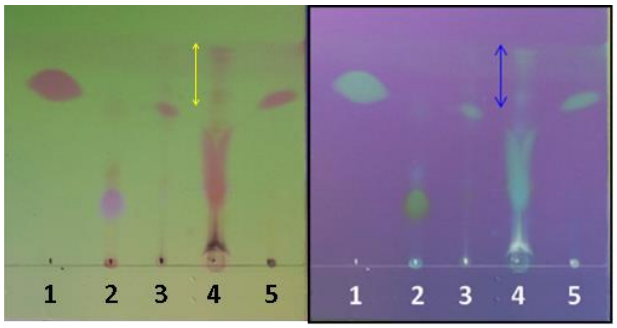

Figure 5.19. Plate a: Tlc plate showing superior purity of material construed using the DMF method (lane 5) compared to pentanol (lane 3). Lane 1: 2,4-dichlorobenzoic acid (2,4-DClBA) ; Lane 2: 2-amino-5-methoxypyridine (2A5MP); Lane 3: 1 equiv. 2,4-DClBA: 1 (2A5MP), refluxed in pentanol (3hrs) Lane 4: Cospot of 1-3 spotted at double the concentration to reveal impurities (see yellow double headed arrow); Lane 5: 1 equiv. 2,4-DClBA: 1 2A5MP reaction in DMF (4 hrs). Plate b) inverted image to reveal impurities more clearly. Solvent system: Ethyl acetate: cyclohexane: acetic acid (60:30:10, v/v/v).

Also, the Dean Stark apparatus recommended by Besly & Goldberg to eliminate water from the reaction was unsuccessful. Excessive heating of the mixture led to formation of side reactions and products not described previously (Figure 5.19, lane 4). Some of these products include the displacement of the halogen *para* to the benzoic acid moiety as well as esters formed during excessive heating. This was readily apparent in electron ionisation spectra.

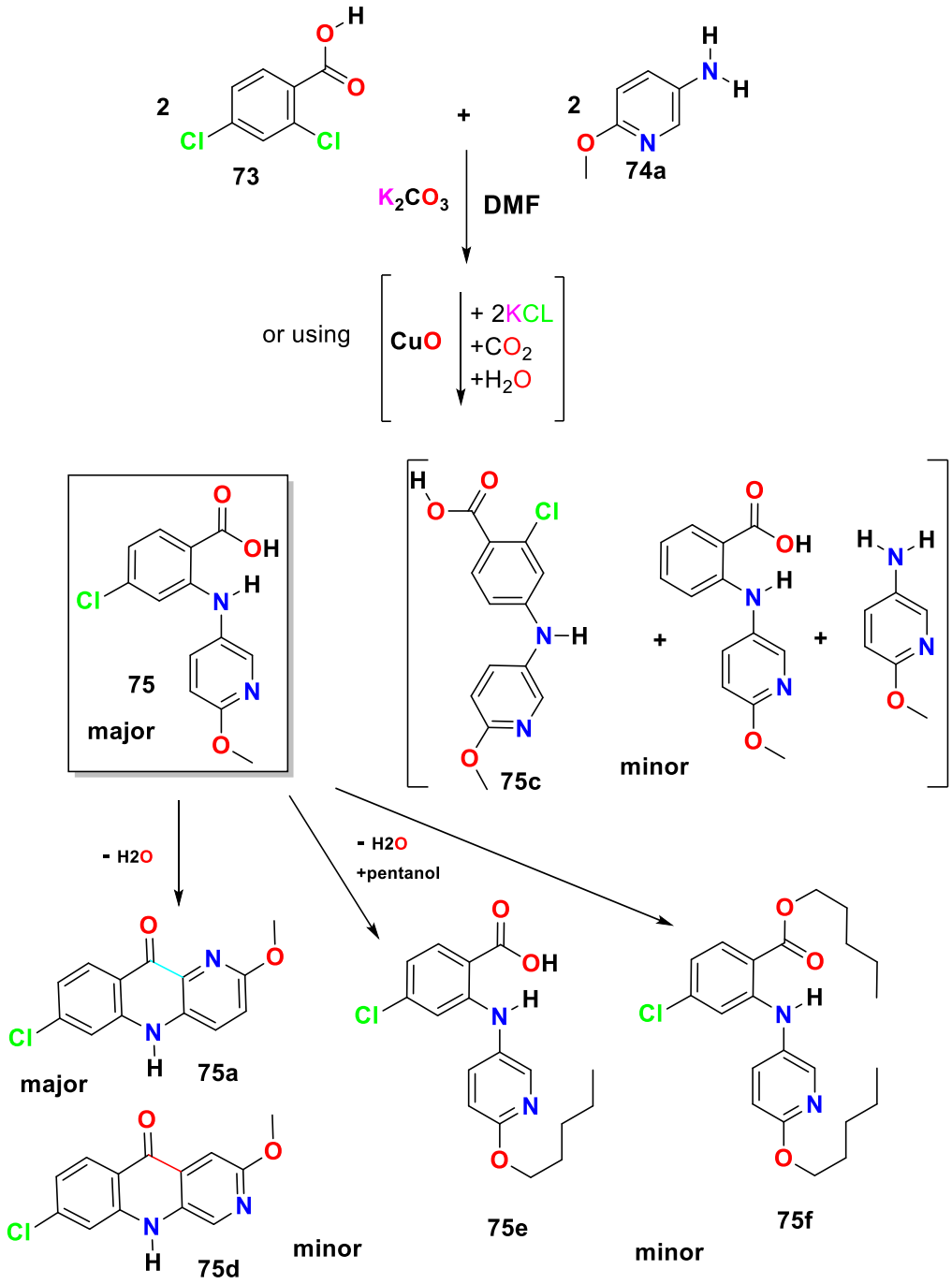

Figure 5.20. **73**:2,4-dichlorobenzoic acid; **74a**:6-methoxypyridin-3-amine; (potassium 2,4-dichloro benzoate; **75:4**-chloro-2-(6-methoxypyridin-3-ylamino)benzoic acid; **75c**:2-chloro-4-(6-methoxypyridin -3-ylamino) benzoic acid; 2,4-bis(6-methoxypyridin-3-ylamino)benzoic acid; **75a**:7-chloro-2-methoxybenzo [*b*][1,5] naphthyridin-10(5H)-one; 75d:8-chloro-3-methoxybenzo[*b*][1,7]naphthyridin-5(*10H*)-one; **75e**:4-chloro -2-(6-(pentyloxy)pyridin-3-ylamino)benzoic acid; **75f**:pentyl 4-chloro-2-(6-methoxypyridin-3-ylamino) benzoate. Blue and red line denotes newly formed bond.

5.4.3. DMF as a solvent for Ullmann Goldberg coupling.

Since difficulties were encountered in removing high boiling alcohols, and the impurity

profile was populated with several undesirable products including condensation of the reactant with alcohols such as *n*-pentanol at high temperature, we explored the use of other solvents to facilitate reaction and noted that DMF had been used by Pellon *et al* (**1997**). Although it was previously known that *N*-phenyl-anthranilic acids could be synthesised by Ullmann- Goldberg condensations, using various solvents and conditions, they systematically explored several common parameters (including catalyst concentration, reaction time and number of base equivalents) on product yield. Notably, using *N,N*-Dimethylformamide as solvent, and the use of one equivalent of K_2CO_3 per mole of o-chlorobenzoic acid allows the use of water in this reaction (Pellón *et al.,* **1993**).

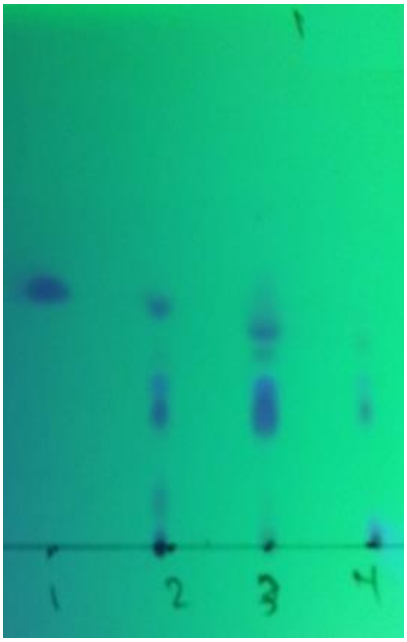

Figure 5.21. 1: 2,4-dichlorobenzoic acid (2,4-DClBA); 2: 2 eqiv. (2,4-DClBA): 1 eqiv. 3-aminopyridine (3AP) in DMF (2hrs) under argon; 3: previous reaction left overnight; 2 eqiv. (2,4-DClBA): 1 eqiv. 3-aminopyridine (3AP) under argon; 4) reaction repeated in air/ DMF/ 2hrs 1 eqiv. (2,4-DClBA): 2 eqiv. 3AP; Solvent system: ethyl acetate: cyclohexane: acetic acid (60:30:10, v/v/v).

When DMF was employed as solvent (Figure 5.20), they suggested it was impossible to eliminate water formed during the neutralization. This water remains in the reaction media and can affect the copper complex formation when an excess of K_2CO_3 is present. However, by inserting a Pasteur pipette plugged with glass wool at the constriction and filled with molecular sieves, previously dried in a hot oven at 120°C, whilst standing vertically in the flask (extending into the condenser) could be used to produce anhydrous conditions. The results are illustrated in the TLC above (Figure 5.21):

The desired product has the same R_f as the starting material 2,4-dichlorobenzoic acid. It was discovered that the product fluoresces blue under 366 nm light (Figure 5.22) but the

starting carboxylic acid does not. Consequently, the DMF method developed in the current study was superior to that of Besly & Goldberg since tar formation was suppressed.

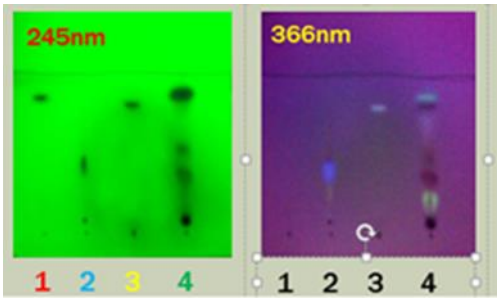

Figure 5.22. After extraction with ethyl acetate, four columns were spotted: 1: 2,4-dichloro benzoic acid; 2: 2 methoxy5amino-pyridine; 3: Authentic 4-chloro-2-((6-methoxypyridine-3-yl)amino)benzoic acid; 4: reaction mixture.

More recently, Kincaid *et al* have achieved the same reaction using micellar catalysis (using TPGS-750-M (2% by weight) and using CuI (10% mol)) in 99% yield but it requires centrifugation to remove the catalysts as filtration produces a foam (Kincaid *et al.*, **2022**).

This is a major disadvantage if such a reaction was to be scaled up and is unlikely to attract industrial production. We had already explored micellar catalysis and phase transfer catalysts but found it difficult to remove them from the product without chromatography and consequently abandoned such routes early (Ismail and Alizadeh unpublished).

Table 1: The R_f value of starting materials, reference material and purified product in TLC analysis.

	Log P	**Retention factor (R_f)**
2,4-dichlorobenzoic acid	2.6	0.72
5-amino-2-methoxypyridine	0.4	0.35
4-chloro-2-(6-methoxy-3-pyridylamino) benzoic acid	2.7	0.73
product after extraction	N/A	0.73

5.4.4. Production of regioisomers.

Cyclisation of *o*-3-Pyridylaminobenzoic acids (**75**) may give rise to the 9-hydroxy- or the 9-chloro-derivative of benzo[*b*][1,5]or [1,7]naphthyridin-5(*10H*)-one (**75j**), according to whether cyclisation is promoted upon either the 2- or the 4th position of the pyridine ring.

Similar types of cyclodehydrations occur with 2-(3-nitrophenylamino) benzoic acid which cyclises principally upon the 2nd position (Albert and Linnell, **1938**).

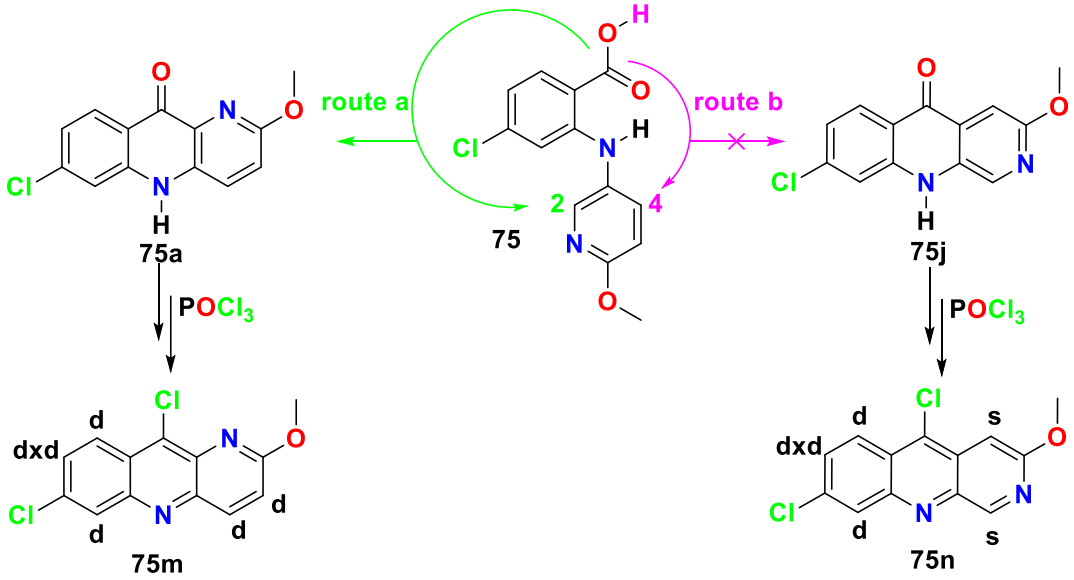

Figure 5.23. The regioselective cyclisation determined by examination of NMR of crude mixtures (not shown). Only signals corresponding to route 'a' were detected. DFT suggest that both routes are likely but only **75m** was ever isolated. S is singlet, d, doublet, dxd, doublet of doublet.

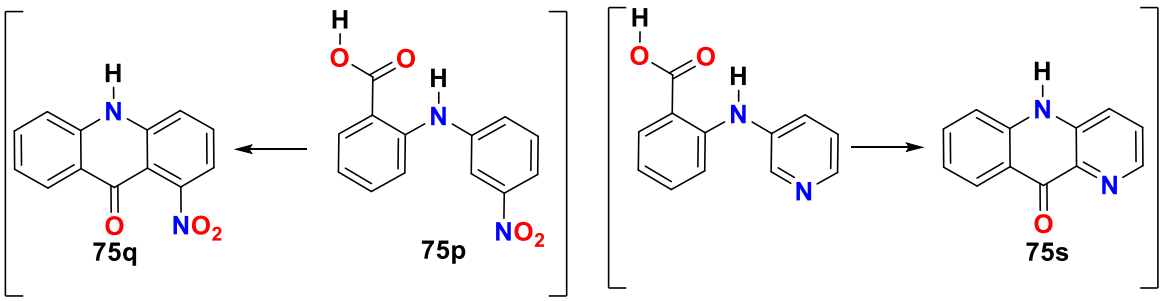

Figure 5.24. Cyclisation reaction of 2-((3-nitrophenyl)amino)benzoic acid and 2-(pyridin-3-ylamino)Benzoic acid bioisosteres.

Besly & Goldberg had noticed the striking similarity between the substitution reactions of pyridine and nitrobenzene. Elderfield, (**1950**), suggests that *o*-3-pyridylamino-benzoic acids would cyclise in a similar fashion i.e. upon the 2-position of the pyridine ring (Figure 5.24).

A substituent blocking the 2- (but not of the 4-) position allows cyclisation and the converse suppresses it. *p*-chloro-2-(6-methoxy-4-methyl-3-pyridy1amino)benzoic acid is, and 4-chloro-2-(6-methoxy-2-methyl-3-pyridylamino) benzoic acid is not, cyclo-dehydrated by sulphuric acid or phosphoryl chloride.

Cyclodehydration of *o*-3-pyridylaminobenzoic acids in strong acid proceeds by the initial protonation of the carbonyl oxygen followed by the attack of the carbonium ion onto the pyridine nucleus.

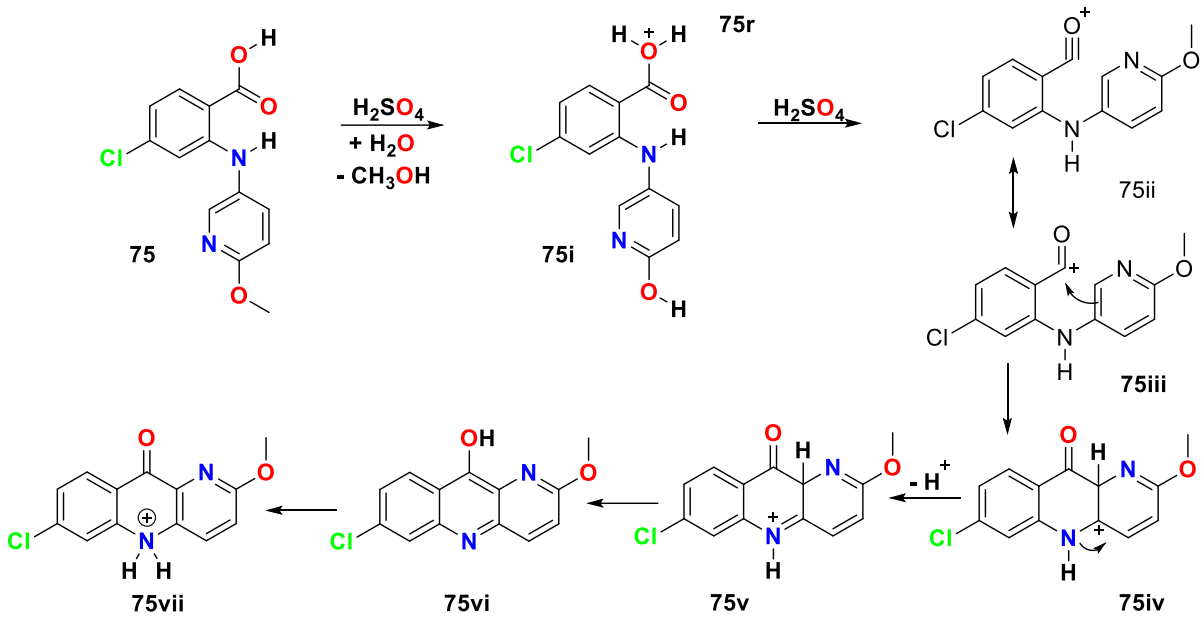

Figure 5.25. Postulated cyclisation of the Acridine ring.

Besly and Golberg (**1954**) suggested that, the reaction will proceed if the electron density at the available points for ring closure C(2) and C(4) of the pyridine ring is sufficiently high, its direction being governed by the relative electron densities (Longuet-Higgins *et al.*, **1947**) found A the 2-position in pyridine is considerably higher than it is at the 4-position, citing examples of the halogenations of 3-aminopyridine in acid (Schick *et al.*, **1936**) and the Skraup cyclisation exclusively at the 2-position (Klisiecki and Sucharda, **1927**). DFT calculations (Prof Drew, Reading University) do not support this view and suggest that other as yet undetermined factors may be at play. It may well be that the isomers are more water soluble than expected and were lost during the work up. It is suggested that *o*-3-pyridylaminobenzoic acids fail to cyclise, which differs from the data obtained by Price & Roberts (**1946**) and that found in the current study. Hence the explanations given by Besly & Goldberg (**1954**) must be considered with caution, and as future works we shall seek an alternative explanation to the route of cyclisation (Figure 5.25, compound **75**).

The regioselective cyclisation was clearly apparent by the detection of four doublets, only one of which demonstrated a *meta* coupled doublet (Figure 5.26). The remaining doublet of doublets (resonating at 7.6 ppm) clearly demonstrates the presence of an AMX system.

Brief reflux in H_2SO_4 for 2 minutes, microwave, at 180°C, protons were determined using ^{1}H-^{1}HCOSY experiments seen on the base line (e.g. 7.6 ppm). GC-MS revealed that the impurity was consistent with material containing chlorine atoms and it was found that refluxing beyond 4 hours in $POCl_3$ caused demethoxyhalogenation to produce 2,7,10-trichlorobenzo[*b*][1,5]naphthyridine. This is a known compound first reported by Takahashi (Takahasi & Hayase, **1945**; Kincaid *et al.*, **2022**) from the same starting materials used in our

study but also from the cyclisation of 2-(6-(benzylmethoxy)pyridin-3-ylamino)-4-chlorobenzoic acid (Besly & Goldberg, **1954**):

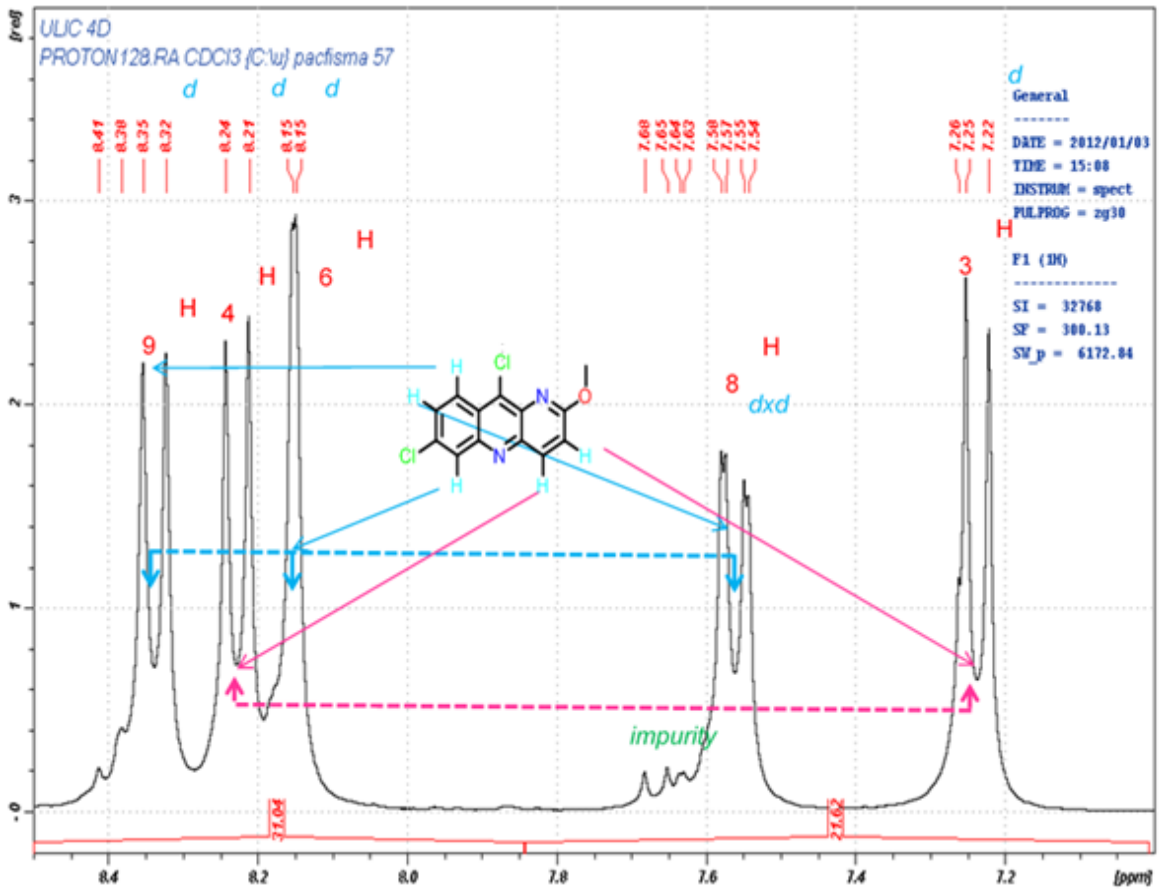

Figure 5.26. ^{1}H NMR of cyclised of the Acridine ring (compound **75m**).

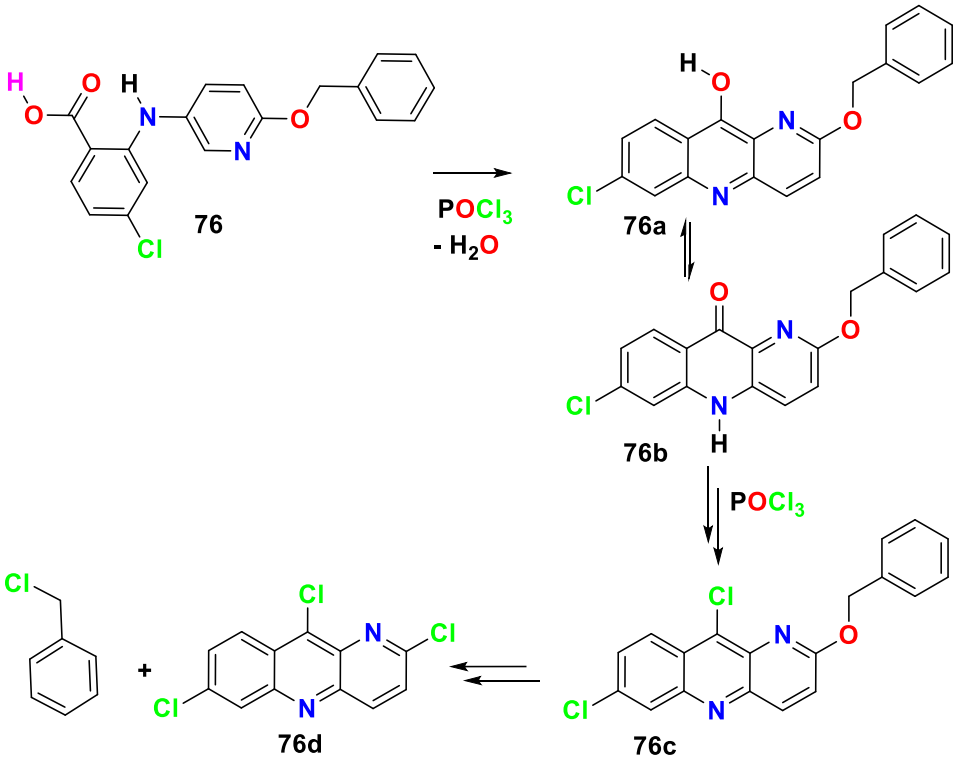

Figure 5.27. Conversion of benzyl substituted pyridyl anthranilic acids.

The leaving group -benzyl alcohol- is converted *in situ* to benzyl chloride (Figure 5.27) by excess thionyl chloride which acts as both reactant and solvent (Mouesca *et al.*, **1993**).

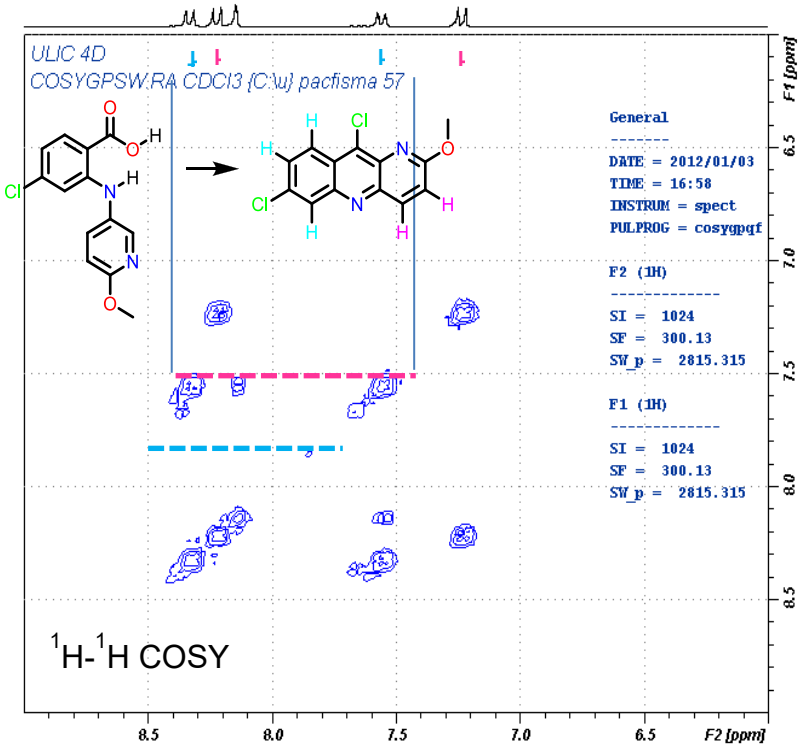

Figure 5.28. 300MHz NMR cosy of Converted benzyl substituted pyridyl anthranilic

acids (compound **75** & **75m**).

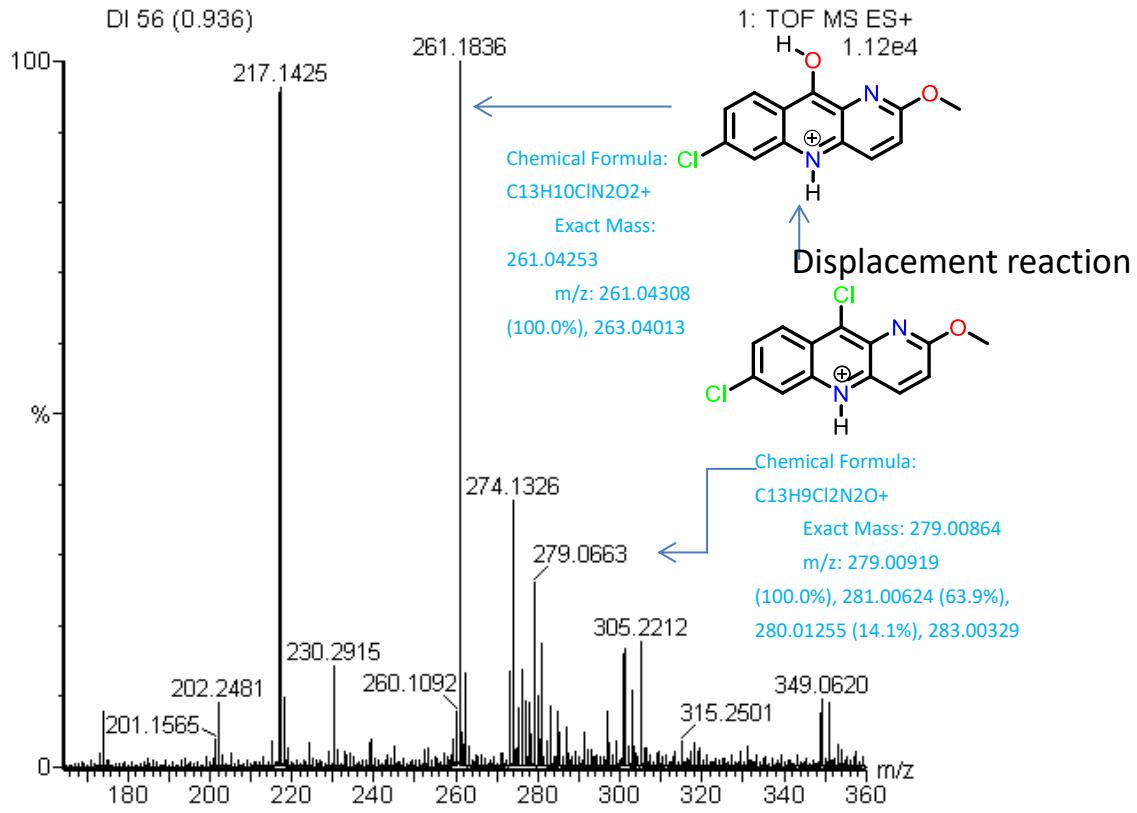

Figure 5.29. Base peak at 261.1836. Failure to maintain basic conditions during work up results in hydrolysis of 7,10-dichloro-2-methoxybenzo[*b*][1,5]naphthyridine to 7-chloro-2-methoxybenzo[*b*][1,5]naphthyridin-10-ol.

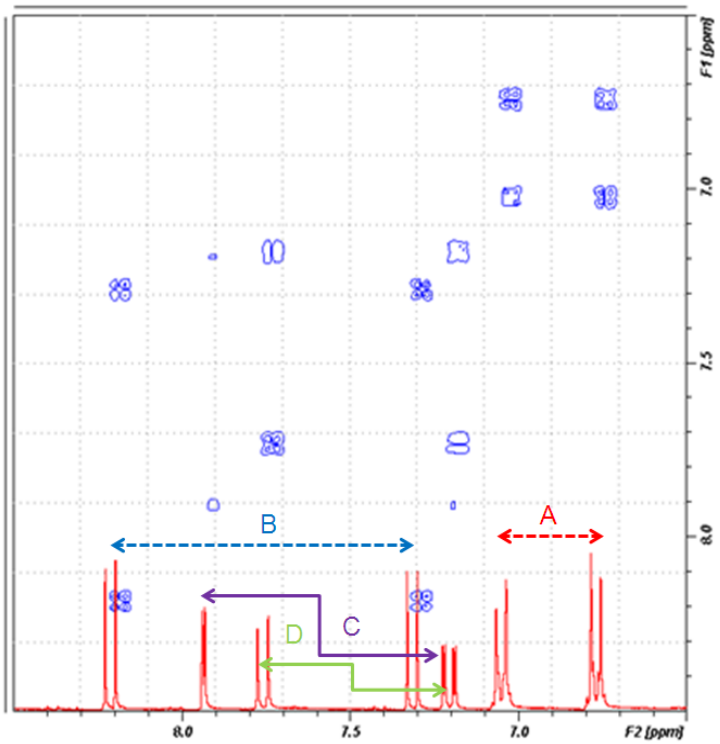

Figure 5.30. COSY spectroscopy for **75m**.

5.4.5. Coupling with *p*-aminophenol.

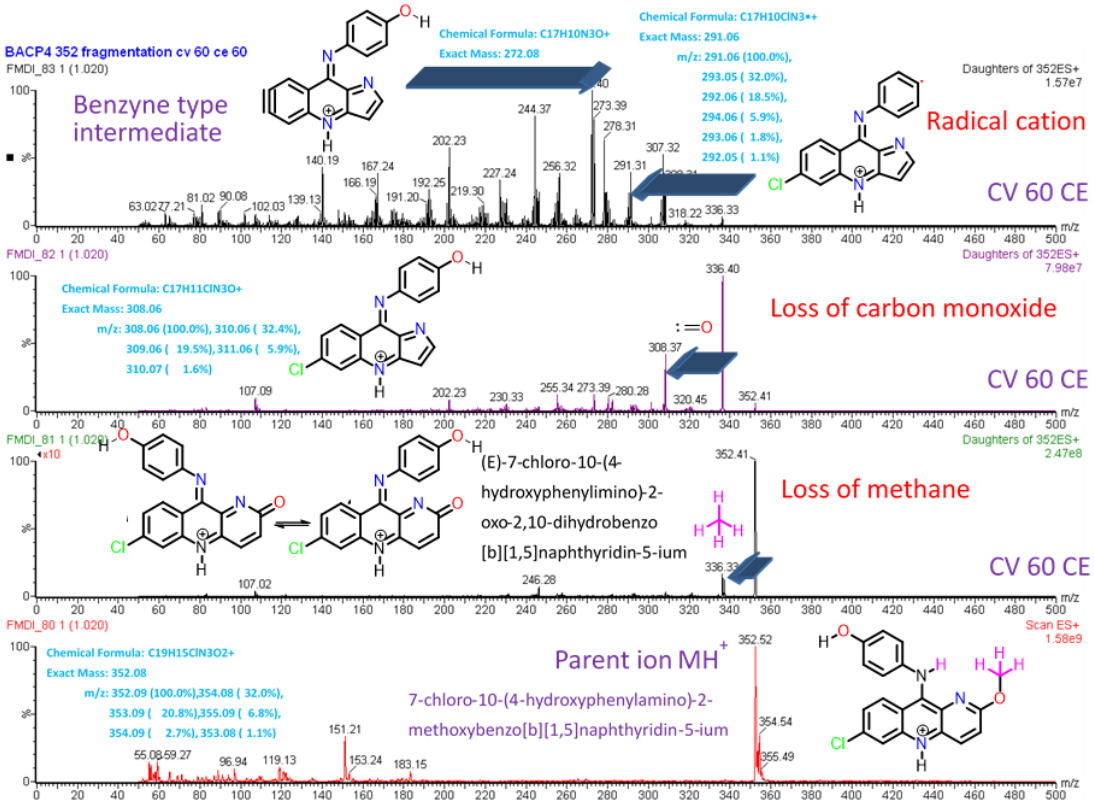

Figure 5.31. Pyronaridine MS fragmentation, Loss of radical cation, CO, CH_3.

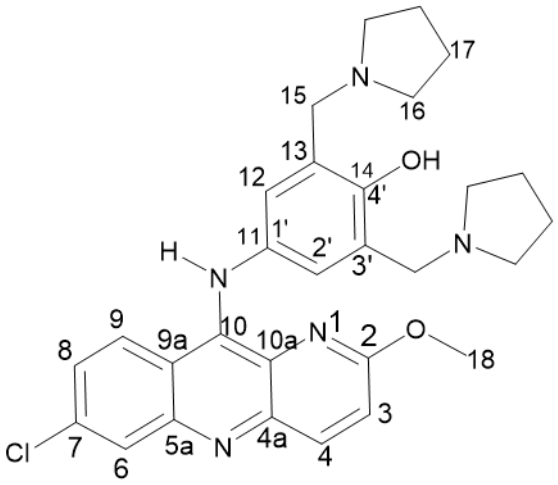

Figure 5.32. Numbering system. Then main ring system numbered according to current IUPAC recommendations. However, the complexity of the side chain utilises a sequential numbering system to facilitate discussion about NMR assignments.

5.5. Analysis and discussion.

A partial 90 MHz ^{1}H NMR spectrum analysis of the free base of pyronaridine, in deutro-chloroform was published by Zheng (Zheng, **1982**). At 6.96-7.07 ppm, a multiplet was found (m, 3H benzene C2-H and C6-H) but the integration was given as three rather than 2 which is incorrect. Subsequently, a further paper appeared involving the synthesis of carbon-14-labelled pyronaridine tetraphosphate (Park *et al.*, **2007**). Again, no firm assignment was advanced regarding the identity of each ^{1}H or ^{13}C atom. It would appear that multidimensional experiments were not run by either group. Initially, we examined the free base of pyronaridine and related analogues but found that long term stability was poor with formation of the quinone (Ismail *et al.*, **2009**) compared to the tetraphosphate so only the salt form data is reported here.

The integration for the initial proton spectra was calibrated to the methylene peak (H17) at δ1.88 setting this to 8 protons. The COSY spectrum confirmed the relationship to the other downfield methylene protons (H16) (δ3.033) of the pyrrolidine rings, integrating to 8 axial and equatorial hydrogens. These peaks appeared as broad singlets, unable to resolve the coupling at this temperature or frequency in DMSO-d_6. The compound was also investigated in solvents that hydrogen bond to the molecule and these are discussed in a subsequent section. The integration of the remaining 2 peaks simply allowed their assignment as δ3.83 (3 protons) as the methyl ether protons (H18) and δ4.10 (4 protons) as the remaining 4 methylene protons (H15) adjoining the two pyrrolidine disposed *ortho* to the phenol moiety. A broad peak resonating at δ6.46 is attributed to water of hydration within the phosphate salt which coalesced exchangeable hydroxyl and amine peaks.

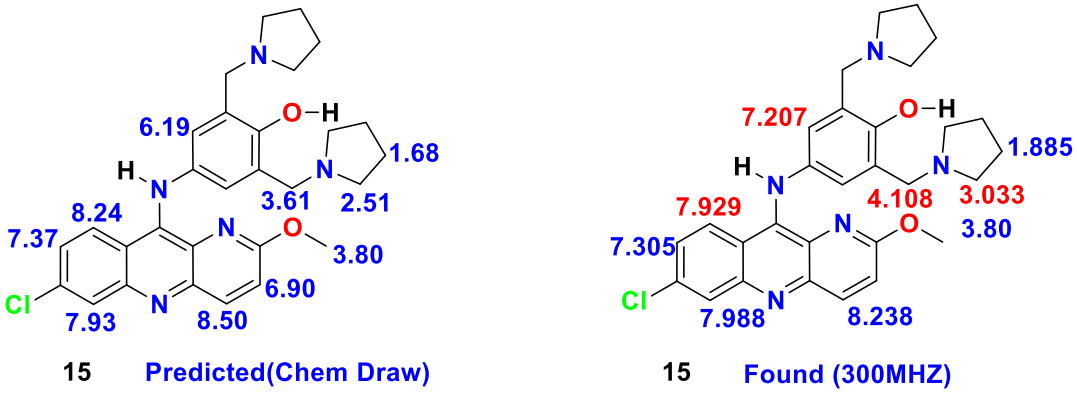

Figure 5.33. H3 and H8 are almost coincidental in 1-D spectra but vicinal connectivity was established using COSY spectra.

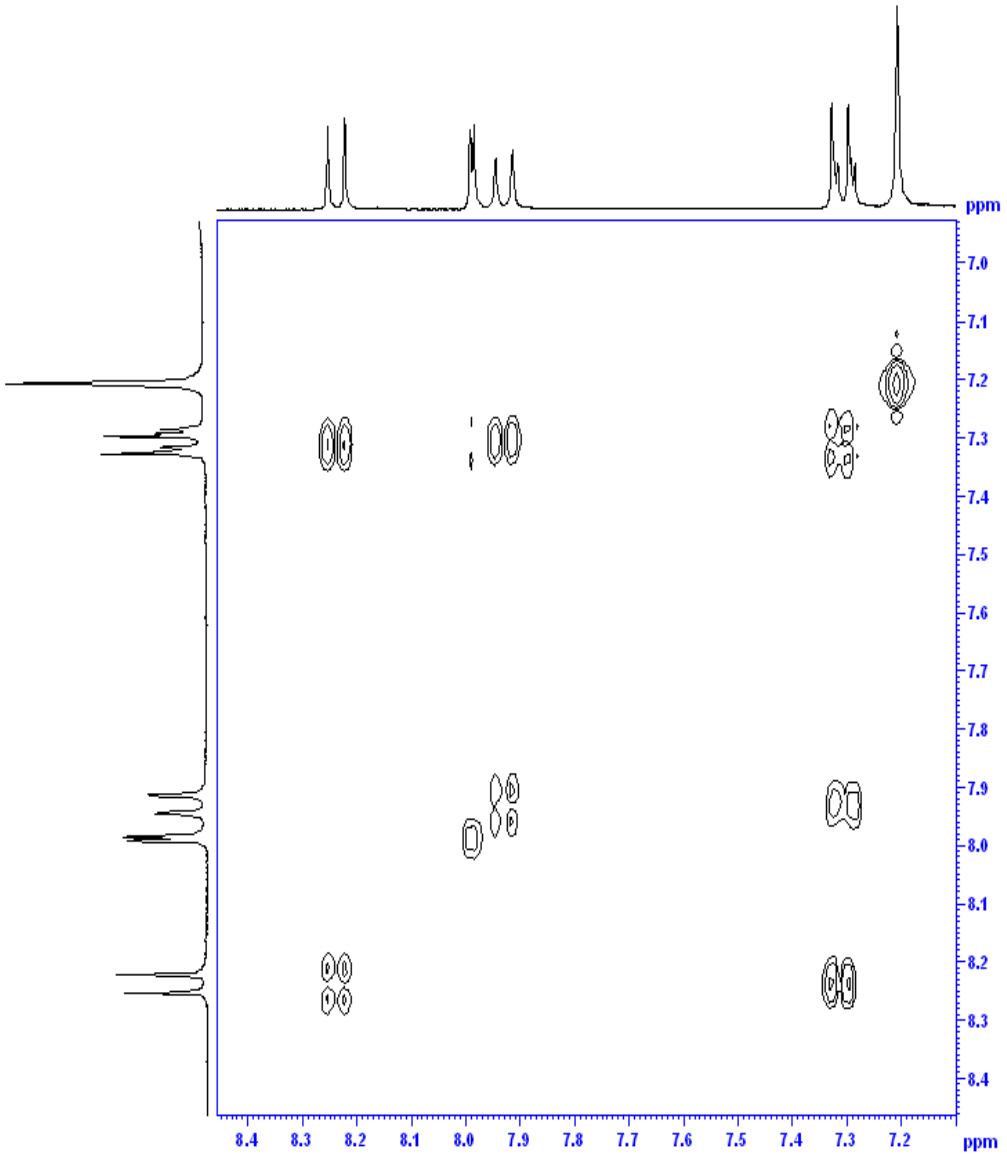

Figure 5.34. COSY spectroscopy also confirmed the coupling between H3 and H4. Initial assignment of the downfield peak at δ8.24 was attributed to H-4 since this was "*para*-" to the nitrogen in the aromatic system. Finally, the corresponding upfield doublet at δ7.31 was ascribed to H3. COSY spectroscopy also confirmed the coupling between H3 and H4. (Pyronaridine Phosphate (10mg in 0.7ml) COSYGPSW.SH DMSO).

The 2-proton singlet, from the phenol ring protons (H12), resonated at δ7.21 ppm (Figure 5.33). Based on the coupling constants, only one set of *meta*- couplings was found between (H6) and (H8) and the *ortho* coupling providing a doublet of doublets confirms the presence of an AMX system (Silverstein *et al.,* **2005**). Consequently, the *meta* coupled *J* value doublet at δ7.988 is assigned to (H6) and the corresponding doublet of doublets resonating at δ7.30 was assigned to (H8). The COSY spectrum confirmed further coupling within this ring and allowed assignment of (H9) at δ7.93 (Figure 5.33).

Proton Spectra in D_2O and TFA-*d* reveal sites of protonation in DMSO-d_6, the aliphatic side chains show free rotation producing broad apparent singlets. However, in the presence of

TFA-*d*, protonation occurs and fine structure appears within the upfield rotationally constrained bonds almost splitting the peak into two. This process is more pronounced when D_2O was used as the solvent. Significant shift positional differences are also seen (as expected) with changes when dissolved in TFA-*d* being more pronounced than in the presence of D_2O.

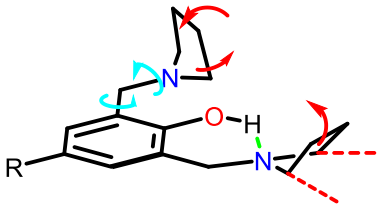

Figure 5.35. Diagram showing conformational flexibility of the pyrrolidine ring. Green dotted line indicates hydrogen bonding.

Mobility is constrained by either protonation on the nitrogen and/or formation of hydrogen bonds with the solvent. Reduced conformational mobility is demonstrated by the appearance of fine structure (i.e. splitting is apparent but coupling constants could not be established at room temperature).

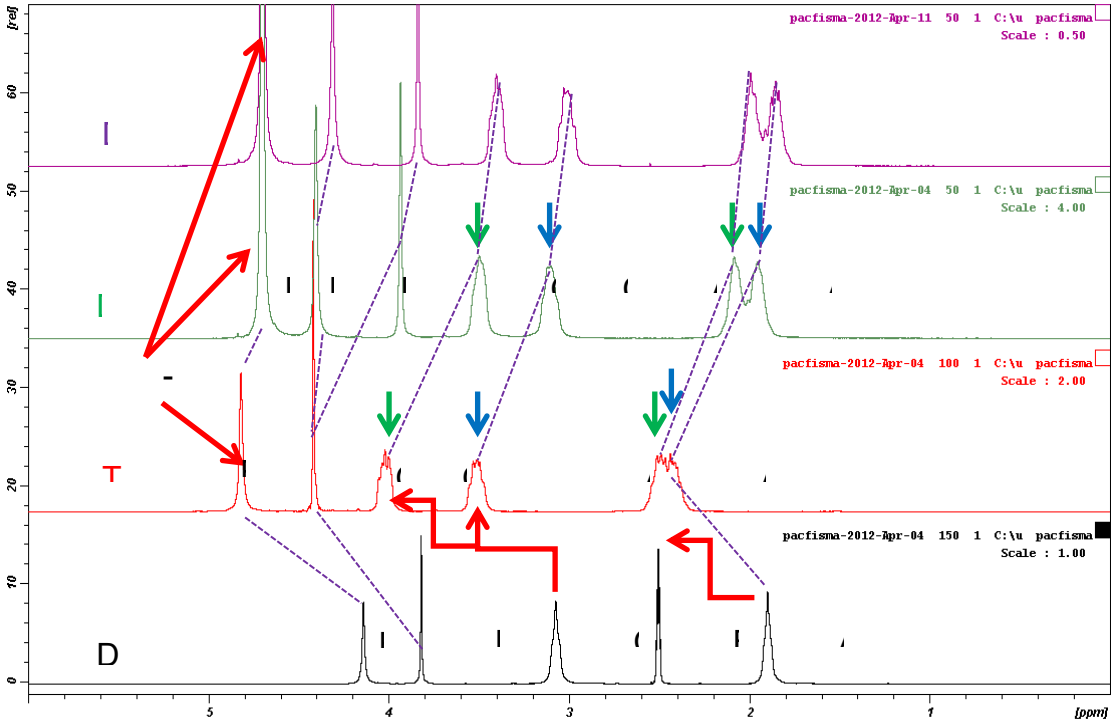

Figure 5.36. Aliphatic portion of pyronaridine phosphate in various solvents. Ascending, DMSO-d_6 (Black), TFA-*d* (Red), D_2O (Green) aged D_2O sample after one week (magenta).

A similar situation is found in D_2O. In samples aged for one week in D_2O, there are no significant further changes in either the methoxyl group or the aliphatic portions of the molecule. During a change in dielectric constant moving from DMSO-d_6 to highly polar

solvents, the methoxyl resides in a polar, solvated region, therefore, resulting in large chemical shifts downfield. This could have significance as they may correspond to sites of drug-receptor interactions (i.e. close polar contacts).

^{13} Carbon Spectra: deduction of multiplicity and connectivity from one to multiple bonds and Polarization transfer experiments such as distortionless enhancement by polarization transfer (DEPT) and insensitive nuclei enhanced by polarization transfer (INEPT) are widely employed to decode the spectra of complex molecules into their individual multiplicities (Sorensen, 1**989**, Nolis & Parella, **2007**). The DEPT experiment is routinely used to edit ^{13}C NMR spectra into sub-spectra (Chandrakumar, **1984**, Doddrell *et al*., **1988**). Distortionless enhancement by polarization transfer including the detection of quaternary nuclei (DEPTQ) experiment was developed by Burger and Bigler (Burger & Bigler, **1998**). This experiment is based on DEPT and gives multiplicity information for all carbons including quaternary carbons. In the later part of the work the advantages of the DEPTQ experiment with respect to similar experiment such as DEPT and sub-spectral editing with a multiple quantum trap (SEMUT) were also discussed in detail by Burger and Bigler **1998**. However, to avoid difficulties with locating the quaternary(4°C), in the later part of the study, improved versions of DEPTQ experiments were utilised to re-investigate pyronaridine tetraphosphate (Bigler *et al.,* **2008**). The carbon spectrum clearly indicated the 20 carbon environments possible in this molecule, four aliphatic and 16 aromatics. There is only one methyl group and the DEPT spectra confirm this, therefore the methyl (C18) is at δ53.50. The upfield signal at δ22.54 is attributed to the methylene carbons (C17) resonating at expected positions and this is confirmed by the HSQC experiment. The HSQC also allows the assignment of the other aliphatic peaks (C15) at δ53.31 and (C16) at δ52.64. The DEPT spectra confirmed there are 6 aromatic methine carbons and examination of the HSQC allows their assignments as δ140.12 (C4), δ127.25 (C6), δ126.51 (C9), δ126.22 (C12), δ123.62 (C8) and δ118.99 (C3). In some experiments when additional equivalents of amino methylating agent were employed, more than two pyrrolidine side chains could be introduced but this is evidently not the case here.

Using the HMBC data quaternary carbons were assigned. The methylene protons (H15) showed 4 correlations, 2 of which were are already assigned via the HSQC experiment. Of the remaining 2, the downfield peak at δ152.49 is most likely due to C14 (by invoking the presence of the electronegative oxygen) and the remaining correlation at δ122.48 for C13. The remaining aromatic proton in the head group, H12, similarly details correlations to C15, C14 and C13 along with a further correlation, which we can assume to be C11 at δ135.87.

The protons attached to the single methyl carbon (H18) show a through bond correlation exists across the ether to carbon (C2) at δ159.023. This carbon also possesses a cross correlation with H11, thereby allowing assignment of C10a at δ127.98 ppm. Finally, C4a can then be assigned to the peak resonating at δ142.77 ppm due to its correlation with H3.

One strong correlation to carbon at δ147.73 is ascribed to H9 being a 3-bond correlation to C10. Similarly, one strong correlation to the carbon resonating at δ143.70 ppm from H9 is

assigned to C5a (Figure 5.33).

As further evidence for these assignments, weaker, longer-range correlations, are noted: The final 2 carbons are less convincingly assigned as δ116.06 as C9a and δ133.71 as C7 based on the intensities of the correlations and the relative chemical shifts. DFT predictions may prove useful in confirming all these assignments. Further papers have appeared in the literature but they have not produced 2-D connectivity data.

The concerted application of the preceding 1D and 2D NMR experiments, allows for confident assignment of the proton spectra and assignment of the carbon spectra. To enable a complete confident assignment for the carbon spectra, either the use of a higher field instrument would be required. Removal of the residual water, may allow the assignment of the -NH and -OH protons and thus they will assist in the assignment of the quaternary carbons via the HMBC. Unequivocal proof was achieved by crystallizing the free base of pyronaridine.

5.6. Experimental.

Authentic sample of 4-Chloro-2-((6-methoxypyridin-3-yl)amino)benzoic acid (**75**) were obtained from both Professor Wallace Peters and David C. Warhurst. All reagents were obtained from Sigma-Aldrich Chemical Co, GB or Lancaster synthesis and were used without further purification. All chromatographic separations were monitored by TLC analyses and performed using glass plates precoated with 0.25mm 230–400 mesh silica gel impregnated with a fluorescence indicator (254 nm). Solvent removal was accomplished with a Buchi rotary evaporator using a Leybold solvent resistant vacuum pump. Microwave assisted organic synthesis was carried out using a CEM focused microwave. Electron Ionisation mass spectra were determined using a VG Analytical (Floats Road, Altrincham, Manchester, UK) 70–250 MS, with a DEC PDP 11/24 data system, at 70eV and a source temperature of ~200°C; trap current 200 μAmps).

Samples were admitted by a direct insertion probe heated to 250–300°C. Positive ion high resolution electrospray mass spectrometry (PIHRESMS) was conducted by direct infusion of the sample (20μlmin^{-1}) into a Micromass LCT orthogonal acceleration time of flight (TOF) mass spectrometer (Waters, Micromass U.K. Ltd. Manchester U.K.). High resolution measurements were made (It can be used for very large molecules with a typical resolving accuracy of 1 part per 10000) using a Lockmass accessory with leucine enkapholin reference. LC-MS analysis used a Waters Alliance 2695 separations module coupled to the Micromass LCT in ESI positive mode and Waters 486 UV detector at 246nm. The HPLC method used a C18 XBridge analytical column (2.1 x 50 mm, 3.5 um particle size); column temperature 25°C, flow rate 0.2 mlmin^{-1}; initial mobile phase 98 % A (A: 0.1% formic acid): 2% B (B: 0.1% formic acid in methanol).

The final composition of 50% A: 50% B was attained using a linear gradient over a 10-minute analysis period. Operational settings for the LCT were: capillary voltage: 3000 V, sample cone voltage: 30 V, RF lens: 250 V, acceleration voltage: 200 V, desolvation temperature: 200°C, source temperature: 100°C, cone gas flow: 22 L/h and desolvation gas flow 750 L/h. LCT calibration was performed using NaICsI solution. Leu-Enk 1ngml^{-1} post column split for 0.2 mlmin^{-1} flow was 5:1 UV:LCT. Optimised HPLC conditions: for the analysis of the synthesised products, an effective HPLC separation system was set up using the chosen XBridge column.

After numerous isocratic systems were tried using different ratios of acetonitrile: water; a gradient system adapted from (Hodel *et al.*, **2009**), was determined to be most effective. The HPLC conditions used were as follows; mobile Phase: solvent A: water: 0.2% ammonium formate: 0.5% formic acid; solvent B: acetonitrile: 0.5% formic acid UV-Detector: ultraviolet detector; column: C_{18} XBridge, 3.5µm column 4.6x50mm; temperature: 25°C; flow rate: 0.3 ml/min; injection: 10 µm. 4-Chloro-2-((6-methoxypyridin-3-yl)amino)benzoic acid was

synthesised according to Besly and Takahashi. Synthesis of pyronaridine was carried out by a modification of the method described by Zheng *et al* (**1982**).

5.6.1. 45. 4-Chloro-2-((6-methoxypyridin-3-yl)amino)benzoic acid: Ullmann coupling using pentanol.

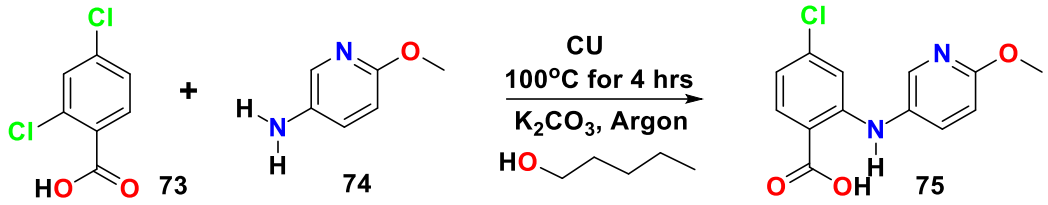

Figure 5.37. Scheme 48. Ullmann coupling reaction, using pentanol, argon, reflux.

2:4-Dichlorobenzoic acid (**73**) (19.10g, 0.1 moles), anhydrous potassium carbonate, freshly fused over a Bunsen flame and stored in the oven at 160^{o}C, (6.91g), copper (II) oxide (Cupric oxide; 0.99 g) catalyst and pentanol (100 ml) in a 3-necked flask (equipped with a condenser, gas inlet tube and thermometer) was stirred at ca. 100°C for 4 hr. Producing the potassium salt of dichlorobenzoic acid in a voluminous state (Figure 5.37).

Then 5-amino-2 methoxypyridine (**74**) (12.41g, 0.1mole) was added by cannula under dry argon and the mixture was stirred for 3hrs under reflux. Water formed was continuously removed by anhydrous molecular sieves (3Å) held in a constricted tube in the neck of the reflux condenser. A Dean-Stark condenser proved ineffective.

Progress of the reaction was monitored by TLC. After the reaction was complete (3 hrs), mixture was poured into water and basified with potassium carbonate water it could hydrolyse (pH was checked by universal indicator paper). Subsequently, the pentanol was removed by steam distillation under reduced pressure using a rotary evaporator. The residual aqueous liquor was decanted from the blue-black tar. Acidification to pH 6.5 precipitated more blue-black tar; after removal of this with charcoal, the solution was stirred at ca. 80^{o}C, and adjusted to pH 4 by addition of conc. hydrochloric acid dropwise. The precipitated 4-chloro-2-(6-methoxypyridin-3-ylamino)benzoic acid (**75**) was filtered at the pump and washed with boiling water to remove unchanged starting material. A bluish white powder was produced (17.0 g, 61%). The pure acid separated from ethyl methyl ketone in colourless needles. λ_{max} = 227 nm; HPLC retention time: 12.46 min. (m. p. 178-180°C).

5.6.2. (46) 4-Chloro-2-((6-methoxypyridin-3-yl)amino)benzoic acid: Ullmann coupling using anhydrous DMF.

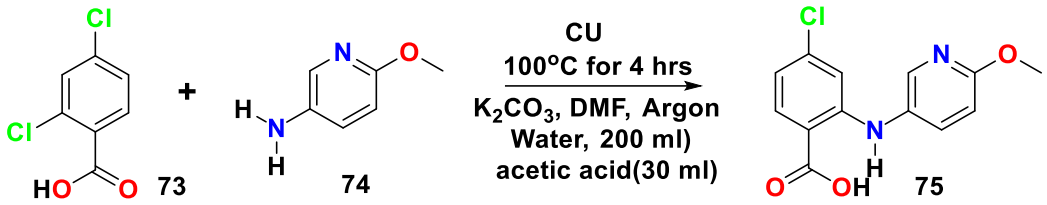

Figure 5.38. Scheme 49. Ullmann coupling reaction, using DMF, argon, reflux.

To a solution of 2,4-Dichlorobenzoic acid (**73**) (2.0 g, 0.0105 mol) in DMF (50 mL) was added 5-amino-2-methoxypyridine (**74**) (0.87 g, 0.007 mol), potassium carbonate (2.00 g, 0.0145 mol) and copper nano powder (0.20 g, 0.0031 mol). After heating at 100°C (20 hrs), the reaction mixture was cooled to room temperature, and poured to water (200 mL) and acetic acid (30 ml), followed by extraction with ethyl acetate. The condensed organic phase was then separated by flash column chromatography using a mixture of petroleum ether (b.p. 40-60) and ethyl acetate (4/1: v/v) as the eluent to give a cream solid (1.08 g, yield 55 %) (Figure 5.38).

Molecular Formula = $C_{13}H_{11}ClN_2O_3$. ^{1}H NMR (300 MHz, $CDCl_3$) δ: 11.73 (1H, s), 9.16 (1H, s), 8.11 (1H, s), 7.94 (1H, d, *J* = 3.7 Hz), 7.50 (1H, dd, *J* = 8.8, 2.3 Hz), 6.82 (1H, d, *J* = 8.6 Hz), 6.76 (1H, s), 6.69 (1H, d, *J* = 8.6 Hz), 3.97 (3H, s).

5.6.3. (47) 7,10-dichloro-2-methoxybenzo[*b*][1,5]naphthyridine.

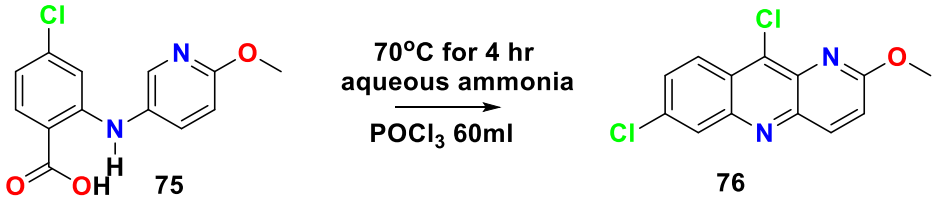

Figure 5.39. Scheme 50. Acridine cyclisation, $POCl_3$, DMF, reflux.

Anhydrous 4-chloro-2-(6-methoxy-3-pyridylamino)benzoic acid (**75**) (27.8 g, moles)) was refluxed with freshly distilled phosphoryl chloride (60 ml, one drop dry DMF) for 4 hrs. Excess phosphoryl chloride (ca. 40 ml) was pumped off (15 mm Hg, oil bath at 70°C) and the residual viscous liquid was slowly poured on crushed ice (200 g) and aqueous ammonia (60 ml, d 0.88) with constant stirring. More ice and ammonia were added when required to maintain the temperature at 0°C and the mixture was kept just alkaline at all times (universal indicator paper). After 12 hrs at 4°C (refrigerator), the solid precipitate was collected, washed

with ice-water, dried (over solid KOH in a desiccator). The 7,10-dichloro-2-methoxybenzo[b] [1,5]naphthyridine (**76**)(26.6 g) 96% yield was obtained as a light yellow powder, m. p. 181-184°C. Analytical sample recrystallised from acetone: yellow needles, m.p. 186-188°C (Figure 5.39).

Molecular Formula = $C_{13}H_8Cl_2N_2O$. ^{1}H NMR (300 MHz, $CDCl_3$) δ: 8.39 (1H, d, *J* = 9.2 Hz), 8.16 (1H, d, *J* = 9.2 Hz), 7.93 (1H, d, *J* = 8.7 Hz), 7.60 (1H, d, J = 9.2, 1.5 Hz), 7.27 (1H, d), 4.21 (3H, s).

^{13}C NMR (CD_3OD), δ: 54.3(CH_3), 104.3 (CH, C3), 121.3 (Cq, C10a), 122.5 (CH, C4), 125.1 (Cq, C9a), 126.3 (CH, C9), 129.3 (CH, C6), 129.6 (CH, C8), 138.7 (Cq, C7), 139.7 (Cq, C10), 143.5 (Cq, C4a), 149.7 (Cq, C5a), 159.7 (Cq, C2),. MS m/z 278. Calcd for $C_{13}H_8Cl_2N_2O$: C 55.94, H 2.89, Cl 25.40, N 10.04, O 5.73.

5.6.4. (48). 4-((7-chloro-2-methoxybenzo[b][1,5]naphthyridin-10-yl)amino)phenol.

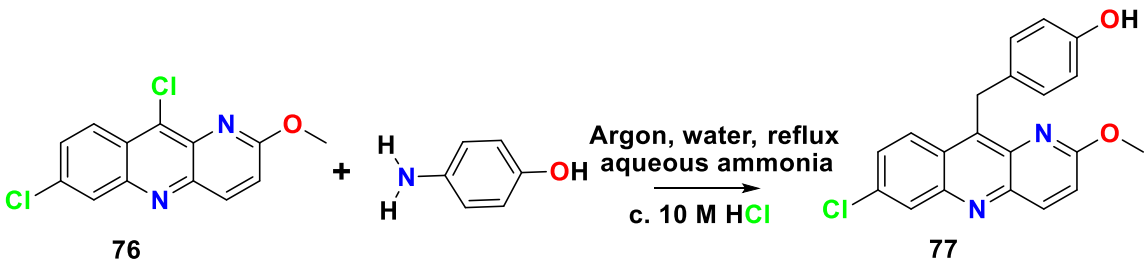

Figure 5.40. Scheme 51. Substitution of chlorine, by *p*-aminophenol on acridine ring.

A flask was charged with both *p*-aminophenol (1.2 g), finely ground 7,10-dichloro-2-methoxy benzo[b][1,5]naphthyridine (**76**)(2.78g) to which was added, degassed and deionised water (30ml) under a blanket of argon. Subsequently, c.10M HCl was added dropwise (1.2ml), and refluxed with magnetic stirring until the yellow mixture fully dissolved and turned orange-red (24 hours). This was then filtered immediately under argon, and washed with dilute ammonia (2M), then washed with ice-cold deionised water, and recrystallized (using excess 95% ethanol). 4-((7-chloro-2-methoxybenzo[b][1,5]naphthyridin-10-yl)amino)phenol (**77**)(2.57g). TLC of free base on a) silica gel: ethyl acetate/hexane 1:1; R_f = 0.72; Product = 0.29%, unknown fluorescent blue spot (corresponding quinone, 4-((7-chloro-2-methoxybenzo[b] [1,5]naphthyridin-10-yl)imino)cyclohexa-2,5-dien-1-one) R_f = 0.17; b) Alumina; R_f =0.70; Product = 0.33 (Figure 5.40).

Molecular Formula = $C_{19}H_{14}ClN_3O_2$. ^{1}H NMR (1mg in 0.7ml DMSO-d_6, 300 MHz) δH: 3.96 (3H, s, (H15, OCH3), 8.23 (1H, d, J=9.00Hz, (H4)), 7.77 (2H, d, J = 9.00, (H13, H13')), 7.05 (2H, d, J = 9.00 (H12, H12')), 7.21 (1H, dd, J = 9.33, 2.19 Hz, (H8)), 7.31 (1H, d, J = 9.07 Hz, (H3)), 7.76 (1H,d, J = 9.33 Hz, (H9)), 7.94 (1H, d, J = 2.19 Hz, (H6)), 9.01 (1H, bs, (1x NH), 9.40 (1H, bs, (1x OH); all peaks assigned using DQF-COSY experiments.

^{13}C NMR (Partial)(DEPTQ) 1mg in 0.7ml DMSO-d_6: 75.5 MHz, 300K, δ: 159.27 (C2, q), 154.33 (C10, q), 153.15 (C14, q)140.38 (C6, CH), 135.87 (C11, q), 133.71 (C5a, q), 127.98 (C7, q), 127.60 (C8, CH), 126.66 (C9, CH), 125.11 (C12, CH), 122.99 (C4, CH), 118.99 (C13, CH), 115.60 (C3, CH), 116.06 (C9a, q), 53.69 (C15, CH_3). 2 of the 9 expected quaternary carbons were not detected, possibly due to poor solubility in DMSO-d_6 (m.p. 178-180°C).

5.6.5. (49) 4-((7-chloro-2-methoxybenzo[b][1,5]naphthyridin-10-yl)amino)-2,6-bis(pyrrolidin-1-ylmethyl)phenol (**15**) Synthesis.

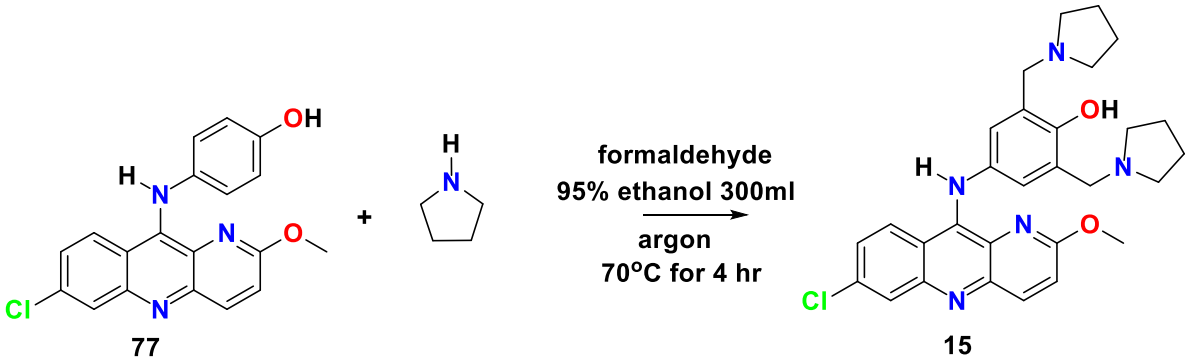

Figure 5.41. Scheme 52. Addition reaction, pyrrolidine, formaldehyde, argon, reflux.

4-((7-chloro-2-methoxybenzo[b][1,5]naphthyridin-10-yl)amino)phenol (**77**) (60g, 0.17 moles)), 30% formaldehyde (78ml) and pyrrolidine (60g, 0.85 moles), was refluxed in 95% ethanol (300ml) for 4 hours until fully dissolved. The ethanol was removed under reduced pressure and condensed to small volume and left in a refrigerator (24 Hrs) under argon to form a red precipitate. This material was recrystallized using ethanol (95%) to give 38.3g of product (yield 43.7%, m.p. 174-176°C, decomposed). $C_{29}H_{32}ClN_5O_2$ Calculated (%) C67.24, H6.18, N13.52, Cl6.85, Found value (%) C67.00, H6.38, N13.54, Cl 7.11. Infrared spectra (KBr cm^{-1}); 3500, 3350, 2800, *v* cm^{-1} (Figure 5.41).

Molecular Formula = $C_{29}H_{32}ClN_5O_2$. ^{1}H NMR (90MHz CDCl3 TMS as internal standard) δH: 1.84-2.42 (8H, m, pyrrolidine ring), 1.84-2.42 (8H, m, pyrrolidine ring), 3.75(4H, s, bibenzyl), 4.12 (3H, s, methoxy), 7.07 (2H, benzene, m, H2' and H6') 7.25, 7.66, 8.28 (3H, d, each, benzonaphthyridine H6, *J* = 10, H8, J=3, H9, *J* = 10). Peaks disappeared at 8.47 (2H) when exchanged with D_2O proved to be hydroxy and amino groups (the most deshielded).

^{13}C NMR (CD_3OD), δ: 23.0, 53.1, 55.3, 119.5, 124.1, 124.7, 126.3, 127.0, 127.9, 135.2, 138.7, 141.9, 148.4, 154.6, 160.3; MS m/z 518.24 [M1]. Calcd for $C_{29}H_{32}ClN_5O_2$: C 67.23, H 6.23, N 13.52. Found: C 66.89, H 6.33, N 13.27.

5.6.6. (50) 4-((7-chloro-2-methoxybenzo[b][1,5]naphthyridin-10-yl)amino)-2,6-bis(pyrrolidin-1-ylmethyl)phenol tetraphosphate hydrate (**78**).

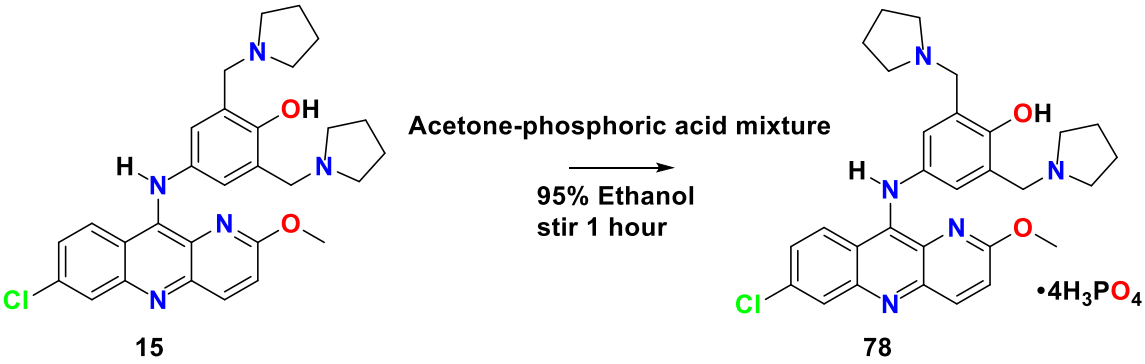

Figure 5.42. Scheme 53. Synthesis of pyronaridine tetraphosphate using Ethanol.

4-((7-chloro-2-methoxybenzo[*b*][1,5]naphthyridin-10-yl)amino)-2,6-bis(pyrrolidin-1-ylmethyl)phenol (**15**) was dissolved in 95% ethanol. To which was added an acetone-phosphoric acid mixture till the solution became acidic, depositing the tetraphosphate hydrate. The solid was recrystallised from ethanol 70% ethanol three times, dried (105°C).

m. p. 223-225°C (decomposed), (lit value M.p. 180-182°C, Park *et al*., 2007) yield, 82%. UV λ_{max} 260, 275nm. $C_{29}H_{32}ClN_5O_2 \cdot 4H_3PO_4$. Calculated value (%) C38.26, H4.83, N7.69, Cl3.69, P13.63, found value (%) C 38.22, H 5.24, N 7.44, Cl 3.95, P 13.61.

Molecular Formula = $C_{29}H_{36}ClN_5O_{14}P_4$. ^{1}H NMR (10mg in 0.7ml DMSO-d_6, 300 MHz) δH: 8.24 (1H, d, J=9.00Hz, (H4)), 7.99 (1H, d, *J* = 2.10 Hz, (H6)), 7.93 (1H, d, *J* = 9.30 Hz, (H9)), 7.31 (1H, d, *J* = 9.00 Hz, (H3)), 7.30 (1H, dd, J = 9.30, 2.40 Hz, (H8)), 7.21 (2H, s, (H13, H13')), 6.46 (5H, bs, (P(OH))), 4.11 (4H, s, (H16, H16')), 3.83 (3H, s, (OCH3)), 1.92-2.90 (8H, bs, pyrrolidine ring), 1.92-2.90 (8H, bs, pyrrolidine ring). (NH peak was not observed, off the chart)

^{13}C NMR DMSO- d_6, 75.5 MHz, 300 MHz): 159.02 (C2, q), 152.49 (C10, q), 147.74 (C15, q), 143.70 (C5a, q), 142.77 (C7, q), 140.12 (C6, CH), 135.87 (C4a, q), 133.71 (C12, q), 127.98 (C14, q), 127.25 (C9, CH), 126.51 (C4, CH), 126.28 (C8, CH), 123.69 (C3, CH), 122.48 (C8, q), 118.99 (C13, CH), 116.06 (C9a, q), 53.50 (OCH_3), 53.31 (C18, CH_2), 52.64 (C16, CH_2), 22.54 (C19, CH_2).

5.6.7. NMR of Pyronaridine in D_2O.

Molecular Formula = $C_{29}H_{36}ClN_5O_2$. ^{1}H NMR (D_2O): δH: 1.80-2.06 (16H, dd, CH_2 , 2", 3", 4", 5"), 3.02-3.22 (4H, s, CH_2), 3.80 (3H, s, OCH_3), 7.12 (2H, , m, H2', H6'), 7.28 (1H, d, H3), 7.42 (1H, dd, H8), 7.42 (1H, d, 1H, d, H6), 7.75 (1H, dd, H9), 8.09 (1H, d, H4).

^{13}C NMR (D_2O): δ: 21.6, 52.3, 52.7, 53.7, 111.7, 118.5, 121.3, 122.7, 123.1, 125.5, 126.7, 129.3, 130.9, 132.5, 138.7, 139.3, 152.3, 153.7, 158.9.

5.6.8. 51. Synthesis of pyronaridine tetraphosphate from pyronaridine (15)(II).

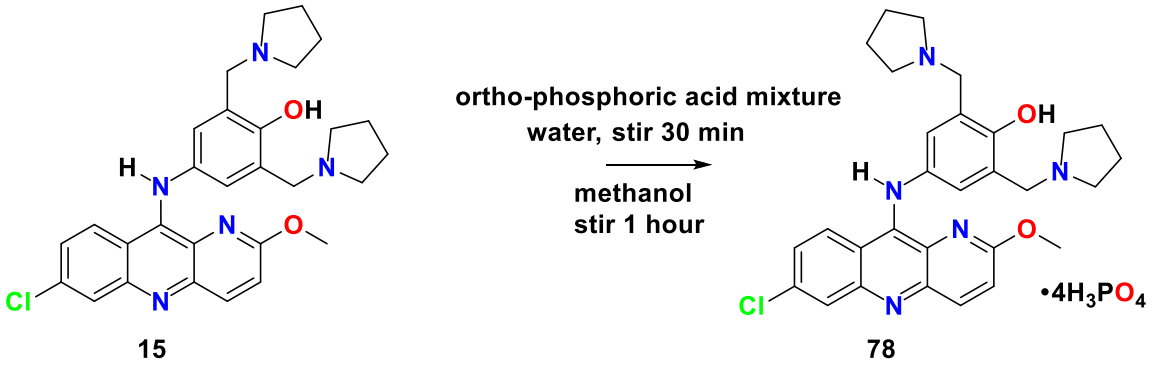

Figure 5.43. Scheme 54. Synthesis of pyronaridine tetraphosphate using methanol.

Pyronaridine (**15**) (0.246 g, 0.0005 mol), distilled water (2.5 ml) and *ortho* phosphoric acid (2.5 ml) were mixed and stirred at RT for 30 min. The mixture was filtered and washed with distilled water. Methanol (0.325 mL) was added to the crude product and stirred at 5–10°C for 1 hr. Then acetone was added to the mixture until pyronaridine tetraphosphate (**78**) particles were observed, filtered and washed with acetone again. The residue was added to a mixture solution of 70% ethanol (5 mL) and *ortho* phosphoric acid (5ml) and stirred at around 60°C for 1 hr. Then it was filtered and washed with acetone (Figure 5.43). The solid sample was dried under vacuum to yield 95%. M.p. 183-185°C. IR (KBr): *v* 3406, 2949, 1631, 1577, 1551, 1526, 1489, 1459, 1389, 1350,1285, 1091, 991 cm^{-1}.

Molecular Formula = $C_{29}H_{36}ClN_5O_{14}P_4$. ^{1}H NMR ($D_2O$), δ: 1.81-2.00 (16H, dd, CH_2 , 2", 3", 4", 5"), 3.03 (4H, s, CH_2), 3.88 (3H, s, OCH_3), 7.01 (2H, m, H2', H6'), 7.38 (1H, d, H3), 7.42 (1H, dd, H8), 7.73 (1H, d, H6), 8.02 (1H, d, H4). NH and OH were not observed.

^{13}C NMR (D_2O): δ 22.4, 53.2, 54.0, 54.5, 111.3, 118.5, 122.1, 123.2, 124.9, 126.1, 127.4, 130.8, 131.3, 132.5, 132.7, 139.7, 140.7, 152.2, 154.5, 160.9; MS m/z 518.4 [M1_(H_3PO_4)]. Calcd for $C_{29}H_{32}ClN_5O_2$: C 38.27, H 4.87, N 7.70.

5.6.9. 52. 4-((7-chloro-2-methoxybenzo[b][1,5]naphthyridin-10-yl)amino)-2,6-bis(pyrrolidin-1-ylmethyl)phenol trihydrochloride dehydrate.

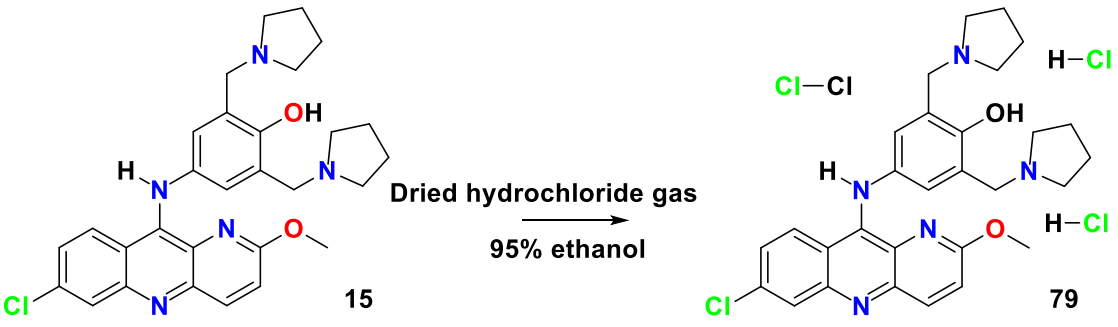

Figure 5.44. Scheme 55. Synthesis of pyronaridine trihydrochloride.

Dried hydrogen chloride gas was passed into the free base of pyronaridine suspended in acetone solution to form the hydrochloride salt (**79**). This material was crystallized with ethanol (95%) to give a product with a melting point of 218-220°C (decomposed) (Figure 5.44), $C_{29}H_{32}ClN_5O_2 \cdot 3HCl \cdot 2\ H_2O_2$ (Check HCl and H_2O_2) calculated value (%) N10.55, Cl 21.41, H_2O 5.61, Found value (%) N10.61, Cl 21.28, H_2O 5.41.

IR (KBr): *v* cm^{-1} 3307, 2965, 2872, 2806, 1621, 1571, 1519,1493, 1465, 1403, 1377, 1305, 1271, 1094, 1068, 1000, 927, 867, 834, 808 cm^{-1}.

Molecular Formula = $C_{29}H_{36}ClN_5O_2$. ^{1}H NMR (CD_3OD), δ: 1.81-2.61 (16H, dd, CH_2 , 2", 3", 4", 5"), 3.74 (4H, s, CH_2), 4.05 (3H, s, OCH_3), 7.01 (2H, , m, H2', H6'), 7.27 (1H, d, H3), 7.64(1H, dd, H8), 7.87 (1H, d, H6), 7.95 (1H, dd, H9), 8.13 (1H, d, H4). NH and OH were not observed.

^{13}C NMR (CD_3OD), δ: 23.0, 53.1, 55.3, 119.5, 124.1, 124.7, 126.3, 127.0, 127.9, 135.2, 138.7, 141.9, 148.4, 154.6, 160.3; MS m/z 518.24 [M1]. Calcd for $C_{29}H_{32}ClN_5O_2$: C 67.23, H 6.23, N 13.52. Found: C 66.89, H 6.33, N 13.27.

5.7. Microwave method.

5.7.1. 53. Cyclisation of acridine ring.

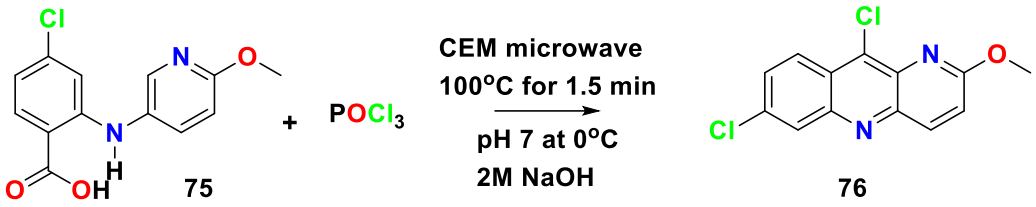

Figure 5.45. Scheme 56. Acridine cyclisation, $POCl_3$, irradiation.

A sample of anhydrous 4-chloro-2-(6-methoxy-3-pyridylamino)benzoic acid (**75**)(0.28 g, 0.0001 mol) was suspended in phosphorus oxychloride (0.5 ml) and heated in the CEM microwave reactor at 100°C for 1.5 min. The mixture was poured onto ice and neutralized dropwise to pH 7 at 0°C with cold 2M NaOH (6.5 ml). The dense yellow-green precipitate obtained was filtered, dried by suction, and sublimed at 60°C, (7,10-dichloro-2-methoxy benzo[b][1,5] naphthyridine)(76) (Figure 5.45).

Molecular Formula = $C_{13}H_8Cl_2N_2O$. ^1H NMR (300 MHz, $CDCl_3$) δ: 8.39 (1H, d, *J* = 9.2 Hz), 8.16 (1H, d, *J* = 9.2 Hz), 7.93 (1H, d, , *J* = 8.7 Hz), 7.60 (1H, d, J = 9.2, 1.5 Hz), 7.27 (1H, d), 4.21 (3H, s).

^{13}C NMR (CD_3OD), δ: 54.3(CH_3), 104.3 (CH, C3), 121.3 (Cq, C10a), 122.5 (CH, C4), 125.1 (Cq, C9a), 126.3 (CH, C9), 129.3 (CH, C6), 129.6 (CH, C8), 138.7 (Cq, C7), 139.7 (Cq, C10), 143.5 (Cq, C4a), 149.7 (Cq, C5a), 159.7 (Cq, C2),. MS m/z 278. Calcd for $C_{13}H_8Cl_2N_2O$: C 55.94, H 2.89, Cl 25.40, N 10.04, O 5.73.

5.7.2. 54. Synthesis of pyronaridine (PND, **15**) from 4-((7-chloro-2-methoxybenzo[b] [1,5]naphthyridin-10-yl)amino)phenol by a microwave irradiation technique.

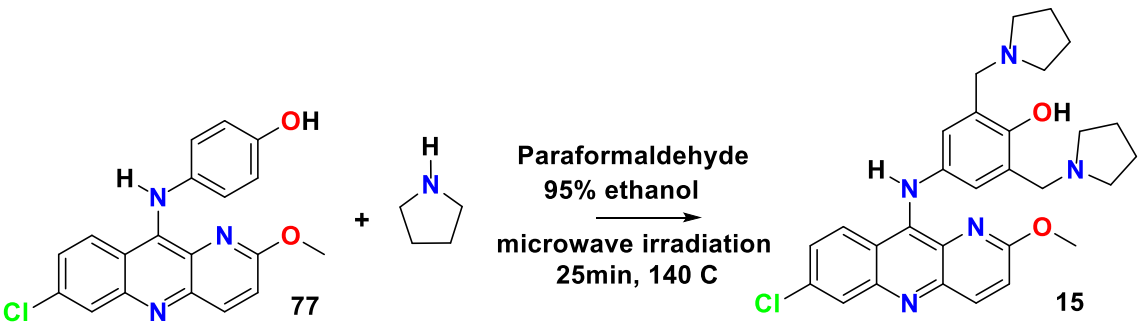

Figure 5.46. Scheme 57. Synthesis of pyronaridine by microwave irradiation.

A 250mL round bottom flask containing a magnetic stirrer was washed with DDW under

an ultra-sonication. Then, paraformaldehyde (5 ml), pyrrolidine (5 ml) and anhydrous ethanol (2.5 ml) were refluxed at 50–60°C for 1hr (Figure 5.46).

4-((7-chloro-2-methoxybenzo[b][1,5]naphthyridin-10-yl)amino)phenol (**77**) (0.419 g, 0.0012 mol) was added to complete the reaction mixture and it was irradiated in a microwave reactor for 25min at 140°C. On completion of the reaction, distilled water (4.2 mL) was added to the mixture and stirred at 15–25°C for 1h, then filtered. The residue was dissolved in anhydrous methanol (4.2 mL) and stirred at 5–10°C for 2 h, then filtered and washed with excessive methanol. The residue was dissolved in a mixture of dimethyl sulfoxide (1.3mL) and dichloromethane (1.3 mL). The mixture was filtered and washed with methanol and finally dried to yield 0.233g (45%) of **15**. m. p. 223-225°C. IR (KBr): n 3307, 2962, 2780, 1620, 1559, 1519, 1494, 1468, 1402, 1377,1301, 1273, 1096, 1070, 1000, 929, 867, 836, 808cm^{-1}.

Molecular Formula = $C_{29}H_{32}ClN_5O_2$. ^1H NMR (CD_3OD), δ: 1.81-2.61 (16H, dd, CH2 , 2'', 3'', 4'', 5''), 3.74 (4H, s, CH2), 4.05 (3H, s, OCH3), 7.01 (2H, , m, H2', H6'), 7.28 (1H, d, H3), 7.65 (1H, dd, H8), 7.87 (1H, d, H6), 7.95 (1H, dd, H9), 8.13 (1H, d, H4). NH and OH were not observed.

^{13}C NMR (CD_3OD): δ: 23.0, 53.1, 55.3, 119.5, 124.1, 124.7, 126.3, 127.0, 128.1, 135.2, 138.7, 145.9, 148.4; MS m/z 518.24 [M1]. Calcd for $C_{29}H_{32}ClN_5O_2$: C 67.23, H 6.23, N 13.52. Found: C 66.36, H 6.13, N 13.06.

5.8. Conclusion.

The synthesis of Pyronaridine, was successfully carried out, using both conventional methods and Microwave synthesis.

All spectral data from authentic samples matched that of synthetic materials produced in this study.

5.9. References.

Acheson, R. M. 1956. Acridines, New York, *Interscience Publishers*.

Albert, A. 1951. The acridines; their preparation, physical, chemical, and biological properties and uses, London, *E. Arnold*.

Albert, A. 1966. The acridines; their preparation, physical, chemical, and biological properties and uses. 2nd ed, London, *Edward Arnold & Co*.

Albert, A., Linnell, W. 1938. 6. Chemotherapeutic studies in the acridine series. Part III. 4-Amino-, 1: 3-, 1: 7-, and 3: 6-diaminoacridines. *Journal of the Chemical Society* (*Resumed*)**.** 22-26.

Alin, M. H., Bjorkman, A., Ashton, M. 1990. *In vitro* activity of artemisinin, its derivatives, and pyronaridine against different strains of *Plasmodium falciparum*. *Trans R Soc Trop Med Hyg.* 84**,** 635-637.

Allen, C., Mckee, G. 1939. Reliable Methods for the Preparation of Acridone. *Organic syntheses*.

Auparakkitanon, S., Chapoomram, S., Kuaha, K., Chirachariyavej, T., Wilairat, P. 2006. Targeting of haematin by the antimalarial pyronaridine. *Antimicrob Agents Chemother.* 50**,** 2197-2200.

Auparakkitanon, S., Wilairat, P. 2000. Cleavage of DNA induced by 9-anilinoacridine inhibitors of topoisomerase II in the malaria parasite *Plasmodium falciparum*. *Biochem Biophys Res Commun.* 269**,** 406-409.

Baker, M. 2016. 1,500 scientists lift the lid on reproducibility. *Nature*. 533, 452–454. https://doi.org/10.1038/533452a.

Babalola, C. P., Scriba, G. K., Sowunmi, A., Alawode, O. A. 2003. Liquid chromatographic determination of pyronaridine in human plasma and oral dosage form. *J Chromatogr B Analyt Technol Biomed Life Sci.* 795**,** 265-272.

Bachman, G. B., Barker, R. S. 1949. Derivatives of the pyridoquinolines. *J Org Chem.* 14**,** 97-104.

Baciocchi, E., Illuminati, G., Marino, G. 1958. Electronic Transmission Through Condensed Ring Systems. III. The Evaluation of epi and cata Sigma Constants from Dissociation and Methoxydechlorination Data on Substituted 1-*Aza*-4-chloronaphthalenes. *J. Am. Chem. Soc.* 80**,** 2270-2273.

Bacon, R., Hill, H. 1965. Copper-promoted reactions in aromatic chemistry. *Quarterly Reviews, Chemical Society.* 19, 95.

Barlin, G., Tan, W. 1986. Potential Antimalarials. III N4 -Substituted 7-Bromo-1,5-naphthyridin-4-amines. *PCT/AU*1986/000142.

Basco, L. K., Le Bras, J. 1992. *In vitro* activity of pyronaridine against African strains of *Plasmodium falciparum*. *Ann Trop Med Parasitol.* 86**,** 447-454.

Basco, L. K., Le Bras, J. 1994. *In vitro* susceptibility of Cambodian isolates of *Plasmodium*

falciparum to halofantrine, pyronaridine and artemisinin derivatives. *Ann Trop Med Parasitol.* 88**,** 137-144.

Basco, L. K., Mitaku, S., Skaltsounis, A. L., Ravelomanantsoa, N., Tillequin, F., Koch, M., Le Bras, J. 1994. *In vitro* activities of furoquinoline and acridone alkaloids against *Plasmodium falciparum*. *Antimicrob Agents Chemother.* 38, 1169-1171.

Basco, L. K., Ringwald, P., Bickii, J. 1996. *In vitro* activity of antimalarials against clinical isolates of *Plasmodium falciparum* in Yaounde, Cameroon. *Am J Trop Med Hyg.* 55**,** 254-258.

Beletskaya, I., Cheprakov, A. 2004. Copper in cross-coupling reactions. *Coordination Chemistry Reviews.* 248**,** 2337-2364.

Besly, D., Goldberg, A. 1954. Antimalarial 2-alkoxy-6-chloro-9-dialkylaminoalkylamino-1 : 10-diaza-anthracenes. *Journal of the Chemical Society (Resumed)*. 2448-2455.

Bigler, P. 2008. Fast ^{13}C-NMR Spectral Editing for Determining CHn Multiplicities. *Spectroscopy Letters.* 41, 162-165.

Bigler, P., Kummerle, R., Bermel, W. 2007. Multiplicity editing including quaternary carbons: improved performance for the ^{13}C-DEPTQ pulse sequence. *Magn Reson Chem.* 45**,** 469-472.

Bonse, S., Santelli-Rouvier, C., Barbe, J., Krauth-Siegel, R. L. 1999. Inhibition of Trypanosoma cruzi trypanothione reductase by acridines: kinetic studies and structure-activity relationships. *J Med Chem.* 42, 5448-5454.

Bunnett, J. F. 1958. Mechanism and reactivity in aromatic nucleophilic substitution reactions. *Quarterly Reviews, Chemical Society.* 12(1), 1-16.

Bunnett, J. F., Zahler, R. 1951. Aromatic Nucleophilic Substitution Reactions. *Chemical Reviews.* 49(2), 273-412.

Burckhalter, J. H., Tendick, F. H. Jones, E, M., Jones, P, A., Holcomb, W. F., A. L. Rawlins, A, L. 1948. Aminoalkyl phenols as antimalarials (heterocyclicamino)-alpha-amino-o-cresols; the synthesis of camoquin. *J Am Chem Soc.* 70**,** 1363-1373.

Burger, R., Bigler, P. 1998. DEPTQ: distorsionless enhancement by polarization transfer including the detection of quaternary nuclei. *J Magn Reson.* 135, 529-534.

Cain, B. F., Seelye, R. N., Atwell, G. J. 1974. Potential antitumor agents. 14. Acridylmethanesulfonanilides. *J Med Chem.* 17, 922-930.

Carrasco, R., Pellon, R., Elguero, J., Goya, P., Paez, I. 1989. Ullmann and Goldberg Reactions-copper Catalyzed C-N-, C-O- and C-S-Coupling. *Synthetic Communications.* 19, 2077-2080.

Chandrakumar, N. 1984. Polarization transfer between spin-1 and spin- nuclei. *Journal of Magnetic Resonance.* 60, 28-36.

Chang, C., Lin-Hua, T., Jantanavivat, C. 1992. Studies on a new antimalarial compound: pyronaridine. *Trans R Soc Trop Med Hyg.* 86**,** 7-10.

Chavalitshewinkoon-Petmitr, P., Pongvilairat, G., auparakkitanon, S., Wilairat, P. 2000. Gametocytocidal activity of pyronaridine and DNA topoisomerase II inhibitors against multidrug-resistant *Plasmodium falciparum in vitro*. *Parasitol Int.* 48**,** 275-280.

Chen, W. H., Yang, D., Wang, W. Y., Zhang, J., Wang, Y. P. 2010. Cellular electrophysiological effects of changrolin isolated rat cardiac myocytes. *Eur. J. OF Pharmacol*. 647, 139-146.

Childs, G. E., Hausler, B., Milhous, W., Chen, C., Wimonwattrawatee, T., Pooyindee, N., Boudreau, E. F. 1988. *In vitro* activity of pyronaridine against field isolates and reference clones of *Plasmodium falciparum*. *Am J Trop Med Hyg,* 38**,** 24-29.

Chin. *Chem. Lett*. 31, 2020, pp. 404-408.

Chorvat, R. J., Black, L. A., Ranade, V. V., Barcelon-Yang, C., Stout, D. M., Brown, B. S., Stampfli, H. F., Quon, C. Y. 1993. Mono- and bis(aminomethyl)phenylacetic acid esters as short-acting antiarrhythmic agents. 2. *J Med Chem.* 36, 2494-2498.

Co., M. A., Tsung-Ying, S., Walford, G. L., Witzel, B. E. 1971. *Pyridon- und Thiopyridonderivate,die als entzuendung shemmende Mittel geeignet sind*. DE19702059358.

Corbett, R., Sweetman, B. 1963. Synthesis of Pyrido[3,4-b]quinolin-5(*10H*)-one and Pyrido[3,2- b]-quinolin-1O(5H)-one. *J. Chem. Soc*. 6058-6059.

Craig, J., Johns, S., Moyle, M. 1963. Amine Exchange Reactions. Mannich Bases from Primary Aliphatic Amines and from Amino Acids. *The Journal of Organic Chemistry.* 28, 2779-2783.

Croft, S. L., Duparc, S., Arbe-Barnes, S. J., Craft, J. C., Shin, C. S., Fleckenstein, L., Borghini-Fuhrer, I., Rim, H. J. 2012. Review of pyronaridine anti-malarial properties and product characteristics. *Malar J.* 11, 270.

Cummings, T., Shelton, J. 1960. Mannich Reaction Mechanisms. *The Journal of Organic Chemistry.* 25, 419-423.

Dabira, E. D., Hachizovu, S., Conteh, B., Mendy, A., Nyang, H., Lawal, B., Ndiath, M. O., Mulenga, J. M., mwanza, S., Borghini-Fuhrerorg, I., Arbe-Barnes, S., Miller, R., Shin, J., Duparc, S., D'alessandro, U., Manyando, C., Achan, J. 2022. Efficacy, Safety and Tolerability of Pyronaridine-artesunate in Asymptomatic Malaria-infected Individuals: a Randomized Controlled Trial. Clinical infectious diseases: *an official publication of the Infectious Diseases Society of America*. 74(2), 180–188.

Dai, Q., Chen, J., Gao, C., Sun, Q., Z. Yuan, Z., Jiang, Y. 2020. Design, synthesis and biological evaluation of novel phthalazinone acridine derivatives as dual PARP and Topo inhibitors for potential anticancer agents. *Chinese Chemical Letters*. Volume 31, Issue 2, February, Pages 404-408

Dai, Q., Chen, J., Gao, C., Sun, Q., Z. Yuan, Z., Jiang, Liu, Y., Xiao, B., Chen, C. 2018. Highly sensitive and selective “naked eye” sensing of Cu(II) by a novel acridine-based sensor both in aqueous solution and on the test kit. *Tetrahedron*. Volume 74, Issue 44, November, Pages 6459-6464.

Denny, W. A., AtwelL, G. J., Cain, B. F. 1977. Potential antitumor agents. 25. Azalogues of the 4'-(9-acridinylamino)methanesulfonanilides. *J Med Chem*. 20, 1242-1246.

Dimmock, J., Kumar, P. 1997. Anticancer and cytotoxic properties of Mannich bases. *Current Medicinal Chemistry*.

Doddrell, D., Pegg, D., Bendall, M. 1982. Distortionless enhancement of NMR signals by polarization transfer. *Journal of Magnetic Resonance.* 48, 323-327.

Elderfield, R. C. 1950. Heterocyclic compounds, New York, *Wiley*.

Elueze, E. I., Croft, S. L., Warhurst, D. C. 1996. Activity of pyronaridine and mepacrine against twelve strains of *Plasmodium falciparum in vitro*. *J Antimicrob Chemother,* 37**,** 511-518.

Evano, G., Blanchard, N., Toumi, M. 2008. Copper-mediated coupling reactions and their applications in natural products and designed biomolecules synthesis. *Chem Rev.* 108**,** 3054-3131.

Fanta, P. E. 1946. The Ullmann synthesis of biaryls. *Chem Rev.* 38, 139-196.

Feng, Z., Jiang, N. X., Wang, C. Y., Zhang, W. 1986. [Pharmacokinetics of pyronaridine, an antimalarial in rabbits]. *Yao Xue Xue Bao.* 21, 801-805.

Feng, Z., Wu, Z. F., Wang, C. Y., Jiang, N. X. 1987. [Pharmacokinetics of pyronaridine in malaria patients]. *Zhongguo Yao Li Xue Bao*. 8, 543-546.

Fu, S., Bjorkman, A., Wahlin, B., Ofori-Adjei, D., Ericsson, O., Sjoqvist, F. 1986. *In vitro* activity of chloroquine, the two enantiomers of chloroquine, desethyl chloroquine and pyronaridine against *Plasmodium falciparum*. *Br J Clin Pharmacol.* 22**,** 93-96.

Goldberg, A. A. 1956. Substituted litd-diaza-anthracenes. *United States patent application*.

Goldberg, A. A., Kelly, W. 1946. Synthesis of diaminoacridines. *J Chem Soc,* 102-111.

Goldberg, A. A., Kelly, W. 1947. Synthesis of diaminoacridines. *J Chem Soc*. 595-597.

Goldberg, I. 1907. Ueber Phenylierung von primaren aromatischen Aminen. *Berichte der deutschen chemischen Gesellschaft.* 40, 4541-4546.

Goldberger, I. 1906. Ueber Phenylirungen bei Gegenwart von Kupfer als Katalysator. . *Berichte der deutschen chemischen Gesellschaft.* 39, 1691-1692.

Graebe, C., Lagodzinski, K. 1892. Ueber Phenylantranilsäure und *Acridon. Ber. Dtsch. Chem. Ges*. 25, 1733–1736.

Gwizdek, C., Leblanc, G., Bassilana, M.1997. Proteolytic mapping and substrate protection of the Escherichia coli melibiose permease. *Biochemistry*. 36:8522–8529. https://doi.org/10.1021/bi970312.

Hanoun, J., Galy, J. Tenaglia, A. 1995. A Convenient Synthesis of N-Arylanthranilic Acids Using Ultrasonics in the Ullmann-Goldberg Condensation. *Synthetic Communications.* 25, 2443-2448.

Hodel, E. M., Zanolari, B., Mercier, T., Biollaz, J., Keiser, J., Olliaro, P., Genton, B., Decosterd, L. A. 2009. A single LC-tandem mass spectrometry method for the simultaneous determination of 14 antimalarial drugs and their metabolites in human plasma.

J Chromatogr B Analyt Technol Biomed Life Sci. 877, 867-886.

Huang, L. S., Zhengh, X.Y., Chen C., Yao S.P. 1979. Synthesis of M6407, a new anti-malarial agent. 14(9), 561-562.

Ingold, C. 1969. Structure and mechanism in organic chemistry, Ithaca, *Cornell University Press*.

Ismail, F., Dascombe, M., Drew, M. 2009. Modulation of drug pharmacokinetics and pharmacodynamics by fluorine substitution. *Chimica Oggi:Chemistry Today.* 27**,** 18-22.

Ismail, F., Drew, M., Navaratnam, S., Bisby, R. 2009. A pulse radiolysis study of free radicals formed by one-electron oxidation of the antimalarial drug pyronaridine. *Research on Chemical Intermediates.* 35**,** 363-377.

Jourdan, F. 1885. Neue Synthesen von Derivaten des Hydroacridins und Acridins. *Berichte der deutschen chemischen Gesellschaft.* 18**,** 1444-1456.

Kermack, W., Wetherhead, A. 1942. Some Anilinopyridine Derivatives. *J.Chem. Soc.*, 726-727.

Kincaid, J., Kavthe, R. D., Caravez, J. C., Thaka, B. S., Thakore, R. R., Lipshutz, B. H. 2022. Environmentally Responsible and Cost-Effective Synthesis of the Antimalarial Drug Pyronaridine. *Organic letters*. 24(18), 3342–3346. https://doi.org/10.1021/acs.orglett.2c00944.

Klisiecki, L., Sucharda, E. 1927. Ueber eine Synthese des 1.5-Naphthyridins. *Berichte der deutschen chemischen Gesellschaft (A and B Series).* 7**,** 204.

Kornblum, N., Kendall, D. 1952. The Use of Dimethylformamide in the Ullmann Reaction. *J. Am. Chem. Soc.* 74, 5782-5782.

Kotecka, B. M., Barlin, G. B., Edstein, M. D., Rieckmann, K. H. 1997. New quinoline di-Mannich base compounds with greater antimalarial activity than chloroquine, amodiaquine, or pyronaridine. *Antimicrob Agents Chemother*. 41, 1369-1374.

Lee, H. H., Wilson, W. R., Ferry, D. M., Van Zijl, P., Pullen, S. M., Denny, W. A. 1996. Hypoxia-selective antitumor agents. 13. Effects of acridine substitution on the hypoxia-selective cytotoxicity and metabolic reduction of the bis-bioreductive agent nitracrine N-oxide. *J Med Chem.* 39, 2508-2517.

Lee, J., Son, S., Chung, J., Lee, E. S., Kim, D. H. 2004. *In vitro* and *in vivo* metabolism of pyronaridine characterized by low-energy collision-induced dissociation mass spectrometry with electrospray ionization. *J. Mass Spectrom.* 39, 1036–1043

Lee, D. W., Lee, S. K., Cho, J. H., Yoon, S. S. 2014. Improved Manufacturing Process for Pyronaridine Tetraphosphate." *Bulletin of the Korean Chemical Society.* 35, no. 2, February, 521–24. doi:10.5012/BKCS.2014.35.2.521.

Lesnianski, W., Dziewonski, K. 1929. Acridone compounds. *Przemysl Chemiczny.* 13, 13,401-13,402.

Ley, S. V., Thomas, A. W. 2003. Modern synthetic methods for copper-mediated C(aryl)[bond]O, C(aryl)[bond]N, and C(aryl)[bond]S bond formation. *Angew Chem*

Int Ed Engl. 42, 5400-5449.

Liu, Y., Zhang, Z., Wu A., Yang, X., Zhu, Y., Zhao, N. 2014. A Novel Process for Antimalarial Drug Pyronaridine Tetraphosphate. 2014. *Organic Process Research & Development. 18* (2), 349-353. DOI: 10.1021/op400357f.

Longuet-Higgins, H. C., Coulson, C. A. 1947. A theoretical investigation of the distribution of electrons in some heterocyclic molecules containing nitrogen. *Trans. Faraday Soc.* 43, 87.

Mackeigan, J., Martin, K., Xu Huaqiang, E., Xu, Y. 2012. *patent Methods for Treating Autophagy-Related Disorders*.

Magidson, O., GRigorovskii, A. 1933. Formation of meso-chloroacridines, and the mobility of chlorine in the mesoposition. Berichte der Deutschen Chemischen Gesellschaft, *Berichte der Deutschen Chemischen Gesellschaft, (Abteilung) B: Abhandlungen* 66B, 866-872.

Mannich, C., Krosche, W. 1912. Ueber ein Kondensationsprodukt aus Formaldehyd, Ammoniak und Antipyrin. *Arch. Pharm. Pharm. Med. Chem.* 250, 647-667.

Mouesca, J. M., Rius, G., Lamotte, B. 1993. Single-crystal proton ENDOR studies of the [Fe4S4]3+ cluster: determination of the spin population distribution and proposal of a model to interpret the 1H NMR paramagnetic shifts in high-potential ferredoxins. *J. Am. Chem. Soc.* 115**,** 4714-4731.

Muci, A., Buchwald, S. 2001. Practical Palladium Catalysts for CN and CO Bond Formation. *Topics in Current Chemistry.* 219.

Nolis, P., Parella, M., T Perez-Trujillo, T. 2007. CN-HMBC: a powerful NMR technique for the simultaneous detection of long-range $^{1}H,^{13}C$ and $^{1}H,^{15}N$ connectivities. *Organic letters*. 9(1), 29–32. https://doi.org/10.1021/ol062511h.

Park, S., Jeong, Y., Pradeep, K. 2009. Synthesis of [2H]- and [13C]-labeled pyronaridine tetraphosphate-an antimalarial drug. *J Label Compd Radiopharm, 52(2)***,** 56-62.

Park, S., Pradeep, K., Jang, S. 2007. Synthesis of carbon-14-labelled pyronaridine tetraphosphate. *J Label Compd Radiopharm.* 50, 1248-1254.

Pellon, R., Carrasco, R., Rodes, L. 1993. Synthesis of N-Phenylanthranilic Acids Using Water as Solvent. *Synthetic Communications.* 23, 1447-1453.

Pellon, R., Carrasco, R., Rodes, L. 1996. Synthesis of 11 H-Pyrido[2,1-b]quinazolin-11-one and Derivatives. *Synthetic Communications. 26(20)*, 3869-3876.

Peters, W., Robinson, B. L. 1992. The chemotherapy of rodent malaria. XLVII. Studies on pyronaridine and other Mannich base antimalarials. *Ann Trop Med Parasitol.* 86, 455-465.

Pradines, B., Tall, A., Parzy, D., Spiegel, A., Fusai, T., Hienne, R., Trape, J. F., Doury, J. C. 1998. *In-vitro* activity of pyronaridine and amodiaquine against African isolates (Senegal) of *Plasmodium falciparum* in comparison with standard antimalarial agents. *J Antimicrob Chemother*. 42, 333-339.

Price, C. C., Roberts, R. M. 1946. 4-Chloro-2-(3-pyridylamino) benzoic acid and its conversion to 6-chloro-9-hydroxypyrido [3,2-b] quinoline. *J Org Chem.* 11, 463-468.

Price, C. C., Roberts, R. M. 1946. The synthesis of 4-hydroxyquinolines; through ethoxymethylene malonic ester. *J Am Chem Soc.* 68, 1204-1208.

Puhl, A. C., Gomes, G. F., Damasceno, S., Godoy, A. S., Noske, G. D., Nakamura, A. M., Gawriljuk, V. O., Fernandes, R. S., Monakhova, N., Riabova, O., Veras, F. P., Batah, S. S., Fabro, A. T., Oliva, G., Cunha, F. Q., Alves-Filho, J. C., Cunha, T. M., Ekins, S. 2022. Pyronaridine Protects against SARS-CoV-2 Infection in Mouse. ACS Infectious Diseases. *Advance online publication*.

Ringwald, P., Bickii, J., Basco, L. 1996. Randomised trial of pyronaridine versus chloroquine for acute uncomplicated *falciparum* malaria in Africa. *Lancet.* 347, 24-28.

Ruscoe, J. E., Tingle, M. D., O'neill, P. M., Ward, S. A., Park, B. K. 1998. Effect of disposition of mannich antimalarial agents on their pharmacology and toxicology. *Antimicrob Agents Chemother.* 42**,** 2410-2416.

Schick, O., Binz, A. and Schultz, A. 1936. Sulfur of *o*-diaminopyridines with a benzyl substituent attached to the ring or exocyclic. *Berichte.* 69, 2593.

Schroeter, G., Eisleb, O. 1909. Ueber dimolekulare Anhydride der Anthranilsaure. *Justus Liebigs Ann. Chem.* 367(1-2), 101-167.

Schulenberg, J., Archer, S. 1965. The Preparation of 2-Methyl-1-phenylbenzimidazole 3-Oxide. *Organic Reactions*. 30, 4, 1279–1281

Silverstein, R., Webster, F., Kiemle, D. L. 2005. Spectrometric identification of organic compounds, New York, N.Y. *John Wiley & Sons*.

Song, H., Chen, T, S. 2001. *p*-Aminophenol-induced liver toxicity: tentative evidence of a role for acetaminophen. *J. Biochem. Mol. Toxicol*. 15, 34-40

Sorensen, O. 1989. Polarization transfer experiments in high-resolution NMR spectroscopy. *Progress in Nuclear Magnetic Resonance Spectroscopy.* 21, 503-569.

Sperotto, E., Van Klink, G. P., Van Koten, G. De Vries, J. G. 2010. The mechanism of the modified Ullmann reaction. *Dalton Trans.* 39, 10338-10351.

Stone, W., Mahamar, A., Sanogo, K., Sinaba, Y., Niambele, S. M., Sacko, A., Keita, S., Youssouf, A., Diallo, M., Soumare, H. M., Kaur, H., Lanke, K., Ter Heine, R., Bradley, J., Issiaka, D., Diawara, H., Traore, S. F., Bousema, T., Drakeley, C., Dicko, A. 2022. Pyronaridine-artesunate or dihydroartemisinin-piperaquine combined with single low-dose primaquine to prevent *Plasmodium falciparum* malaria transmission in Ouélessébougou, Mali: a four-arm, single-blind, phase 2/3, randomised trial. *The Lancet. Microbe*. 3(1), e41–e51. https://doi.org/10.1016/S2666-5247(21)00192-0.

Takahashi, H. 1945. Synthesis of pyridine containing rings. *Yakugaku Zasshi,* 65, 7-8A.

Takahashi, T., Shimada, S., Hayase, K. 1945. Synthesis of heterocyclic compounds of nitrogen. XII. Synthesis of 7-chloro-2-methoxy-10-(4-diethylamino-1-methylbutylamino) pyrido[3,2-b]quinolone. *Yakugaku Zasshi.* 2A, 5-6.

Terrier, F. 1982. Rate and equilibrium studies in Jackson-Meisenheimer complexes. *Chemical Reviews.* 82, 77-152.

Ullmann, F. 1903. Ueber eine neue Bildungsweise von Diphenylaminderivaten. *Berichte der deutschen chemischen Gesellschaft.* 36, 2382-2384.

Ward Blenkinsop & company. Goldberg A. A. 1956. Substituted 1.10-Diaza-anthracenes. *US patent*.

Warsame, M., Wernsdorfer, W. H., Payne, D., Bjorkman, A. 1991. Positive relationship between the response of *Plasmodium falciparum* to chloroquine and pyronaridine. *Trans R Soc Trop Med Hyg*. 85, 570-571.

Wattanavijitkul, T. 2010. Population pharmacokinetics of pyronaridine in the treatment of malaria. *PhD Thesis*, University of Iowa, http://ir.uiowa.edu/etd/622.

Yamaguchi, M., Maruyama, N., Koga, T., Kamei, K., Akima, M., Kuroki, T., Hamana, M., Ohi, N. 1995. Novel antiasthmatic agents with dual activities of thromboxane A2 synthetase inhibition and bronchodilation. VI. Indazole derivatives. *Chem Pharm Bull (Tokyo).* 43, 332-334.

Zeng, P., Zhou, H., Han, Y., Fu, S., Zheng, Y., Xu, X. 2009. Study on Pharmaconkinetics of Pyronaridine in Mice, School of Chemistry and Biology Engineering. *Drug Dev Ind Pharm.* School of Chemistry and Biology Engineering: Chongqing University of Technology.

Zheng, X. L. 1979. [Diagnosis and surgical treatment of pancreatic cyst (author's transl)]. *Zhonghua Wai Ke Za Zhi.* 17, 238-239.

Zheng, X. Y., Chen, C., Gao, F. H., Zhu, P. E., Guo, H. Z. 1982. [Synthesis of new antimalarial drug pyronaridine and its analogues (author's transl)]. *Yao Xue Xue Bao.* 17, 118-125.

Zheng, W. Y., Chen, C., Huang, L. S. *Chin. J. Pharmaceut*. 1990, *21*, 200-204.

Chapter 6

Conclusion.

Index of Contents chapter 6.

Figure of contents chapter 6.

6.1. Conclusion.

One critical issue of concern within science is the poor reproducibility of published work. This was addressed in this thesis for the production of promising antimalarials. This can be traced back to *Organic Syntheses* 1921 (Figure 6.1) which was established to facilitate production of chemicals which could not be imported from Germany due to the first world war: i.e. “to be absolutely certain that each set of directions can be repeated, every experiment has been carried out in at least two laboratories. Only after exact duplication of the results, in both laboratories are the directions considered ready for publication”.

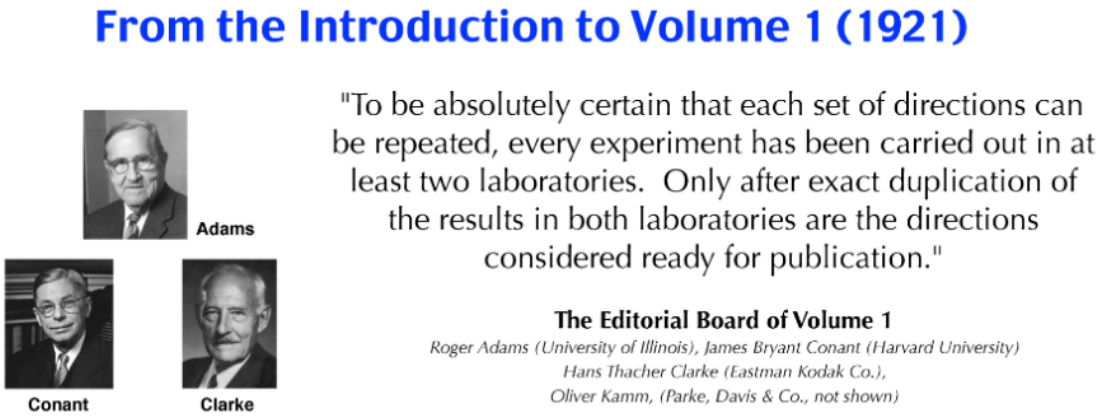

Figure 6.1. (Baker, 2016). "1,500 scientists lift the lid on reproducibility".

This study followed the protocol mentioned in organic synthesis. It was found that in the authors hands, many literature procedures were difficult to reproduce or scale up, whilst methods provided here are entirely reproducible especially for *meta*-quine (**25a**) (Figure 6.4) (Quinoline and *bis*quinoline synthesis, chapter **2**) and have been carried out multiple times at various scales from mg (chapter **4**) to multigram and in some cases at Kg quantities (pyronaridine (**15**), chapter **5,** unpublished work) (Figure 6.2). In addition, where possible structures were fully characterised by spectroscopy (principally NMR) and spectrometry (chemical ionisation and electrospray mass spectrometry).

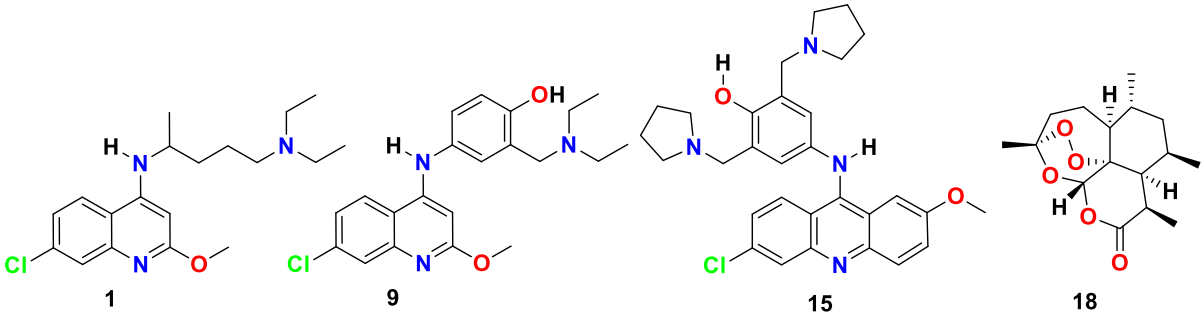

Figure 6-2. chloroquine (**1**), amodiaquine (**9**), pyronaridine (**15**), artemisinin (**18**).

Notable papers for antimalarial work included the article on chloroquine (**1**) (Figure 6.2) manufactured by Kenyon, which was seen as a model approach for reporting work in a reproducible fashion at scale (Kenyon *et al*. **1949**).

A substantial percentage of tropical infections including malaria, which mostly affect economically deprived people, their livestock and pets, are caused by increasingly resistant parasites that have become resistant to medications many of which were the only ones available at the outset of this study (Ismail *et al*., **2020**).

Naturally occurring substances such as artemisinin (**18**) (Figure 6.2), which are isolated from *Artemisia annua* L. which were first discovered and then isolated in China. This can be likened to the original discovery of quinine from the bark of cinchona tree. The cultivation of these plants has successfully led to the provision of suitable clinically useful compounds. Despite intensive global searches of plant extracts, from traditionally used medications as well as plants not currently used as medications, discovering affordable, safe and effective natural products that meet modern safety standards and most importantly, high potency *in-vivo* remain quite rare. Consequently, affordable and safe synthetic or semi-synthetic compounds will fulfil this need until such time an affordable and effective vaccine is produced and successfully introduced in malaria endemic areas and solve the problems of patient compliance. Currently, distinct compounds with mechanisms of action different to those associated with acquired drug resistance are now being sought using new techniques that target multiple parts of the malaria life cycle. These are now being given more consideration than drugs derived from the prototypes of quinoline and acridine. However, most of these molecules are synthesised in industry, through expensive, multi-step synthetic methods which are unaffordable by developing nations.

Therefore, one of the main objectives of this study, pharmacological research into unexplored drug-receptor chemical spaces, could help to select/design new, or to improve established prototypes, that could be appropriately developed for additional clinical use.

*Mono*quinolines, e.g. compounds 36-39 were synthesised (chapter **2**, schemes 1-4, pages 81-83); *bis*quinolines, aliphatic bridged *bis*quinolines (schemes 5-23, Pages 83-95) and aromatic bridged *bis*quinolines (schemes 24-27, pages 95-98) were synthesised using conventional procedures. Some of the proceeding compounds were also synthesised using microwave radiation (schemes 27-38, pages 98-102). Some of these procedures were optimised and characterised. Overall, 39 schemes were introduced in chapter **2**, they are new. They are

improved and reproduceable methods of synthesis for synthesis and production of *mono*- and *bis*quinolines.

The paradigm that "a small change in structure can lead to a large change in potency" was explored in the current study. For instance, in the *bis*quinoline chapter a strategy in producing *ortho*-, *meta*- and *para*- *bis*quinolines allowed a hypothesis first advanced by Cheng (Cheng, **1976**) to be tested. Variation in chemical geometry allowed identification of the most potent members of this small series which were *meta*-analogues that are active at *ca*. 1mg/kg (Ismail *et al*., **1998**). The accumulation of drugs into acidic vacuole compartments of parasites is reliant on a so called "weak base effect" (Pulcini *et al*., **2015**).

It is accepted that polyamine importation pumps steal amines required for parasitic growth from the host. This thesis, hypothesised that the same mechanisms may be allowing antimalarial medications, such as chloroquine (**1**)(Figure 6.2), to be (inadvertently) imported into the parasite, in a "Trojan horse fashion". Consequently, it was hypothesised that by appending various side chain polyamines linked to various heterocycles, that such molecules could surreptitiously be imported thereby by-passing parasite resistance mechanisms (Carter *et al*., **2015**).

Another aspect explored in the current thesis was to allow transition to "green solvents", replacing more toxic *N*-methyl pyrrolidinone used by earlier investigators in making aryl bridged *bis*quinolines. This was successfully achieved for aryl bridge antimalarials. However, this procedure could not be used to make alkyl bridged compounds, including Ro47-7737. Using methanol as a green solvent, this was successfully achieved, however such compounds still require a green solvent to replace NMP. Phenol, which is biodegradable, but still highly toxic, is a possible candidate. This having been used successfully in a few small scale reactions. Extension to other compounds, and developing a scaling up procedure is part of future work.

The current study addressed concerns of affordability by using known inexpensive feedstocks especially 4,7-dichloroquinoline. This features in chapter **2** where compounds originally described in the patent literature were synthesised and characterised using more modern methods of analysis. The following chemicals (Figure 6.3) were used to make possible antimalarials in chapter **2**, and some selected syntheses are also presented (Figure 6.4).

1- cyclohexanamine

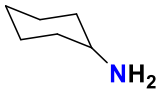

2- 1-adamantamine

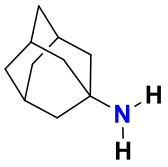

3- 2-adamantamine

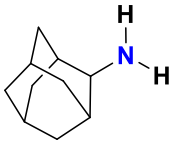

4- 2,4-dichloroaniline

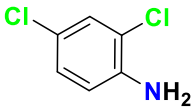

5- (±)-1,2-diaminocyclohexane

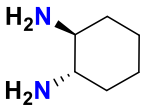

6- cis-1,2-diaminocyclohexane

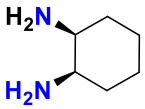

7- Ethane-1,2-diamine

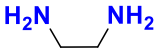

8- Propane-1,3-diamine

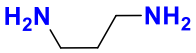

9- Butane-1,4-diamine

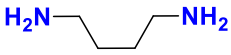

10- Pentane-1,5-diamine

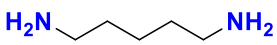

11- Hexane-1,6-diamine

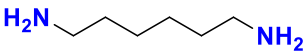

12- heptane-l,7-diamine

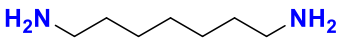

13- Octane-l,8-diamine

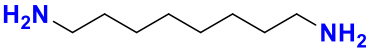

14- nonane-l,9-diamine

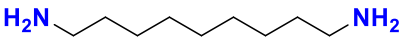

15-decane-l,10-diamine

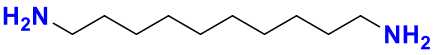

16-Dodecane-1,12-diamine

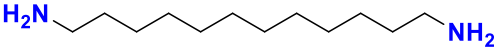

17- α,α'-diamino-p-xylene

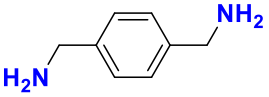

18- phenylene diamine

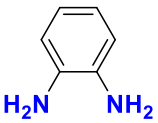

18- 1,3-phenylene diamine

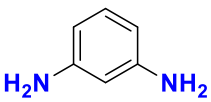

19- 1,4-phenylene diamine

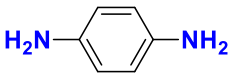

Figure 6.3. Chemicals used to make quinolines and *bis*quinolines in chapter 2.

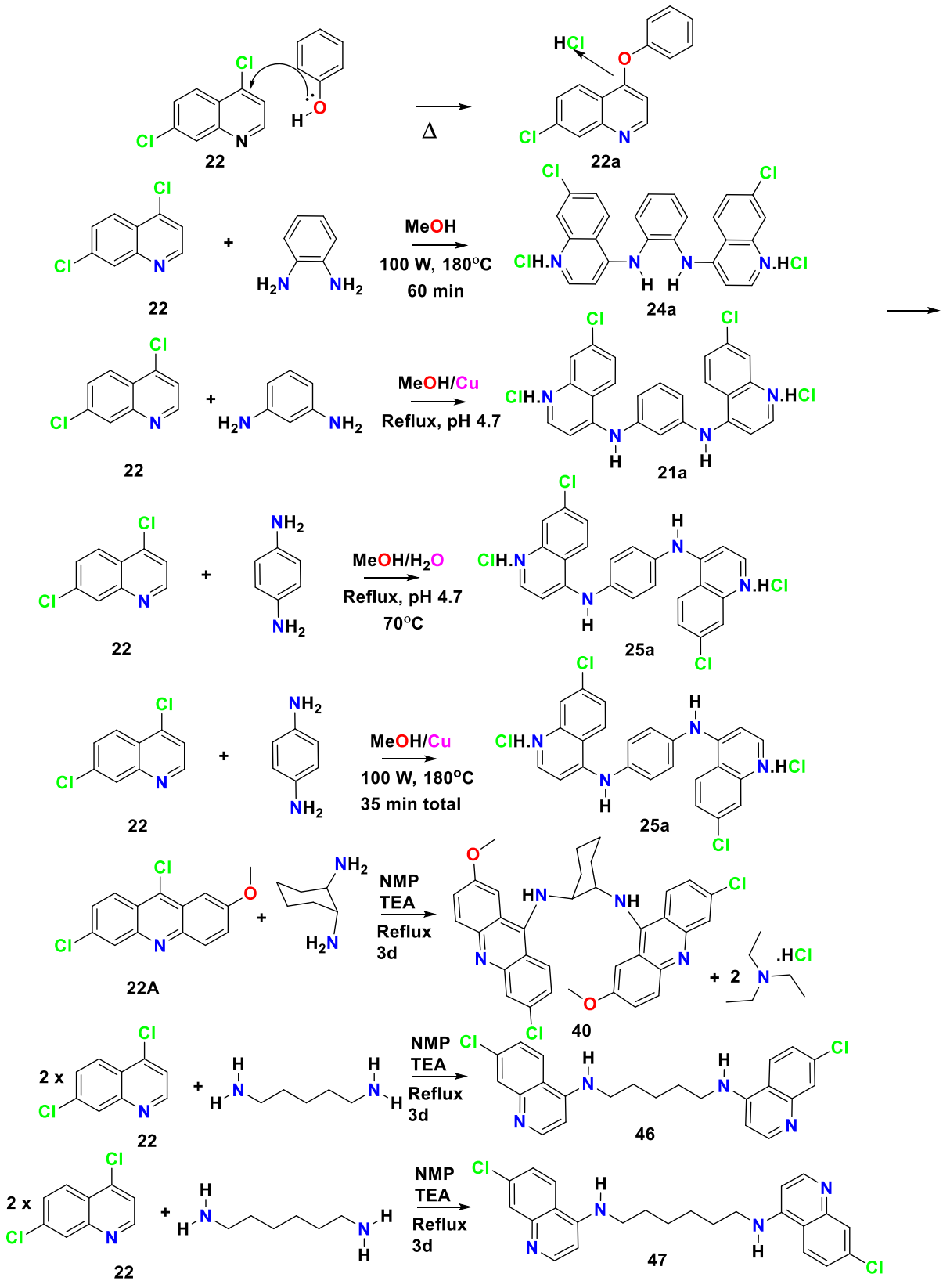

Figure 6.4. Selection of quinoline and *bis*quinolines synthesised in chapter 2.

During pharmacological evaluation, this study demonstrated that a simple aromatic ring could replace the more complex side chains found in amodiaquine (**9**) and pyronaridine (**15**) (Figure 6.2), and that such drugs were absorbed by the oral route, an important step in developing this class of compounds for eventual clinical applications. The toxicological evaluation of such compounds to assess the therapeutic index were beyond the scope of this study. It can be concluded that the best methods for making "aromatic *bis*quinolines" are microwave procedures that produce the desired compounds such a *meta*-quine (**25a**) (Figure 6.4) in less than 2 minutes, therefore making them highly affordable, due to reduced energy costs. Conversion of such processes into recently developed flow protocols can form the basis of future continuous manufacturing (Figure 6.4). if they do prove safe in detailed toxicological safety studies (Lei *et al*., **2024**)

Contributions to determining drug-receptor interaction required specialized hybrid compounds (chapter **3**, schemes 40-42, pages 137-139, fluorinated *bis*quinolines) that resulted in a major study published in Chemistry, A European Journal (Fielding *et al*. **2017**). The large quantities of material synthesised allowed insightful EPR studies to be conducted that highlighted electron transfer from the quinoline drug to inert iron III, converting it to haem Fe (II), which is toxic to *Plasmodia* (Fielding *et al*. **2017**). This important observation demonstrates that antimalarial action should be evaluated in terms of efficient electron transfer from drug to haem within the parasite.

Another strategy explored in this work was to incorporate an additional nitrogen into a quinoline in various positions. This replacement of a methine group in a quinoline to make naphthyridines was extensively explored by Cheng (1925-2016) in his development of a clinically useful anticancer agent mitoxantrone.

Importantly, Cheng & McCaustland's work in **1970**s established that the 5th position (N5) in the chloroquine (**1**) (Figure 6.2), not only had improved the biological activity but also reduced the toxicity. In the current author's experience, none of the previously described synthetic routes could be scaled up to produce multi-gram quantities required for pharmacological and EPR studies. Recently, the N5 has been described as "The necessary nitrogen atom: A versatile high impact design element for multiparameter optimisation" (Lewis *et al*., **2015**).

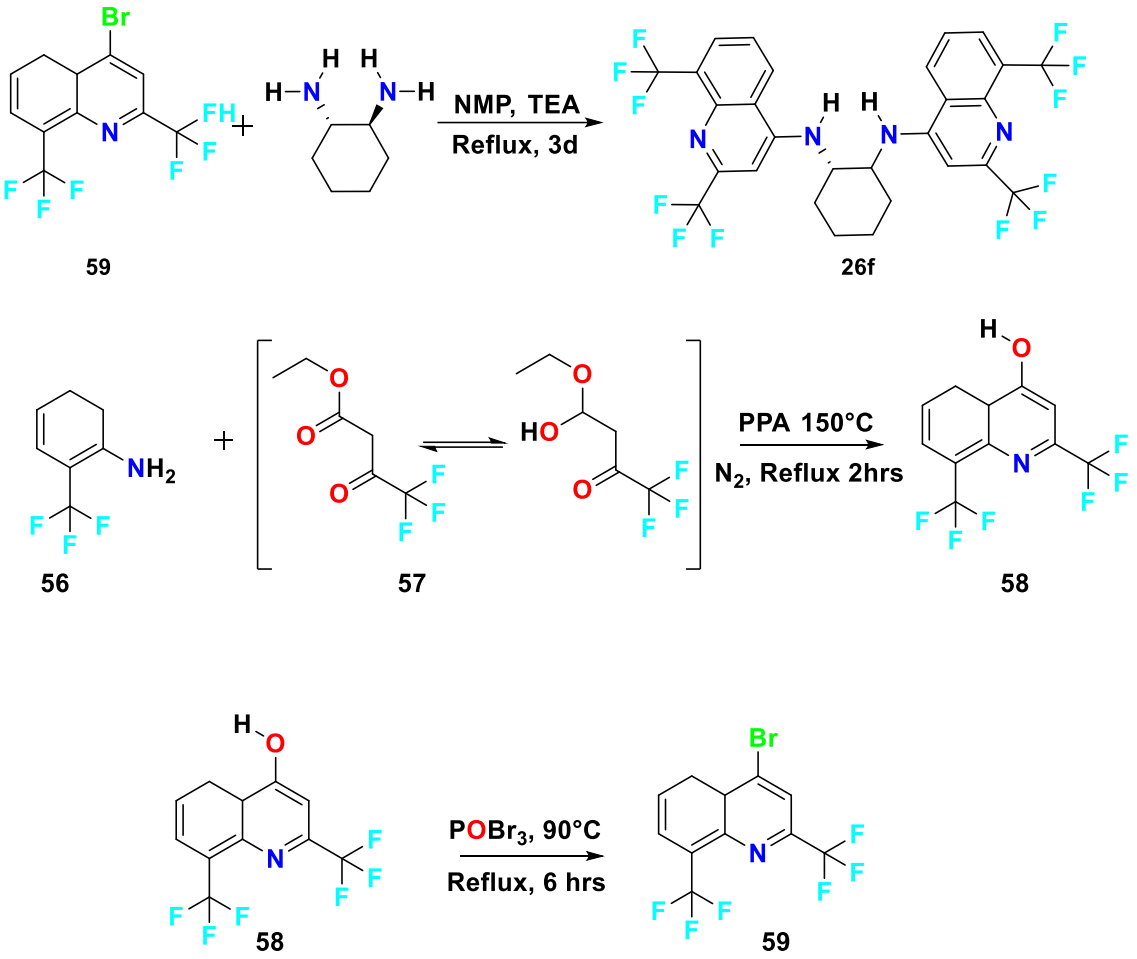

Figure 6.5. Fluorinated compounds, measured using EPR studies (Fielding *et al*. 2017).

Making naphthyridines (chapter **4**, schemes 43-47, pages 158-181) was fraught with difficulties. Consequently, routes were sought to investigate the reproducible production of the key 1,5-napthyridine material (4-hydroxyquinoline) to explore the scalability of naphthyridine productions. This could be an important relay molecule for the production of 7-chloro-1,5-naphthyridin-4-ol, which was not explored in this study. Notably it was found that the compound could be recrystallized from distilled water and expensive chromatography was avoided. Also, the multistep route was telescoped into a single step in which the desired compound sublimed onto the walls of the reaction vessel- a serendipitous result for which a novel mechanism for this process was explored using DFT (Figure 6.5).

More contemporary methods can now be used to directly insert nitrogen into a homocycle compound, as noted in Peplow's essay "Almost magical" in the synthesis of naphthyridines (Peplow, **2023**).

An important observation made by McCaustland & Cheng (**1970**), demonstrated that 5-*aza* chloroquine was much safer than chloroquine (**1**). This prompted a search for exploring affordable methods of making 4-hydroxy,1,5-napthyridine a compound that had proven difficult to make reproducibility. Consequently, methods were developed that allowed gram to multi-gram scale synthesis to be produced. Importantly, a mechanism was discovered in which the sublimate found was the desired compound allowing the reaction to be telescoped into a single step and a method that allowed recrystallization from water, a further green protocol.

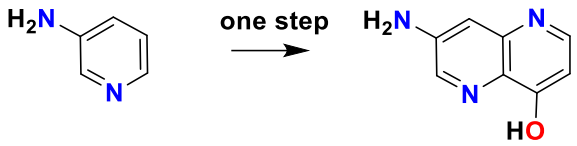

Figure 6.6. One step, one pot unforeseen thermal method of syntheses 4-hydroxy, 1,5 Naphthyridine.

Full NMR characterisation, as well as a single crystal x-ray diffraction study allowed rapid chromatography-free purification which makes this reaction industry friendly. Methods to introduce a halogen in the 7th position were planned but there was insufficient time to explore this further. This would allow cost effective production of 7-*aza*-chloroquine (Figure 6.7).

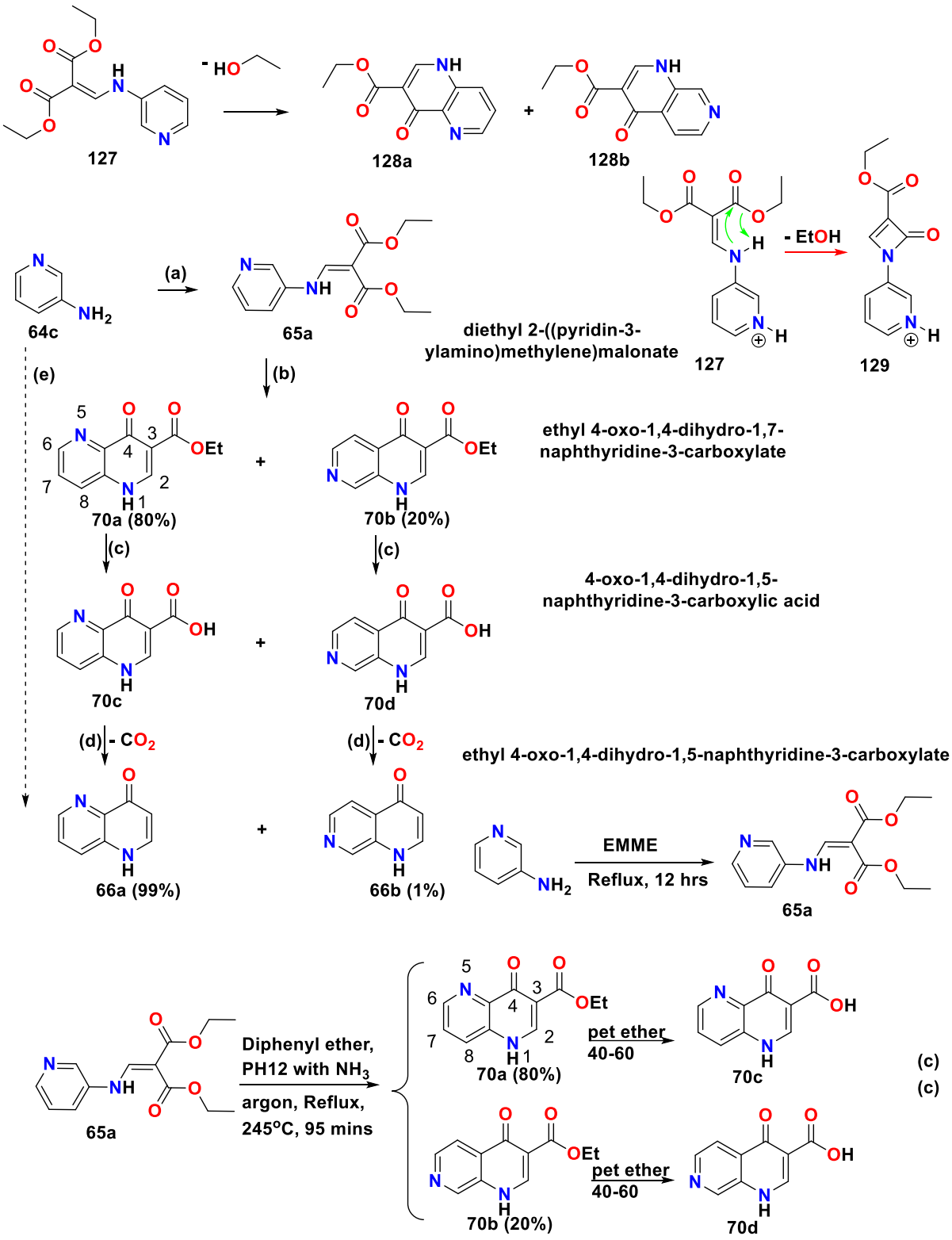

Figure 6.7. Synthesis of Naphthyridines in chapter 4.

Finally, synthesis of Pyronaridine (**15**) (Figure 6.2), was successfully investigated, using both conventional methods and microwave synthesis. At the onset of this study, pyronaridine

was not in clinical use. However, it was fully characterised and methods used to manufacture this at kilogram scale were investigated just after this study was complete (Figure 6.8).

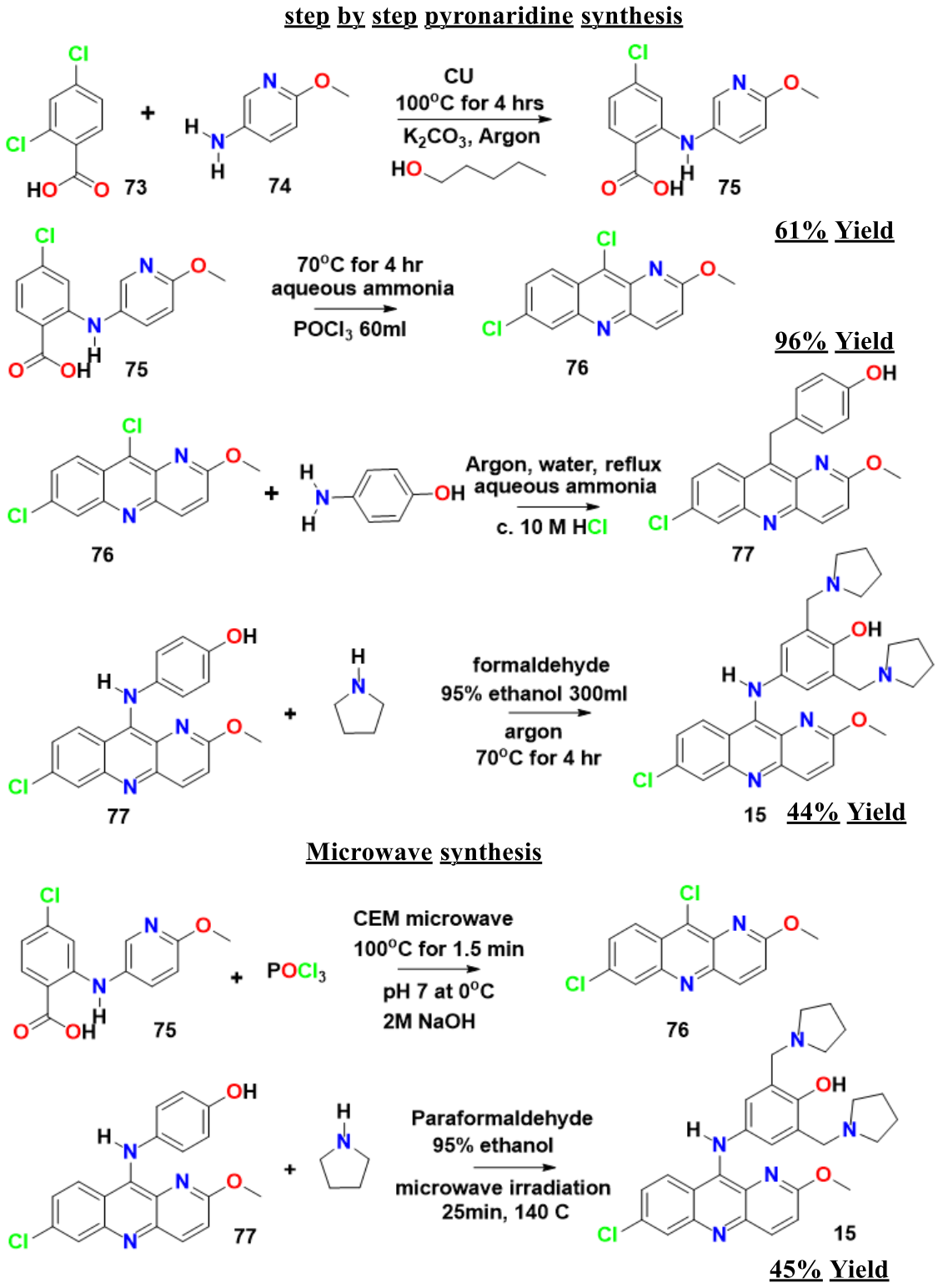

Figure 6.8. Pyronaridine (**15**), conventional synthesis and microwave synthesis.

In this thesis, using Ullmann coupling approach, the acridine ring was constructed (scheme

48-50, pages 228-230). Then using *p*-amino phenol, the first part of head group was synthesised (scheme 51, page 231), after which pyrrolidine was used for addition to phenol moiety (scheme 52, page 232). Synthesis of pyronaridine was also carried out using microwaves, with successful results (scheme 56-57, pages 236-237). On the whole, more than one hundred procedures were carried out, of which the key procedures are described in this study (chapter **5**, schemes 48-57, pages 229-236).

In conclusion, this work established robust, scalable protocols for the synthesis of putative antimalarial drugs and their critical intermediates, rendering them ideal for industrial processing.

A number of publications detailing the work are mentioned at the end of this conclusion.

6.2. Future works.

All the drugs synthesised, (schemes 1-57) should be examined using soft mechanochemical synthesis and analysis by ESI-MS. More Importantly, further NMR studies using INADEQUATE spectroscopy are required to allow further substantiation of the proposed molecules.

A possible contender for scalable synthesis, will be the use of microwave, especially with evolution of new microwave synthesisers under conditions of flow chemistry. There is now a huge potential to synthesise organic molecules and drugs at significantly higher volume, and the industry has begun to embrace this paradigm shift.

6.3. References.

Baker, M. 2016. 1,500 scientists lift the lid on reproducibility. *Nature* (News Feature). *Springer Nature*. 533 (7604): 452-454. Bibcode:2016Natur.533.452B. doi:10.1038/533452 DOI: 10.1021/acs.oprd.2c00374.a

Banerjee, B., Singh, A., Sharma, A., Priya, A., Kaur, M., Gupta V.K. 2023. A Simple and Efficient Method for the Synthesis of Benzo[3,4-a]Phenazin-5-Ols and Benzo[f]Pyrido[b]Quinoxalin-5-ol Derivatives Using Trisodium Citrate as an Efficient Organo-Catalyst at Room Temperature, *Polycyclic Aromatic Compounds*, https://doi.org/10.1080/10406638.2023.2238869

Carter, N. S., Kawasaki, Y., Nahata, S. S., Elikaee, S., Rajab, S., Salam, L., Alabdulal, M. Y., Broessel, K. K., Foroghi, F., Abbas, A., Poormohamadian, R., & Roberts, S. C. (2022). Polyamine Metabolism in Leishmania Parasites: A Promising Therapeutic Target. *Medical sciences* (Basel, Switzerland), 10(2), 24. https://doi.org/10.3390/medsci10020024

Cheng, C.C. 1976. Structural similarity between febrifugine and chloroquine, *Journal of Theoretical Biology*, 59 (2), 497-501, https://doi.org/10.1016/0022-5193(76)90186-710.1016/j.molstruc.2019.06.025

Da Silva, L.C., Lindner, A., Cavalcanti, L.N., Da Costa, E.P., Azevedo, M.M., Araújo, R.M., De Freitas, R. S., De Souza, A.F., Machado, V.G., Menezes, F.G. 2019. One-pot synthesis and structural elucidation of polyfunctionalized quinoxalines and their use as chromogenic chemosensors for ionic species. *Journal of Molecular Structure*, Volume 1195, 5, 936-943. https://doi.org/10.1016/j.molstruc.2019.06.025

Fielding, A. J., Lukinovic, V., Evans, P. G., Alizadeh-Shekalgourabi, S., Bisby, R. H., Drew, M.G.B., Male, V., Del Casino, A., Dunn, J.F., RandlE, L.E., Dempster, N.M., Nahar, L., Sarker, S.D., Cantu Reinhard, F.G., De Visser, S.P., Dascombe, M.J., Ismail, F.M.D., 2017. Modulation of Antimalarial Activity at a Putative Bisquinoline Receptor *In-Vivo* Using Fluorinated *Bis*quinolines. *Chemistry*. 23(28):6811- 6828.. https://doi.org/10.1002/chem. 2016050995 . Epub 2017 Apr 21. PMID: 28261884.

Iseminger, P.W., Gregory, M., Weakley, T.J., Caple, G., A.G. Sykes, A. G. 1997. Characterization of 3-Aminophenazin-2-ol Isolated from the Chemical Oxidation of of Phenylenediamine, *J. Org. Chem*. 62, 2643-2645.

Ismail, F. M., Nahar, L., Zhang, K, Y., Sarker, S, D. 2020. Chapter Four-Antiparasitic natural products, Editor(s):Satyajit D. Sarker, Lutfun Nahar, Annual Reports in Medicinal Chemistry, *Academic Press*, 55. https://doi.org/10.1016/bs.armc.2020.03.001

Kenyon, R.L., J. A. Wiesner, J.A., C. E. Kwartler, C.E. 1949. Chloroquine Manufacture. *Industrial & Engineering Chemistry*. 41 (4), 654-662. https://doi.org/10.1021/ie50472a0021

Lei, Zh., Ang, H.T., Wu, J. Advanced In-Line Purification Technologies, *Organic Process Research & Development*. 2024 28 (5), 1355-1368 DOI: 10.1021/acs.oprd.2c00374

Mc Caustland, D., Cheng, C. P. 1970. 1,5-naphthyridines. Synthesis of 7-chloro-4-(4- di-

ethylamino-1-methylbutylamino)-2-methoxy-1,5-naphthyridine and related compounds. *Journal of Heterocyclic Chemistry*. 7, 467-473.

Pennington, L.D., Moustakas, D.T. 2017. The Necessary Nitrogen Atom: A Versatile High-Impact Design Element for Multiparameter Optimization. *Journal of Medicinal Chemistry*. 60 (9), 3552-3579. https://doi.org/10.1021/acs.jmedchem.6b01807

Peplow, M. 2023. 'Almost magical': chemists can now move single atoms in and out of a molecule's core. *Nature*, 618(7963), 21–24. https://doi.org/10.1038/d41586-023-01735-1

Pulcini, S., Staines, H., Lee, A. 2015. Mutations in the *Plasmodium falciparum* chloroquine resistance transporter, PfCRT, enlarge the parasite's food vacuole and alter drug sensitivities. *Sci. Rep*. 5, 14552. https://doi.org/10.1038/srep14552;

https://www.cheminfo.org/flavor/structuralAnalysis/IR/IR_spectra_prediction/index.html.

6.4. Publications.

Dascombe, M. J., Drew, M. G., Morris, H., Wilairat, P., Auparakkitanon, S., Moule, W. A., Alizadeh-Shekalgourabi, S., Evans, P. G., Lloyd, M., Dyas, A. M., Carr, P., Ismail, F. M. 2005. Mapping antimalarial pharmacophores as a useful tool for the rapid discovery of drugs effective *in-vivo*: design, construction, characterization, and pharmacology of *meta*-quine. *J Med Chem*. 48, 5423-5436. https://doi.org/10.1021/jm0408013

Fielding, A. J., Lukinovic, V., Evans, P. G., Alizadeh-Shekalgourabi, S., Bisby, R. H., Drew, M.G.B., Male, V., Del Casino, A., Dunn, J.F., RandlE, L.E., Dempster, N.M., Nahar, L., Sarker, S.D., Cantu Reinhard, F.G., De Visser, S.P., Dascombe, M.J., Ismail, F.M.D., 2017. Modulation of Antimalarial Activity at a Putative Bisquinoline Receptor *In-Vivo* Using Fluorinated *Bis*quinolines. *Chemistry*. 23(28):6811- 6828.. https://doi.org/10.1002/chem. 2016050995 . Epub 2017 Apr 21. PMID: 28261884.